



NTNU – Trondheim
Norwegian University of
Science and Technology

The Performance and Potential for PV systems at Northern Latitudes

Eirik Oksavik Lockertsen

Master of Energy and Environmental Engineering

Submission date: June 2015

Supervisor: Ole-Morten Midtgård, ELKRAFT

Co-supervisor: Øystein Kleven, Solbes A/S

Norwegian University of Science and Technology
Department of Electric Power Engineering

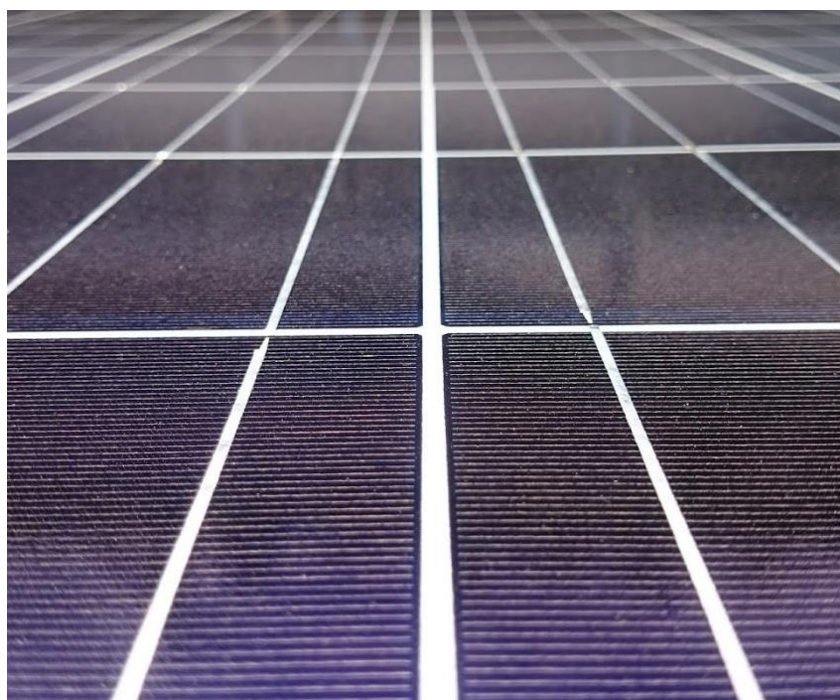
MSc student Eirik Oksavik Lockertsen

The Performance and Potential for PV systems at Northern Latitudes

Trondheim, spring 2015

NTNU
Norwegian University of
Science and Technology
Faculty of Information Technology,
Mathematics and Electrical Engineering
Department of Electric Power Engineering

Trondheim, spring 2015



NTNU

Norwegian University of
Science and Technology

Front-page photo from the Acusticum PV system.

Photo by Eirik Oksavik Lockertsen

Sammendrag

Hva er ytelsen og potensialet til PV systemer på nordlige breddegrader, er forskningsspørsmålet til denne avhandlingen. For å svare på dette er det blitt utført en litteraturstudie, en case studie med tilhørende besøk til et 236 kWp PV system i Piteå, Sverige. Dette systemet har blitt simulert med utgangspunkt i gjennomsnittsårs data fra systemet selv, og meteorologiske data, for å kunne sammenligne den faktiske ytelsen mot den simulerte. Den balanserte levetidskostnaden (LCOE) har blitt kalkulert gjennom et utviklet verktøy. Og det har blitt undersøkt om hvorvidt et slikt system er lønnsomt i Norge.

Det ble funnet at kvaliteten på databaser med innstrålingsdata for nordlige breddegrader er lav. Den beste generiske databasen funnet er NASA/SSE. De lave solinnstrålingsverdiene på nordlige breddegrader kan ha en negativ effekt på likeretterens ytelse. Optimal vinkel på modulene burde være basert på snøakkumulasjon i tillegg til solgeometri og komposisjon av solinnstrålingen

Simuleringen av 236 kWp PV systemet ga en ytelsesratio på 0.850, spesifikk produksjon på 897 kWh/kWp, og en årlig produksjon på 208 kWh. Dog viser sammenligninger mellom simuleringer basert på faktisk værdata, og rapporter fra systemet på levert energi, at likeretterens effektivitet er på 89.1 % istedenfor de 96.3 % som er satt av produsenten.

PV systemets LCOE ble kalkulert til å være 0.132 EUR/kWh. Kostnadsnivået som ble funnet er tett opptil beste praksis i verden.

Et scenario med et 15 kWp PV system for en privat husholdning ga en energikostnad fra et PV system for en privat husholdning i Norge gav en energikostnad på 0.12 EUR/kWh, 0.02 EUR/kWh over strømprisen fra veggkontakten. Indirekte inntekter peker på en mer fordelaktig prising på elektrisitet fra PV som gjør dette til det beste valget.

Det er noen momenter som en må være på vakt mot, men konklusjonen blir at ytelsen og potensialet for PV systemer på nordlige breddegrader er svært god.

This page intentionally left blank

Abstract

What is the performance and potential for PV systems at northern latitudes, is the research question for this thesis. In order to answer this a literature review have been done and a case study of, and visit to, a 236 kW_p PV system in Piteå, Sweden have been conducted. Simulations of this system have been done for average years, through extracted system data, and meteorological data, in order to compare to the actual performance of the system. The levelized cost of energy from the PV system have been calculated through a constructed tool. And the investment profitability in Norway have been investigated.

It was found that the quality of irradiation databases available for northern latitude is low. The best generic database found was the NASA/SSE. The low irradiation conditions in northern latitudes might have a negative effect on inverter performance. The optimal module tilt and azimuth should be based on snow accumulation in addition to solar geometry and irradiation composition

The simulation of the 236 kW_p PV system gave a performance ratio of 0.850, specific production of 897 kWh/kW_p, and an annual yield of 208 kWh. Although comparison between simulation based on actual weather conditions and reported delivered energy from the system suggests an inverter efficiency of 89.1 % instead of 96.3 % as suggested by the manufacturer.

The PV system LCOE was calculated to be 0.132 EUR/kWh. The cost level was found to be close to world best practice.

A scenario with a 15 kW_p PV system for a private household in Norway gave a cost of energy from a PV system of 0.12 EUR/kWh, 0.02 EUR/kWh above the socket electricity price. Indirect revenues points to a higher value of PV electricity, making this the preferred choice.

There are some issues to be aware of, but the end conclusion is that the performance and potential for PV systems in northern latitudes is overall very good.

This page intentionally left blank

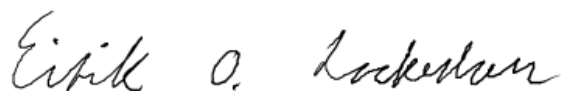
Preface

This is my master thesis in my 10th semester at the MSc programme, Energy and Environmental Engineering at NTNU. The master thesis counts 30 ECTS.

The reason for writing a master thesis on photovoltaic systems is that I think this technology will be a very significant global contributor in the supply of electricity in the future. I have four main arguments for this. First, price is passing grid parity at a rapid pace all over the world, and the rate of price reduction does not seem to decline any time soon. Second is that it is for most systems a maintenance less technology, which means the operational cost should be at a minimum in a world where labour is becoming more and more expensive. Third, it is a technology that can be deployed almost anywhere at any scale. And fourth, it is a technology for a sustainable future. A more detailed picture of where the opportunities and threats are for photovoltaic systems is therefore of great interest for me. What about Norway? In light of the arguments above?

This thesis answers and discusses a lot of questions, but raises even more.

In order to be able to complete this thesis several helpful and most competent persons have contributed and guided me along the way. First I would like to thank my supervisor, Professor Ole-Morten Midtgård at the Department of Electric Power Engineering, for very useful guidings at the start of the semester. Øystein Kleven, researcher for NORUT and managing director at Solbes for hours of interesting discussions and feedback, a most interesting excursion to the PV system in Piteå and some very helpful last minute data samples. Patric Jonsson head of Research and Development at Pite Energi for valuable data this thesis. And last but not least Silje Nørsett for valuable support along the way.



MSc student, Eirik Oksavik Lockertsen

Trondheim, 18th of June 2015

Table of Contents

SAMMENDRAG	III
ABSTRACT	V
PREFACE	VII
TABLE OF CONTENTS	IX
LIST OF FIGURES	XII
LIST OF TABLES	XXI
1 INTRODUCTION.....	2
1.1 PV AS A PARTICIPANT IN THE NEW ENERGY SYSTEM.....	2
1.2 THE COST OF PV ELECTRICITY	7
1.3 THESIS PROBLEM FORMULATION	13
1.4 THE ACUSTICUM PV SYSTEM IN PITEÅ, SWEDEN	13
1.5 LIMITATIONS, DELIMITATIONS AND ASSUMPTIONS.....	15
1.6 THESIS OUTLINE	15
2 THE SOLAR ENERGY POTENTIAL AT NORTHERN LATITUDES	16
2.1 THE SUN AS A RESOURCE.....	16
2.1.1 <i>Power from the sun to the earth's atmosphere</i>	16
2.1.2 <i>The power from the sun at sea level</i>	17
2.1.3 <i>The suns path as seen from a point on earth</i>	21
2.2 THE QUALITY OF SOLAR ENERGY DATA SOURCES (AT NORTHERN LATITUDES)	24
2.2.1 <i>Measurements and modelling of surface irradiation</i>	25
2.2.2 <i>Solar irradiation databases</i>	33
2.2.3 <i>Unshaded solar potential in Piteå</i>	41
2.2.4 <i>Irradiation composition impact on optimal solar energy collector orientation</i>	42
2.2.5 <i>Summary of the quality of solar energy data sources at northern latitudes</i>	46
2.3 THE PV SYSTEM AND DIRECT INFLUENCING FACTORS	47
2.3.1 <i>PV modules</i>	47
2.3.2 <i>Shading of solar modules</i>	59
2.3.3 <i>The inverter</i>	68
2.3.4 <i>Cabling</i>	75
2.3.5 <i>PV system mechanical aspects</i>	76

2.4	PV SYSTEM MODELLING.....	78
2.4.1	<i>Important terms related to PV system performance.....</i>	78
2.4.2	<i>Software for PV systems</i>	79
2.4.3	<i>Summary of input parameters to simulation program</i>	80
2.5	EXPECTED ENERGY PRODUCTION.....	82
2.6	ACTUAL VS EXPECTED ENERGY PRODUCTION FOR MAY 2015	86
3	COST OF ELECTRICITY FROM ACUSTICUM PV SYSTEM	94
3.1	COST OF ELECTRICITY METHODOLOGY	94
3.2	INSTALLATION COST	101
3.2.1	<i>PV module</i>	101
3.2.2	<i>Balance of system cost</i>	103
3.2.3	<i>Total installation cost and comparison</i>	106
3.3	ANNUAL COST	108
3.3.1	<i>PV system life expectancy.....</i>	109
3.3.2	<i>Other annual costs.....</i>	111
3.4	THE COST OF CAPITAL	111
3.5	THE LCOE FOR THE ACUSTICUM PV SYSTEM.....	114
3.6	LCOE FUTURE DEVELOPMENT	118
4	PV SYSTEM INVESTMENT PROFITABILITY IN NORWAY.....	122
4.1	INDIRECT REVENUES AND COST.....	122
4.1.1	<i>Advantages and disadvantages for transmission system operators.....</i>	122
4.1.2	<i>Social responsibility costs and opportunities</i>	124
4.1.3	<i>Other indirect revenues or costs.....</i>	128
4.2	POLICY INSTRUMENTS AND THEIR INFLUENCE ON PV PROFITABILITY.....	129
4.2.1	<i>Investment support.....</i>	129
4.2.2	<i>Feed in tariffs (FiT) and Green certificates</i>	130
4.3	ELECTRICITY PRICE DEVELOPMENT.....	132
4.3.1	<i>Annual average.....</i>	132
4.3.2	<i>Grid rent cost, tax, VAT and development in these</i>	135
4.3.3	<i>Demand- and price fluctuations during the day.....</i>	138
4.4	PV SYSTEM INVESTMENT PROFITABLE IN NORWAY?.....	140
4.4.1	<i>Reaching socket parity</i>	140
4.4.2	<i>Self-use and self-sufficient.....</i>	144

5	CONCLUSION	148
5.1	SUMMARY.....	148
5.2	FURTHER RESEARCH	149
5.3	RECOMMENDED READING	151
	REFERENCES.....	152
	APPENDIX 1 – EXTRACTION OF STRÅNG DATA.....	160
	APPENDIX 2 – EXTRACTION OF PVGIS-CLASSIC DATA	161
	APPENDIX 3 – EXTRACTION OF NASA/SSE DATA	162
	APPENDIX 4 – EXTRACTION OF METEONORM 7.1 DATA.....	165
	APPENDIX 5 – EXTRACTION OF METEONORM 6.1 DATA.....	166
	APPENDIX 6 – EXTRACTION OF SATEL-LIGHT DATA.....	167
	APPENDIX 7 – INVERTER SIMPLIFICATION CALCULATIONS FOR PVSYST	169
	APPENDIX 8 – SIMULATION REPORT. EXPECTED SCENARIO.....	170
	APPENDIX 9 – ACUSTICUM AC ENERGY REPORT MAY 2015	176
	APPENDIX 10 – SIMULATION REPORT. MAY, ACUSTICUM DATA.	177
	APPENDIX 11 – SIMULATION REPORT. MAY, STRÅNG DATA.....	183
	APPENDIX 12 - SIMULATION REPORT. MAY, E-ROOF.....	189

List of Figures

Figure 1 - Atmospheric greenhouse gas concentration over the last 2000 years [2].	2
Figure 2 - Global mean surface temperature, from 1880 to 2012,	2
Figure 3 - World total installed PV [4].	3
Figure 4 - Average annual growth rates of renewable energy capacity production	4
Figure 5 - Historical and projected global installed electrical generation capacities [7].	4
Figure 6 - Net power generation capacities added in the EU in 2013 [8].	5
Figure 7 - Installed PV capacity per habitant in Europe in 2013 [8].	5
Figure 8: Annually installed PV capacity in Norway in KWp [9].	6
Figure 9 - Renewable energy investments in 2012 classified by technology [6].	7
Figure 10 - PV price experience curve.	7
Figure 11 – LCOE for residential PV systems from Q2 2010 to Q2 2014 [12].	8
Figure 12 – LCOE development of residential PV systems by country .[12]	9
Figure 13 - LCOE for small (households), large (business partnerships) and utility size PV systems for different GHI values [1, 15].	10
Figure 14 - LCOE for sites in Sweden, Norway and Germany [18].	10
Figure 15 – LCOE projections for European countries. Red and green lines represent a 20 % and 15 % learning rate, respectively [19].	11
Figure 16: LCOE estimates for a 5 KWp PV system at the left followed by a 100 KWp system, and a1MWp system. Orange graphs are the expected cost. The blue and gray are the low and high estimates [21].	12
Figure 17 - Geographical location of the Acusticum PV system. Maps by Google.	14
Figure 18 - Arial photo by the roof the Acusticum PV system is built on.	14

Figure 19: Spectrum of solar irradiance at earth. At the edge of the atmosphere and at sea level compared to the ideal blackbody. Graph from Wikipedia.com. 17

Figure 20 - Illustration of the three radiation components hitting a collector surface. The direct beam, diffuse and reflected. (Albedo is reflection factor.) [26]. 17

Figure 21 - Solar spectrum at AM1, 1.5, 2, 3, 4 and 5. 18

Figure 22: Air Mass (AM) relative to the solar zenith angle [26]..... 18

Figure 23 – AM at Piteå for different times a year and day. Source: PVSYST v6.32..... 19

Figure 24 – Part of diffuse radiation received by an inclined collector surface 20

Figure 25 – Reflected radiance to collector..... 21

Figure 26 - The sun position at solar noon at different times a year..... 21

Figure 27 - Differences in length of a solar day 22

Figure 28 - The Analemma..... 22

Figure 29 – Sun path diagram for Piteå (top), Rome and Kampala (bottom) drawn by PVSYST v6.32..... 23

Figure 30: GHI is obtained by subtracting cloud attenuation from a clear-sky background [26]. 24

Figure 31: Irradiance components plotted for clear and cloudy periods as measured by pyrhemeters (A: DNI) and pyranometers (B: GHI; C: DHI). Corresponding images of the sky during a day below the graph. Site: Golden, Colorado, July 19, 2012 [26]. 26

Figure 32: World Radiation Data Centre radiation monitor stations world coverage [34].26

Figure 33: Baseline Surface Radiation Network stations [35]..... 27

Figure 34 – Ground irradiation measurement stations in Sweden [36]..... 27

Figure 35: World weather satellites orbiting earth [41]..... 29

Figure 36: Geostationary weather satellites from the United States, Germany, India, and Japan are shown [26]. 30

Figure 37 - Meteostat-9 13th October 2012 [42].....	30
Figure 38: Coverage of a polar orbiting satellite [26]......	32
Figure 39 - Comparison between the SolarGis model and actual measurements.....	34
Figure 40 - Monthly irradiation for Trondheim.	35
Figure 41 - Global irradiation estimates in Europe by PVGIS [57, 60].	37
Figure 42 - Global irradiation estimates in Norway from PVGIS [57, 60]......	38
Figure 43 - Yearly sum of GHI from Meteoronorm 7.2. Uncertainty of 8% [61]......	39
Figure 44: Ground measurement stations for the STRÅNG solar radiation model [63]. .	40
Figure 45 – Annual global irradiation development in Sweden [65]......	41
Figure 46 – Annual irradiation in Piteå. Comparison between six different irradiation models. Units in [kWh/m ² /year]......	42
Figure 47 – GHI composition in Hamburg.	43
Figure 48 – GHI composition in Braunschweig.	43
Figure 49 - Irradiation composition over the year for Piteå. Generated by PVSYST v6.32 from Meteoronorm 7.1 data.....	43
Figure 50 - Annual solar yield in St. Petersburg.	44
Figure 51 - Iso-transposition diagram for Piteå using Meteoronorm 7.1 data. Calculated by PVSYST v6.32.....	45
Figure 52 - Iso-transposition diagram for Piteå using Meteoronorm 6.1 data. Calculated by PVSYST v6.32.....	45
Figure 53 - Iso-transposition diagram for Piteå using NASA/SSE data. Calculated by PVSYST v6.32.....	45
Figure 54 - Best research-cell efficiencies [74].	48
Figure 55 - Flow of electrons due to an electrical potential difference [25].	49

Figure 56 - Illustration of photon energy and the crystalline silicon utilization of this for different wavelengths [75]..... 50

Figure 57 - Energy available in the solar spectrum for crystalline silicon based PV cells [76]. 50

Figure 58 - Utilization of the solar spectrum for different semiconductors with different band gaps [24]..... 51

Figure 59 - Plotting the IV-characteristic of a cell based on various loads [75]..... 51

Figure 60 - Original planned placement of the PV module on the Acusticum. Picture by Google Maps and illustration by Øystein Kleven [77]..... 53

Figure 61 – The PV system at the Acusticum. Photo taken from the tower to the west. Photo by Eirik Oksavik Lockertsen. 54

Figure 62 – Parts of the PV system at the Acusticum. Photo taken from roof I. Photo by Eirik Oksavik Lockertsen. 54

Figure 63 - Different IV-curve characteristics depending on solar irradiance [24]. 55

Figure 64 - IV-curves for different irradiation levels for the module used in later simulations. Data from PVSYST v6.32 database. 55

Figure 65 - Different IV curves for different cell temperatures..... 56

Figure 66 - IV-curves for different temperatures for the module used in later simulations. Data from PVSYST v6.32 database. 56

Figure 67 - Reduction in energy yield due to increase in temperature 57

Figure 68 - PV cell performance at STC and as a function of cell temperature 58

Figure 69 - Serial connected PV cells [24]. 60

Figure 70 - 36 cell solar module with associated IV-curve. 60

Figure 71 - The effect on the IV-curve with different number of bypass diodes..... 61

Figure 72 - The effect of shading on a thin film module 62

Figure 73 - Shading on vertical and horizontal mounted PV modules	63
Figure 74 - Near shading from a tree at roof A. Photo by Eirik Oksavik Lockertsen.....	63
Figure 75 - 3D model of the PV module layout and near shading at the Acusticum by Øystein Kleven and Eirik Oksavik Lockertsen.	64
Figure 76 - Beam shading factor for the Acusticum. The top illustration is all roofs except I and G, next is roof I, and the bottom illustration is roof G. Exports from PVSYST v6.32 based on Acusticum 3D model.....	65
Figure 77 - Shading due to soiling.....	66
Figure 78 - Shading due to frost.	66
Figure 79 - Thermography of shading due to soiling.....	66
Figure 80 - Snow on the roof of the Acusticum. Roof A is the largest roof in the picture. Shot at 9 th of February 2015. Photo by Øystein Kleven.....	67
Figure 81 - Operating points for a fixed resistance load at different insolation levels vs. MPP [75].	68
Figure 82 - Efficiency characteristic curves for different inverter manufactures.....	69
Figure 83 - Comparison of Euro and CEC efficient factors with two different inverters [24].	70
Figure 84 - Different grid connected inverter concepts.	71
Figure 85 - The inverters at the Acusticum. Photo by Eirik Oksavik Lockertsen.....	72
Figure 86 - The efficiency characteristic curves for SolarEdge SE17K [84].	73
Figure 87 - Number of hours of total irradiation for different insolation values in Piteå in a reference year [71]. PVSYST v6.32 and Meteonorm 7.1 database.....	73
Figure 88 - Shattered, severely bent, and minor bent modules at the Acusticum PV system. Photos by Eirik Oksavik Lockertsen.	76

Figure 89 – Snow covering PV modules at roof A. The shattered module is the 4th in the middle row. Shot at 27th of March 2015. Photo by Øystein Kleven. 77

Figure 90 – Snow accumulation difference on standard framed and frame-less modules [87].
..... 78

Figure 91 - An overview of different decision support software for PV systems 79

Figure 92 - Urban rooftop solar potential in Stockholm [88]..... 80

Figure 93 - Loss diagram of the expected energy output. Generated by PVSYST v6.32.. 84

Figure 94 - Loss factors for the expected energy output split into months. Generated by PVSYST v6.32..... 84

Figure 95 - Loss diagram of the expected energy output, but no near shading and loss due to soiling. Generated by PVSYST v6.32..... 85

Figure 96 - Loss diagram of the expected energy output, but no near shading and module tilt (48°) and azimuth (0°) to optimize energy production. Generated by PVSYST v6.32.
..... 85

Figure 97 - Loss factors for the expected energy output split into months, but no near shading and loss due to soiling. Corresponding to the loss diagram in Figure 95. Generated by PVSYST v6.32. 85

Figure 98 - Placement of the Acusticum temperature-, wind- and irradiance sensors. Photo by Eirik Oksavik Lockertsen..... 87

Figure 99 - The Acusticum wind- and irradiance sensors. Photo by Eirik Oksavik Lockertsen..... 87

Figure 100 - Acusticum loss diagram for May 2015 based on temperature-, wind- and irradiation data from the Acusticum sensors. 88

Figure 101 - Acusticum PV system inverter efficiency in May 2015. 89

Figure 102 - Acusticum PV system inverter efficiency in May 2015 for power input above 2 kW..... 90

Figure 103 - Acusticum loss diagram for May 2015 based on temperature-, wind data from the Acusticum sensors, and STRÅNG data for the irradiation.....	91
Figure 104 - Acusticum E-roof loss diagram for May 2015 based on temperature-, wind- and irradiation data from the Acusticum sensors.....	92
Figure 105 - In plane global irradiance (Azimut of 39° (ref south), and tilt of 27°) at the Acusticum 30 th of May 2015.	93
Figure 106 - Estimation of system LCOE in Germany for an increasing share of solar PV of the final electricity market. FLH is the full-load hour reduction of conventional electricity plants [102].....	100
Figure 107 - Not to scale validity of a few valuation estimate methodologies for investors vs. society.....	100
Figure 108 - PV module average retail price in 2012 currency [104].....	102
Figure 109: PV BoS cost breakdown. Global average and best practice [12].....	103
Figure 110: Residential PV system installation labor hours and cost in the US and Germany [105].....	105
Figure 111: Labor and cost of permitting, interconnection, inspection (PII) and incentive application in the US and Germany [105].	106
Figure 112 - PV system prices in European countries in 2011 currency [104].	107
Figure 113: PV system median price development for systems smaller than 10 kWp [105].	107
Figure 114: Residential PV system cost difference between Germany and the US in 2011 [105].....	108
Figure 115 - Estimated global average PV installation cost, 2009 to 2014 [12].	108
Figure 116 – Historical PV module degradation rates split by technology. The diamonds represents the mean and 95% confidence interval. [107].....	109
Figure 117 - The LCOE for the Acusticum PV system.	114

Figure 118 - The Acusticum LCOE sensitivity related to relative change in input parameters.....	116
Figure 119 - LCOE as a function of a variation in the load factor (5 % discount rate) [92].	117
Figure 120 - LCOE sensitivity for different discount rate for different technologies [92].	117
Figure 121 – Different LCOE scenarios for PV systems from 2010 to 2030 [113].....	118
Figure 122 - LCOE forecasts for different energy technologies [1, 15].....	119
Figure 123 - Different storage technologies for corresponding power system applications [93].	123
Figure 124 - Life cycle stages of crystalline PV system [117].	124
Figure 125 - Results of carbon footprints of Si-PV modules	125
Figure 126: Utilization of Italian pumped hydro storage and installed PV capacity [93].	128
Figure 127 – LCOE reduction for residential PV from Q2 2008 to Q2 2014 [12].	130
Figure 128 - Green certificates price development 01.2012 - 05.2015 [128].	131
Figure 129 - Forecasted Nordic spot price of base load power in real 2012 Euros	133
Figure 130 - Future bids for Nordic electricity in EUR/MWh. Data from Nordpool [130].	133
Figure 131 - Shift in merit-order and system price with the introduction of renewables	134
Figure 132 - Grid rent statistics for private households in Norway. Blue is grid rent for a household using 20 000 kWh, purple is tax and VAT, and line is prices in 2015 currency [131].	135
Figure 133 - Investment in the central grid. Historically and prognosis [132].	136
Figure 134 - Actual and projected energy demand during a single day in March from the California Independent System Operator Corporation (CAISO) [134, 135].	137

Figure 135 – Shift in the spot market price structure. Germany 2006-2012 [93].	137
Figure 136 – Net load and the impact of solar PV generation in Italy. Left: A sunny day in July 2012. Right: Simulated doubling of PV capacity [93].....	138
Figure 137 - Nordic and German average price of electricity in 2013 [136].	139
Figure 138 – LCOE for different energy technologies in Germany 2013 [1].	140
Figure 139 – The LCOE compared to the variable portion of electricity tariffs in selected countries [5, 133].....	142
Figure 140 - The population distribution in Norway as of 1st of January 2015 [137]. ...	142
Figure 141 - The influence on electricity demand and supply by a PV system on a office building in southern France [5].....	144
Figure 142 - Self-use and self-sufficiency shares by PV system size and consumer segment [5].	145
Figure 143 - Electricity consumption profiles for building types in Germany [3].	146
Figure 144 – PV system profitability for different rates of self-use [5]. Profitability index = $1 + \text{net present value}/\text{investment}$. A value over 1 means the project is profitable.	146

List of Tables

Table 1 - Yearly validation and interannual variability analysis.	34
Table 2 - Detailed Monthly irradiation for Trondheim.	35
Table 3 - Numbers of modules and their orientation on each roof at the Acusticum.....	53
Table 4 - Temporary shading loss factors.	67
Table 5 - Inverter setup on the Acusticum. The ratio is the module STC power divided by the rated power of the transformer [77].	74
Table 6 - PVSYST sub-array input.	81
Table 7 - Exchange rates used for calculations.....	101
Table 8 - CO ₂ -eq., NO _x and SO ₂ emissions from different sources of energy [123].....	126

1 Introduction

1.1 PV as a participant in the new energy system

The emission of greenhouse gases has increased dramatically after the industrial revolution as shown in Figure 1 and is an important reason for the observed increase in the global mean surface temperature shown in Figure 2. The research community is almost unanimous that the humane race have played, and are playing, a vital role in this context. The burning of fossil based fuel for the production of energy carries a lot of this burden.

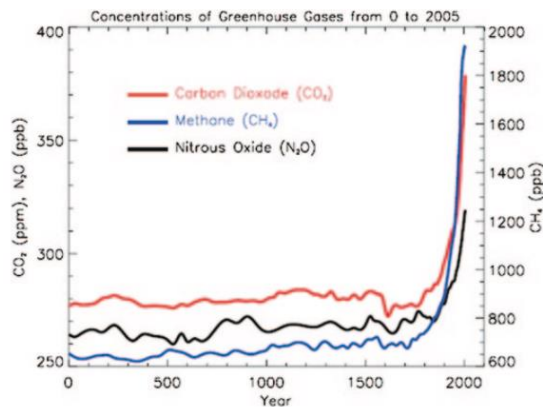


Figure 1 - Atmospheric greenhouse gas concentration over the last 2000 years [2].

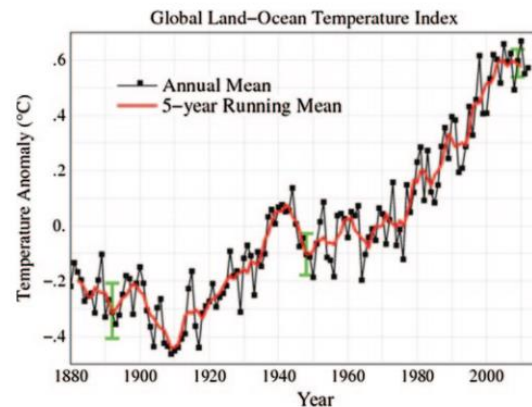


Figure 2 - Global mean surface temperature, from 1880 to 2012,

relative to the base period of 1951–1980 [2].

In order to move away from a fossil base energy source, efforts are put into the development and use of renewable energy sources (RES) in order to mitigate some of these emissions and make the shift to a path towards a sustainable future. The shift is not easy. The existing infrastructure is adapted for the use of easy to control and reliable power plants, largely based on fossil fuels.

RES, with the exception of water and bio, are uncontrollable and an unreliable, and is for several sources well suited for distributed generation. Mixed with the fact that electricity must be produced the moment, at least in the old system, one are facing some challenges.

World energy outlook: predicted an 80% increase in electricity demand between 2006 and 2030.

High shares of VRE is likely to necessary in order to reach the vision of a decarbonised electrical system future. (With it comes some challenges)

From 2010 to present it have been installed more PV capacity than the previous four decades. In 2013, new systems were installed at a rate of 100 MW of capacity per day. Early in 2014 the total installed PV system capacity overtook 150 GW [3]. At the end of 2014 this number had risen to 177 GW. These systems alone are expected to produce at least 200 TWh of electricity during 2015 [4]. The incremental yearly development per world region can be seen in Figure 3. By 2020 the installed PV capacity is expected to reach 400 to 515 GW [5].

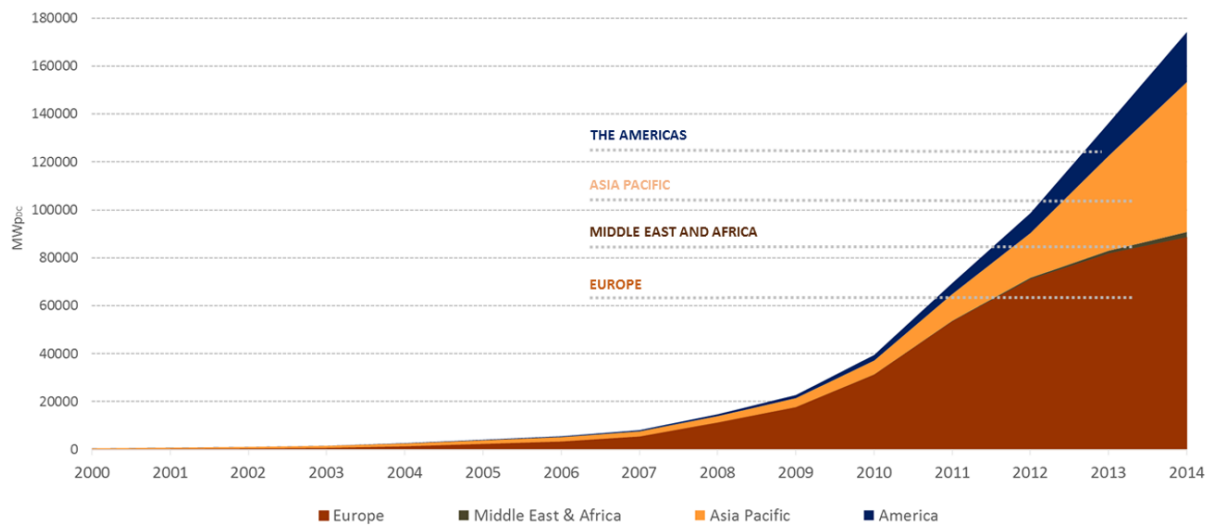


Figure 3 - World total installed PV [4].

When it comes to annual growth rates, no other renewables are even close as illustrated in Figure 4. For 2014, both China and the US had about 50 % increase in cumulative installed PV capacity, while Japan and the UK almost doubled their capacity. These are the top four countries for annual installed capacity in 2014 [4].

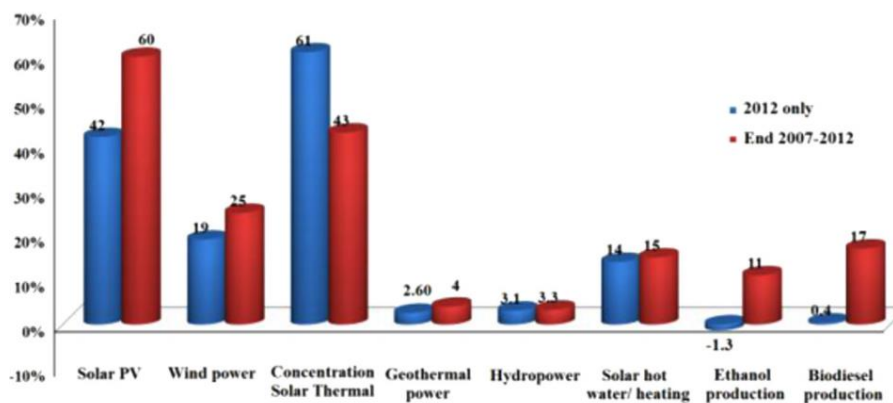


Figure 4 - Average annual growth rates of renewable energy capacity production , end-2007–2012 [6].

The PV share of the total world electricity market is still very small as illustrated in Figure 5. The prospects for growth are though good. In the 2014 IEA Technology Roadmap for Solar PV Energy, they updated their 2010 envisioned PV share of the global electricity composition in 2050 from 11% to 16% in just four years [3]. If their envisioned PV share continue to rise with about 50% every four year, they will not envision any other source of electricity than PV in 2025.

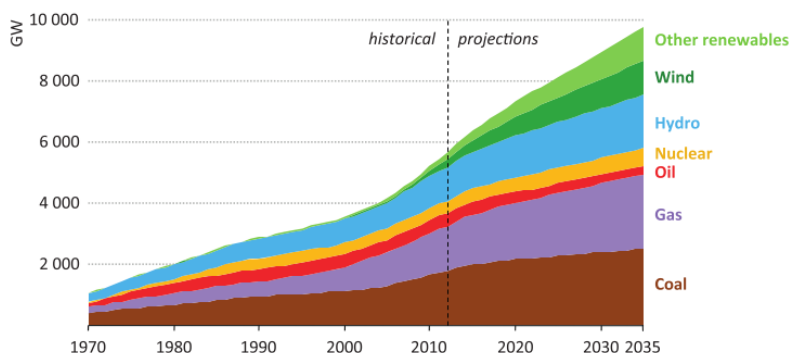


Figure 5 - Historical and projected global installed electrical generation capacities [7].

Looking at the net power generation capacities added in EU in 2013, no other energy source are even near PV and wind. In fact, fuel oil, gas and coal is instead in recession. The EU is definitive moving in the right direction.

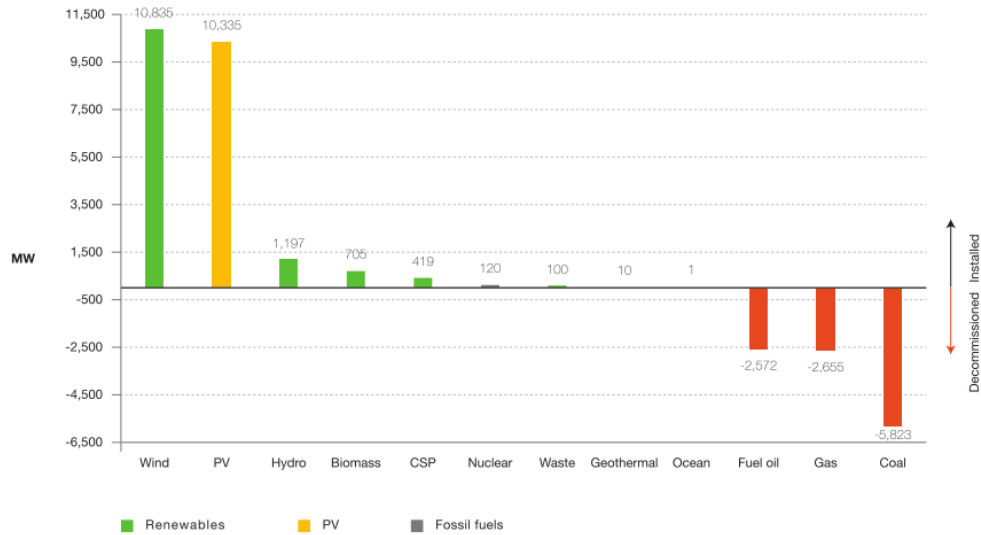


Figure 6 - Net power generation capacities added in the EU in 2013 [8].

When it comes to Norway, it is somewhat special as most of its electricity comes from renewable hydro already. Because of this, the incentive to invest in other RES. This becomes very clear when comparing the installed PV capacity per habitant to the rest of Europe as seen in Figure 7.

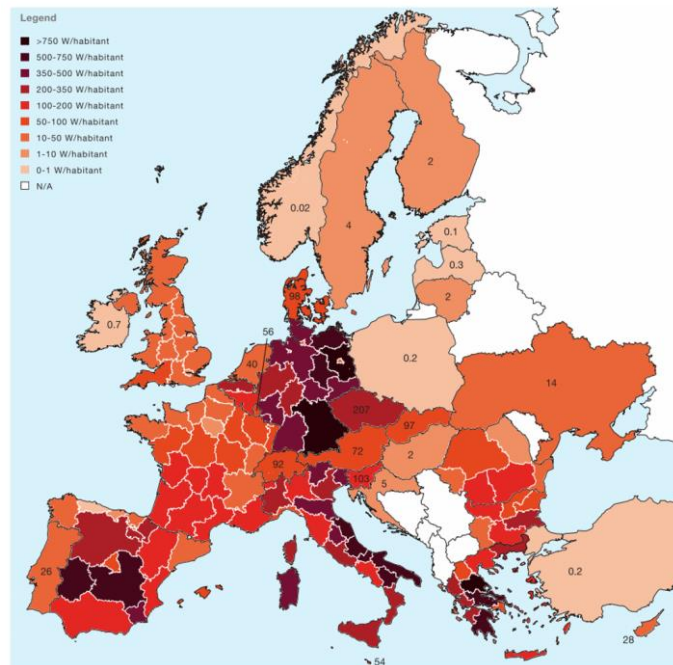


Figure 7 - Installed PV capacity per habitant in Europe in 2013 [8].

However, 2014 might represent a turning point for the PV industry in Norway. Not only was it installed over three times as much PV capacity compared to the earlier top year in 2013, but 1.42 of the 2.24 MW_p of capacity was grid connected. The earlier best year, also 2013, this number was 0.10 MW_p [9]. Though, still some distance from the annual installed capacity of about 7 500 MW_p Germany had in 2010, 2011 and 2012 despite more inhabitants [8].

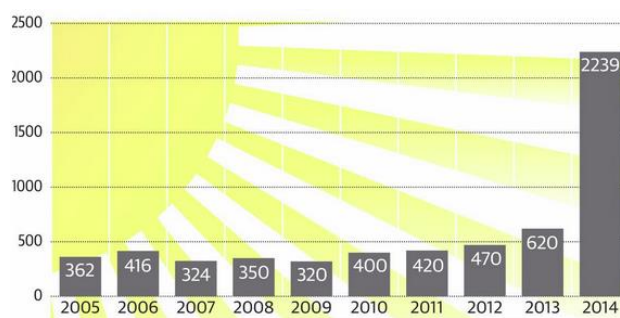


Figure 8: Annually installed PV capacity in Norway in KW_p [9].

1.2 The cost of PV electricity

The PV system prices have been divided by three in the last six years in most markets [3]. The price has followed an almost perfect exponential downwards curve the last four decades as seen in Figure 10, and there are no signs of a stall in this development. The global investment in the solar industry was bigger than all of the other renewable sectors combined in 2012 as seen in Figure 9.

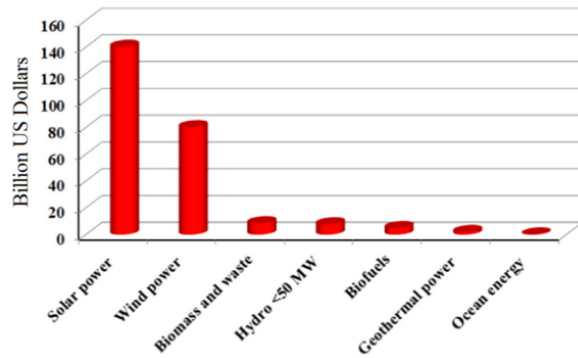


Figure 9 - Renewable energy investments in 2012 classified by technology [6].

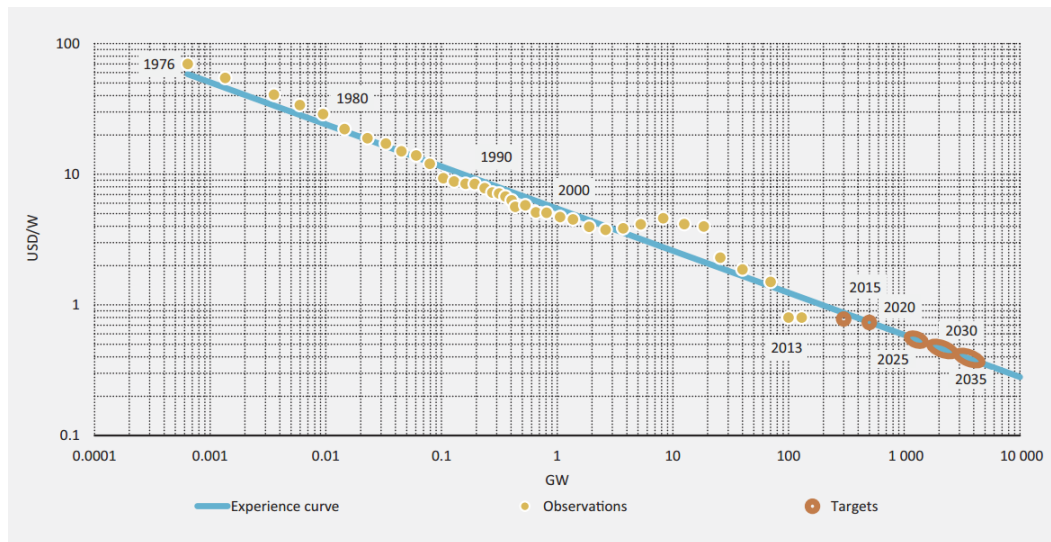


Figure 10 - PV price experience curve. Yellow dots indicate past module prices, orange dots are expectations and the oval ones are predictions [10].

In order to go from the module investment prices to an energy price, it has become common to use the levelized cost of electricity (LCOE). The LCOE is the expected total lifetime cost of the PV system levelled out over the total expected electricity production. It describes the total lifetime production cost as a per kWh unit, making it comparable to other electricity generating technologies. More details in the LCOE methodology chapter at 3.1.

Reinchelstein et al. (2013) found a LCOE of 0.122 USD/kWh in the US for a commercial-scale best case scenario in the fourth quarter of 2011. They include a tax effect where new solar installations get a 30% Investment Tax Credit (ITC) and the 5-year accelerated depreciation schedule. The removal of these tax incentives would raise the LCOE by about 75%. Despite of this, they conclude that commercial-scale PV will reach grid parity within a decade, even without the tax subsidies. In favourable scenarios they already are. However, they also concludes that PV will not be cost competitive in many northern locations, including Germany, for decades. [11].

According to statistics from the International Energy Agency, the average LCOE of utility-scale PV has been cut in half from 2010 to 2014 as illustrated in Figure 11. The best projects are now delivering electricity for USD 0.08/kWh without financial support. Projects with an estimated LCOE of down to USD 0.06/kWh are now being realised [12].

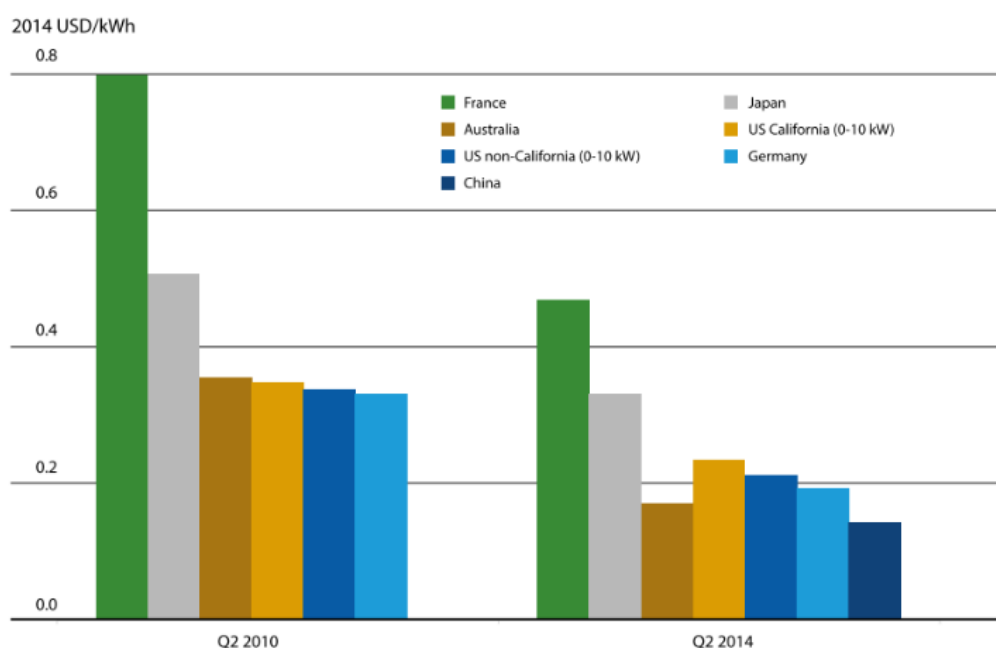


Figure 11 – LCOE for residential PV systems from Q2 2010 to Q2 2014 [12].

Looking more closely to residential PV systems, the average LCOE fell from above 0.3 USD/kWh in 2010 to half of this in 2014 as seen in Figure 12.

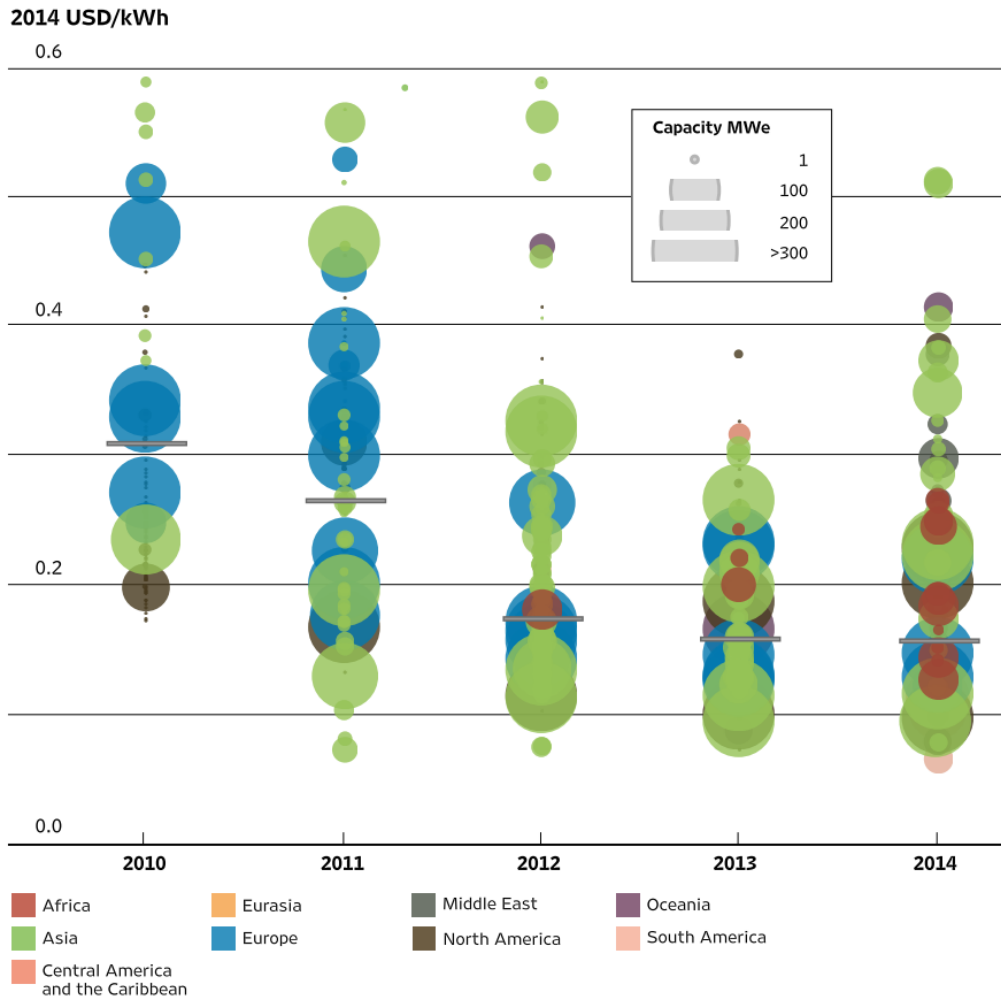


Figure 12 – LCOE development of residential PV systems by country .[12]

In late 2014, Brazil announced the results of the auction of 20 year power supply contracts which is due start to deliver 1st of October 2017. Projects in a total of 889.7MW was auctioned with an average price of R\$215.12/MWh. With today's currency rates, this equals to about 0,087 USD/kWh or €69/MWh [13, 14].

Moving into Europe, the Fraunhofer Institute for Solar Energy presented in 2013 statistics for the German PV marked, showing remarkable PV LCOE for the relatively low levels of solar energy compared to places where the sun is more prominent as seen in Figure 13. In fact, Kost et al. (2014) concluded that electricity produced from all types of PV power plants, form household size to utility size, are beneath the average household price of

electricity in Germany. Even in Northern Germany where highest priced PV electricity from household systems are between 0.12 and 0.14 EUR/kWh [15]. What is interesting is that these levels of solar energy is in line with southern parts of the Scandinavian Peninsula.



Figure 13 - LCOE for small (households), large (business partnerships) and utility size PV systems for different GHI values [1, 15].

Going back some years to 2006 in Sweden, Swedish Elforsk found a LCOE of 8.2 SEK/kWh for an 11 KW PV system and 4.3 SEK/kWh for a 64 KW PV system, both in Malmö. Predicting a LCOE of 0.45 SEK/kWh for 2020 [16]. The findings in 2006 was however study was already outdated when it was published because the development went so fast [17].

In 2011 Good et al. conducted a LCOE calculation for Piteå where a LCOE of 0.27 EUR/kWh was found for an optimal fixed system with Mono-Si modules illustrated in [18].

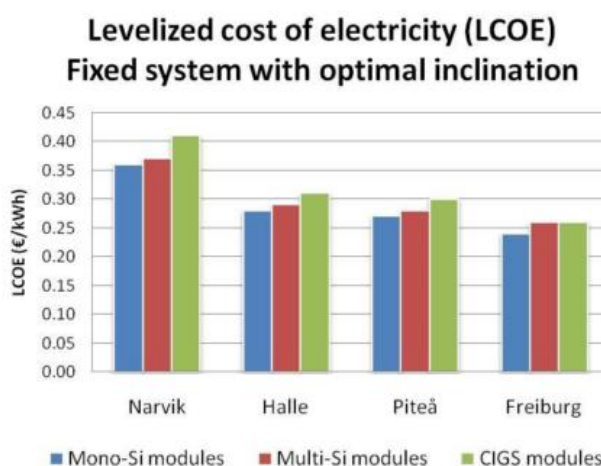


Figure 14 - LCOE for sites in Sweden, Norway and Germany [18].

In 2013 Breyer and Gerlach conducted a global overview on when the LCOE reaches the price paid by the consumers. Their result for Europe can be seen in Figure 15. The LCOE is quite in line with the findings of Good et al. in 2011. Also, an interesting observation is that the whole PV LCOE range for private households in 2016 in Norway are lower than the total price of electricity from the grid.

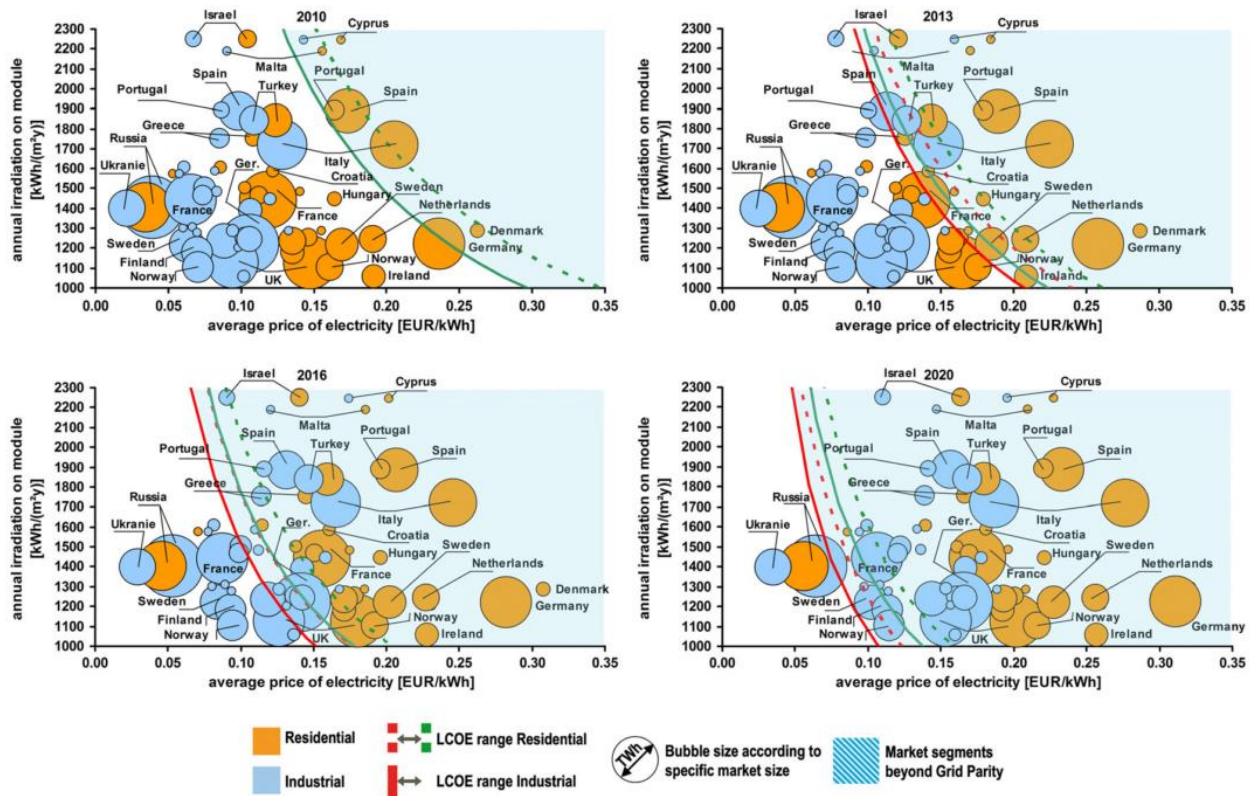


Figure 15 – LCOE projections for European countries. Red and green lines represent a 20 % and 15 % learning rate, respectively [19].

Multiconsult, on assignment from Enova SF, conducted a cost study for PV in Norway in 2013. They found a LCOE in the range of 2.2 to 3.0 NOK/kWh for an average 7 kW_p PV system dependent on the geographical location of the system. The LCOE range for a 100 kW_p system was found to be between 1.8 and 2.6 NOK/kWh [20].

In 2015 NVE published “Costs in the energy sector” (based on the Enova report) where the expected LCOE for residential houses (5 kW_p) was in the range of 1.5 to just below 2

NOK/kWh depending on the geographical location. The low estimate for Kristiansand was about 1.2 NOK/kWh. For larger PV systems (100 KWp) the expected LCOE was in the range of just below 1.5 NOK/kWh to about 1.9 NOK/kWh. The low estimate for Kristiansand was just above 1 NOK/kWh [21].

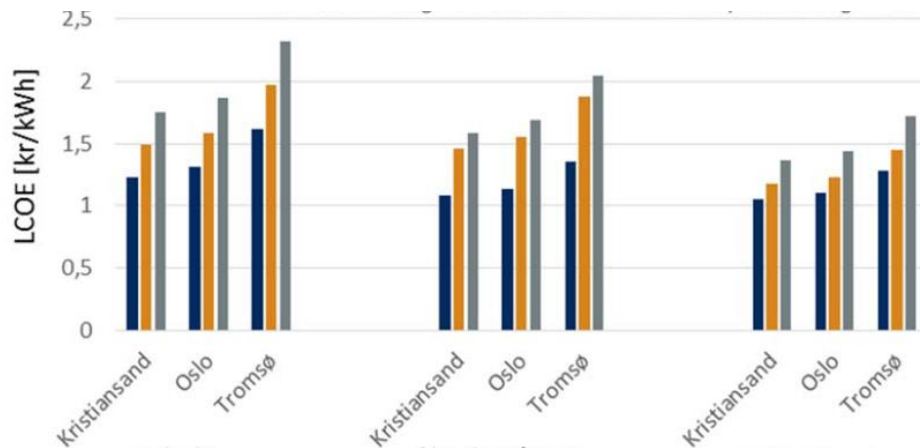


Figure 16: LCOE estimates for a 5 KW_p PV system at the left followed by a 100 KW_p system, and a 1 MW_p system. Orange graphs are the expected cost. The blue and gray are the low and high estimates [21].

Even though the above numbers differs in assumptions and preconditions used, they all indicate that PV solar energy is, or are soon to be, competing in the electricity market without subsidies. With the current rate of cost reduction PV solar energy is experiencing, it will move past other electricity sources rather fast. The CEO of Statnett, Auke Lont, also stated at their annual autumn conference in 2014 that the rapid price reduction of power from PV is one of the big coming game changers [22].

Almost all of the world installed PV capacity is at latitudes south of Norway. Although still few, an increasing number of reports and papers exists on PV for Norway. However, no reports exists having described more closely the factors affecting PV northern latitudes related to the cost of solar electricity.

1.3 Thesis problem formulation

The question this thesis is going to try to give an answer to is;

What is the performance and potential for PV systems in northern latitudes?

As the performance is vital for the PV system potential, and of special interest for northern latitudes, this will be the primary focus. As a case for this a 236 kW_p PV installation in Piteå, Sweden will be used. The performance of this installation will be analysed and compared to simulations. In order to find the potential for PV systems, the Levelized Cost of Energy (LCOE) will be calculated with the basis in the same installation in order to find the direct cost associated with a PV system, comparable to other electricity generating technologies. With the LCOE as a basis, the investment profitability in Norway will be discussed by taking into account costs and revenues not included in the LCOE.

1.4 The Acusticum PV system in Piteå, Sweden

The Acusticum PV system is owned by Pite Energy and built by Solbes at the end of 2014 on the roof of the department of Art, Communication and Learning located in Piteå, but part of the Luleå University. Co-located with the concert hall named Studio Acusticum. It is located in north of Sweden, just under the arctic circle at 65.304N 21.478E. Map of the location of the Acusticum PV system and the roof it is mounted on can be seen in Figure 17 and Figure 18.

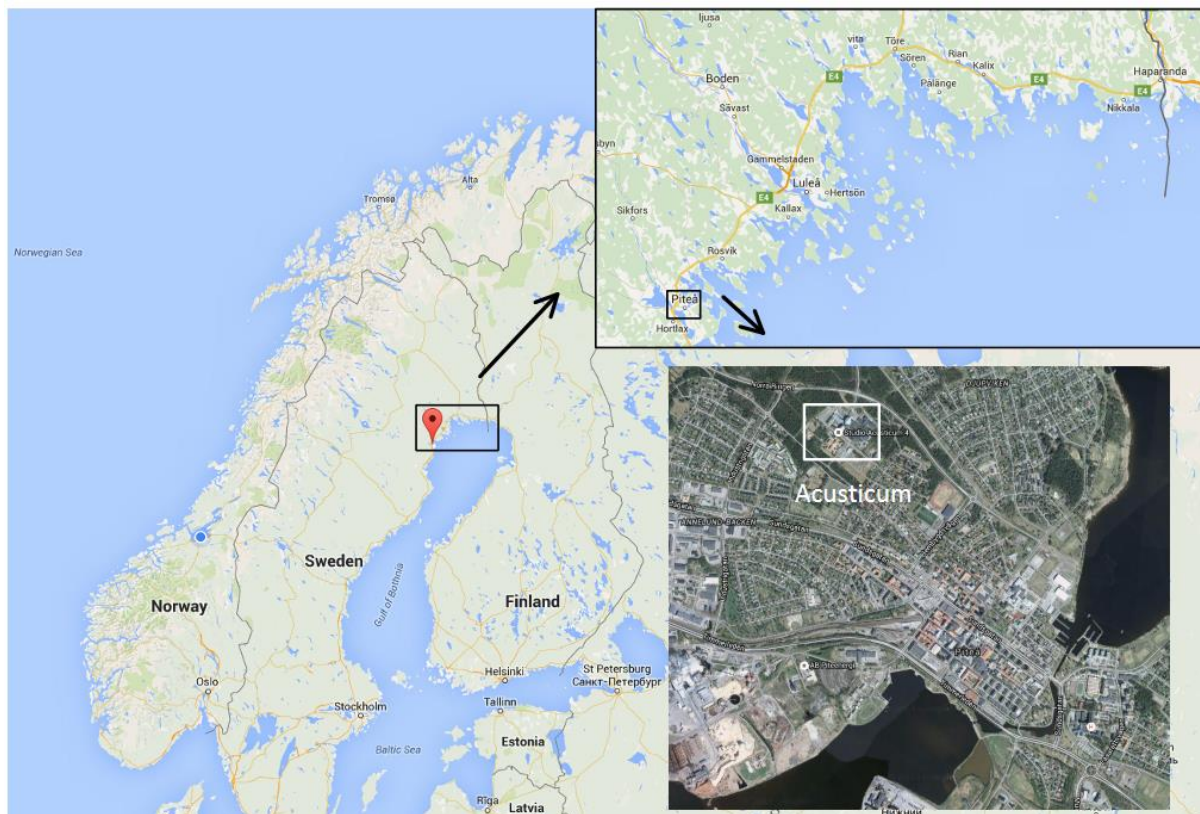


Figure 17 - Geographical location of the Acusticum PV system. Maps by Google.

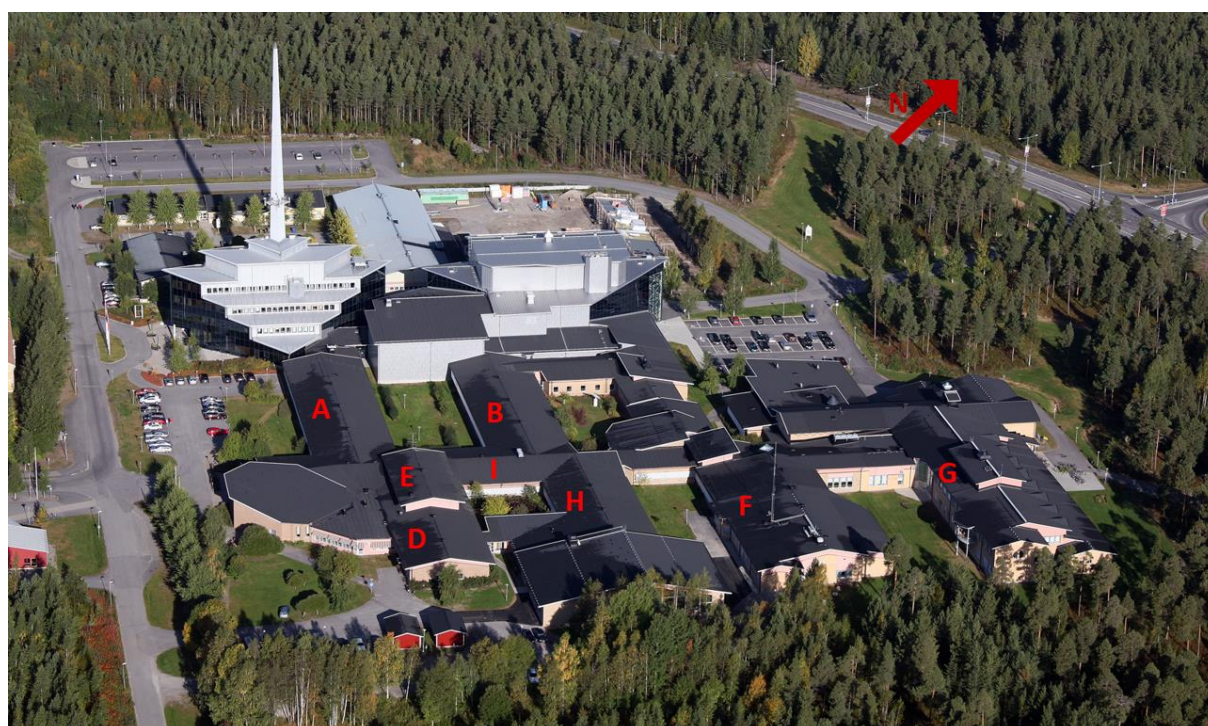


Figure 18 - Aerial photo by the roof the Acusticum PV system is built on.

1.5 Limitations, delimitations and assumptions

Northern latitudes is limited to Norway and Sweden mainland.

As Acusticum PV system is just built data availability is scarce, meaning only one month of data will be compared to simulations

Other Limitations, delimitations and assumptions will be given in each chapter.

1.6 Thesis outline

In order to answer the problem formulated, the first chapter will be answering the question regarding the performance of PV systems in northern latitudes by assessing the solar energy potential for PV systems, and particular for the Acusticum PV system

Chapter two is designated to the calculation of the levelized cost of energy of the Acusticum PV system.

Chapter three is looking at the LCOE environment, more precisely the investment profitability in Norway. Discussing cost elements beyond the scope of the LCOE methodology and the revenues, both in a Norwegian setting.

Chapter four presents a short summary of the findings, gives some recommendations on future actions to be taken to ensure the possibility and validity of further measurements, and some suggestions on further reading is presented at the end.

2 The solar energy potential at Northern Latitudes

To assess the solar energy potential at Northern Latitudes a large numbers of variables have to be assessed. Each section first in a generic term, then assessed more closely with regards to northern latitudes, and towards the end of this chapter down to Piteå and the PV system at the Acusticum. The city of Rome in Italy will also in some cases be used for comparison purposes.

First the sun as a resource, from the energy origin to a given point on earth, will be assessed. Next, the different elements concerning the quality of solar energy sources will be discussed and also illustrated with the different solar potential assessments for Piteå. Further the PV system itself and direct influencing factors will be evaluated. From this a simulation model will be made and the expected energy production from the PV system at the Acusticum will be assessed. At the end of this chapter on solar energy potential at northern latitudes a comparison between the simulated expected vs the actual energy production in May 2015 will be made.

2.1 The sun as a resource

To describe the sun as a resource, first the actual power from the sun itself will be illustrated. Next, the different components making up the solar power at sea level will be described, and last you will be taken through the geometry regarding the sun path as seen from a point on earth.

2.1.1 Power from the sun to the earth's atmosphere

The sun continuously radiates about 3.846×10^{26} W of power [23]. Only a small fraction of this hits the Earth, and the power per unit area naturally decreases by increasing distance. Because the earth's orbit is elliptical, the distance to the sun varies between 147 and 152 million km. This is one of the reasons that the radiance fluctuates between $1,325$ W/m² and $1,420$ W/m² at the edge of the earth atmosphere [24, 25]. The yearly average is called the solar constant (SC) and is $1,367$ W/m² [23-25].

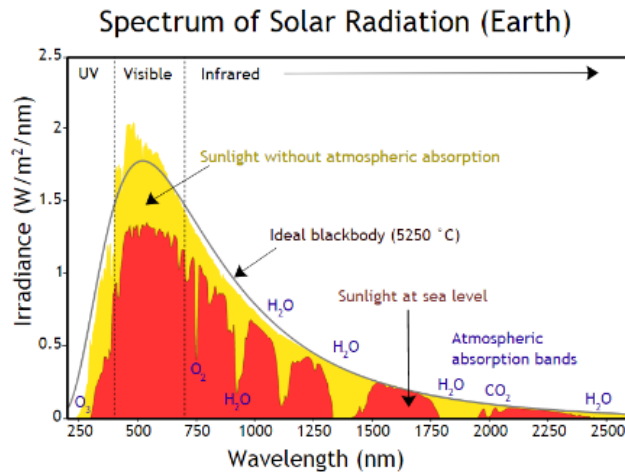


Figure 19: Spectrum of solar irradiance at earth. At the edge of the atmosphere and at sea level compared to the ideal blackbody¹. Graph from Wikipedia.com.

2.1.2 The power from the sun at sea level

The power from the sun at sea level are made up by three components. The direct-, diffuse- and the reflected components [25]. This is illustrated in Figure 20. These components are described more closely in the next three sections. The total power from the sun on an object is referred to as the Global Irradiance.

Be aware that the literature on the sun are not consistent in the terminology used in describing the power, and later energy, from the sun. In this thesis “radiance” will be used to describe the power from an object, and “irradiance” the power on an object.

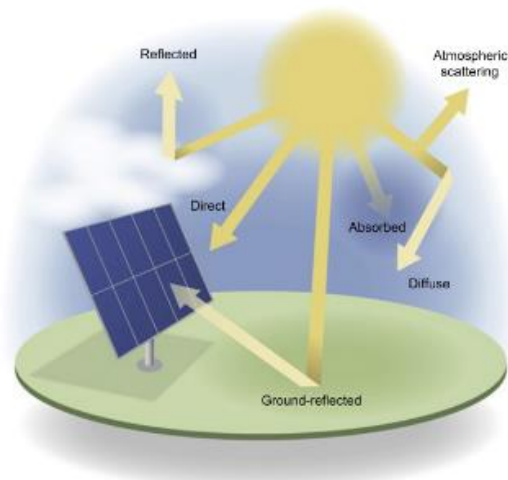


Figure 20 - Illustration of the three radiation components hitting a collector surface. The direct beam, diffuse and reflected. (Albedo is reflection factor.) [26].

¹ The ideal blackbody is the theoretical radiance spectrum of an object that emits or absorbs power through radiance.

2.1.2.1 Direct irradiance

As the sun's radiance passes through the earth atmosphere, the power is reduced. If we for now do not take the weather into account, this is due to reflections in the atmosphere, absorption by molecules in the atmosphere, scattering of molecules and scattering from impurities in the air [23, 24]. The result is a lower and different solar spectrum at the earth surface than at the edge of the atmosphere. Because earth position relative to the sun always shifts, so does the amount of air the radiance have to travel through to get to a given point at the surface. The relationship between the inclination of the sun to a given point at earth is called the air mass ratio (AM). When the sun is perpendicular to the Earth we have $AM=1$, noted AM1. In comparison, we say that we have AM0 at the edge of the atmosphere. For different elevation angles, we naturally get different spectrums at different AM as seen in Figure 21. An AM1.5 is often assumed as an average solar spectrum for the earth's surface.[23-25]. For AM1.5 the direct irradiance is 835 W/m^2 [23].

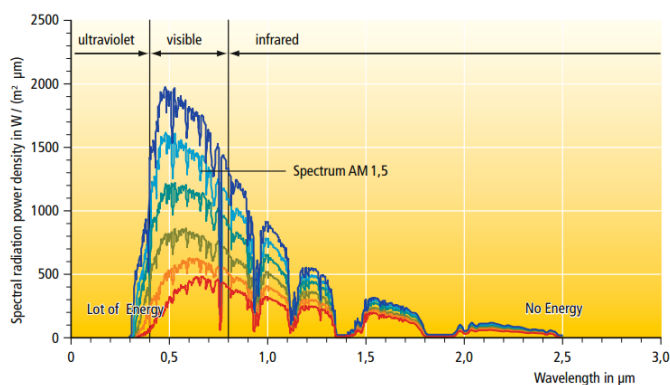


Figure 21 - Solar spectrum at AM1, 1.5, 2, 3, 4 and 5. [24]

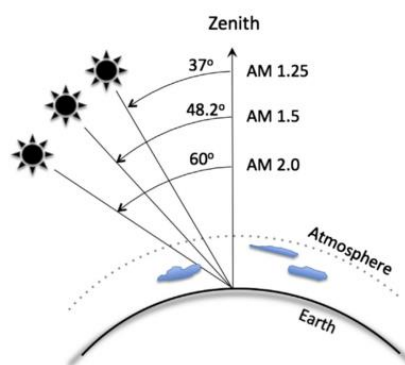


Figure 22: Air Mass (AM) relative to the solar zenith angle [26].

For northern latitudes the AM is for large periods of the year and day above 1.5 as seen in Figure 23, and AM1.5 is most likely a too low estimate for northern latitudes. However, this is accounted for in most simulation software used for energy calculations as illustrated in Figure 23.

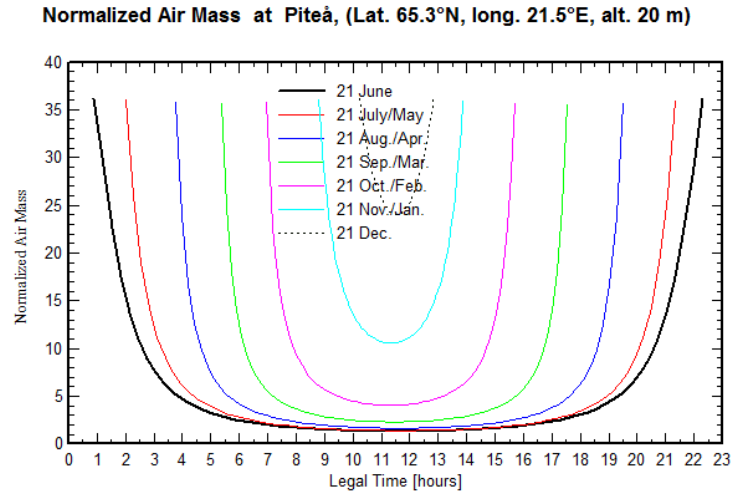


Figure 23 – AM at Piteå for different times a year and day. Source: PVSYST v6.32

The direct irradiance is often referred to as direct normal irradiance with its abbreviation DNI. “Normal” because it is the power from the solar beam itself on a surface perpendicular to the incoming beam.

2.1.2.2 Diffuse and global horizontal irradiance

As the radiance travels through the atmosphere, some of the direct radiance gets scattered. A good approximation is that one can assume that the radiance gets scattered equally in the atmosphere, and thereby that the diffuse radiance arrives to a given surface with equal intensity from all directions [25]. For a horizontal collecting surface, this means it will receive all available insolation from the diffuse radiance. How much the incoming radiance is diffused is dependent on the composition of the atmosphere. There among the weather.

The Diffused Horizontal Irradiance is often referred to by its abbreviation DHI. For a horizontal surface the total irradiance is referred to as the Global Horizontal Irradiance (GHI) [23] and is

$$GHI = DHI + DNI \cos \beta \quad (1)$$

which corresponds to the formulation used in [27-30]. How much each of these two parts contribute to the GHI is dependent on the specific site of measurement.

Even though the irradiance at AM1.5 is 835 W/m^2 as mentioned in chapter 2.1.1, the total horizontal irradiance have been measured at values up to 1300 W/m^2 [23]. This is because of the addition of the diffuse radiance component. Some literature uses the notation AM_D and AM_G to separate the direct and global, but most do not as it is double communication when the GHI and DNI is already given.

For an inclined non-moving surface, it will only receive the diffuse radiance from the part of the sky that is visible from the surface as illustrated by Figure 24 [25].

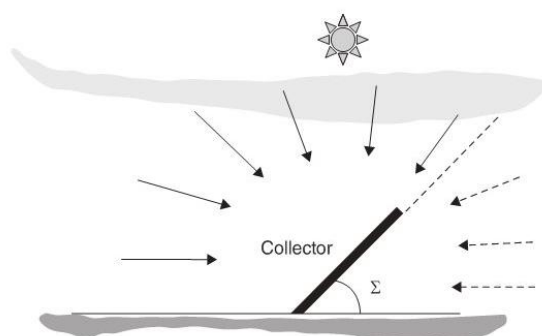


Figure 24 – Part of diffuse radiation received by an inclined collector surface [25].

2.1.2.3 Reflected irradiance

The third component of total insolation on a collector surface is the radiance that is reflected by the ground surface hitting a collector surface. Both the direct beam radiance and the diffuse radiance is reflected. The ground's ability to reflect the radiance is described by a fraction between zero and one and is called the albedo [24]. Typically an albedo of 0.2 is used as it represents i.e. grass. An albedo of 0.8 is fresh snow [24, 25]. This means that the amount of irradiance on a surface can almost be doubled in areas where there is snow present and the collecting surface is inclined optimal for this. As illustrated in Figure 25, reflected radiance is from both diffuse and direct beam component.

The importance of the reflected irradiance is of course increasing with the latitude.

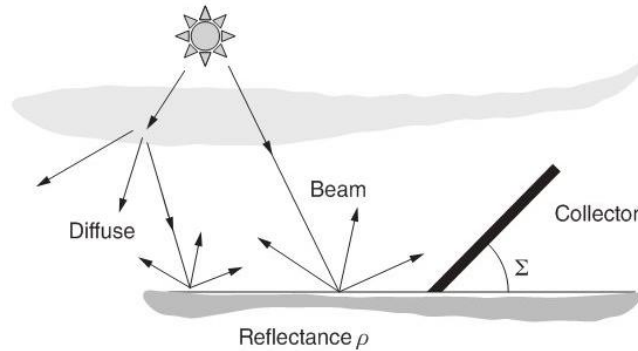


Figure 25 – Reflected radiance to collector [25].

2.1.3 The sun's path as seen from a point on earth

The solar position changes all day and all year. To have a reference point it is common to use the time when the sun is at its highest. This happens at the northern hemisphere at solar noon June 21st or 22nd, depending on the point on earth, at all other dates the sun will have a different declination as shown in Figure 26.

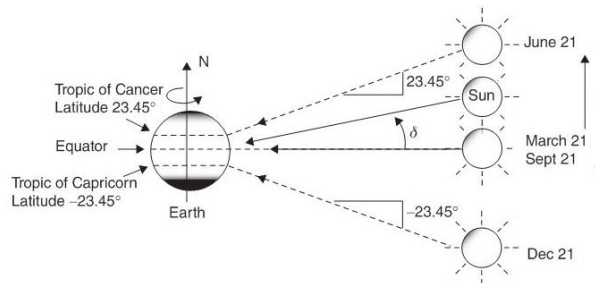


Figure 26 - The sun position at solar noon at different times a year [25].

As solar noon is the time when the sun reaches its highest elevation angle at a given point at Earth, this means of course that solar noon and clock noon only is the same at 24 longitudes on earth. All other longitudes it will have a relative difference. One differentiates between solar time (ST) and clock time (CT) where ST is related to the solar position, and CT is related to the given time zone on earth.

In addition, the solar noon changes along the year because the length of a solar day changes along the year. This again is a result of the earth's elliptical orbit [25]. This is illustrated in Figure 27.

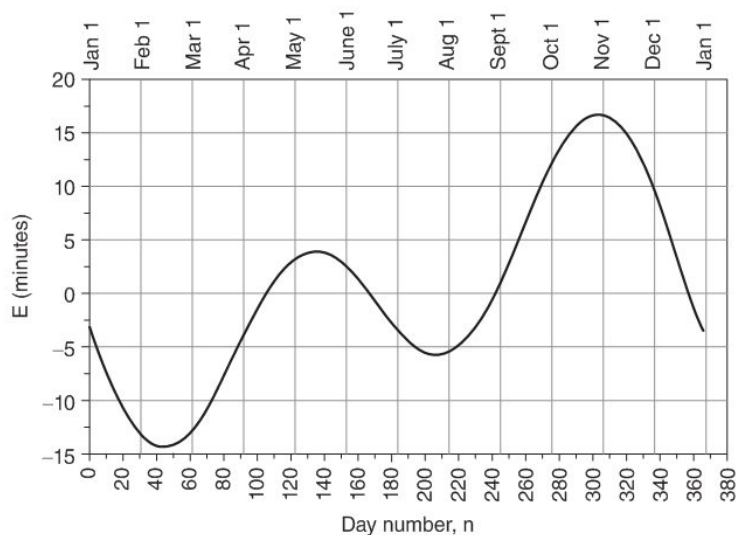


Figure 27 - Differences in length of a solar day relative to a 24h day along a year [25]

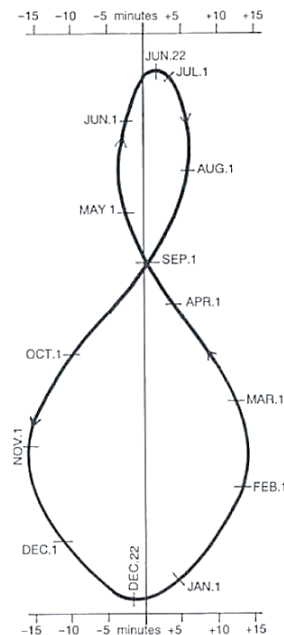


Figure 28 - The Analemma. The solar angle at a given clock time vs solar time plotted for a year [31].

Another way of plotting the equation of time is through what is known as the analemma [31]. See Figure 28. This is a more visual way of showing the difference between a solar day and a clock day, and will be recognized in the sun path diagrams below.

The sun's position plotted in time for a given location results in unique sun path diagrams. Three examples are shown on the following page in Figure 29. The examples are from Piteå at 65.3°N, Rome at 41.8°N and Kampala at 0.3°N. The higher share of the reflective component in global irradiance at northern latitudes is illustrated quite well in this comparison.

Sun path diagrams are particularly useful in order to take into account shading on a collector surface.

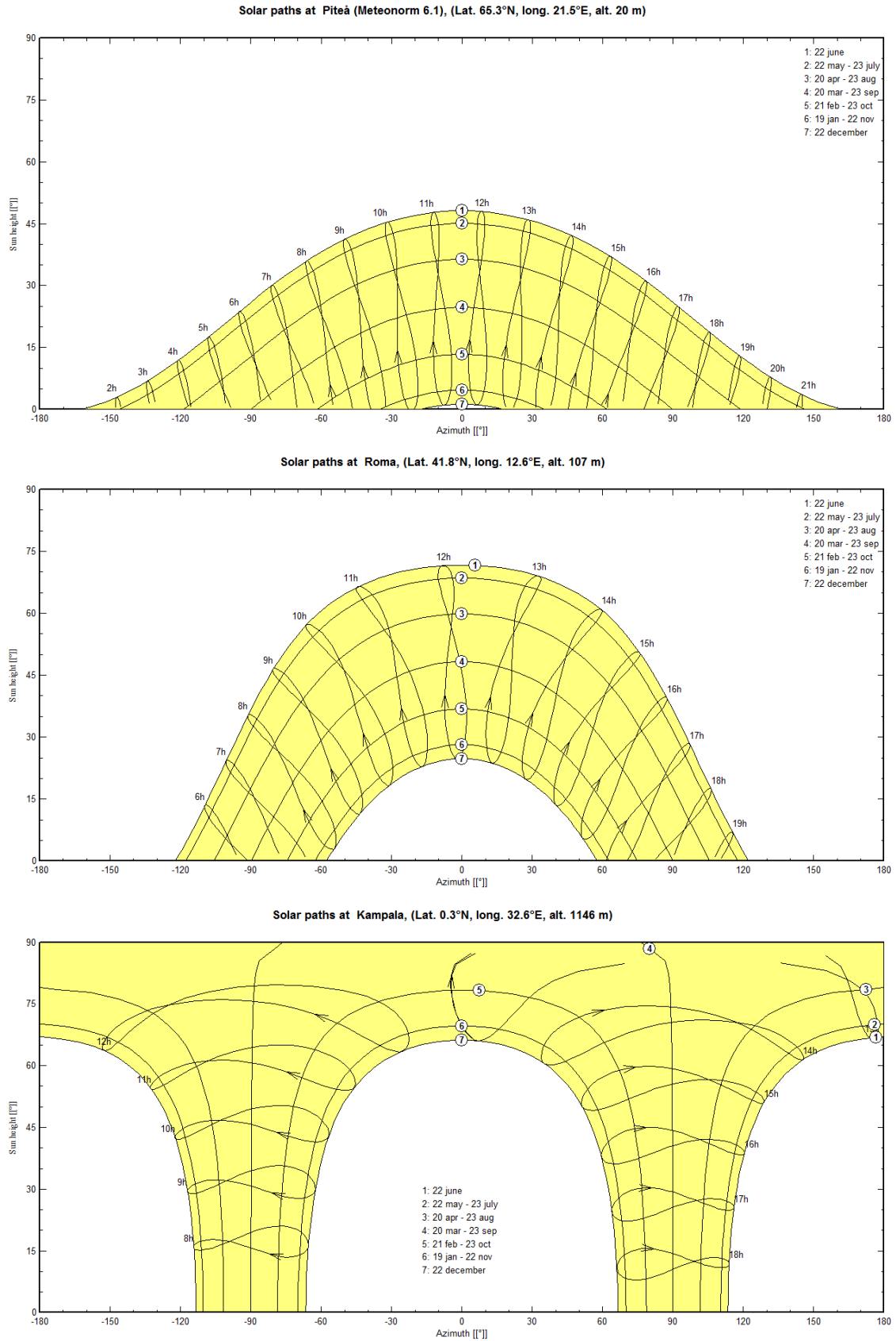


Figure 29 – Sun path diagram for Piteå (top), Rome and Kampala (bottom) drawn by PVSYST v6.32.

2.2 The quality of solar energy data sources (at northern latitudes)

As the immediate irradiance on a surface on earth is of interest especially for the dimensioning of PV equipment, the yield within a given timeframe is more suitable for the overall system analysis. It is also impossible to model the irradiance under varying condition as the weather continuously influences the irradiance as illustrated in Figure 30. So, instead of referring to the irradiance, the power from the sun reaching the surface, a more convenient measurement is irradiation, the energy reaching the surface within a given time interval.

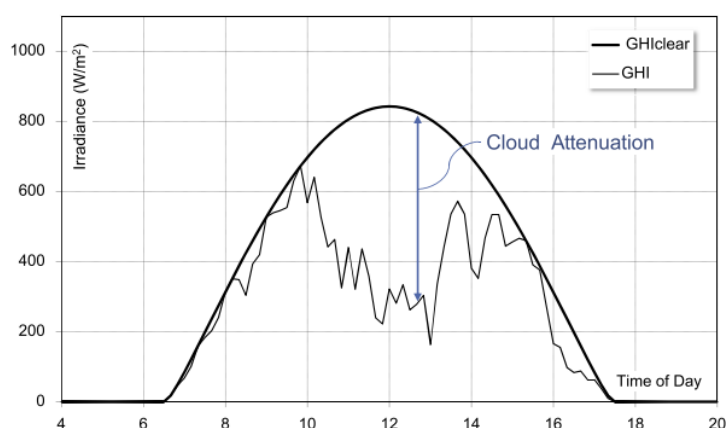


Figure 30: GHI is obtained by subtracting cloud attenuation from a clear-sky background [26].

As earlier mentioned, the literature on solar energy is not consistent in the use of the terms related to the power and energy from the sun. I.e. irradiance vs. irradiation, and radiance vs. radiation. Both used for both power and energy. GHI is referred to as both Global Horizontal Irradiance and Global Horizontal Irradiation. The inconsistency is the case also for reputable authors like the IEA. For this thesis the abbreviations for GHI, DNI and DHI is used for both power and energy. The separation is by the units used. Please refer to the section on important terms and expressions in the start of this thesis for details.

To assess the quality of solar energy data sources for northern latitudes, first a description of different methods for measure and modelling the surface irradiation is done. Next some

of the most used databases for solar irradiation is evaluated with regards to validity in northern latitudes. These are then used to assess the unshaded solar potential in Piteå. Last a discussion on irradiation composition impact on optimal solar collector orientation is done.

2.2.1 Measurements and modelling of surface irradiation

Several models have been constructed with the aim of predicting the annual solar energy yield around the globe. However, the modelling is difficult because of very different atmospheric conditions, mainly the weather, which naturally changes by both time and place [32]. Even though the weather have been an important factor for most likely the entire human history, the actual irradiation level measurements and predictions has a short history as the demand for irradiation data have been low. The increasing use of solar energy increases the demand for accurate irradiation data as the market increases and the profit margins of the investments becomes smaller.

The weather data can be measured and modelled in several different ways. One of the most important component to calculate the solar energy yield is the irradiation. Irradiation estimation is done mainly by ground measurements but also by satellites. These, and briefly some other methods for irradiation calculations, are described in the following chapters.

2.2.1.1 Ground measurements

Data from ground sources are preferred as they represent the actual conditions for the potential solar energy system, but they are difficult to obtain. For the data to be reliable it has to be collected in a rigorous manner with well-maintained and calibrated instrumentation [26]. In order to get the highest precision measurements for solar radiance, a pyranometer for GHI, a pyrhelimeter for DNI and a pyranometer coupled with a shade disk for DHI is recommended [30]. Their associated margin of error are; thermopile pyrhelimeter $\pm 2.8\%$, thermopile pyranometer $\pm 4.0\%$ and photodiode pyranometer $\pm 7.6\%$ [26]. An example of a measurements during one day can be seen in Figure 31.

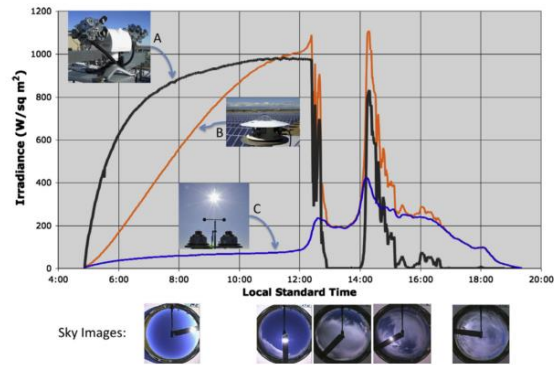


Figure 31: Irradiance components plotted for clear and cloudy periods as measured by pyrbeliometers (A: DNI) and pyranometers (B: GHI; C: DHI). Corresponding images of the sky during a day below the graph. Site: Golden, Colorado, July 19, 2012 [26].

There are two large worldwide surface radiation networks operation today: World Radiation Data Centre (WRDC) and Baseline Surface Radiation Network (BSRN) [33].

The WRDC is a part of the World Meteorological organization. The coverage in mainland Europe is quite good, but they only have one station in Norway: Bergen. There are 16 stations in Sweden, and Finland has five [34].

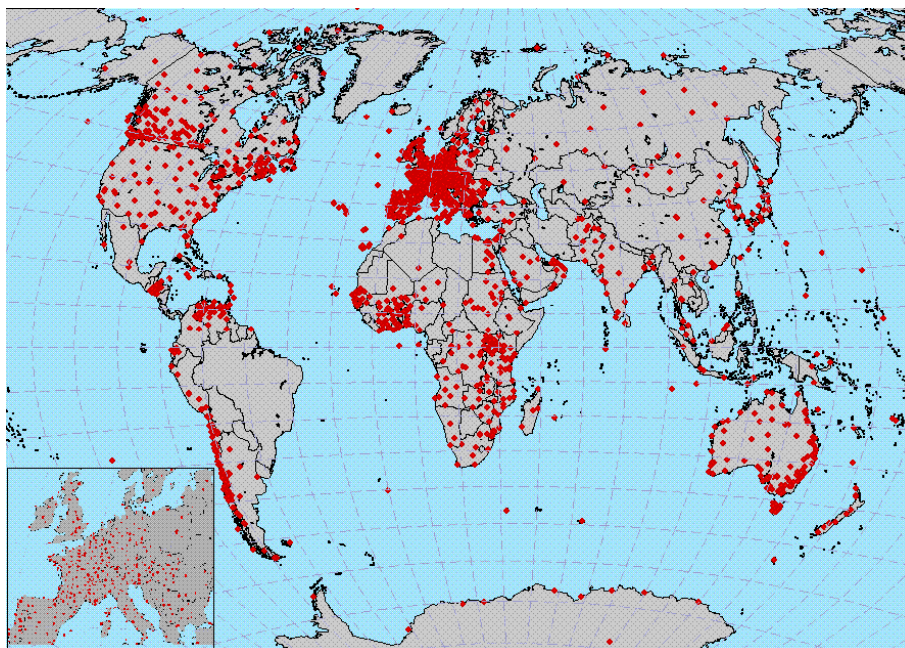


Figure 32: World Radiation Data Centre radiation monitor stations world coverage [34].

The BSRN network is part of the World Radiation Monitoring Centre and has considerably less stations than the WRDC. One of them in Scandinavia as seen in Figure 33.



Figure 33: Baseline Surface Radiation Network stations [35].

Sweden has several stations scattered over the country as seen in Figure 34, most of them reporting to the WRDC.



Figure 34 – Ground irradiation measurement stations in Sweden [36].

In Norway only one station reports to an international radiation network. However, Kjeller Vindteknikk made in 2013 a report on resource mapping of solar energy in Norway for Oslo Renewable Energy and Environment Cluster. They collected solar data from 68 stations in Norway and Sweden, where 51 of those have more than 10 years of data. The quality of the data is questionable as the measure equipment used ranges from sun hour durations to more advanced measurement devices. Also the maintenance of the measurement equipment have large variations [37]. The data from these stations have not been validated, but a master thesis by MSc student Sigbjørn Grini at NMBU are aiming at validating five of these stations during the spring of 2015 [38].

Ideally, the best solar irradiation dataset would come from a high-quality site-specific solar-monitoring station that is well maintained and with measurements taken over 30 years or longer [26]. However, these results have only a limited validity. In Sweden i.e., it has been measured that the town of Visby had on average 12% less irradiation than Växjö. And the year to year variation in all stations operated by SMHI was 15% or more. Visby and Växjö is separated only by 0.75° latitude, and a distance of under 200 km [39].

In fact, studies show that hourly irradiation data derived from satellites is more accurate than data from high-quality ground stations if the site of interest is more than 25 km away from the ground station [26, 40].

2.2.1.2 Satellite data

There exists several satellites used for investigating different aspects of earth's climate as seen in Figure 35. Most of which are geostationary satellites. For Europe the satellites Meteosat-7 and 9 (Second Generation) are used primarily.

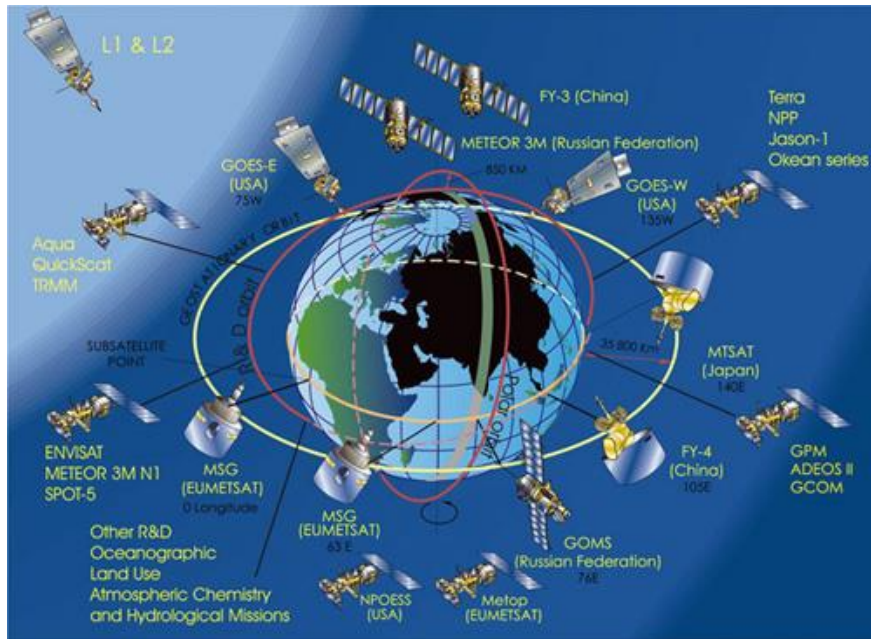


Figure 35: World weather satellites orbiting earth [41].

In order to estimate the irradiation on a given site on the earth surface satellite data can be interpreted through methods ranging from purely physically to purely empirical based methods. Physically based satellite methods are aiming at describing the composition of the atmosphere mathematically by solving radiation-transfer equations. Empirical based methods use regression between the radiation observed by the satellites and the measurements on ground radiation observation stations on the earth surface. Most methods used nowadays for radiation calculations are semi-empirical methods using simple radiative-transfer approaches combined with observations [26].

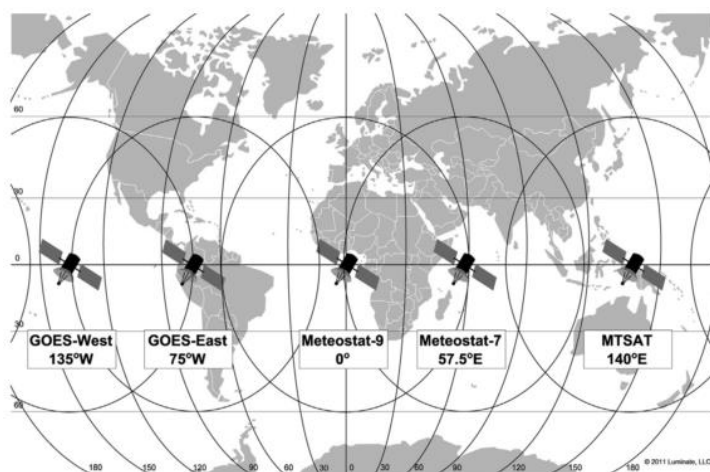


Figure 36: Geostationary weather satellites from the United States, Germany, India, and Japan are shown [26].

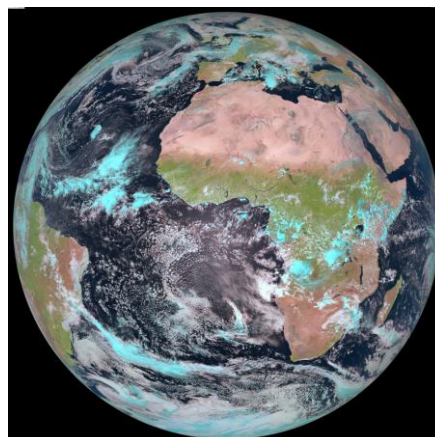


Figure 37 - Meteosat-9 13th October 2012 [42]

The semi-empirical satellite models used depend on the ability to distinguish clouds and the ground a certain amount of dynamic range is needed. In the case of snow the dynamic range is considerable reduced and thereby the accuracy of the models used. Different models use different methods to mitigate this problem, i.e by using the infrared channels from the satellites [26].

In 2010 Gueymard published a comparison of 18 different models for calculating the DNI based on satellite data. Models in the whole available range of empirical to physical models. He concluded that under cloudy conditions no models performed consistently well. Snow even worsen the situation more. He suggested to pursue the path of physics-based methods to achieve models that perform satisfactory [29]. In addition, empirical and physical satellite models is single-step methods. Advantages have been made in two-step methods and will most likely substitute the single-step methods in the long run because of higher precision.

Irradiation data from satellites has a bias confidence level of ± 3 to 6 % of daytime mean irradiance (depending on climate and terrain) and are therefore good for capturing inter annual changes [43]. However, because this is relative numbers a source for calibration is needed. A minimum of one year's worth of ground-based data is described as necessary to reach adequate uncertainty limits [26].

For northern latitudes it is interesting to notice that because of the curvature of the earth this limits the usability of the satellite images. The usability is argued that ends between 60 and 66°N [26]. According to Kleissl (2013) the DNI mean bias error (MBE) for investigated sites above 60°N latitude is -15.7 %, compared to 2.4 % below 60°N [26]. Andersen (2014) found a bias error of up to -19.7 % between measured and predicted annual irradiation in Ås, Norway. The prediction model used was PVGIS and because of the lack of ground stations in Norway, the model results is mainly based on satellites. This might indicate a rather severe underestimating of the solar potential in northern latitudes.

However, Hagen (2011) investigating the validity of satellite derived solar radiation in Scandinavia from the Satel-Light model. This shows that the satellite gives “good estimates” of global radiation for the 11 ground stations compared to. These stations were mainly situated on the west and east side of the Scandinavian Peninsula [44]. It should also be noted that this is one of few studies done on validating radiation data from satellite sources. Both PVGIS and Satel-Light will be further described in chapter 2.2.2.

The models described above are based on geostationary satellites orbiting at about 36 000 km above sea level. But there also exists polar orbiting satellites at about 850 km above sea level [26]. However, these are not mainly for weather purposes and earlier polar orbiting satellites only pass over a given spot on earth two times a day, in comparison to the geostationary satellites that take pictures every 15 minute [37]. Relatively recently the Metop-B polar orbiting satellite, which is a part of the Polar Operational Environmental Satellites (POES), launched September 2012 uses 101.7 minutes orbiting earth [45]. This equals to about 14.1 times around the earth each day.

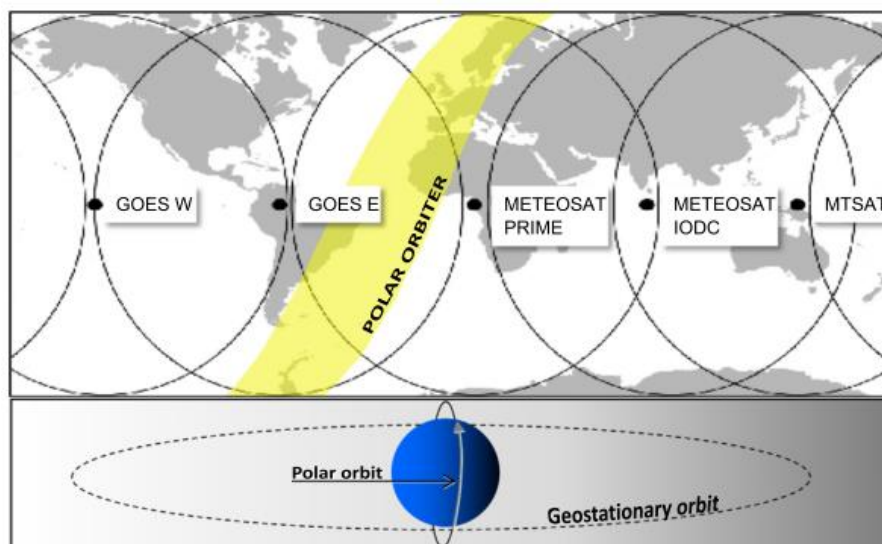


Figure 38: Coverage of a polar orbiting satellite [26].

Liu & Liu (2012) and Godøy (2012) are most likely the only studies using polar-orbiting satellites for the estimating of irradiation potential. They conclude that data from polar-orbiting satellites probably can be used for data validation and improving of the datasets from geostationary satellites [46, 47]. Godøy (2012) also points to the low availability of good quality ground irradiance observations stations for validating the satellite data as one of the major challenges [47].

Uncertainty in satellite derived irradiation data increases for lower sun elevation angles as this affects the air mass ratio and thereby is more dependent on the weather. Also positions where a high occurrence and variability of clouds the uncertainty increases further. It is also higher for areas closer to the satellites images borders because of higher occurrence of reflections and difficulties to determine cloud position. Complex landscapes and variability of water and land also adds to the uncertainty [26]. Most of these affects especially Norway and in light of the other challenges related to accurate irradiation data mentioned earlier in this chapter, the uncertainty must be described as relatively high. On the positive side, the uncertainty is at its highest in the winter months where the possible energy yield also is at its lowest.

2.2.1.3 Other sources

Several other potential sources for irradiation data exists. There are even promising methods for calculating global insolation without any radiation measurements at all² [48, 49]. One study even shows that these artificial neural network (ANN) based models are superior to other available models for calculating the solar potential in regions with few meteorological stations [50].

Also Unmanned Aircraft Systems (UAS) can be a welcome addition for the mapping of the solar resource in northern latitudes. This especially for albedo in the north as this is more important at northern latitudes [51].

No further assessments of these sources will be taken in this thesis.

2.2.2 Solar irradiation databases

As the different ground irradiation measurements are not collected to a common database, and the satellite data can be modelled and interoperated different, several databases has been made with the aim of providing the most accurate irradiation data.

The international Energy Agency (IEA) established the solar heating and cooling program (SHC) in 1977. Task 46 is solar resource assessment and forecasting. One study from 2014 in this task have evaluated long term validity of 13 satellite radiance model products in the European and Mediterranean region. They found that the average for all models provided an absolute mean bias from 2 % to 5 % compared to the measured standard deviation (SD) [52]. The mean measured SD was 2.9 %. The numbers for each site can be found in Table 1. As this study shows, the reliability of the data all these products produce is rather high, with SolarGis as the best. A representative comparison between SolarGis model and Carpentras, city south-east in France are presented in Figure 39. However, the study only includes sites at latitudes between 22°N and 60°N.

² Input used: Temperature, relative humidity, daily sunshine duration, precipitation, daylight hours, daily extraterrestrial radiation, and number of day in the year.

The largest deviation in the above study was in Davos and it was concluded to be because of the snow. The effect of snow has also been mentioned in earlier studies [43].

Table 1 - Yearly validation and interannual variability analysis. The first six are annual average products, and the last seven provide more frequent forecasts. Green is mbd under one SD, orange is mbd under two, and red is over two [53].

Sites	Yearly total [kWh/m ²] 2004-2010	standard deviation 2004-2010	Global irradiation, annual mean bias difference												
			PVGIS-CM SAF	WRDC (1981-93)	RetScreen (1961-90)	NASA-SSE (1983-2005)	MN 7 (1980-2000)	ESRA (1981-90)	Satellite (96-00)	Helioclim (2004-2011)	SolarGis (2004-2011)	Solami (2004-2011)	IRSOLaV (2006-2011)	S2m (2004-2011)	Heliomont (2006-2011)
Almeria	1850	2%	2%		-8%	-8%	-3%		5%	6%	0%	3%	0%	-1%	3%
Bratislava	1176	3%	3%	1%	1%	-1%	2%	4%	-4%	0%	2%	2%	5%	7%	2%
Carpentras	1587	2%	2%	-5%	-15%	-6%	-3%	-5%	0%	2%	1%	4%	2%	0%	1%
Davos	1383	1%	-1%			-8%	2%	-3%	-17%	11%	-5%	-7%	-9%		
Geneva	1282	2%	3%	-6%	0%	0%	-5%	-6%	-1%	0%	5%	7%	4%	24%	3%
Kassel	1048	3%	1%		-6%	-6%	-6%	-7%	-6%	-4%	0%		5%		-3%
Lerwick	810	5%		-4%	9%	9%	-4%	-4%	-3%	3%	0%	4%			-5%
Lindenberg	1120	4%	-4%	-4%	-4%	-10%	-4%	-12%	-4%	-3%	-5%	-3%	2%		-6%
Madrid	1697	5%	3%		-5%	-5%	-3%	-2%	2%	4%	2%	6%	2%	-2%	6%
Nantes	1266	3%	1%	-5%	-3%	-7%	-2%	-1%	-3%	0%	-3%	3%	1%		0%
Payerne	1278	2%	2%	-8%	-3%	0%	-2%	-8%	-3%	-5%	2%	4%	5%	12%	0%
Sede Boqer	2114	1%	-9%	1%	-7%	-4%	-4%			-7%	1%	4%	-1%	2%	
Tamanrasset	2345	2%	-3%	1%	3%	-8%	1%			3%	-1%	-1%		-2%	
Toravere	981	4%			3%	3%	0%		5%	1%	-1%	-1%	-1%		-4%
Valentia	1021	5%	9%	-4%	-5%	8%	-5%	-5%	-4%	2%	-4%	3%	1%		
Vaulx-en-Velin	1304	4%	3%	-8%	-4%	-3%	-6%	-3%	0%	1%	2%	6%	1%		4%
Wien	1175	3%	1%	-7%	-6%	-1%	1%	-7%	-1%	12%	0%	-3%	3%	7%	0%
Zilani	1024	3%	-6%	-3%		2%	-3%		6%	9%	-2%	-3%	-1%		-3%
All sites	1359	3%	0%	-3%	-3%	-3%	-2%	-3%	-1%	2%	0%	2%	1%	2%	0%

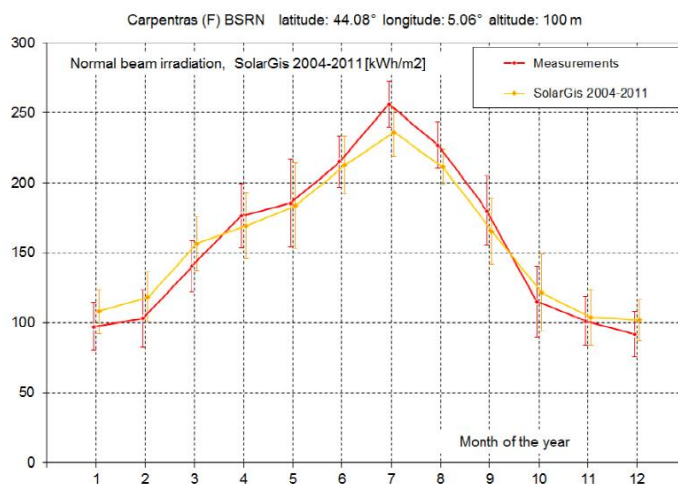


Figure 39 - Comparison between the SolarGis model and actual measurements in Carpentras, south-east France [52].

In Norway, Multiconsult have compared the irradiation data from four different databases. The result for Trondheim can be seen in Figure 40 and more detailed data in Table 2. The difference between the annual irradiation estimate of PVGIS and Meteonorm 7.0 is 7.0 %. It is worth to mention that PVGIS was the database that underestimated the insolation in Ås by almost 20 % as described earlier. Some more details about these databases and some more are taken in the next sections.

Table 2 - Detailed Monthly irradiation for Trondheim. Comparisons between four irradiation providers. Values in [kWh/m²,month]. Data supplied by Stanislas Merlet / Multiconsult

TRONDHEIM	Jan.	Feb.	Mar.	Apr.	May	Jun.	Jul.	Aug.	Sep.	Oct.	Nov.	Dec.	Year
Meteonorm 7.0	5,8	22,7	64,3	110,3	153,0	158,1	153,5	112,2	66,3	29,4	7,8	2,7	885,9
NASA/SSE	5,0	19,3	57,0	106,8	153,8	155,7	144,5	113,8	72,0	32,9	9,0	1,9	871,5
PVGIS	4,6	19,7	56,7	100,5	143,5	156,9	144,2	107,0	58,5	26,7	7,7	2,1	828,2
Satellight	4,6	19,0	59,3	102,6	153,8	137,5	142,7	114,7	73,9	32,3	9,0	2,3	851,8
Median	4,8	19,5	58,2	104,7	153,4	156,3	144,4	113,0	69,2	30,9	8,4	2,2	864,8
Average	5,0	20,2	59,3	105,1	151,0	152,1	146,2	111,9	67,7	30,3	8,4	2,3	859,4

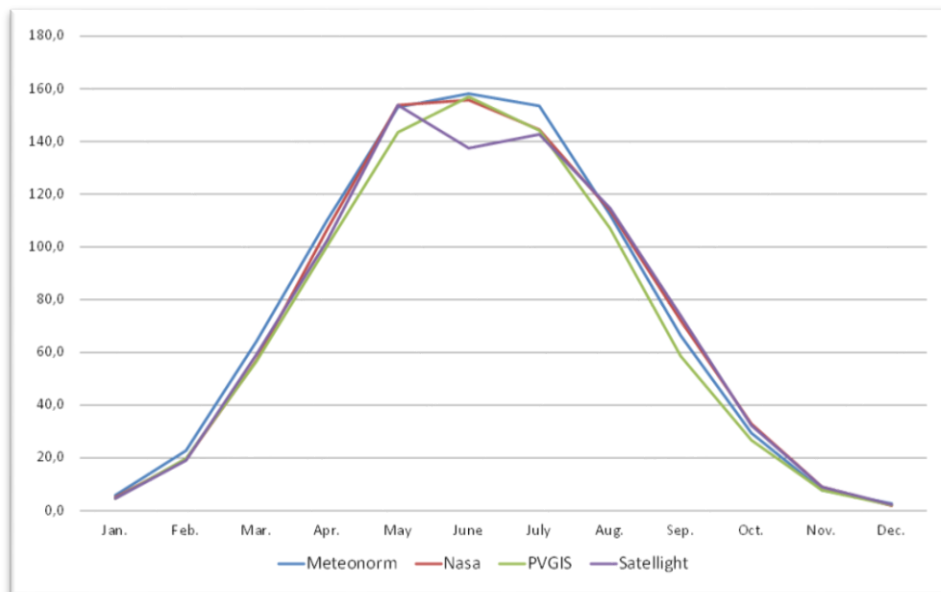


Figure 40 - Monthly irradiation for Trondheim. Comparisons between four irradiation providers. Values in [kWh/m²,month]. Data supplied by Stanislas Merlet / Multiconsult

The Satel-Light database is one of the first online databases to provide irradiation data. It provides monthly means of hourly and daily values from the period 1996 to 2000 and is not updated after that. This is based on data from the Meteosat satellites [33]. Its validity is estimated to reach approximately 66°N [37]. The earlier described work by Hagen (2011) utilizes this database for comparison to measurement stations. The correlation was found to be relatively good for those few stations they were compared to.

NASA Surface meteorology and Solar Energy (NASA/SSE) database includes over 200 satellite-derived (Meteosat) meteorological and solar radiation parameters. Data quality control is carried out by comparison with ground measured data [33]. The NASA/SSE model only have a resolution of 1°, and data of monthly intervals [54]. This low resolution corresponding to 110 km does not make a good foundation for site evaluations, but is sufficient for regional potential evaluation.

The NASA/SSE dataset is the only relatively up-to-date dataset that is freely available over the Internet and that provides worldwide coverage. The dataset is from 1983 to 2005. This is the reason why Good et al. (2011) used the NASA/SSE model when calculating LCOE for a PV tracking system in Piteå [18].

NASA/SSE uses data from the Polar Operational Environmental Satellites (POES) [54, 55]. To what degree this data is utilized is not known and will not be investigated further.

When comparing the NASA/SSE model to BSRN ground stations the mean bias error (MBE) was found to vary several percent depending on the site examined. I.e., the DNI MBE varies from -15.7% above 60°N latitude to 2.4% below 60°N [26]. However, the NSASA/SSE model gave the most accurate forecast of annual yield in Ås, Norway, with a bias error of -0.2% according to the Andersen (2014), although this was the total irradiation [56].

The PVGIS database is in Europe based on an interpolation of 560 ground station measurements down to a 1 km grid. The data is collected in the period 1981–1990 [33]. The quality of the database was tested in 2007. The study found a cross-validation error of 4.5

% for the entire dataset. The latest data from PVGIS are validated and improved through the Climate Monitoring Satellite Application Facility (CMSAF) resulting in an updated database; PVGIS-CMSAF. However, this latest addition to the database does not cover the region north of 58°N. This is due to the high uncertainty of the radiation estimates from the geostationary satellite data that is used [57]. Even though the old database also covers more northern latitudes, it is based on few ground stations. In Norway there is just one, and a few more in the neighbouring countries [58].

Andersen (2014) found a bias error of -19.7% for Ås, Norway when using the PVGIS database [56].

The latest release (2015) of the CMSAF database includes data from 1983 to 2013 and covers the region of ±65° longitude and ±65° latitude with a resolution of 0.05° x 0.05° [59]. The inclusion of these data in PVGIS would be a welcome addition for the northern latitudes.

PVGIS irradiation estimates for Europe and Norway are shown in Figure 41 and Figure 42.

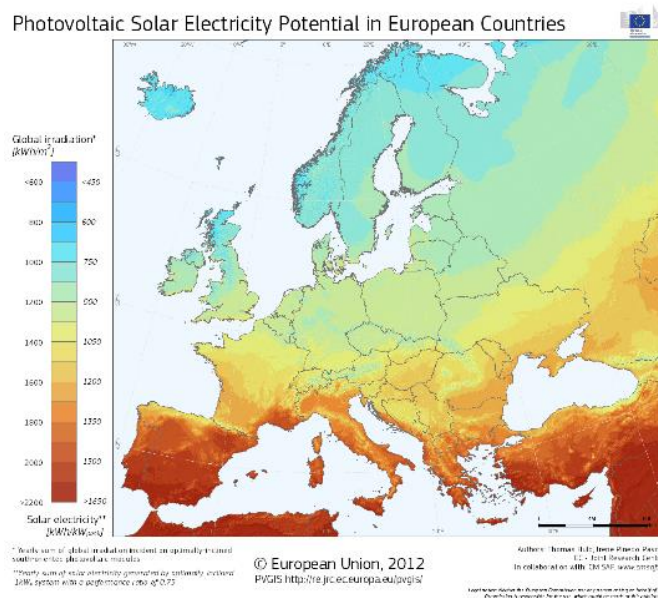


Figure 41 - Global irradiation estimates in Europe by PVGIS [57, 60].

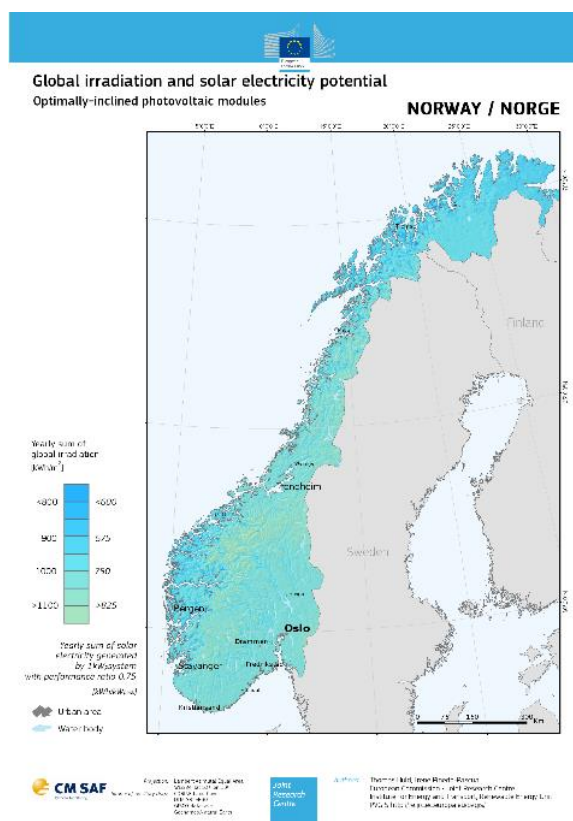


Figure 42 - Global irradiation estimates in Norway from PVGIS [57, 60].

Meteonorm 7 has data from 1961 to 2000. In comparison to the above three models described it has hourly irradiation values. The model is based on ground stations, but enhanced satellite data are used to improve the estimation for areas with low density of weather stations. [33] These satellite data are from 2004 to 2010 of the visible of the infrared channel of Meteosat Second Generation satellites. In Europe, the model is based on 400 stations collecting radiation data [61]. However, only three of these ground stations are in Norway [54].

Meteonorm 7.2 states an uncertainty of 8 % for their annual GHI. Based on their home page coverage map seen in Figure 43, their main coverage area seems to be between about $\pm 60^\circ$ latitude. This is in line with the Meteosat coverage.

One of the few PV LCOE studies done in Norway, written by Multiconsult, uses Meteonorm 7.0 as the main basis [20, 21]. This report is also the basis from which the solar

economic potential for Norway is assessed by the Norwegian Water Resource and Energy Directorate in its 2015 report on costs in the energy sector [21].

Meteonorm is, in contrast to the other three models above, a commercial service and by this reason the underlying methodology is difficult to obtain. I.e. Meteonorm 6.1 gives in most cases a lower irradiation estimate than Meteonorm 7. Whether this is from better modelling or from better data is not known.

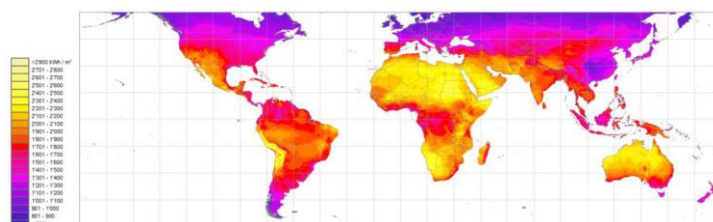


Figure 43 - Yearly sum of GHI from Meteonorm 7.2. Uncertainty of 8% [61].

Those four databases described above, corresponding to the databases assessed in the Multiconsult PV LCOE report, are all based on the Meteosat satellite. Especially since the ground stations used in Norway are at maximum three. The maximum northern coverage is described to be between 58° N and 66° N depending on the accuracy of the model used and the uncertainty limit accepted. Regardless, the quality of the irradiation databases used, and available, cannot be considered to be high. The high dependency of a single satellite also raises the question if the data is prone to a systematic error.

STRÅNG is an irradiation model from the Swedish meteorological and hydrological institute (SMHI) covering northern Europe with a resolution of 11×11 km and a time resolution of one hour. The model is continuously updating having measurements from 1999 and onwards. The work by Lundström (2012) found that the STRÅNG model is only consistent for Sweden and with reasonable good results for mainly Central Europe [62].

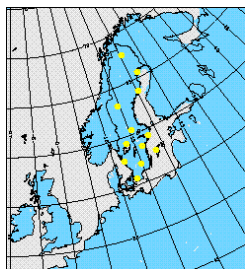


Figure 44: Ground measurement stations for the STRANG solar radiation model [63].

SolarGIS, the database found to be the best in the study mentioned in the start of this chapter, are using satellite data from various sources, astronomical data, data from atmospheric models, terrain models and ground measurements. Though all geostationary satellites for Europe is the Meteosat satellite. They limit their supply of irradiation data to no further than 60°N. They also report a higher uncertainty³ from north of 50° N latitude [64].

That SolarGIS, as one of the best sources for irradiation data, have these rather strict geographical coverage limitations compared to the other models described. One question the validity of other models based on rather similar input data.

As seen in the start of this chapter, several other databases for irradiation exists. However, these are not that common, mostly based on the Meteosat satellite, and have similar limitations in latitude. They will not be discussed in this thesis.

An interesting aspect of all the irradiation databases that exist is that they are static. The prediction is for an average year, with some differences in their time resolution besides the actual irradiance data. However, a study by Persson (1999) finds an average increase in irradiation in Sweden of 7.2 % a decade [39]. This upwards trend, although not that high, is also documented by the SMHI as seen in Figure 45, where the annual increase is found

³ By higher uncertainty they mean: “higher than $\pm 4\%$ for yearly GHI and higher than $\pm 8\%$ for DNI”

to be 0.3 % a year [65]. Will this escalation prevail? If so, to what degree? In a 25 to 30 year perspective usual for PV system, this effect may be worth to take into account.

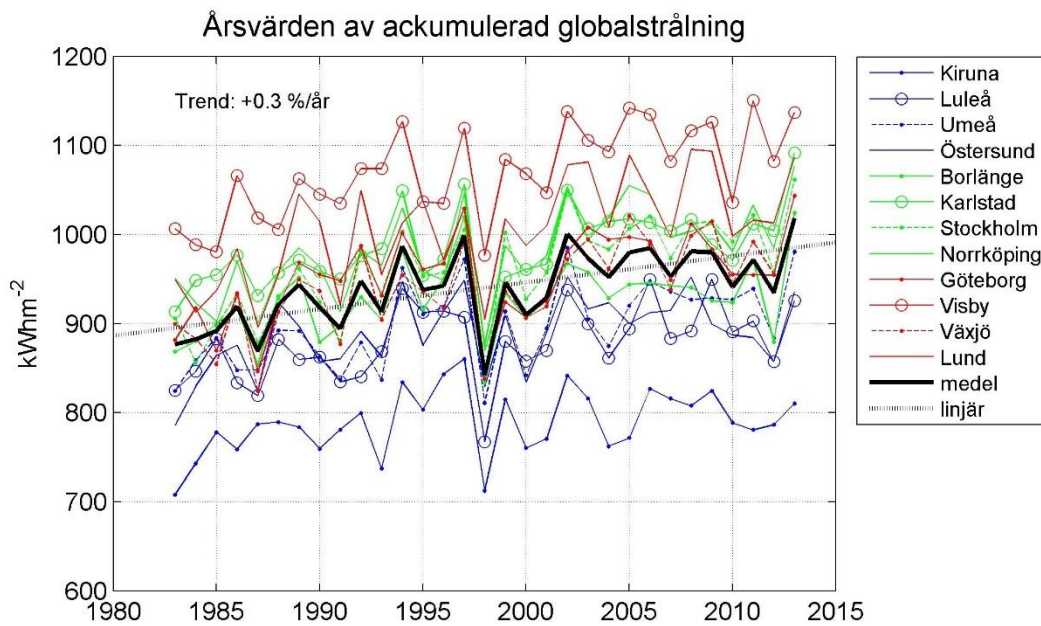


Figure 45 – Annual global irradiation development in Sweden [65].

2.2.3 Unshaded solar potential in Piteå

To estimate the unshaded solar potential in Piteå the same models as used in the Multiconsult PV cost report in Norway (2011) will be used. In addition, an earlier version of Meteonorm and the STRÅNG model will also be included.

As NASA/SSE does not state any values for DHI for December, and no DNI for December and January, zero is assumed. The annual GHI of 898 kWh/m²/year corresponds to the value of 900 kWh/m²/year used in the study by Good et al. (2011) when referring to the NASA/SSE model [18]. STRÅNG does not supply DHI. Satel-Light does not supply DNI [66-71]. The raw data from the data extraction can be found in appendix 1 to 6.

The annual irradiation in Piteå from the irradiation databases is summarised in Figure 46.

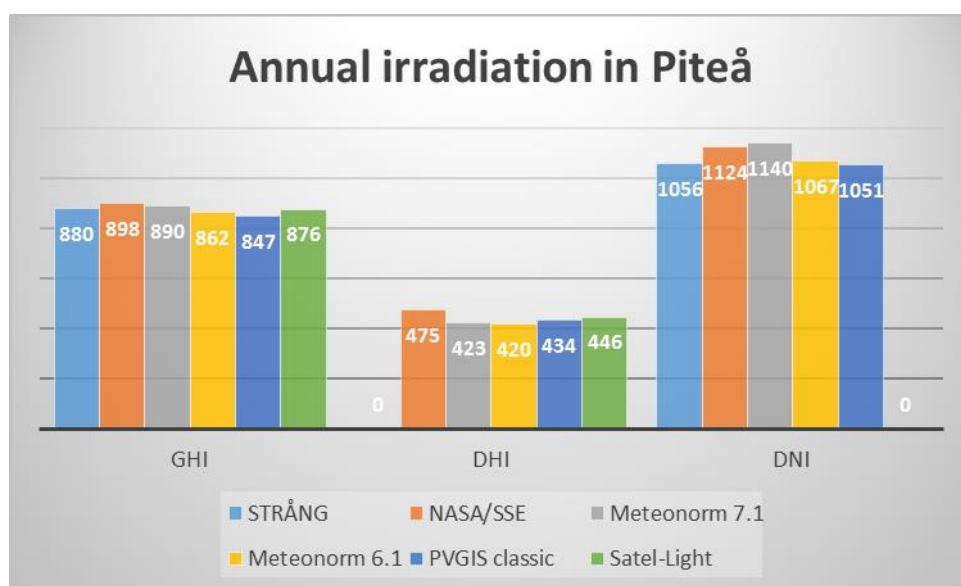


Figure 46 – Annual irradiation in Piteå. Comparison between six different irradiation models. Units in $[kWh/m^2/year]$.

The DHI difference between Meteonorm 7.1 and NASA/SSE is 12 %. For the STRÅNG database to reach their GHI levels with their relatively low DNI estimate, the DHI would have to be even higher than NASA/SSE. As NASA/SSE have some polar orbiting satellites in their samples, and STRÅNG have relatively many validating ground stations in Sweden, this might indicate that the DHI estimates for the other databases might be too low.

2.2.4 Irradiation composition impact on optimal solar energy collector orientation

As seen in the previous section, the differences in irradiation composition between the irradiation databases is even higher than just the GHI itself. In fact, research in the US has shown that the optimal tilt and azimuth angle of the solar collector is not directly proportional to the solar position, but also the weather. *“The optimum tilt was never greater than latitude tilt, but up to 10° less than latitude tilt.(...) Azimuths deviating up to 10° west or east of due south were found for areas with typical daily cloud patterns such as morning fog or afternoon thunderstorms.”* [72] This emphasizes the importance of knowing the local weather, not only to predict the annual yield, but also to know the radiation composition in order to correctly place the PV modules to optimize the yield.

I.e. in Hamburg the diffuse irradiation contributes for almost 60 % of the global horizontal irradiation during a year, see Figure 47, and in Cairo 29 % over a sunny summer day [23]. In Figure 48, you can clearly see the impact from what is most likely morning humidity in the air.

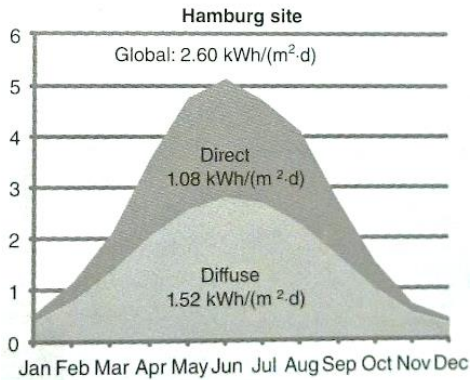


Figure 47 – GHI composition in Hamburg. Y-axis is given in $kWh/m^2/d$ [23].

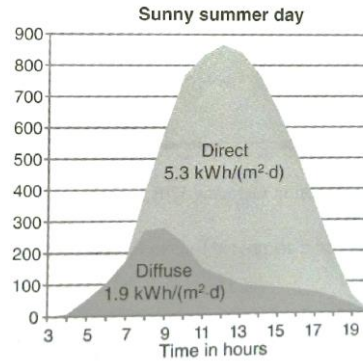


Figure 48 – GHI composition in Braunschweig. Y-axis is given in $kWh/m^2/h$ [23].

For Piteå the annual average irradiation composition can be seen in Figure 49.

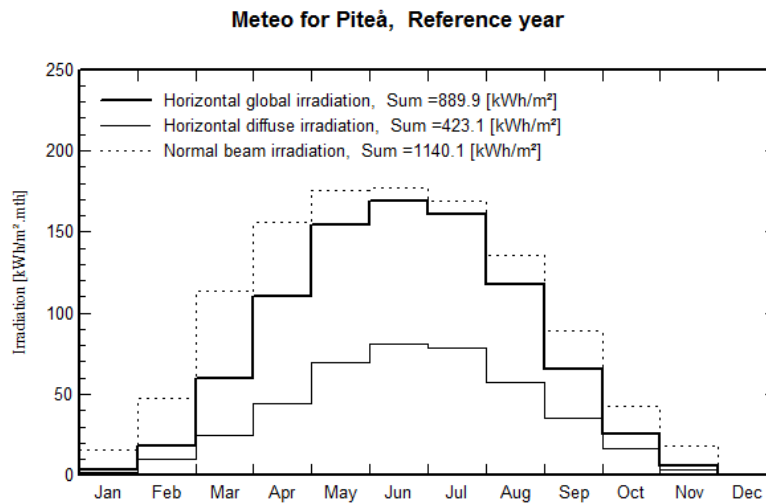


Figure 49 - Irradiation composition over the year for Piteå. Generated by PVSYSY v6.32 from Meteonorm 7.1 data.

Knowing the radiation composition for every time interval is important to maximize the annual yield for a given site. However, this separation does not have a long history. For older datasets average monthly global insolation data available is most common. From these datasets methods for separating the different components have been developed. One procedure for this is described in [25]. If you have hourly global insolation data available you can use a technique described by Bugler et al. [73]. However, the models used for separating GHI into DHI and DNI have been shown to not performance satisfactory [29].

Andersen (2014) points to the lack of adequately separating the different components as a possible reason for a bias error of up to -19.7 % between measured and predicted annual yield at a site in Ås, Norway [56].

As the optimal angle is not directly connected to the solar angle, iso-transposition models are made on the basis of the radiation composition and are used for illustrating how different angles influences the expected annual yield. This is illustrated in in Figure 50.

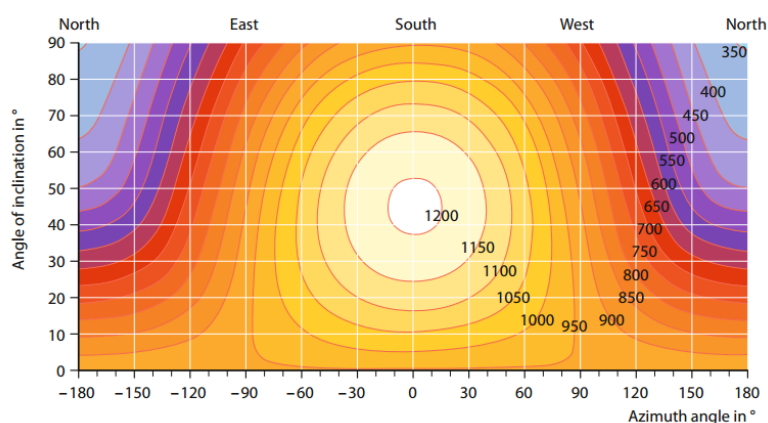


Figure 50 - Annual solar yield in St. Petersburg. Values in kWh/m^2 and as a function of azimuth and solar angle [24].

For Piteå iso-transposition diagrams have been calculated through PVSYS v6.32 based on the data from Meteonorm 6.1 and 7.1, and NASA/SSE. These diagrams can be seen in figure 51 to 53.

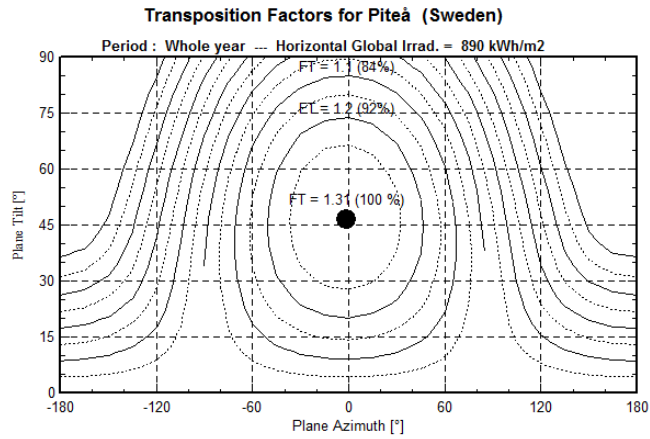


Figure 51 - Iso-transposition diagram for Piteå using Meteor norm 7.1 data. Calculated by PVSYS v6.32.

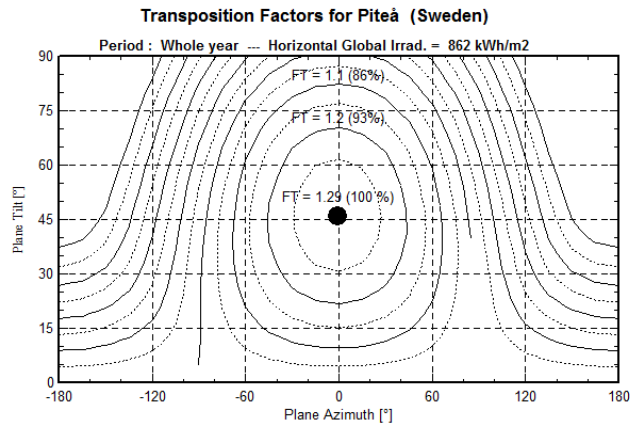


Figure 52 - Iso-transposition diagram for Piteå using Meteor norm 6.1 data. Calculated by PVSYS v6.32.

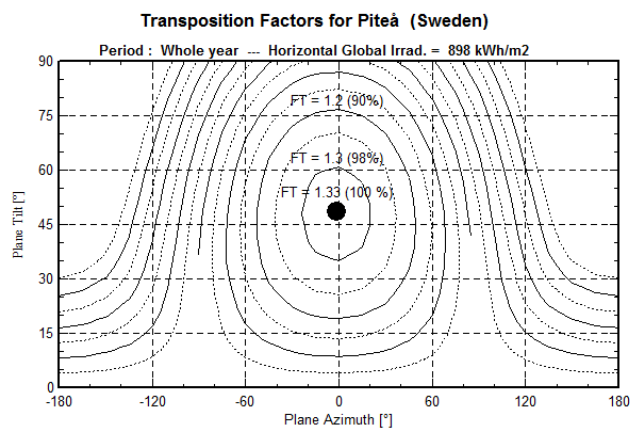


Figure 53 - Iso-transposition diagram for Piteå using NASA/SSE data. Calculated by PVSYS v6.32.

As the figures above illustrate the azimuth angle is consistent. One could expect some deviation between Meteonorm and NASA/SSE as the NASA/SSE database only have monthly data and Meteonorm have hourly. This means that only the Meteonorm database of these two could have found a difference in expected optimal azimuth angle. For a permanent mounted collector the optimal azimuth is most likely due south.

The plane tilt angle is as expected different because of the difference in reported irradiation composition. A difference in the transposition factor, of 3.1 % between Meteonorm 6.1 and NASA/SSE, directly affecting the possible energy yield, is not negligible.

At an optimal tilt between 45° and 50°, the reflected radiance is of a relative high importance at these northern latitudes. However, as the albedo is highly site dependent it will not be covered here, but taken in as a factor during the system modelling. Although one could expect an even higher optimal tilt as there is a possibility of a higher albedo than the relatively industry standard of 0.2 because of the snow.

2.2.5 Summary of the quality of solar energy data sources at northern latitudes

The best irradiation models the expected irradiation through good quality satellite data calibrated through equally good quality ground based stations. The problem for northern latitudes is that the satellites available, mainly just one, are geostationary and does just marginally cover beyond 58°N depending on which database used. I.e. the Multiconsult report (2011) estimating the cost of PV in Norway is based on four models which in turn is based on data from one of those satellites. This might be a source of systematic error. In addition only a few ground stations are available for calibrating these already marginally good satellite data. However, those validating studies that is done indicate that if there is a discrepancies between the models and the actual irradiation level, the models most likely underestimates the irradiation potential.

The irradiation models described in the sectioned above reports an even larger difference between the irradiation component compositions than between the annual irradiation

potential. This influences what the optimal angle of the solar collector surface should be and in the end the actual annual energy yield.

For the rest of this thesis, where only the annual irradiation is of interest the NASA/SSE model will be used as this model holds all three irradiation components and no further uncertainty is introduced while transposing to DHI. Also, this model is also equal valid for Norway. Where a higher data resolution than monthly is needed, Meteonorm 7.1 will be used instead of STRÅNG as those results are more of an illustrative interest. And as this database is already in the simulation software used later on, considerable less effort is used in data preparation and the risk of error is also lower. The STRÅNG model is also not prepared for the use in simulations as an average is not good enough as this does not simulate the limits of the PV systems well enough.

2.3 The PV system and direct influencing factors

There are several factors affecting the potential energy yield, even after the expected irradiation potential has been found. The solar energy has to be converted to electricity through PV modules and these modules can be shaded in several different ways with different effects. Next the direct current has to be converted to alternating current to be able to connect to the grid and these components has to be connected through some cabling, and mechanical secured. This is also how this chapter is organized.

2.3.1 PV modules

In this chapter first a PV technology introduction will be made, giving a brief intro in the basics of photovoltaic and how it works. Next the PV technology used and setup of the modules at the Acusticum will be made. Then a more detailed look into how irradiance and temperature affects the performance of PV cells. At last the PV module standard test conditions are described.

2.3.1.1 PV technology introduction

The ability to utilize larger parts of the solar energy is moving forward. The different PV technologies are with few exceptions all increasing the efficiency as seen in Figure 54. From a few research projects in the 70ties to a relatively large number the last decade.

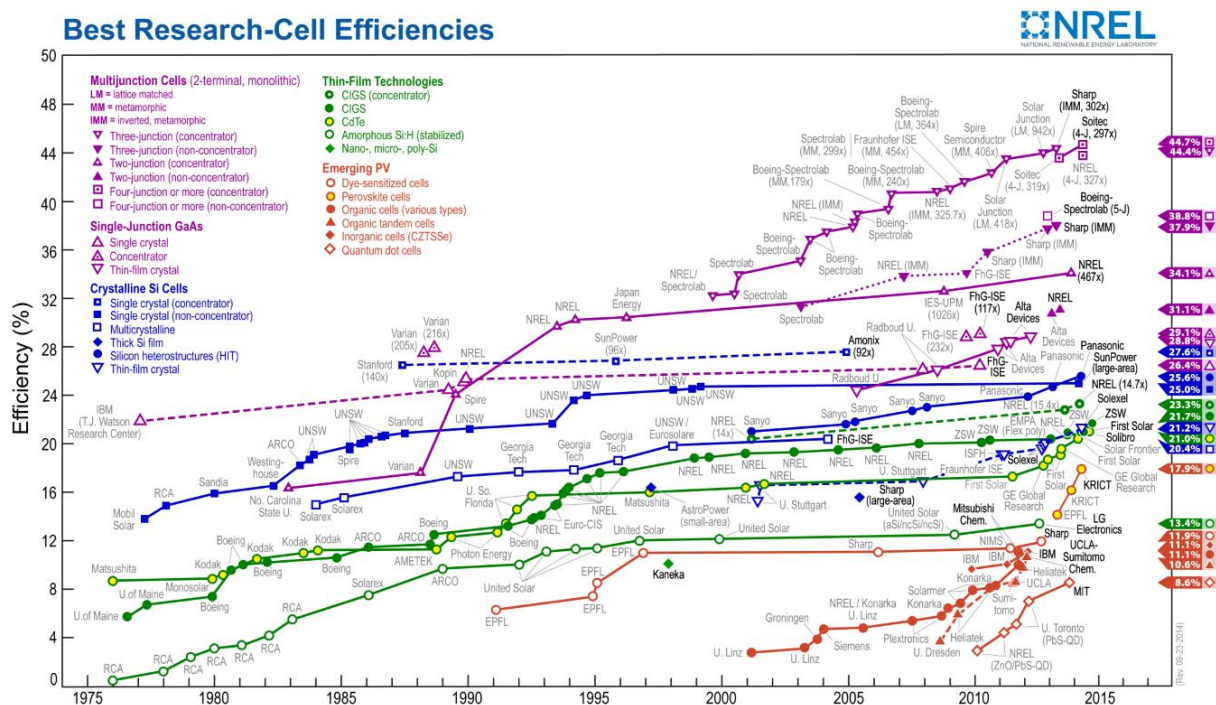


Figure 54 - Best research-cell efficiencies [74].

However, the adaptation of the different technologies in the industry are moving slowly. The PV market today is dominated by the crystalline silicon cells with a marked share of about 90 %. This is technology with almost no development with regards to efficiency the last 20 years. On the other hand the development has been in the production process, resulting in continuously reduction in cost per watt. As will be shown later, the energy from PV systems based on modules with an efficiency of around 15 % are now competing without subsidies with other sources of electricity. Given the present best research cell efficiencies, the future potential is interesting.

The different technologies operate all the same way. Simply put at least one layer of positively and one layer of negatively charged semiconductor are put on top of each other. The positively charged semiconductor can be made by adding small amounts of group 3 elements from the periodical table, i.e. boron, and negatively charged semiconductor by adding small amounts of group 5 elements, i.e. phosphorus. If only two layers are used these charged semiconductors are referred to as p- and n- type materials, and the junction created between these two layers the pn-junction. An illustration of an electrical circuit based on this concept is shown in Figure 55.

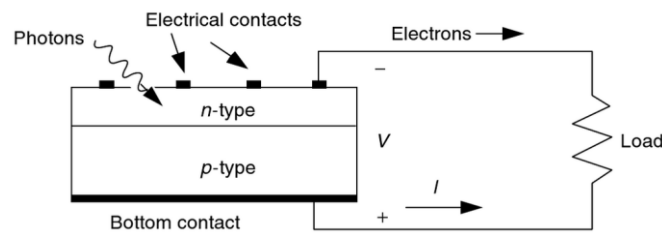


Figure 55 - Flow of electrons due to an electrical potential difference [25].

Electricity is generated through what the quantum theory describes as exciting of electrons, where energy supplied (in this case from photons) forces the electron to change what is called energy band. The energy needed for this is called the band gap energy. In order to excite one electron in crystalline silicon, one photon of at least 1.12 eV is needed. If the energy of the photon is less, the electron will not be excited, and if the energy is higher it will still only excite one electron. Photons have different amounts of energy depending on their wavelength as illustrated in Figure 56. For single pn-junction PV cells based on crystalline silicon this means that there is an upper theoretical efficiency limit of 49.6 % [75].

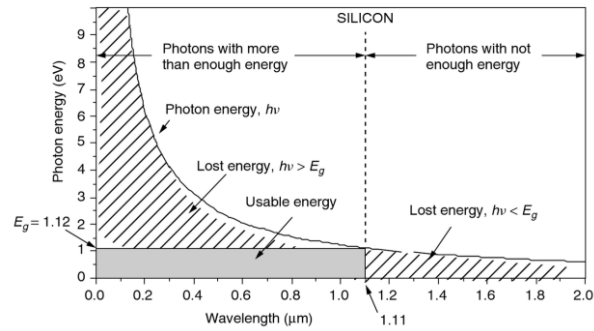


Figure 56 - Illustration of photon energy and the crystalline silicon utilization of this for different wavelengths [75].

An illustration of the available energy from the solar spectrum vs. the energy available for silicon based PV cells can be found in Figure 57.

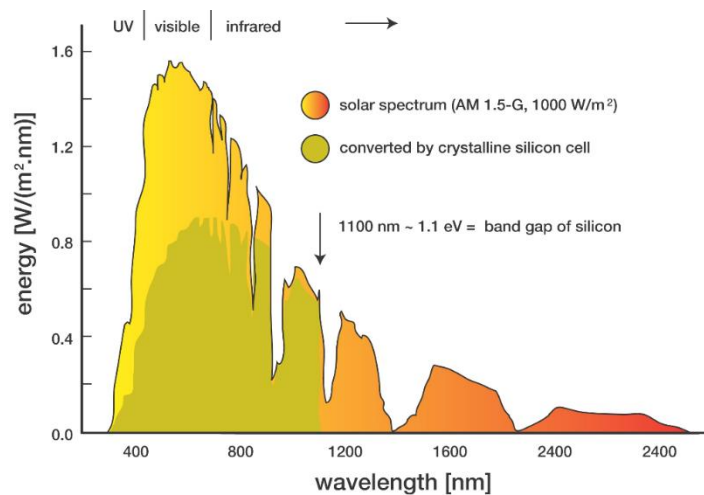


Figure 57 - Energy available in the solar spectrum for crystalline silicon based PV cells [76].

For PV cells based on different materials than silicon, the band gap energy needed is different. This is illustrated in Figure 58. This also illustrates the advantage of multi junction PV cells as these are able of utilize a higher proportion of the solar spectrum.

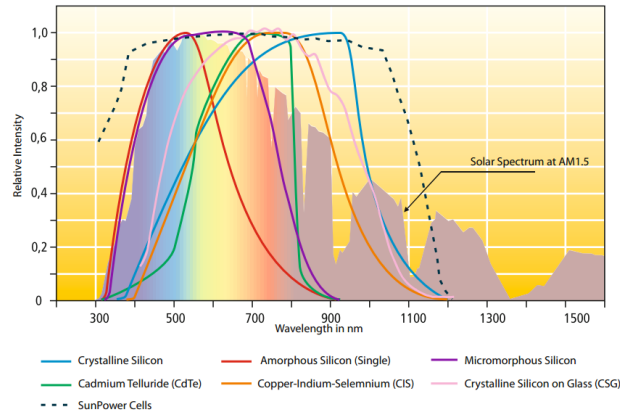


Figure 58 - Utilization of the solar spectrum for different semiconductors with different band gaps [24].

The maximum amount of current a given PV cell can produce for a given amount of irradiance can be found by short circuit the p and n side. Similarly the maximum voltage the pn-junction can uphold can be found by measuring the open voltage. The maximum current and voltage cannot be achieved by the same time, but different degrees. By plotting the values for current and voltage for various loads one get what is called the IV-characteristic illustrated in Figure 59. The point where the product of the current and voltage is the highest is called the Maximum Power Point (MPP). The shape and size of this curve is different for different PV technologies, and also changes for different impacting factors as described in the following sections.

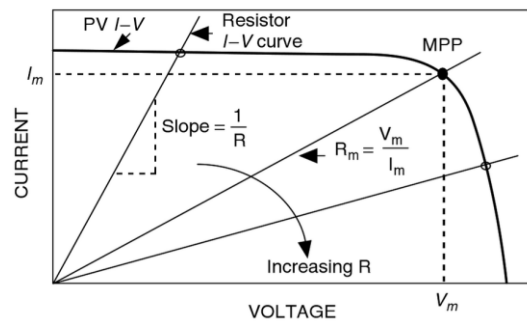


Figure 59 - Plotting the IV-characteristic of a cell based on various loads [75].

2.3.1.2 Acusticum PV modules

The modules used at the Acusticum are Swedish produced from Swemodule. In these modules there have been used four types of cells; Q-Cells 3rd generation, both mono- and multicrystalline silicon, Bosch monocrystalline and SolarWorld multicrystalline. The STC⁴ rated power for the modules based on these cells is all between 260 and 270 Wp [77]. In accordance with module flash list⁵ received from Kleven, the average STC power of the modules is 264.84 Wp. The calculated variation, within two standard deviation, was 2.2 %.

For the simulation the module EcoPlus260 from Innotech Solar will be used. This is because Swemodule does not exist in the module database used by the simulation program later used. However, Innotech Solar was one of the large owners of Swemodule, and technology transfer have most likely been done. The use of EcoPlus in the simulation was also recommended by the CEO at Solbes, Øystein Kleven. Although not exactly the same, this module represent a good average of the modules used.

The EcoPlus260 module have a rated STC power of 260.3 Wp. To adjust for the additional power, a module mismatch loss of -1.7 % will be added to account for this extra power. (Because of the later described Solar Edge inverter architecture the module mismatch loss is before this modifying zero.)

A total number of 891 modules was installed. This gives an installed power of 236 kWp.

Figure 60 shows the original planned placement of the PV modules. However, because roof C was unsuitable due to its unique construction with no places to fasten the mounting equipment, this roof was dropped and an extra row of modules was placed on the west side of roof G in addition to adding three rows of modules on roof I. The orientation and number of modules on each roof can be found in Table 3.

⁴ Description on the Standard Test Conditions (STC) can be found in chapter 2.3.1.4.

⁵ The flash list shows the performance of the modules under STC conditions.

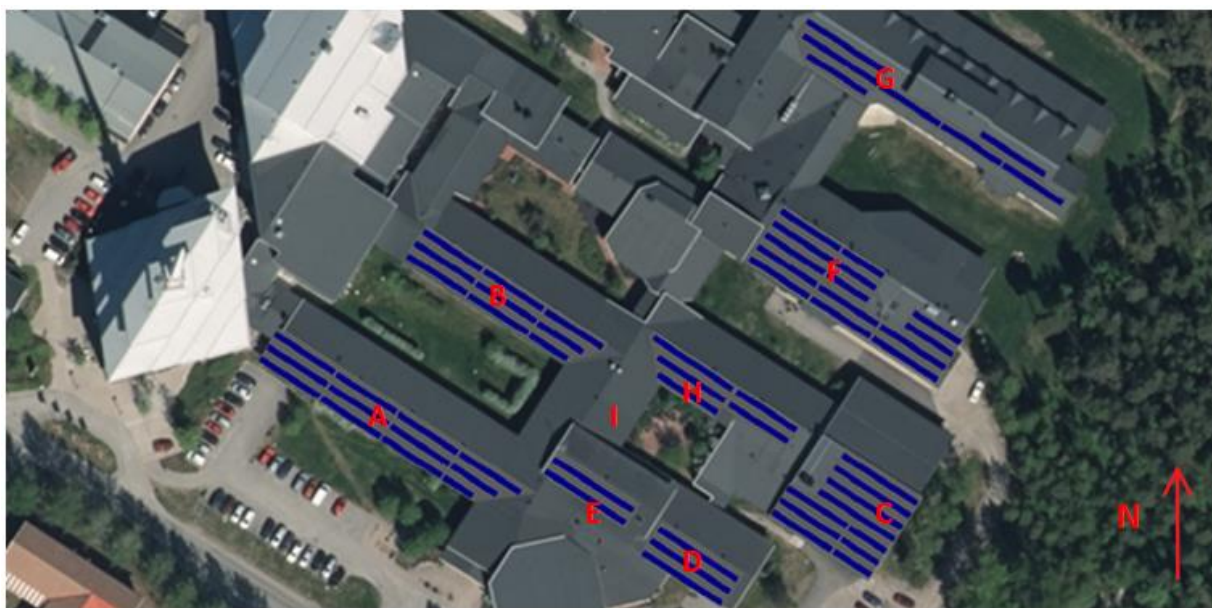


Figure 60 - Original planned placement of the PV module on the Acusticum. Picture by Google Maps and illustration by Øystein Kleven [77].

Table 3 - Numbers of modules and their orientation on each roof at the Acusticum.

Roof	PV module tilt (deg)	Azimuth (0° is S)	# modules
A	27	38.9	168
B	27	38.9	148
D	27	38.9	60
E	27	38.9	40
F	27	38.9	205
G	30	38.9	130
H	27	38.9	93
I	27	-51.1	47
TOTAL			891

A 3D model of the Acusticum with the module placement can be found in chapter 2.3.2.2. Two photos of the system are shown on the following page.



Figure 61 – The PV system at the Acusticum. Photo taken from the tower to the west. Photo by Eirik Oksavik Lockertsen.



Figure 62 – Parts of the PV system at the Acusticum. Photo taken from roof I. Photo by Eirik Oksavik Lockertsen.

2.3.1.3 Irradiance, temperature and rain affecting PV module performance

PV cell external factors affecting the PV cell efficiency is temperature, dust and irradiance [78]. Dust can also be considered a temporary shading as described in the later chapter regarding shading.

The most importantly is off course the level of irradiance as seen in Figure 63, but other factors also have an impact.

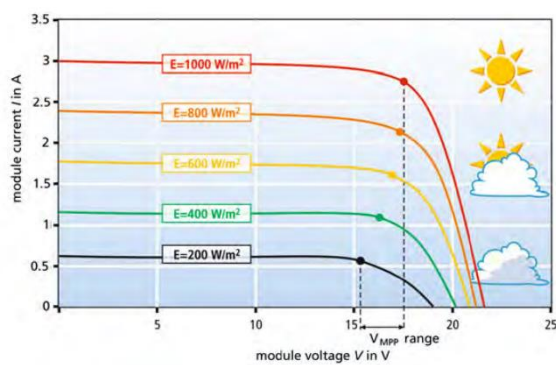


Figure 63 - Different IV-curve characteristics depending on solar irradiance [24].

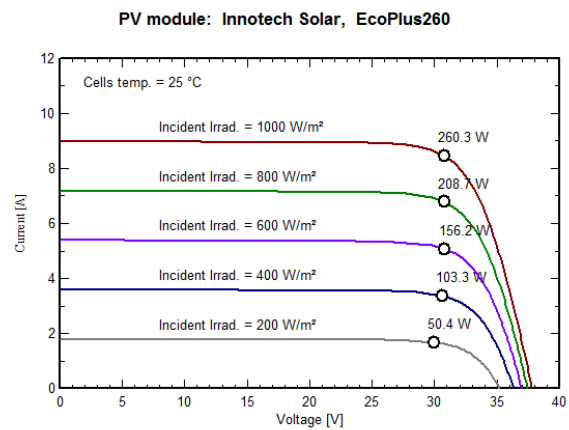


Figure 64 - IV-curves for different irradiation levels for the module used in later simulations. Data from PVSYSST v6.32 database.

Besides the obvious less power output with lower irradiance, Eikelboom and Jansen [79] showed, among other things, that efficiency differences at different irradiance levels are small at irradiance levels over about 400 W/m² for different manufactures, and considerable below about 400 W/m².

Three out of four cells types used in the modules at Acusticum is described to have good to exceptional low light performance [77]. This is an important quality of the cells as a rather big porprtion of the incoming radiance is of rather low power as seen in Figure 87.

As for the impact of the temperature, the effect is inverse proportional. The higher the temperature is, the lower the performance as illustrated in Figure 65 and Figure 67.

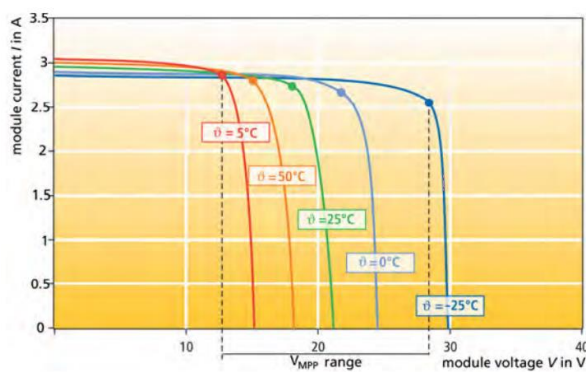


Figure 65 - Different IV curves for different cell temperatures [24].

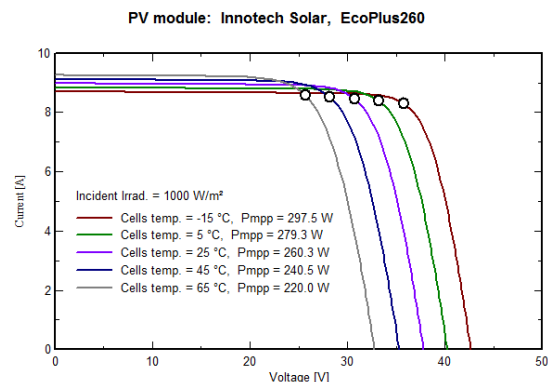


Figure 66 - IV-curves for different temperatures for the module used in later simulations. Data from PVSYSST v6.32 database.

The temperature effect is of great interest when calculating the possible energy yield of a PV system. For this reason the module producers in most cases supply the module characteristics for different temperatures in order to take the temperature into account when calculating the yield. Combined with good quality meteorological data on temperature and wind, it is possible to make some good estimations on PV module performance for a given site.

The increase in power output from 25°C to -15°C is 14.3 % for the module used in later simulation as seen in Figure 66.

It is important to note that it is the cell temperature that is of importance. Of course very closely related to the ambient temperature, but also dependent on the ability to cool down the panels. This is largely dependent on how the modules are mounted and the amount of wind. The effect on energy yield for different mounting options can be seen in Figure 67. At the Acusticum the spacing between the roof and the module are relatively large. In later simulation this is taken into account as this is modelled as “Open construction”.

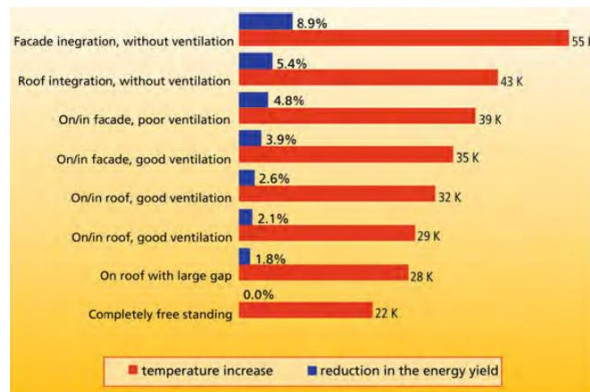


Figure 67 - Reduction in energy yield due to increase in temperature [24].

For northern latitudes, the colder climate is of course a very interesting advantage. The maximum efficiency for a PV system at Nunavut Arctic College at 63.4°N, was found to be best in the period between February to April because of the relative abundance of irradiation, while the temperature was low [80]. In Piteå the temperature will be taken from the NASA/SSE model.

The low temperature can also be a challenge as this increases the voltage MPP range which can be a challenge for the later described inverter. For Piteå a lowest temperature of -15°C will be used.

An interesting characteristic not widely known is that it has been shown that PV modules, operating under low irradiance levels, have a higher performance during rainy than under non-rainy weather conditions by up to 12% [81]. However, this is only one source and further validation has to be done.

2.3.1.4 Standard test conditions (STC)

As the surrounding conditions for PV cells always are changing, the need for a standard in order to be able to compare different cells against each other is needed. For this purpose the STC was stated. The STC consists of three points. (1) perpendicular irradiance of 1000 W/m², (2) defined light spectrum with an air mass of AM1.5 and (3) a cell temperature of

25°C with a tolerance of $\pm 2^\circ\text{C}$ [23-25]. The first condition (1) is often referred to as 1-sun [25]. The kWp rating stated on each module are at STC.

As the cell temperature of 25°C is in most cases an optimistic value for an irradiance of 1000 W/m², the higher temperature is in most cases an additional reduction in module performance when calculating the energy yield. For northern latitudes on the other hand, the case of an average cell temperature of below 25°C is possible and comes as an increase in module performance.

Above 1000 W/m² and cell temperature under 25°C is both possible in northern latitudes – though rarely at the same time.

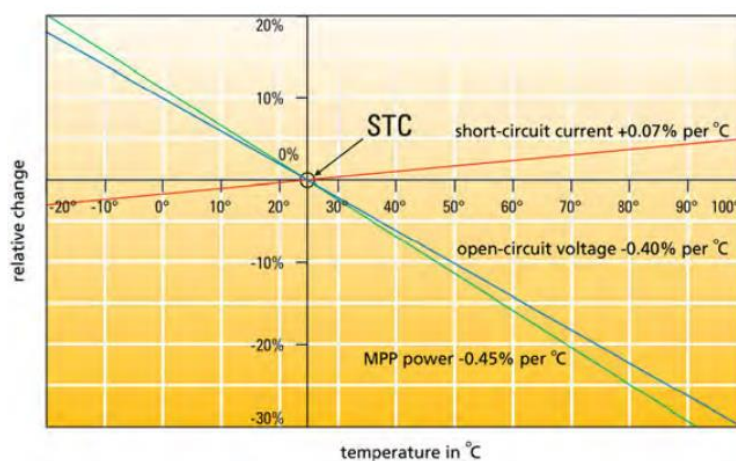


Figure 68 - PV cell performance at STC and as a function of cell temperature [24].

Producers of PV modules often provide a nominal operating cell temperature (NOCT) which is the cell temperature when the radiation is 800 W/m², wind speed is 1 m/s and ambient temperature is 20°C [25]. NOCT is available in PVSYST simulation program, but not recommended option, as this is modelled through parameters as module temperature coefficient, ambient temperature and wind speed.

The STC module information in the module databases, i.e. PHOTON, are in most cases the producers themselves that have put in. Some doubt on these numbers are advised.

2.3.2 Shading of solar modules

There are several ways of classifying shading. One way is to distinguish between far-, near- and temporary shading.

2.3.2.1 Far shading

Far shading is a result of permanent objects in the horizon of the solar collector. Mountains, hills, buildings and vegetation relatively far away from the modules. Far shading affects the whole collector surface in a homogenous way, in comparison to near shading that only affects parts of the PV system. Far shading affects when the DNI might be available, and the maximum amount of DHI.

To gain an accurate horizon profile there exists tools specialized for his task like the SunEye from Solmetric. For the system in Piteå the horizon is flat in all directions so the far shading does not have any mentionable impact.

A shading effect a little difficult to classify is the shading due to the smoke from the Kappa industry in the south. This might have an effect, but how much is not known and difficult to model. This will not be taken into account in the simulation model.

2.3.2.2 Near shading

Near shading is shades only affecting parts of the PV system. Near shading can be a result of vegetation, buildings and other constructions close by, the building the collectors is mounted on and the solar construction itself. Near shading is mostly changing with time and difficult to calculate the effect of manually. 3D models in solar calculating programs are for this a big help.

The relation between shaded area and power output from a collector system is not linear, and solar system design must consider shadows in more ways than just minimizing them. This effect will be explained in more detail in the paragraphs that follow.

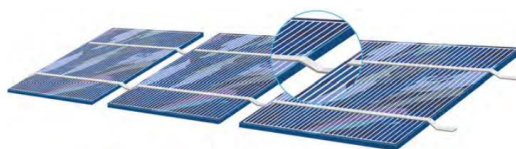


Figure 69 - Serial connected PV cells [24].

As described in chapter 2.3.1.1 the pn-junction, is rather difficult to cross for electrons if they are not excited. Even when the electrical potential on each side of the junction is relative high. This means that if the sun does not excite that many electrons in one PV cell as the other cells in that series, this cell will become a bottleneck. If no electrons are excited, this will almost completely block the flow of electrons from all other cells in that series.

For far shading, as clouds, mountains and other objects that affects the whole PV systems, we must in most cases just take the lower energy yield into account. However, if the radiance is different on different part of a serial connected system as the case for close shading, the PV cell with the lowest irradiance levels will represent a bottleneck, and the potential flow of electrons in the other cells because of more radiance, is not utilized. This is the case of near shading where the shading affects just parts of the system. It is important to emphasize that it is the difference in radiance level that is important. As described earlier only about half of the radiance hitting a collector surface is direct radiance, meaning that even if you block the sun you still might have a radiance level of towards 50 %. Shading is not an on or of phenomena, but degrees.

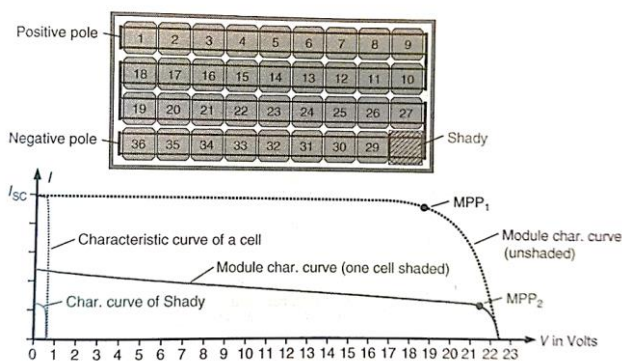


Figure 70 - 36 cell solar module with associated IV-curve. Cells are serial connected and one is shaded [23].

In Figure 70 an illustration of what happens if the radiance levels on a single PV cell in series is considerably reduced. As some electrons is excited the open source voltage is not affected, but as the flow of electrons increase, the bottleneck of the shaded cell becomes apparent. Even at closed circuit, the flow is considerable lower for the whole module.

Apart from the apparent thing to remove the object that is shading, the next measure is to reduce the impact of the shading. This can be done by bypassing the shaded cells i.e. by mounting diodes in parallel of the cells.

To mount a bypass diode over each cell is impractical for the actual module production, temperature increase, cost and so on. Typically one bypass diode is used for every 12, 18, or 24 cells [23]. Different IV-curves for different numbers of bypass diodes can be seen in Figure 71.

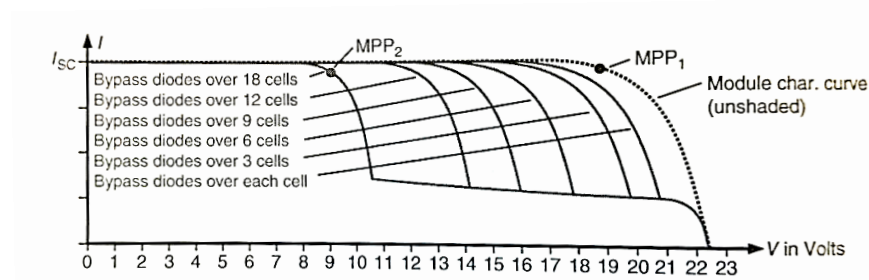


Figure 71 - The effect on the IV-curve with different number of bypass diodes in a PV module [23].

As each module only have a few bypass diodes, the shading i.e. of a proportion of a module might have different effect depending of what part of the module that is shaded. If the shading covers cells in all the serial connected cells, the effect would be greater than the shadowed proportion. However, if the same proportion of shading just covers a single string of serial connected cells, the impact would be much less. It is therefore important to be aware of which strings in the module that have bypass diodes in order to take the near shading into account when deciding on how to mount the modules.

The effect of shading is not uniform for all PV technologies. I.e. thin film is considerably less affected by shading as illustrated in Figure 72. This is because the voltage needed to pass the pn-junction is much lower than for crystalline silicon.

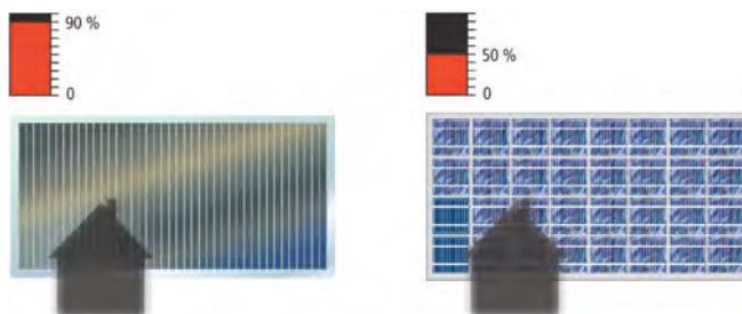


Figure 72 - The effect of shading on a thin film module (left) and crystalline silicon module with no bypass diodes [24].

The same effect as described above related to single modules is also highly important for systems as a whole. How many modules in a string. How to mount them with regards to shadows. And so on. If the modules in Figure 73 are serial connected, and the cells in each module also is serial connected with three bypass diodes and the internal strings going lengthwise, the power output for these systems would be very different. In the system to the right the tree only covers one to two strings in each module, each protected by a bypass diode. Some reduction due to the reduction of irradiance. In the system to the left, the tree covers all strings in three modules. In this case, all three modules must activate their bypass diodes for the system as a whole not to be affected. In this case we highly affected three modules, in comparison to the first case where only two is partly affected.

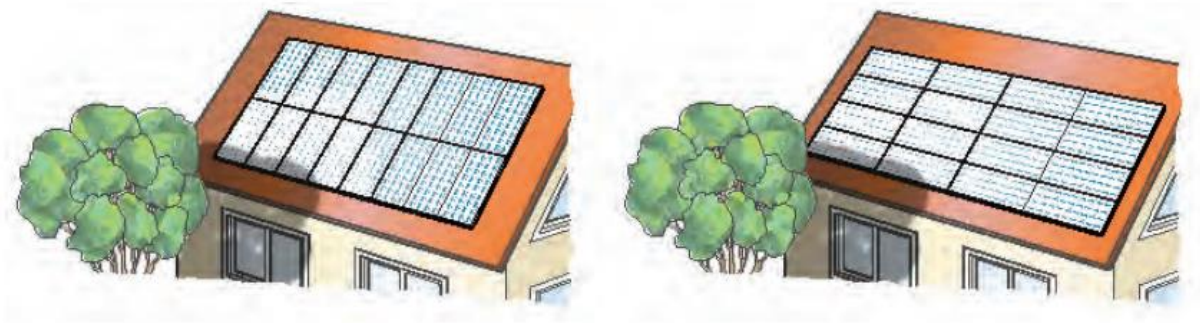


Figure 73 - Shading on vertical and horizontal mounted PV modules [24].

For northern latitudes the sun path is lower than for more central latitudes and by this reason more prone to near shading as seen in the sun path diagrams in chapter 2.1.3.

In order to take the near shading into account a 3D model of the PV module setup and the near shading environment has to be made. The 3D model of the Acusticum was made in PVSYST v6.32 and can be found in Figure 75. The perspective in this illustration is almost the same as in the aerial photo of the Acusticum in chapter 1.4.



Figure 74 - Near shading from a tree at roof A. Photo by Eirik Oksavik Lockertsen.

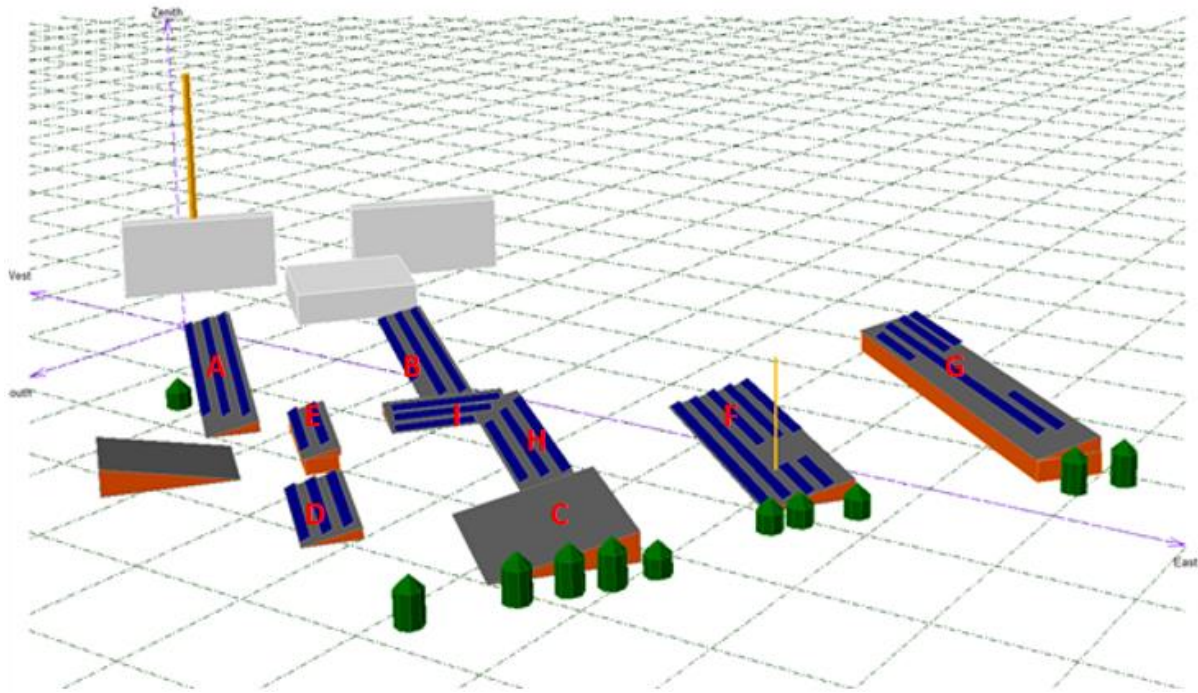


Figure 75 - 3D model of the PV module layout and near shading at the Acusticum by Øystein Kleven and Eirik Oksavik Lockertsen.

As the amount of near shading fluctuates throughout the day and year, this of course results in a % wise amount of shading towards the horizon. This is calculated in PVSYST v6.32 based on the drawn 3D model and illustrated in Figure 76. The tall buildings in the vest can clearly be seen in the top and bottom illustration, and for the middle illustration from roof I, the shading from roof E is also easy to notice.

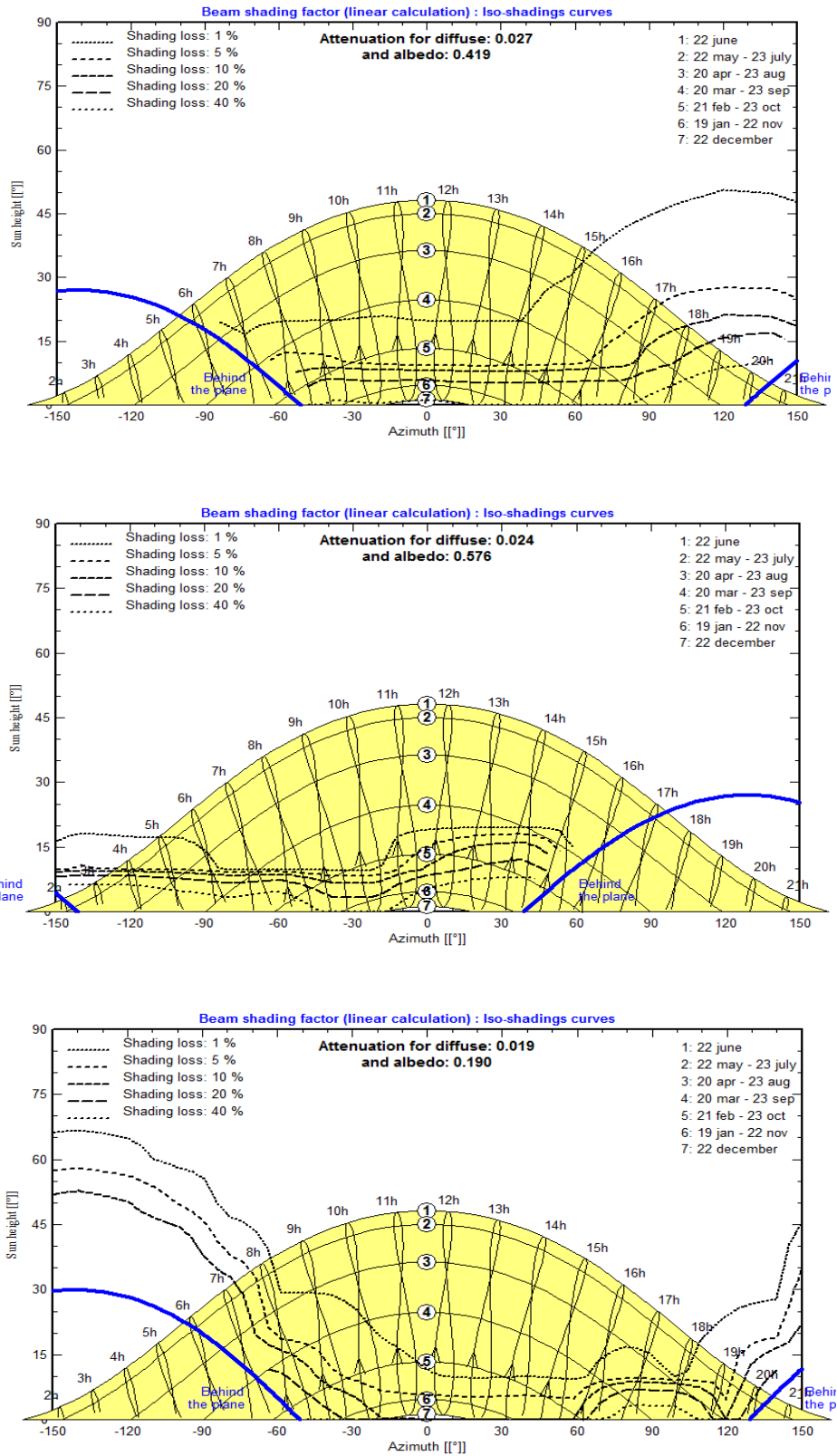


Figure 76 - Beam shading factor for the Acusticum. The top illustration is all roofs except I and G, next is roof I, and the bottom illustration is roof G. Exports from PVSYST v6.32 based on Acusticum 3D model.

2.3.2.3 Temporary shading

Temporary shading is a result of i.e. soiling from the environment and snow. One study argues that loss due to soiling can be assumed to be in the area of two to five %, and losses related to snow are in most cases negligible [24]. However, this is of course very site dependent. One factor of temporary shading by soiling and snow is that one might get a total radiation blocking to the solar surface. From the other shading types, shading only blocks the direct radiation and parts of the diffuse radiation. This is an important difference from the other type of shadings. Some illustrations of temporary shadings can be seen in the figures below.



Figure 77 - Shading due to soiling. Shot at 19th of November 2014. Photo by Eirik Oksavik Lockertsen.



Figure 78 - Shading due to frost. Photo by Eirik Oksavik Lockertsen.

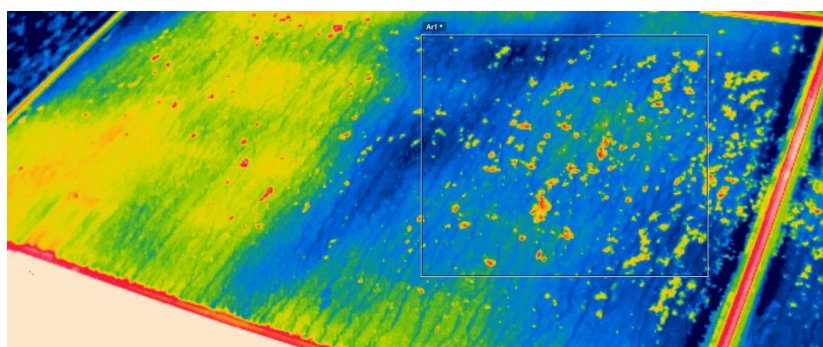


Figure 79 - Thermography of shading due to soiling. Instead of the radiance reaching the cell, the radiation is converted into heat on top of the module. The difference between minimum and maximum temperature within Ar1 is 6.3 °C. Thermography of the same roof as the illustrations above. Picture by Assistant Professor Arvid Dalebaug at NTNU.

At northern latitudes snow naturally is a large contributor to the temporary shading. There exists however no research on the area except the experiences from the Glava Energy Centre (GEC) in Sweden, located inland at about 60°N. These numbers are also those used by Multiconsult (2013) in their LCOE report for PV in Norway. For this report the use of the near shadings for Trondheim as defined by Multiconsult is used [20]. These can be seen in Table 4.

Table 4 - Temporary shading loss factors.

	Jan.	Feb.	Mar.	Apr.	May	Jun.	Jul.	Aug.	Sep.	Oct.	Nov.	Dec.
Trondheim	80 %	80 %	50 %	0 %	0 %	0 %	0 %	0 %	0 %	0 %	0 %	50 %

For the Acusticum, even if the PV system has been operating since December 2014, this winter there have been relatively large amounts of snow as illustrated in Figure 80. One can barely make out the three rows of modules on the roof.



Figure 80 - Snow on the roof of the Acusticum. Roof A is the largest roof in the picture. Shot at 9th of February 2015. Photo by Øystein Kleven.

2.3.3 The inverter

The main functions of an inverter are [23, 24]: The ability to convert DC to AC, preferably with low harmonic distortions. As the optimal voltage of a module changes according to the insolation, the inverter should also be able to track this maximum power point (MPPT) as illustrated in Figure 81. It should also have AC and DC protection schemes as overload and overvoltage protection, and sufficient insulation capabilities for personnel protection. The ability to monitor, store and display operational data of the system. In addition, grid monitoring and management for i.e. utilize reactive power capabilities and avoid islanding of the PV system.

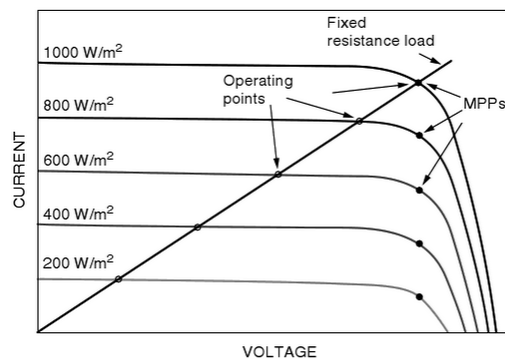


Figure 81 - Operating points for a fixed resistance load at different insolation levels vs. MPP [75].

The above properties and functions of a converter can be implemented in a number of ways. Several different system configurations have therefor been developed as I will illustrate in chapter 2.3.3.2.

In addition I will take little deeper look into the efficiency, DC/AC conversion and considerations related to the grid.

2.3.3.1 Inverter efficiency

Inverter efficiency consists of two components [24]; The adaptive efficiency which is to what degree the inverter manages to keep track of the consciously changing radiation levels

and the subsequent change in power point. The other is the actual conversion itself of input vs. output power.

As the input power naturally varies a lot, this represent a huge challenge for the inverter. Some compromises must be done in order to keep the efficiency up for different power input levels. To describe the efficiency with a single number is therefore difficult as one does not have any control of the input. One way of describing the efficiency of inverters is through efficiency characteristic curves as illustrated in Figure 82.

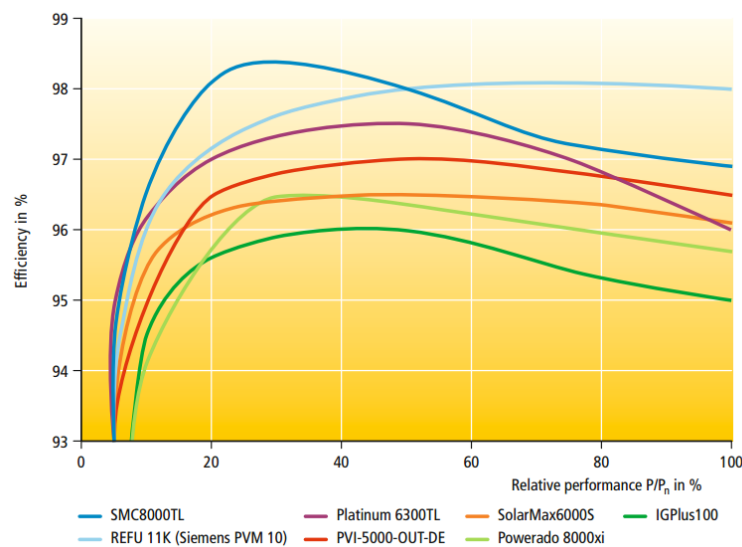


Figure 82 - Efficiency characteristic curves for different inverter manufactures [24].

The comparison of inverters only through graphs, and not numbers, is not ideal. In order to easily compare different inverters on a numeric scale two different efficiency scales have been developed; The European (Euro) and the Californian (CEC) efficiency factors. The difference between them is how much they weight the efficiency of the inverter at different stages up to its nominal power. The reason for this is because in California the radiation is much higher in average than in Europe, and the inverter will therefore be used a longer time towards its nominal power in California than in Europe. In Figure 83 the different weighting for different nominal performance factors is illustrated for two inverters with different optimal markets.

For modern inverters, the difference in efficiency factors between European and Californian efficiency is within the range of half a % [24].

For northern latitudes both the Euro and CEC weighting is rather unsuitable as the distribution of irradiation are rather different.

If the inverters for PV systems at northern latitudes are dimensioned for the peak hours, the inverters would run at low capacity a lot of the time. It is therefore important, at these high latitudes where a large share of the insolation is in the lower

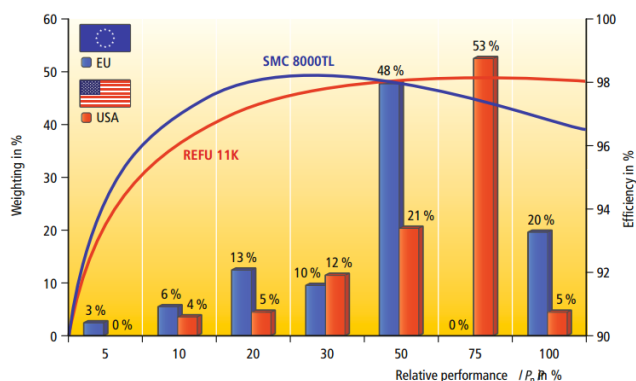


Figure 83 - Comparison of Euro and CEC efficient factors with two different inverters [24].

part of the irradiation scale as seen in Figure 87, to choose an inverter that performs well at these low values. An under dimension of the inverters will result in a cut-off at high input values, but may be an option in order to run the inverters at a higher capacity at a larger proportion of the year. Though can the low temperatures result in performances above the power at STC.

2.3.3.2 Different grid connected inverter concepts

The main type of concepts are shown in Figure 84. What concept to go for in different PV systems depends on the system internal and external factors. At one concept end the central inverter might be a good option if one have relatively many modules, little to no shading and low interferences between modules for same irradiance. At the other concept end we have the module-, also called micro inverters. These can be a good option if the PV system scale is small and further development of it is going gradually, the redundancy and downtime is important, installation simplicity is important, and the top notch efficiencies are not the highest priority. String and multi-string inverters are middle solutions that might also be good options depending on the system characteristics. In addition to the concept

listed, other concepts as the DC bus concept is also emerging. This is similar to the multi-string concept, but each DC-DC converter is placed on each module. Today SolarEdge is inverter producer associated with this technology.

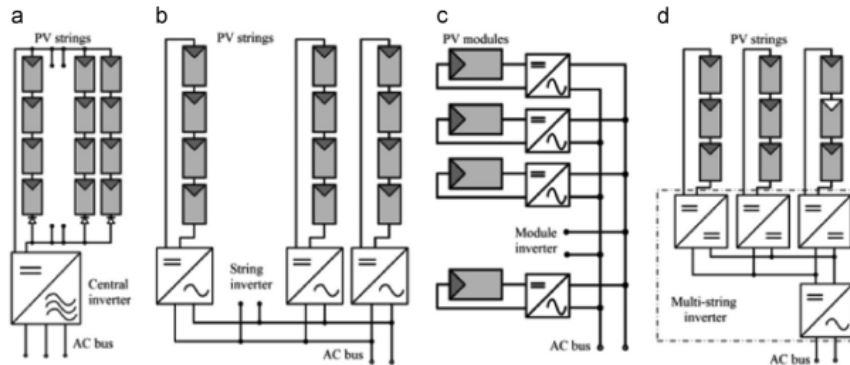


Figure 84 - Different grid connected inverter concepts.

(a) Central inverter, (b) string inverter, (c) module inverter, (d) multi-string inverter [6].

The development in inverters on the micro scale have the last years been noticeable. In addition to the resistance to the shading issue and good handling of module mismatch [82], other positive sides like the low cost of installation, the ease of power output scalability and possibility of eliminating harmonic distortion through intelligently linked micro inverters into swarms [83]. There are also now produced PV modules with integrated micro inverters called AC modules [24]. The MPPT voltage tracking area for these are in most cases relative high, meaning i.e. that if one of three strings in one three bypass-diode-module is shaded, the last two often is out of the MPPT voltage range of the micro inverter. In comparison the DC-DC inverter and MPPT for the DC bus concept for SolarEdge have a MPPT range that also covers down to one string operational in each module.

Another concept rarely used, but could be quite interesting for northern latitudes because of the high share of low irradiance, is the ability to choose how many modules to connect to one inverter depending on the amount of irradiance. I.e. if one have a base system of three string inverters with numbers of modules for each string dimensioned after peak performance. For low irradiance conditions the inverters will normally have to operate at

an efficient level lower than for higher irradiance conditions. But if all three strings could be switched in series onto one inverter for low irradiance conditions, the overall efficiency could be improved because the inverter operates in a more ideal area of operation.

2.3.3.3 Acusticum inverters

Originally offered SMA string inverters, but as PiteEnergy already had inverters from SolarEdge DC bus concept, and the cost different up to this solution in total was assessed to sufficiently small.



Figure 85 - The inverters at the Acusticum. Photo by Eirik Oksavik Lockertsen.

For the Acusticum the SolarEdge inverter SE17K have been chosen. 13 in total as seen in Figure 85. These are located at the eastern wall at the building with the C roof. As the model name indicates the rated and maximum power output of the inverter is 17 kW. The recommended maximum STC DC power input is 21.25 kW and the European weighted efficiency is 97.7 %. The efficiency chart of this inverter can be seen in Figure 86. In addition, Figure 105 illustrate quite well one aspect of the demanding conditions the inverter have to work in with fast fluctuating input.

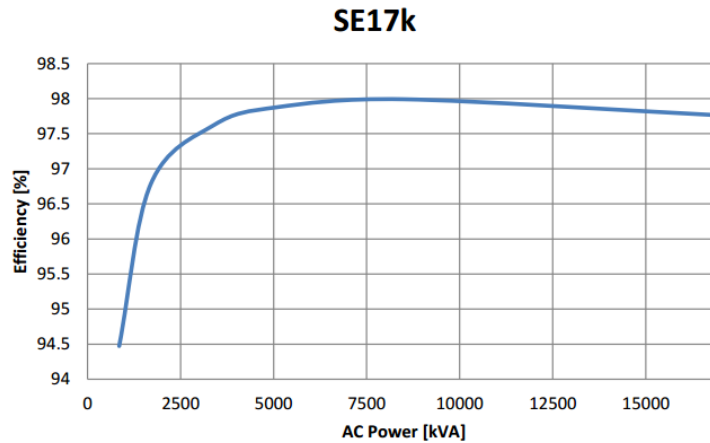


Figure 86 - The efficiency characteristic curves for SolarEdge SE17K [84].

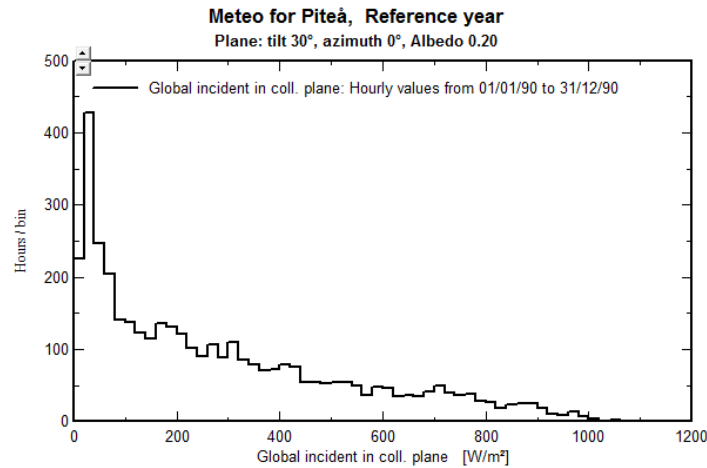


Figure 87 - Number of hours of total irradiation for different insolation values in Piteå in a reference year [71]. PVSYST v6.32 and Meteonorm 7.1 database.

Compared to other inverters, the SE17K have a rather good performance also for low power input. This is an important quality of the inverter as a rather big porprtion of the incoming radiance at these northern latitudes is of rather low power, and thereby low power levels to the inverter, as seen in Figure 87. However, as the figures above illustrates quite good, the high amount of low light power combined by the rapid reduction in efficiency does make it interesting. How will the inverter handel to operate at these low extremes for so much of the time? And is the inverter good enough modelled to accuratly enough calculate the expected energy yield?

The SE17K is specially designed to work with power optimizers. This inverter is accompanied by the SolarEdge power optimizers. 125 of the P350 and 395 of the P600 and 15 of the P700. The number in the model name stands for the rated power input. As seen in chapter 2.3.1.2 regarding the PV modules used, the limit on 600 W per two modules will most likely not represent a mentionable limitation.

A total of 11.25 kW is maximum string power. From Table 5 we see that a maximum of 42 modules was used for a single string. Just below the maximum string power.

The P350 have a MPPT operating range of 8 to 48 V. This is a long interval, even covering the low voltage case if two out of three module internal strings are not operating, i.e. because of shading. The P600 have a MPPT operating range of 12.5 to 80 V. The 40 V per module is closer to the panel limit as seen in Figure 66, but still within the acceptable range.

The P600 and the P700 connects to two modules instead of one. Otherwise practically no differences compared to the P350. The P350 have a weighted⁶ efficiency of 98.8 %, marginally more than for the P600 on 98.6 %.

Table 5 - Inverter setup on the Acusticum. The ratio is the module STC power divided by the rated power of the transformer [77].

Inverter	String 1		String 2		Total	
	# modules	String name	# modules	String name	# modules	Ratio
7E18255C-17	31	G1	34	G2	65	1.018
7E18253B-F6	32	G3	33	G4	65	1.018
7E182562-1D	33	F4	35	F5	68	1.065
7E18257B-36	38	F6	32	F2	70	1.097
7E182540-FB	32	F3	35	F1	67	1.050
7E18257A-35	39	A5	32	B1	71	1.104
7E182573-2E	33	A3	34	B2	67	1.043
7E182550-OB	40	B3	30	A2	70	1.091
7E18254F-0A	42	B4	30	A1	72	1.121
7E18256E-29	36	A4	33	HI1	69	1.096
7E182569-24	40	HI3	29	HI4	69	1.082
7E182571-2C	38	HI2	30	D2	68	1.066
7E182561-1C	40	E1	30	D1	70	1.091
TOTAL					891	1.068

⁶ What kind of weighting is not given in the data sheet.

As Table 5 shows the ratio between the modules STC power divided by the rated power of the transformer in most strings is just above 1. One inverters have a ratio of 1.121. Combined with low temperatures and a high level of irradiation one might see periods of saturation. Although these periods will most likely be very short and negligible. On the other hand, pushing the ratio to the max reduces the time the inverters will have to operate in low power conditions where the efficiency is particular low. This is important for these northern latitudes where a higher proportion of the radiance is rather low compared to further south.

2.3.4 Cabling

Concepts like microinverters and the SolarEdge architecture have an advantage when it comes to safety. For installation the optimizer/microinverter will not produce any electricity before it is connected to the grid or is given any other activating signal. It is just the short non-lethal distance between the module and the optimizer/microinverter that potentially delivers power during installation, not whole strings. In addition, in case of fire in the building with an installed PV system, when the fire department as normal procedure cuts power, also all the power to the optimizer/microinverter is stopped. This is not the case of string inverters, where potential harmful levels of electricity is flowing in wires in the building – even after cutting the power to the grid.

For the Acusticum this is an advantage as there is in total about 7 km of cables installed in the PV system, connecting the power optimizers and the inverters.

The cables used has a thickness of 6 mm². Combined with the relatively high nominal operating voltage between the power optimizers and the inverters of 750 V, and the relatively low numbers of modules per string of around 35, this gives rather low losses. Øystein Kleven calculated these losses to about 0.8 %. Also the cable thickness used is also compatible with standard MC-4 socket, making installation much simpler and faster.

2.3.5 PV system mechanical aspects

For northern latitudes the climate is rougher than further south. This puts more strain on the PV system, and especially the modules which is the most exposed.

I.e. snow is a natural aspect to consider. SweModule, the PV modules used at the Acusticum, follows the UL 1703 standard which states that the modules should withstand a downwards pressure of up to 5400 Pa (550 kg/m²) if mounted according to instructions [85]. This weight equals to considerable amounts of snow, and for modules mounted at exposed sites this weight will most likely never be reached.

For the Acusticum PV system, one module was shattered during the winter, around 15 modules had rather sever damages to the lower frame, and a considerable amount of modules had indications on a bent lower frame. This illustrated in Figure 88.



Figure 88 - Shattered, severely bent, and minor bent modules at the Acusticum PV system. Photos by Eirik Oksavik Lockertsen.

How could this have happened? As seen in Figure 80 and Figure 89 there was snow on the modules this winter, but not enough to reach the limits set by the standard. But as the

standard states, this is downwards pressure. These modules are mounted at 27° and 30° tilt making a considerable pressure on the frame. First pulling the frame out of position, and thereby weakening the module construction is probably the cause of the shattered module. The SweModule installation manual does not mention any tilt angles to avoid [85]. The mounting manual for REC Peak energy series modules states that “*Site-specific loads such as wind or snow which may exert forces in a different way need to be taken into consideration to ensure this limit is not exceeded for each respective mounting option.*” [86] Although not mentioning any particular tilt angles, one might expect a tilt angle interval where the angle is too low for most of the snow to fall off, and too high to be within the boundaries of the module pressure limit. This might be the work on further research and updated standards for modules used in northern latitudes. In fact, work on elaborating and enforcing the performance standards for PV modules and systems in various climatic environments is one of four non-economic barriers suggested by the International Energy Agency that should be addressed in the next five years [3].



Figure 89 – Snow covering PV modules at roof A. The shattered module is the 4th in the middle row. Shot at 27th of March 2015. Photo by Øystein Kleven.

A possible solution to circumvent the problem might be to use frame-less modules. The snow will not have a frame to strain and thereby not weakening the module construction. An illustration of frame-less vs. framed modules can be seen in Figure 90.

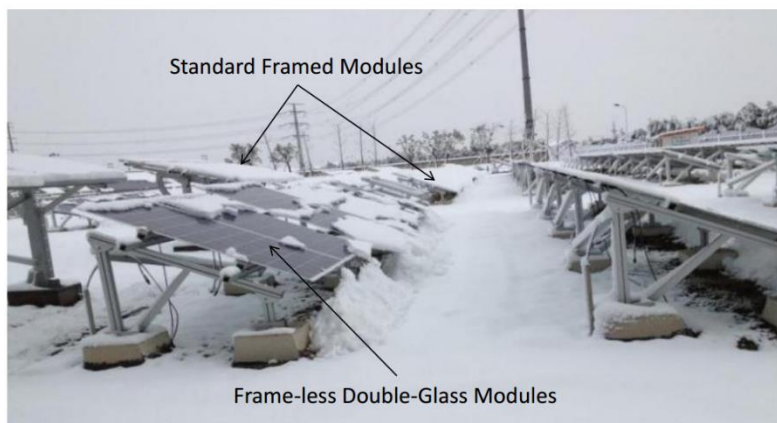


Figure 90 – Snow accumulation difference on standard framed and frame-less modules [87].

2.4 PV system modelling

In this chapter first some important terms related to PV system performance is given, next a brief overview of different software available for helping the PV system planning process, and last a summary of the input variables for the PV simulation software PVSYST is given.

2.4.1 Important terms related to PV system performance

Some of these have been mention earlier, but will be repeated her as a reminder.

$[kW_p]$ is the performance of the module under STC (see 2.3.1.4). This is not far from the top of what one could anticipate from the module with close to perfect conditions. (The “p” stands for peak.)

$[kWh/kW_p, Year]$ can be used several ways. One is to compare average numbers between geographical sites to predict energy yield towards installed W_p . Other is to compare different system configuration efficiencies at the same geographical region.

Performance Ratio (PR) is the ratio between the actual energy production and a system with no loss.

2.4.2 Software for PV systems

The process of designing an optimal PV system for given locations can be very difficult. There are many factors to take into considerations, some static, but also dynamic. The need for decision support systems in one or several parts of this process have been made up through the years. Several of the available systems are shown in Figure 91.

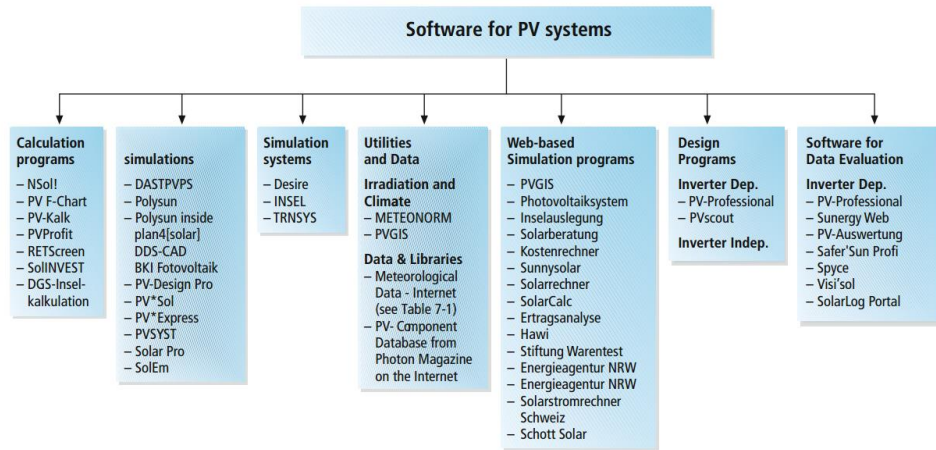


Figure 91 - An overview of different decision support software for PV systems [24].

A comprehensive and relatively easy to understand description of several of these softwares can be found in “Planning and installing photovoltaic systems” by the German Solar Energy Society from 2013 [24].

For fast initial PV system potential assessment the web-based simulation program from PVGIS is a good start. An interesting approach on solar potential simulation is to do the simulation not for a single site, but for whole areas. An example of this is the sun map of Stockholm as seen in Figure 92. Here the rooftop potential for Stockholm have been calculated down to the orientation of each roof. This makes the information on solar potential very easy accessible and user friendly. The data is based on the STRÅNG irradiation database.

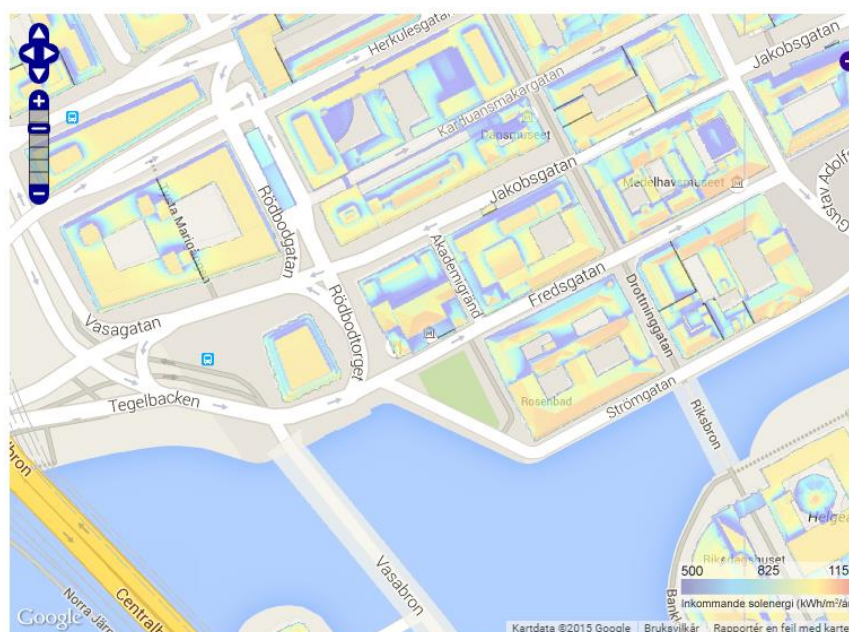


Figure 92 - Urban rooftop solar potential in Stockholm [88].

An example on a little more holistic perspective, also considering the economy of the PV system is the program Solelekonomi. Fairly easy to use, and gives some fast insight to the bottom line of a PV project [89, 90].

The program that will be used later in this thesis is PVSYST v6.32. Its development started in 1992 at the University of Geneva and is considered as a classic among PV system simulation softwares. It has abundance of functions, but comes at a price of high complexity. The program target audience is those who have a very good knowledge of the theory of PV systems [24].

2.4.3 Summary of input parameters to simulation program

The EcoPlus260 module has a rated STC power of 260.3 Wp. The Module average was found to be 264.84 Wp. To adjust for the additional power, a negative loss of 1.7 % will be added to the mismatch loss component as this does not inflict any loss on the system due to the SolarEdge architecture.

According to recommendations from PVSYST the near shading should be simulated as “Linear”. This means that the string setup has no influence on the estimated energy output

from the PV system. This is as expected for a system based on individual module MPPT tracking.

PVSYST v6.32 only supports eight sub-array configurations. Their suggested method for simulating systems with the SolarEdge architecture is to have one sub-array for each string length. Each sub array then multiplied by the number of strings with that particular length. This will off-course not correspond to the number of inverters, so the number of inverters are given in fractions for each sub-array. As seen in Table 5 on page 74, the Acusticum have 12 different string lengths. For the simulation four of these strings have been added or subtracted to a string similar in length to get below the boundaries set by PVSYST v6.32. These calculations can be found in appendix 7. The final sub-array configuration input to PVSYST v6.32 is shown in Table 6.

Table 6 - PVSYST sub-array input.

PVSYST string name	# modules	# strings	Sum modules	Total fraction of inverter used	Azimuth used (0° is south)	Tilt used
5x30	30	5	150	2,135	38.9	27
5x32	32	5	160	2,355	38.9	27
4x33	33	4	132	1,964	38.9	30
2x34	34	2	68	1,031	38.9	27
3x35	35	3	105	1,559	38.9	27
3x38	38	3	114	1,651	38.9	27
3x40	40	3	120	1,723	38.9	27
1x42	42	1	42	0,583	-51.1	27
			891	13		
			# modules	# inverters		

Roof I has an azimuth of -51.1 degrees with a southern reference. This roof has 47 modules which are simulated in 42 module string named “1x42”. Roof G has a tilt of 30 degrees. This roof has 130 modules and are simulated under the name “4x33”. The differences between actual situation and simulation setup are too small to have a mentionable influence the end result. Please use the 3D model in chapter 2.3.2.2 for reference. In comparison, Multiconsult uses in their PV LCOE report (2011) a tilt of 27° for private households, 20°

for office- and industrial buildings and 30° for ground mounted utility size systems for all sites in their report. Taken the relatively rather big geographical differences between the sites this is an interesting choice.

The power optimizer SolarEdge P350 will be used for simulations. The differences between this the other power optimizers installed are considered negligible because of very similar characteristics.

The meteorological data used, irradiation, wind and temperature, is collected through the NASA/SSE database.

Shading due to soiling is set equal to the factors in Table 4.

Lowest temperature is set to -15°C.

The albedo is set to 0.2 all year as the vicinity is mostly trees.

In the thermal parameter section the PV module mounting is set to “«Free» mounted modules with air circulation”.

Other values are default in PVSYST v6.32 and can be seen in the simulation report in appendix 8.

All files used and produced in PVSYST is attached as a file in the electronic publication of this thesis.

2.5 Expected energy production

For the first simulation all parameters are as earlier described. This is the expected result. The essence of the simulation results are shown in the loss diagram in Figure 93. As this shows, the first year energy production is expected to be 208 MWh. The performance ratio is 0.850 and the specific production is 897 kWh/kWp. The complete simulation report can be found in appendix 8.

From the loss diagram the loss due to soiling clearly stands out as the biggest loss contributor with a loss of 7.1 %. This is also shown more clearly in the monthly loss factors in Figure 94. The added irradiation due to the module tilt and azimuth is 17.5 %. The loss due to soiling was defined on the background of findings at the Glava Energy Center, but these values are of course very site dependent. As seen in both Figure 80 and Figure 89 the amount of snow at the Acusticum PV system, at least this winter, is probably higher than what is simulated. Point being, how much should one take the optimal irradiation tilt and azimuth into consideration vs best positioning for minimizing snow accumulation? In addition, will the use of frame-less modules in light of this be an even better choice for northern latitudes? I.e. instead of separate rows, would interconnecting frame-less modules mounted at the edge of the roof be a better option? Further research is needed to answer this.

To illustrate the influence of the loss due to soiling (snow) and the near shading, these factors were reduced to zero. The main result can be seen in Figure 95 and Figure 97. Expected energy yield is now 231.5 MWh with a performance ratio of 0.948 and specific production up to 999kWh/kWp.

To illustrate the influence of optimizing the tilt and azimuth a simulation was done with these optimized and no near shading. The loss diagram for this scenario can be seen in Figure 96. Expected energy yield is 228.4 MWh, less than the previous scenario.

As these two illustrations show, it might be better to minimize snow accumulation before irradiation optimization for PV systems in northern latitudes.

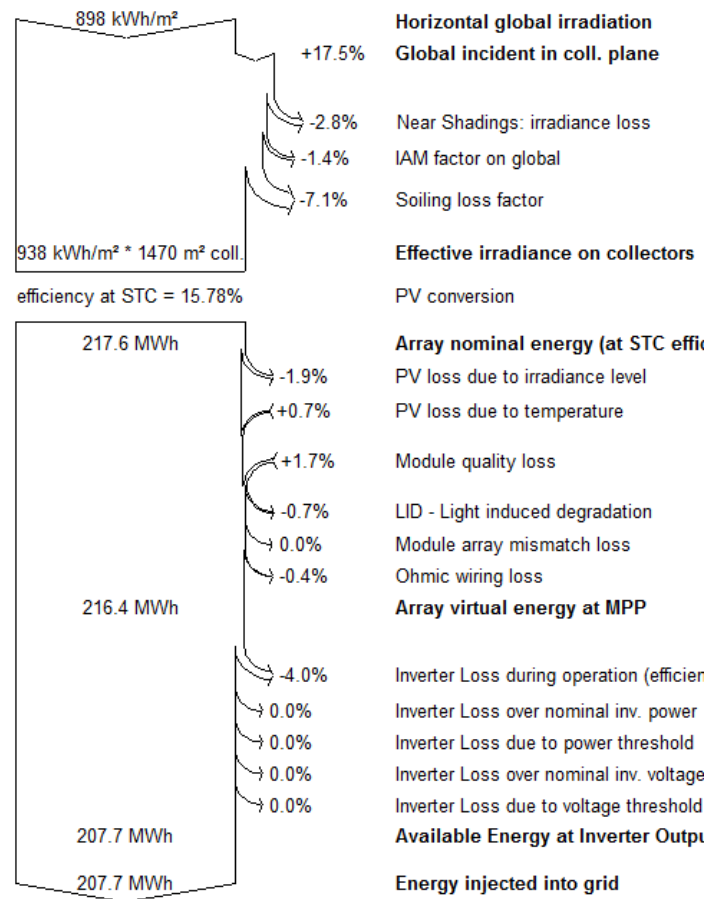


Figure 93 - Loss diagram of the expected energy output. Generated by PVSYSYST v6.32.

Normalized productions (per installed kWp): Nominal power 232 kWp

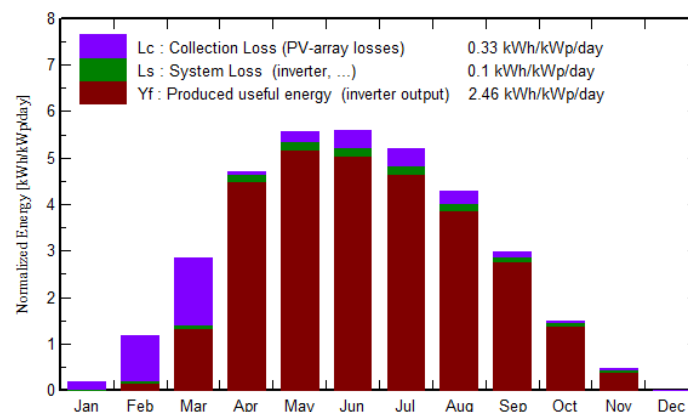


Figure 94 - Loss factors for the expected energy output split into months. Generated by PVSYSYST v6.32.

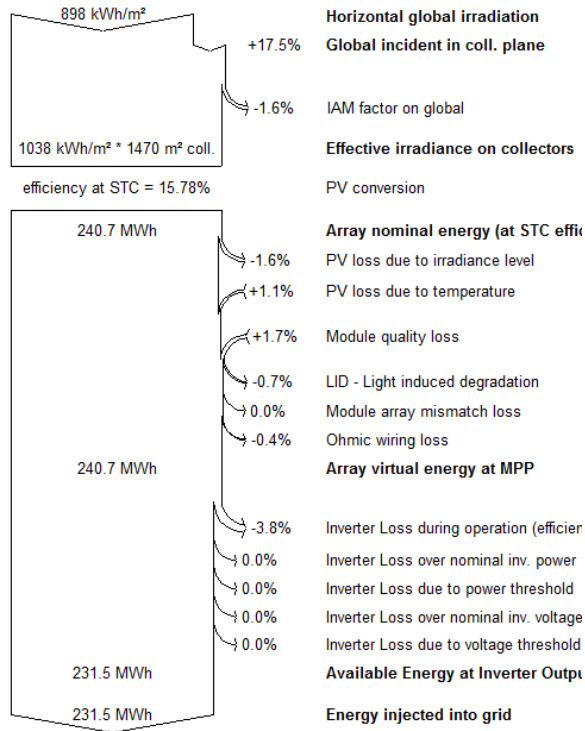


Figure 95 - Loss diagram of the expected energy output, but no near shading and loss due to soiling. Generated by PVSYST v6.32.

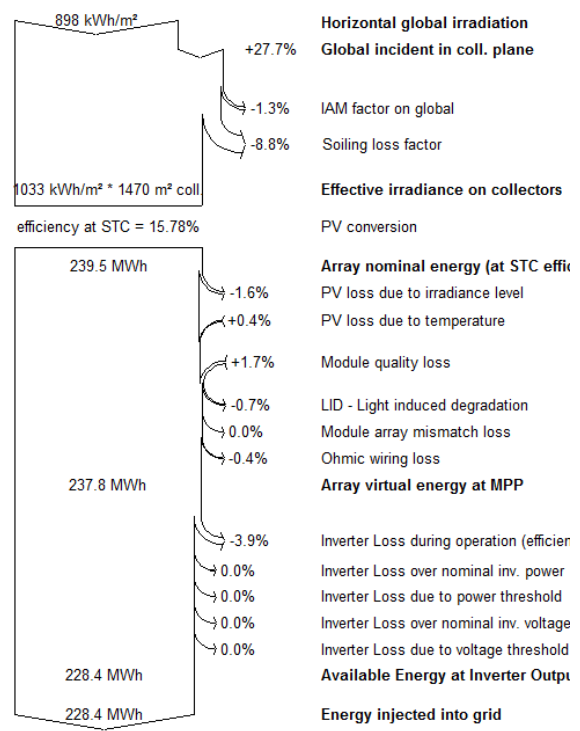


Figure 96 - Loss diagram of the expected energy output, but no near shading and module tilt (48°) and azimuth (0°) to optimize energy production. Generated by PVSYST v6.32.

Normalized productions (per installed kWp): Nominal power 232 kWp

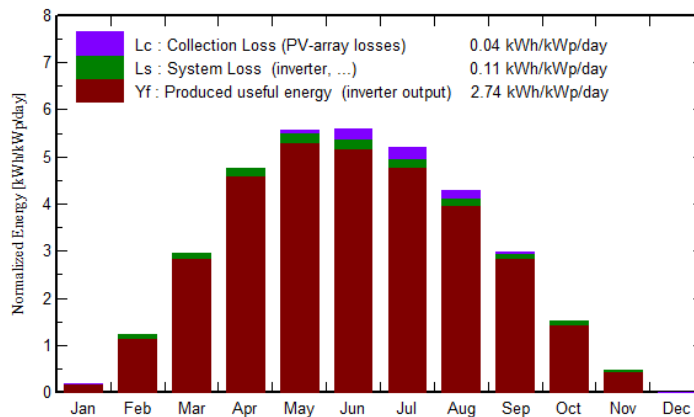


Figure 97 - Loss factors for the expected energy output split into months, but no near shading and loss due to soiling. Corresponding to the loss diagram in Figure 95. Generated by PVSYST v6.32.

For the later economical calculations the first year energy yield of 208 MWh will be used.

2.6 Actual vs expected energy production for May 2015

Because of especially large amounts of snow this last winter in Piteå, some PV modules was covered by snow also in April. In order to have a full month to compare to and as few biases as possible May 2015 was chosen.

The energy production is reported by the SolarEdge system itself, through an access restricted portal. Access to this was granted by Øystein Kleven. The total energy at the inverter outputs (AC energy) produced by the PV system at the Acusticum May 2015 was 25.81 MWh. This AC energy report can be found in appendix 9.

In order to compare this actual energy production to the expected, an average meteorological May month for Piteå is obviously not satisfactory, and actual meteorological parameters is needed.

The PV system at the Acusticum is equipped with a temperature-, wind- and irradiation sensor. The temperature sensor is located a few meters north of the inverters, on the eastern wall of the C roof building. The wind- and irradiation sensor is located on top of the C roof at the eastern end. These sensors can be seen in Figure 98 and Figure 99. As seen from these pictures, and earlier aerial photos, the threes to the east will most likely influence the results.

The irradiation sensor is a silicon irradiance sensor from Mencke & Tegtmeyer, model nr Si-01TC-T. It is placed in-plane with most of the modules. Tilt of 27° and azimuth of 39° (0° is South). Measuring as seen global irradiance. These data are also stored and available through the SolarEdge restricted portal.

As the irradiation is of particular high importance, hourly GHI and DNI data from May 2015 was exported from the STRÅNG database [66]. The position used as input is as earlier described for the Acusticum. This was the only database freely available, and as discussed in an earlier chapter, of relatively high quality.

The hourly data from the sources above are gathered in a single file for import to PVSYST. This file can be found as an add-on to the electronic publication of this thesis.



Figure 98 - Placement of the Acusticum temperature-, wind- and irradiance sensors. Photo by Eirik Oksavik Lockertsen.



Figure 99 - The Acusticum wind- and irradiance sensors. Photo by Eirik Oksavik Lockertsen.

Based on the temperature-, wind- and irradiance data from the Acusticum the AC energy production from the Acusticum PV system was estimated to be 28.46 MWh as seen in the loss diagram in Figure 100. This is 10.3 % higher than the reported from SolarEdge. The full PVSYST report can be found in appendix 10.

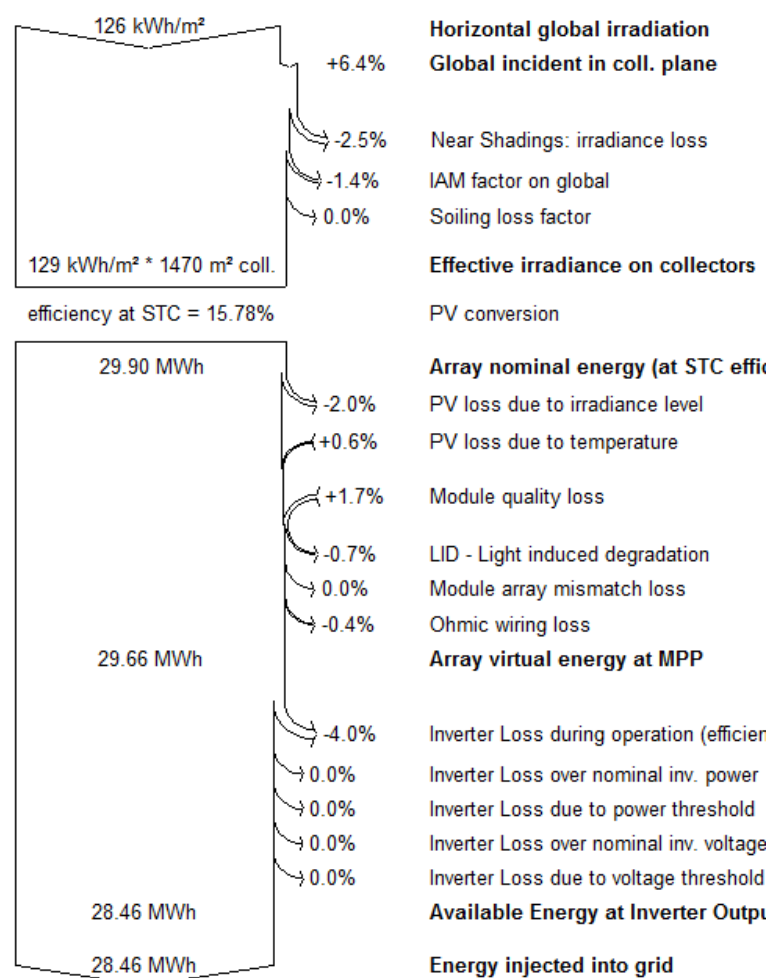


Figure 100 - Acusticum loss diagram for May 2015 based on temperature-, wind- and irradiation data from the Acusticum sensors.

How trustworthy are the irradiation data from the from the Acusticum sensor? In the dataset the irradiation at night never goes below 25.556 Wh/m²/h during the darkest night hours. It is getting lighter during the night this close the Arctic Circle, but the same numbers is reported the every night during May. This effect can also be seen in Figure 105. The total in-plane irradiation reported by the Acusticum irradiation sensor is 139.6 kWh/m². If 25.556 Wh/m² is subtracted of every hour the total would be 120.6 kWh/m². This is a reduction in irradiation of 13.6 %. A 13.6 % reduction of the estimated 28.65 MWh would result in a yield of 24.75 MWh. If one take into account that the sensor itself has some

rather serious shading to the east this might be the reason for the difference between the actual and the expected energy production.

Another possible explanation is a possible higher loss in the inverters. This might be because of the high levels of low light irradiance as discussed in the inverter chapter. To further investigate this, the hourly average power from every hour for all the strings was divided by the corresponding hourly average power for all the inverters. This was then plotted against the average inverter power input. The plot can be seen in Figure 101.

-

Figure 101 - Acusticum PV system inverter efficiency in May 2015.

As this figure clearly indicates is that it is in fact not the efficiency at low power levels, but the rest. This becomes more clearly when disregarding the values below 2 kW input as illustrated in Figure 102.

Figure 102 - Acusticum PV system inverter efficiency in May 2015 for power input above 2 kW.

Calculating a weighted average against the string power gives an average inverter efficiency of 89.1 %. This is far more than the expected, and calculated, efficiency of 96 % according to the loss diagram in Figure 100. Using the calculated loss gives an expected energy output of 26.42 MWh.

In addition, from the real system nine modules have not been working properly according to the SolarEdge web interface. As this is 1 % of the modules, this can in fact explain the last percent difference. Also, it should be mentioned that the earlier described shattered module is producing at almost similar levels as the working modules next to it.

A more trustworthy source of irradiation data is the STRÅNG database. Although not that geographical precise. Using STRÅNG irradiation data and wind- and temperature data from the Acusticum sensors results in an estimated AC energy of 28.65 MWh. This is almost exactly the same as reported using the Acusticum irradiation data. This indicates that the irradiation results from the Acusticum irradiation sensor might be correct and further strengthens the findings behind the reason for mismatch between the simulations and the reported energy output.

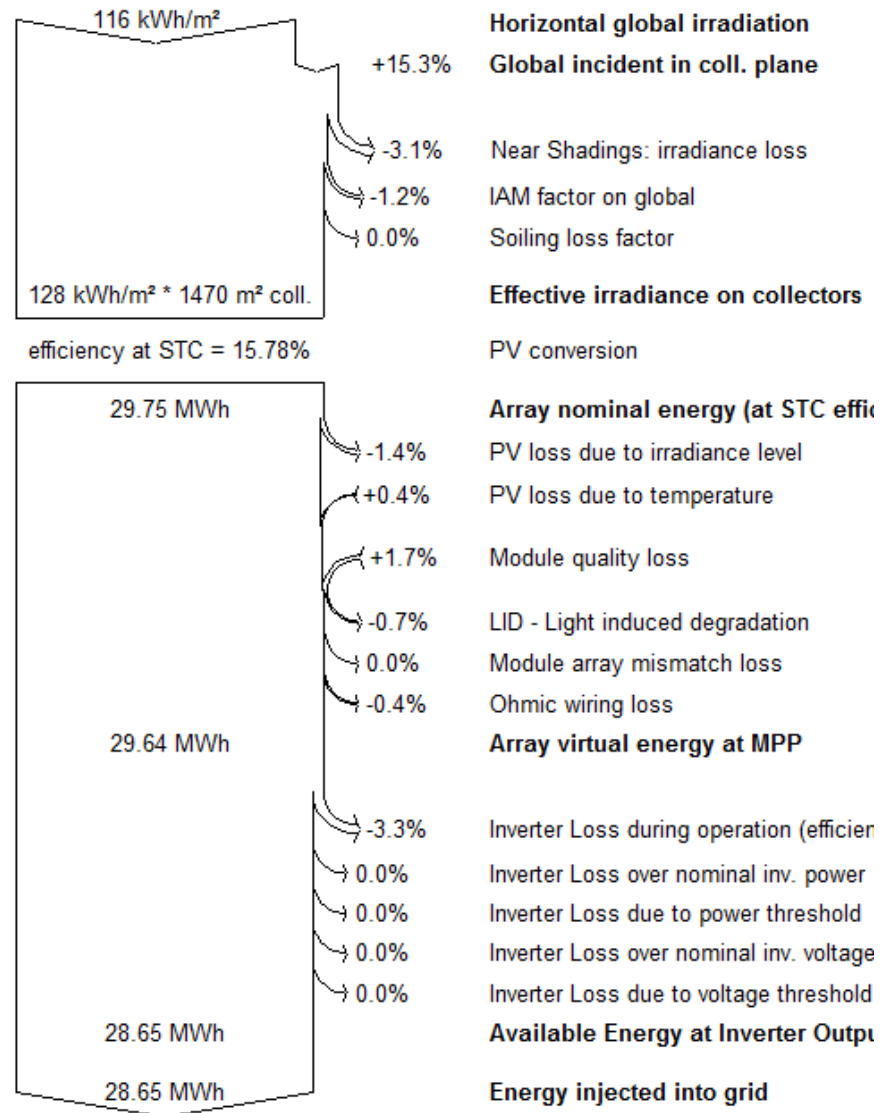


Figure 103 - Acusticum loss diagram for May 2015 based on temperature-, wind data from the Acusticum sensors, and STRÅNG data for the irradiation.

In order to reduce the complexity of the system, and thereby possible causes of faults, the PV system at the Acusticum was reduced to a model of only the E roof. This roof is not shaded and all modules have been working properly all of May.

From the SolarEdge portal the E roof reports an energy production of 1230 kWh during May 2015. The data can be found in the add-on file to the electronic publication of this thesis. Using the Acusticum meteorological data PVSYST calculates an AC energy production of 1317 kW as seen in the loss diagram in Figure 104. The complete report form PVSYST can be found in appendix 12. Correcting the simulated energy output with the found inverter efficiency gives a new energy injected to the grid of 1222 kWh. Marginally below the actual production.

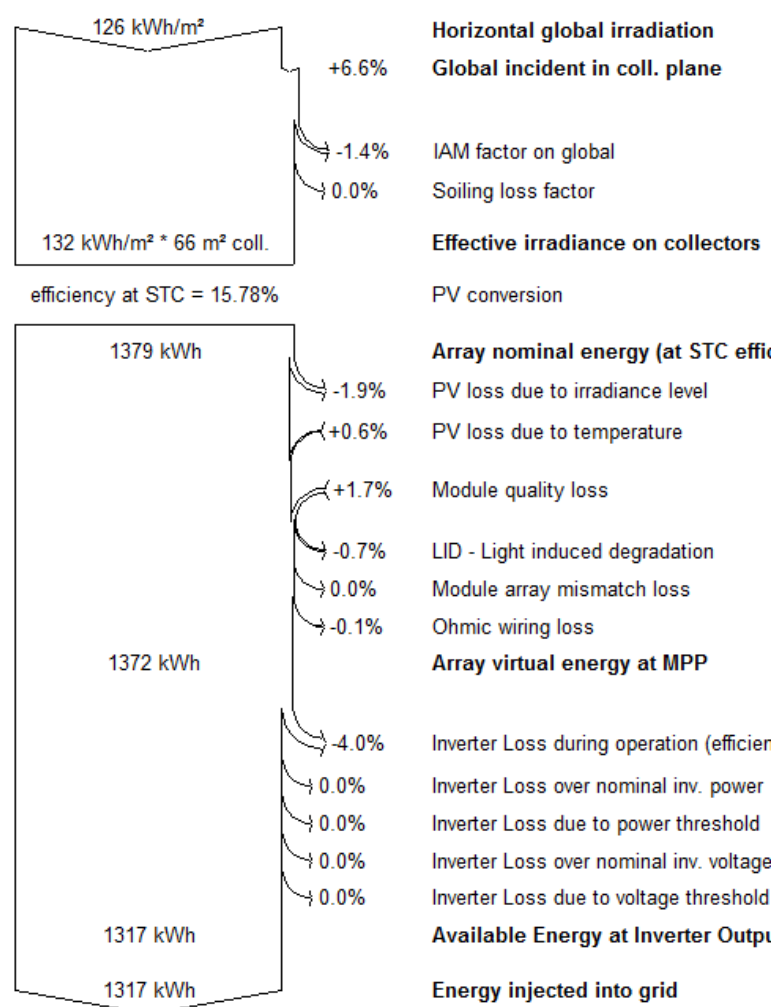


Figure 104 - Acusticum E-roof loss diagram for May 2015 based on temperature-, wind- and irradiation data from the Acusticum sensors.

However, the question remains; why the big difference between the reported efficiency by SolarEdge and the actual performance?

As the performance of an inverter is not only dependent on the power level input, but also how much and fast the irradiance is changing, this might be a possible cause. May did not have any stable weather. The irradiation sensor on the Acusticum PV system observed fast changing irradiance behaviour on several days in May. A detailed graph over the irradiance at the Acusticum 30th of May can be found in Figure 105, and as seen the fluctuations is both rather fast and rather high. This puts strain on the inverters. As the data before the power optimizer is not logged, any further investigation will not be done.

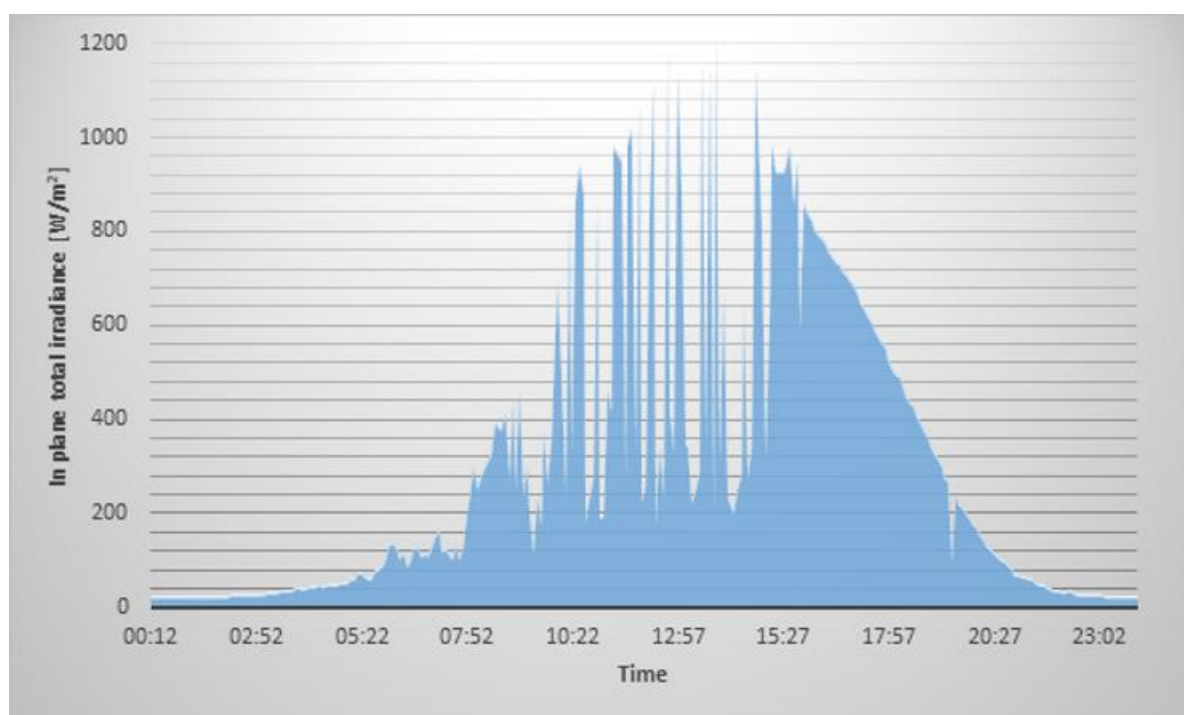


Figure 105 - In plane global irradiance (Azimuth of 39° (ref south), and tilt of 27°) at the Acusticum 30th of May 2015.

Because this actual vs expected energy is only over one month, the possible reduced yield is not taken into account in the later calculations. However, this is far from insignificant and should by all means be taken into consideration if the difference is shown to persist.

3 Cost of electricity from Acusticum PV system

What the actual cost of electricity from the Acusticum PV system is depends on the perspective and boundaries set by the analyser. As seen in the introduction the cost of electricity from PV systems differs a lot, an important reason is off course the geographical location as several studies indicates, but there are several other factors that have to be addressed.

In chapter 2, factors affecting the potential energy yield and especially for northern latitudes was discussed, and the expected energy from the Acusticum PV system was found to be 208 MWh for the first year of production. This is off course an important input factor for the cost of electricity from PV systems.

In this chapter first the methodology used for the cost calculations is described, next the installation- and annual cost of the Acusticum PV system will be given. A chapter on the cost of capital is then gone through before the cost of energy for the system is presented.

3.1 Cost of electricity methodology

The generation of electricity can be done in a numerous ways. Varying in resource needs, efficiency, geographically dependencies, land use, environmental impact, investment needs, operational needs and so on. But, when seen as a time independent good the finish product is homogenous and can thereby be compared.

To make it time independent the cost of the system is levelized throughout the systems lifetime. Hence the expression Levelized Cost of Electricity (LCOE). Notice that LCOE is the abbreviation for both Levelized Cost Of Energy [5, 20, 91], and Levelized Cost Of Electricity [12, 92, 93].

The LCOE can be considered a comprehensive way of comparing different technologies used to generating electricity as it reduces all variables down to a cost per energy unit expressed as [cost/kWh]. This makes LCOE value easy to understand and easy to compare different LCOE to other alternatives even if the technology used, and thereby cost structure, of generating the electricity is very different.

The LCOE can be seen as the revenue per unit energy of an electricity generating investment where the net profit, the net present value (NPV), over the financial period equals to zero [92].

$$\textit{Lifetime Revenues} - \textit{Lifetime Costs} = 0 \quad (2)$$

As the value of a given cost or revenue is higher today than tomorrow this must be taken into account when calculating the total revenue and cost. They need to be discounted by the factor $(1+r)^t$ where r is the discount rate and t is the given year.

For a LCOE, assumed fixed, and a discount factor that does not change from year to year the lifetime revenues equals to

$$\textit{Lifetime revenues} = \textit{LCOE} * \sum_t \textit{Electricity}_t * (1 + r)^{-t} \quad (3)$$

where

$$\textit{Electricity}_t = S * (1 - d)^t \quad (4)$$

and

S = Estimated electricity produced in the first year of production

d = The predicted annual change in electricity output. I.e. degradation.

If most the electricity is consumed by the producer itself, like i.e households, the producer will not have any cash flow revenues, but enjoys instead the benefit of the electricity directly. However, the value is still the same and the revenues are expressed here in monetary terms.

The same calculation goes for the cost:

$$Lifetime\ costs = \sum_t Cost_t * (1 + r)^{-t} \quad (5)$$

Where the cost structure used by Organisation for Economic Co-operation and Development and the Nuclear Energy Agency (OECD/NEA) [92] among others and discussed later, is

$$Cost_t = Investment_t + O\&M_t + Fuel_t + Carbon_t + Decommissioning_t \quad (6)$$

And

Investment_t = Investment cost in year *t*

O&M_t = Operations and maintenance cost in year *t*

Fuel_t = Fuel cost in year *t*

Carbon_t = Carbon cost in year *t*

Decommissioning_t = Decommissioning cost in year *t*

As the total costs is all costs related to the lifetime of a given project, the term Life-Cycle Cost (LCC) can also be used. Also worth mentioned is that the term Long Run Marginal Cost (LRMC), which is a more generic term than LCOE as it is not restricted to energy, is used by many utilities instead of LCOE [94].

By combining (3) and (5) we get

$$LCOE = \frac{\sum_t [Cost_t * (1 + r)^{-t}]}{\sum_t [Electricity_t * (1 + r)^{-t}]} \quad (7)$$

Or simply put

$$LCOE = \frac{\textit{Lifetime cost}}{\textit{Lifetime Electricity Production}} \quad (8)$$

The discounting of a physical value as the electricity might by first glance look non-intuitive. However, it is important to look at the flow of electricity as a flow of cash, and the same amount of money in worth less tomorrow than today. The discount rate essentially reflects the cost of capital invested in the project [92].

This method for calculating the LCOE is the one used by the International Energy Agency, Organisation for Economic Co-operation and Development and the Nuclear Energy Agency [92], Fraunhofer Institute for Solar Energy Systems [1] and several other papers and reports calculating the LCOE [15, 20, 21, 91, 95-100]. However, the calculation of LCOE and the assumptions made still differs between each other as there is no defined and finite method for the calculations. Branker et al. (2011) described the utilization of the the LCOE method as “(...)deceptively straightforward and there is lack of clarity of reporting assumptions, justifications showing understanding of the assumptions and degree of completeness, which produces widely varying results.” [96] I.e. Reichelstein et al. (2013) suggests a method for calculating the LCOE that differs from the ones above in mainly that it includes the positive value of the tax effect [11]. Models like the System Advisor Model (SAM) to the National Renewable Energy Laboratory (NREL) uses this method [101]. But the last years a lot of LCOE literature, as shown above, that have been published, indicating a more unified LCOE understanding in line with method details described earlier.

However, even if the LCOE seems to have reach a somewhat common understanding it is still important to understand the limitations of it and the close related methods. IEA (2014) goes as far as writing that “Whenever technologies differ according to the when, where and how of their generation, a comparison based on LCOE is no longer valid and may be misleading.” [93] This underlines the importance of knowing the limitations of the LCOE given in order to

evaluate it under the correct perspective, as almost no electricity generating technologies are homogenous under these preconditions.

For stakeholders in given electricity generation projects the LCOE contains too few details to make an investment decision on. I.e. the LCOE method does not reflect the risk related to the specific electricity generating technology. These risks include those at the plant, market regulations and policy [92]. I.e. it could be argued that PV have a lower uncertainty than fossil based electricity generation because most of the expenses is at the start of the project. But on the other side, PV is more dependent on a future price of electricity of precisely the same reason. In addition special for variable renewable energy (VRE), the time of electricity generation can also not be decided. It is a good one does not know the precise delivery of and by this reason not directly comparable to other non VRE generating technology. For a VRE vs. fossil based technology with equal LCOE, this favours the fossil based option.

As the LCOE sets its boundaries very close to the place where the electricity is generated, a huge portion of the total costs related to a given technology are not paid by anyone, but still faced by society. For fossil based technology these can be cost related i.e. to the increased numbers of natural disaster, reduced life expectancy, higher healthcare cost, premature deaths and so on. 1.1 million People die annually for diseases related to indoor air pollution due to the use of solid fuels. 1.5 million People die annually from air pollution caused by urban transportation. These early deaths and other health impacts is estimated to cost USD 325-825 billion per year worldwide in 2010. The cost related to human induced climate change due to CO₂ emissions is considerable and comes on top on this. IRENA have estimated the total additional cost for society to be in the range of USD 0.01/kWh and 0.13/kWh, depending on the carbon intensiveness of the electricity generation systems [12]. As these externalities focuses on fossil technologies, all technologies have a wider impact. The question is in most cases how much.

The cost of integrating the variable renewable energy (VRE) like PV into the existing system is an important limitation of the LCOE PV calculations [102]. These costs arise as the current power system is designed around a specific composition of electric generation technologies. Each with its own strengths and weaknesses. This means that the question of when, where and how the electricity is generated are components not taken into account into the LCOE. A comparison towards other technologies purely based on the LCOE is therefore not valid and may be misleading [93]. I.e. as the LCOE only reflects the long term energy yield, in other words; energy, and not the power, it has been shown that PV does not reduce peak capacity requirements [102].

In light of the fact that a big proportion of the renewables planned and being built cannot be controlled when it comes to timing of power generation: Is a large share of VRE sustainable? The International Energy Agency has concluded that a VRE share of up to 45% of annual electrical generation can be integrated into the power system in the long run, without significant increase in the total power system cost [103]. If the share exceeds that, a system wide transformation is needed. To tackle this challenge they suggest focusing on system-friendly VRE deployment, improved system and market operation, and investment in additional flexible resources [103].

In order to take the actual grid cost into account when calculating the cost of VRE, a method called System LCOE has been developed. This method aims at not only taking the generation cost into account, but also the extra cost of integrating the VRE into the grid. An illustration of this can be seen in Figure 106. However, when considering the total system LCOE when introducing VRE, IEA suggests not rely on methods just using integration costs in addition with generation cost, but instead develop and use simulation tools capable of taking the specific operation conditions into account [93].

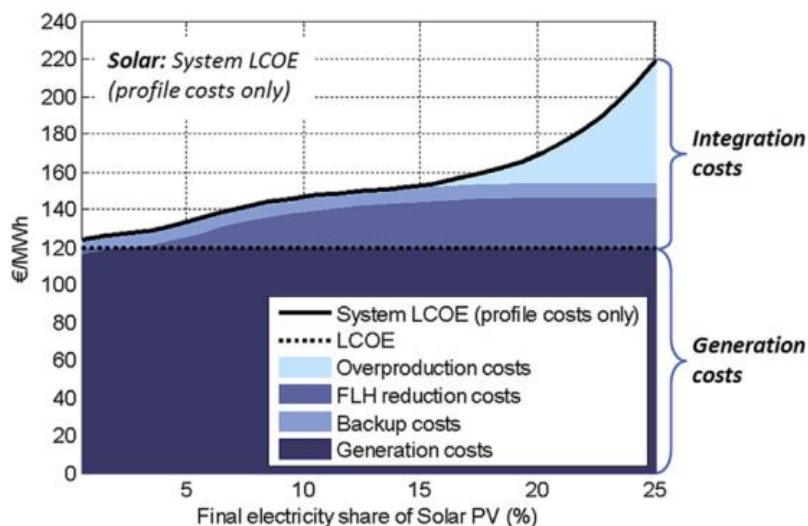


Figure 106 - Estimation of system LCOE in Germany for an increasing share of solar PV of the final electricity market. FLH is the full-load hour reduction of conventional electricity plants [102].

As discussed above, the LCOE have too few details to be a foundation for given energy project, but is especially narrow to be an instrument for policy makers. Though as rough estimate and easy energy comparison between projects and technologies it serves its purpose as a starting point for both. A schematic illustration of the LCOE method compare to other cost estimation method is shown in Figure 107.

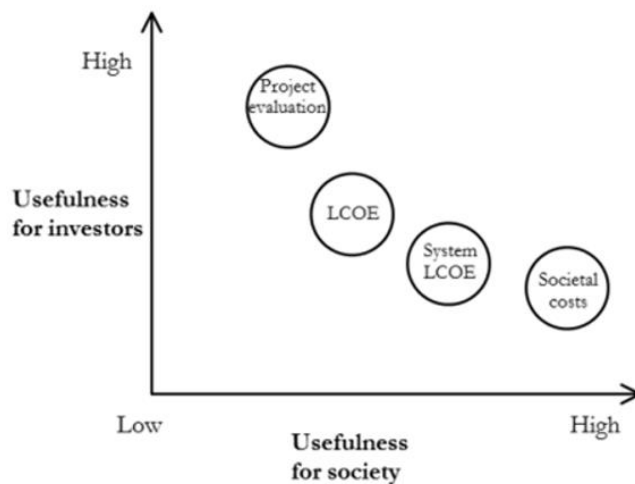


Figure 107 - Not to scale validity of a few valuation estimate methodologies for investors vs. society.

However, as the scope of the LCOE is so narrow, indirect revenues and costs related to PV systems are discussed to some extent in chapter 4.

For a more detailed discussion around the economic methodology around PV power, Bazilian et al. [94] is highly recommended, in addition to the methodology chapter in the report “Renewable Power Generation Cost” by IRENA [12].

3.2 Installation cost

In this chapter all direct costs related to the Acusticum PV system is gone through. The cost are divided into PV modules and balance-of-system (BoS) cost. Historically BoS cost have been a relatively small part of the total installation cost and by this reason collected under the BoS concept. However, because the cost of PV modules are declining faster than the BoS costs, this is now a very significant cost element. The BoS cost are here split into several sub categories.

Cost will be given in total and cost per W_p in order to better compare the cost to other projects. The exchange rates used are found in Table 7.

Table 7 - Exchange rates used for calculations.

USD/EUR	USD/GBP	EUR/SEK	NOK/SEK
0.8899	0.6432	9.2535	1.1111

All costs related to the Acusticum PV system are from mail correspondences with Øystein Kleven at Solbes and interview with Patric Jonsson, head of Research and Development at Pite Energi.

3.2.1 PV module

As seen in the PV module experience curve in Figure 10 the module price have with a steady pace being going down with a learning rate⁷ of 19 to 22 % [11], some arguing of up to 22.8 % [19]. If one only looks at the learning rate from 2009 it is considerable higher.

⁷The learning rate is the price reduction after doubling of cumulative production.

This sudden change can also be seen in Figure 108. Regardless, as the price per W_p is continuously getting lower, PV electricity is getting more and more competitive and as a result the demand is increasing. Whether this demand is steady or not is not known as the LCOE the last and coming years have and are reaching parity with other electricity sources, meaning a sudden shift might occur.

The price paid for the 924 modules at the Acusticum was SEK 1 454 824. This is a price per W_p of SEK 5.95 or USD 0.722. Only 891 modules was used as the C roof was not considered usable for PV installation. If the price per W_p would be the same, the module cost would have been SEK 1 403 030. This cost will be used for later calculations.

If one compare the price per watt to the expected price in 2015 from the experience curve in Figure 10, one can see that the price per watt in the Acusticum system is lower than the expected price. It should also be noted that these modules, in according to Øystein Kleven, are considered to be of some of the best quality available, despite the last winter bending of several module frames.

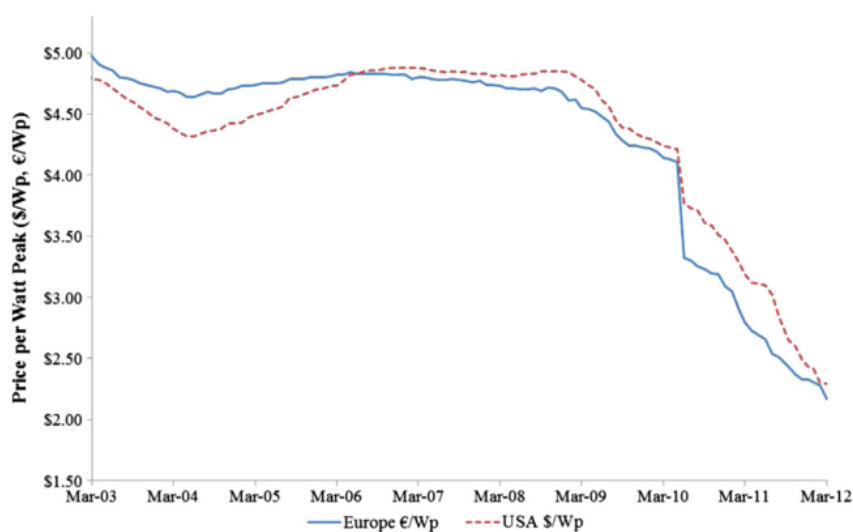


Figure 108 - PV module average retail price in 2012 currency [104].

3.2.2 Balance of system cost

The total BoS cost for the Acusticum PV system was SEK 1 687 452. This is SEK 7.15 or USD 0.853 per Wp. This is far better than the global average and close to the global best practice found in “Renewable Power Generation Costs in 2014” by the International Renewable Energy Agency (2015) and is illustrated in Figure 109. In order to better understand the reason for this difference, a more detailed description of BoS cost composition is taken in the following chapters.

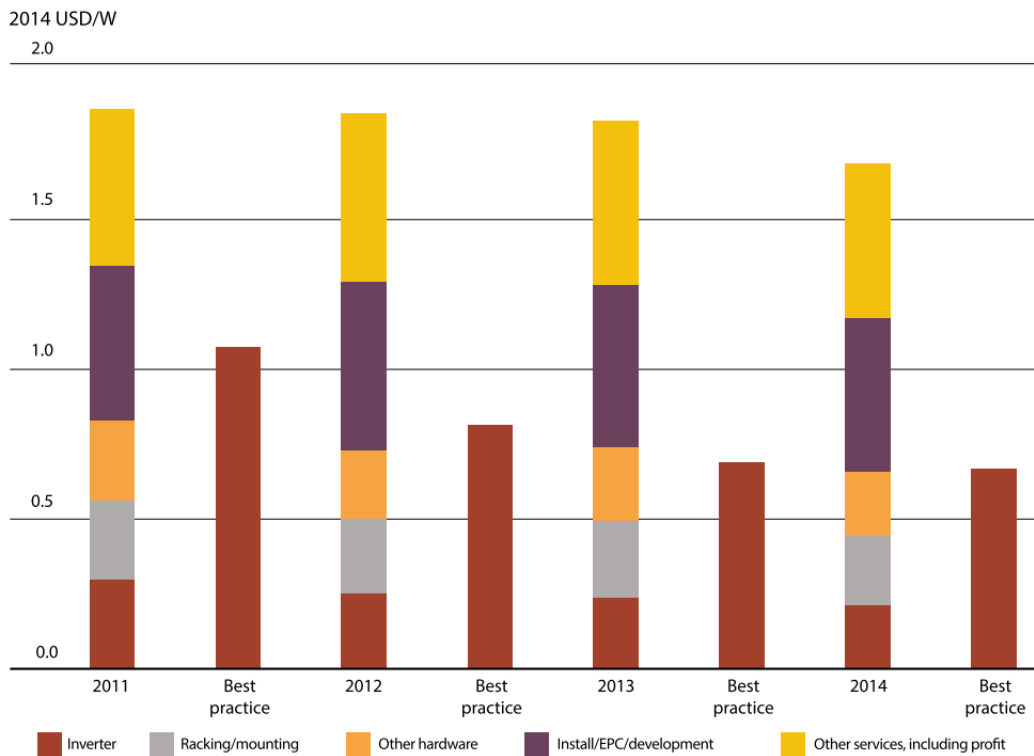


Figure 109: PV BoS cost breakdown. Global average and best practice [12].

Inverter

The Acusticum inverter system, consisting of the actual inverters (The 13 inverters was SEK 145 600.), power optimizers and sensors, was SEK 380 000. This is SEK 1.61 per Wp or USD 0.196 per Wp. As seen in Figure 109 this is about the global average price. However, the SolarEdge system is considered to be one of the high-end systems and is also placed there price wise.

Mounting system

At the Acusticum the mounting system was SEK 410 910. This is SEK 1.74 per Wp or USD 0.211 per Wp. Compared to global average as seen in Figure 109, this is marginally less.

Other BoS hardware

Other BoS costs, primarily cables, was SEK 52 450. This is SEK 0.22 per Wp or USD 0.0270 per Wp. This is considerable lower than the world average as seen in Figure 109.

Installation labour

At the Acusticum PV system this was SEK 520 758, which is SEK 2.21 or USD 0.268 per Wp. As seen in Figure 110 this is under half of the 2010 USA cost, and almost at the level of 2011 Germany according to Seel (2014).

The difference between Germany and the USA as seen in Figure 110 is because of a lower overall wage, fewer total installation labour hours and a lower share of electrician labour in Germany [105]. In Scandinavia, the common understanding is that the wages is relatively high, so intuitively the installation time then should be lower to explain this cost. However, as this is a pioneer PV system where also several of the work staff was new to the installation of PV, a fast installation time do not sound much plausible. Further investigation into the installation labour cost and comparison to other projects in Scandinavia could have been interesting.

As the installation labour is a large contribution to the total BoS cost, this explains a lot of the low BoS cost compared to global average. It should also be noted that in addition to customer acquisition, labour cost also represents the largest cost differences between the US and Germany [105].

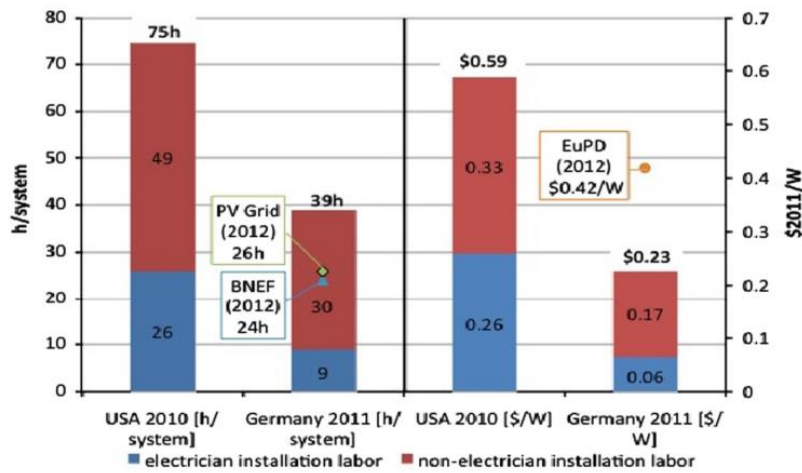


Figure 110: Residential PV system installation labor hours and cost in the US and Germany [105].

Permitting, interconnection, inspection (PII)

At the Acusticum Solbes used SEK 152 633 for design, preparation and inspection. Pite Energy used SEK 100 000 for connecting the PV system to the grid. In total this equals to SEK 252 633, which is SEK 1.07 or USD 0.130. Although this is about half of the 2010 USA cost and should by this reason alone be considered very good, it is almost four times the 2011 cost in Germany, both found by Seel (2014) and is illustrated in Figure 111. However, in Germany, solar PV prices are among the lowest globally, partly due to the large amounts of PV installations, facilitating for the streamlining of procedures and the following cut of PII cost.

If adding the cost per Wp for the installation labour cost from the previous section we get USD 0.398 which is less than world average as seen in Figure 109.

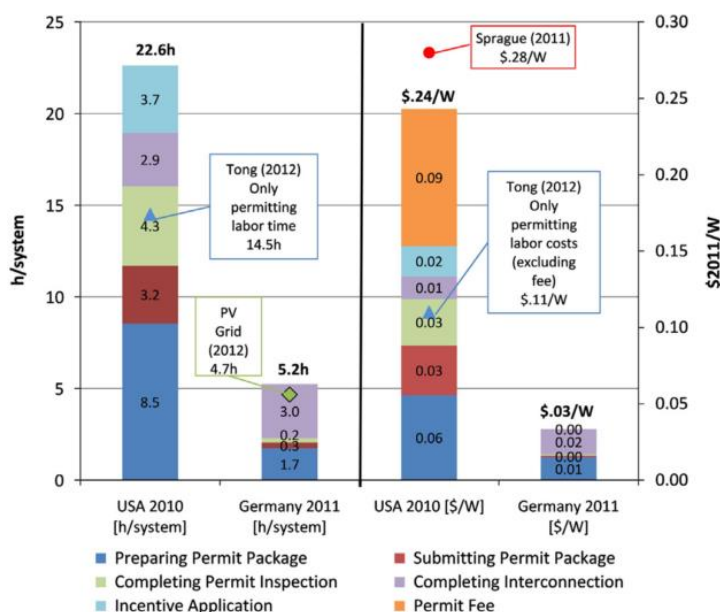


Figure 111: Labor and cost of permitting, interconnection, inspection (PII) and incentive application in the US and Germany [105].

Other BoS non-hardware

Logistics was included in the price of each component, and no sales tax applied as this was a company purchase. A profit of SEK 70 701 was made by Solbes

As this is considered pioneer work, some other surrounding cost could also be attributed to the Acusticum PV system. However, research and development assets of SEK 280 000 was granted and are used to covered these expenses and are not considered in the further calculations.

3.2.3 Total installation cost and comparison

The total installation cost is then SEK 3 090 482, equal to SEK 13.10, USD 1.562 or GBP 1.023 per Wp. Compared to the 2011 and 2012 costs illustrated in Figure 112, Figure 113 and Figure 114 the total installation cost for the Acusticum PV system is far below.

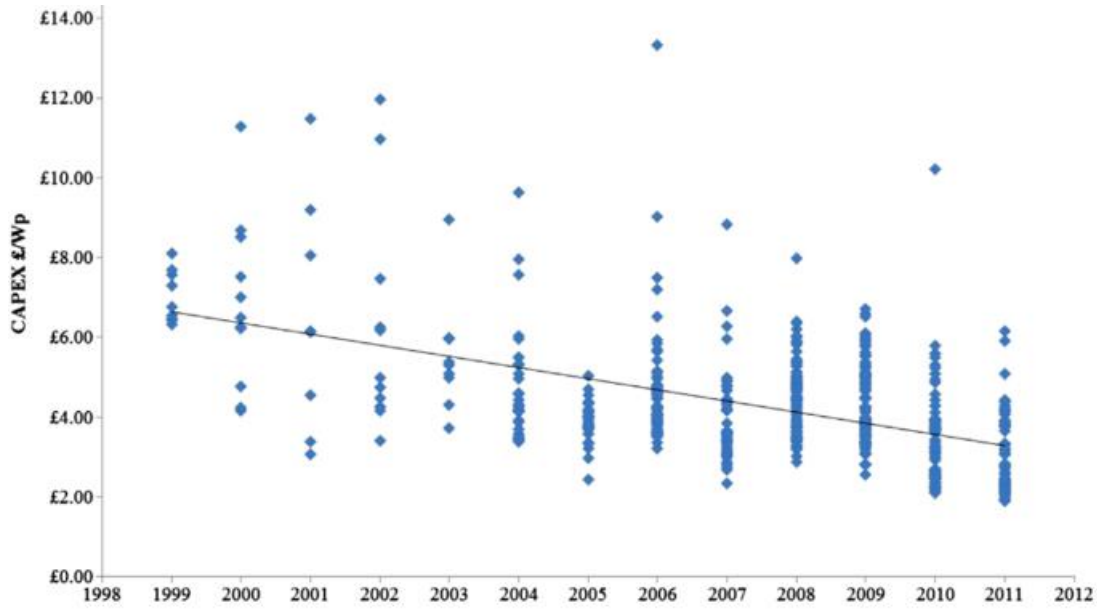


Figure 112 - PV system prices in European countries in 2011 currency [104].

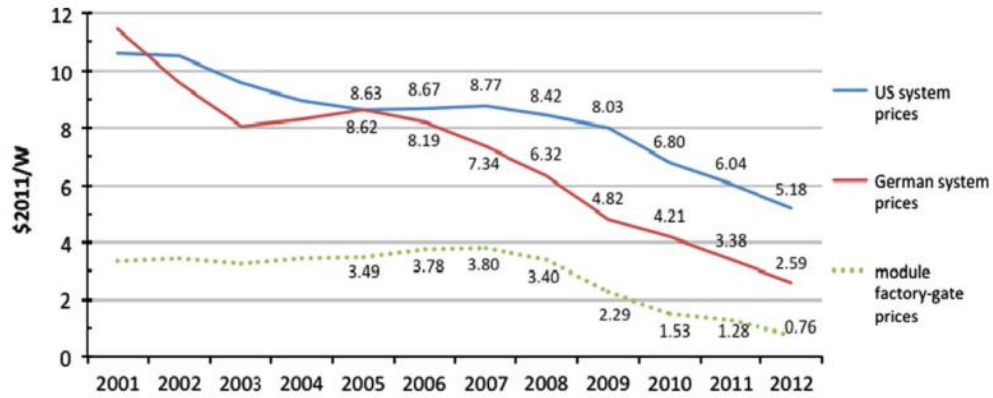


Figure 113: PV system median price development for systems smaller than 10 kWp [105].

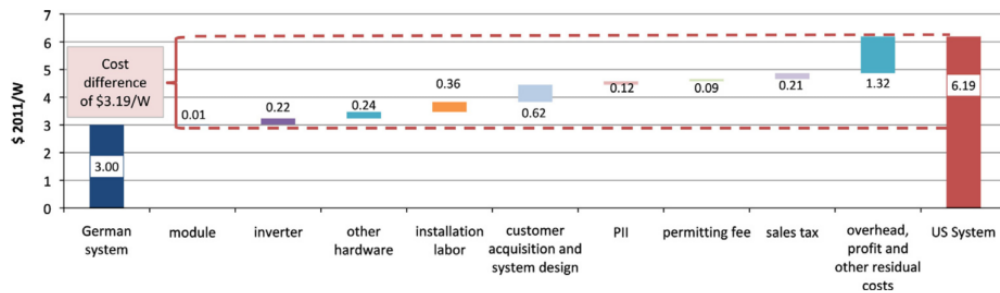


Figure 114: Residential PV system cost difference between Germany and the US in 2011 [105].

Comparing the Acusticum PV system installation cost to the IRENA (2015) “Renewable Power Generation Costs in 2014” one can see that the cost is one of the lowest of the utility scale PV systems. For Solbes to reach this level is remarkable.

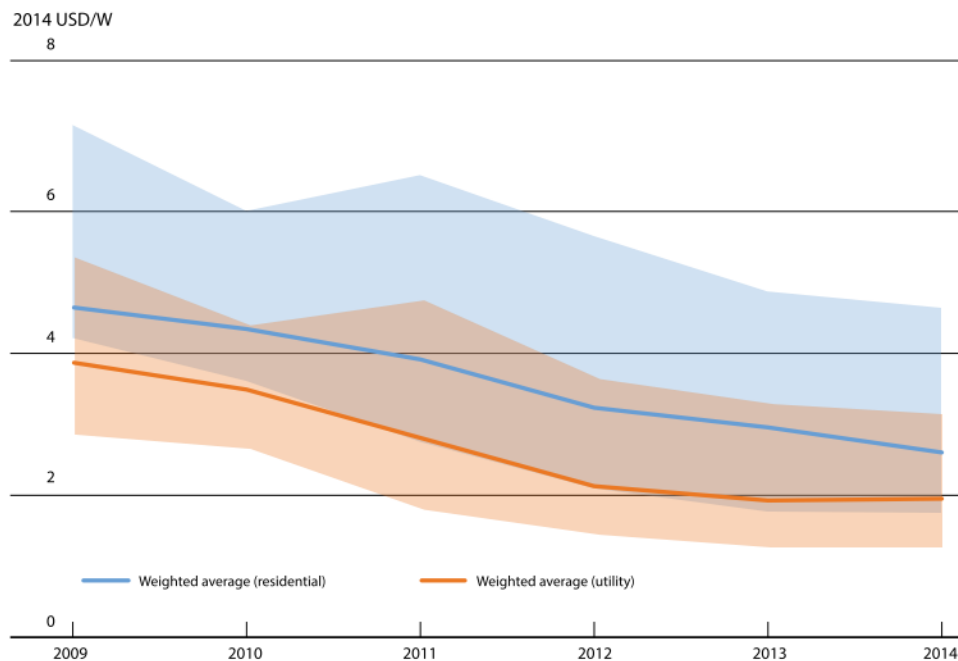


Figure 115 - Estimated global average PV installation cost, 2009 to 2014 [12].

3.3 Annual cost

One of the most important elements of annual costs is how many years they will occur. This is also an important input for how many years the PV system will generate electricity. The PV system life expectancy will be discussed first, before going through other annual costs related to the Acusticum PV system.

3.3.1 PV system life expectancy

The life expectancy and warranty is often closely related. The life expectancy a little more than the warranty. In this chapter a closer look at the life expectancy of the module and the inverter will be taken.

3.3.1.1 Module degradation

The industry warranty standard has become 25 years. Meaning the module after 25 years will have 80 % of its original STC rated output. When it comes to life expectancy, one can wonder with this relative high output after 25 years if the life expectancy may be longer than just over the warranty. In fact, some research suggests 40 years, and even 50 years [94]. For further calculations a life expectancy of 30 years is used. Most LCOE calculations uses 25 or 30 years.

The International Energy Agency (IEA) concluded in their 2014 report “Review of Failures of Photovoltaic Modules” that the statistics indicate a mean degradation rate of 0.8 % for crystalline silicon PV modules [106]. This is also the conclusion by Jordan & Kurtz (2012 & 2013) [107, 108]. Results illustrated in Figure 116.

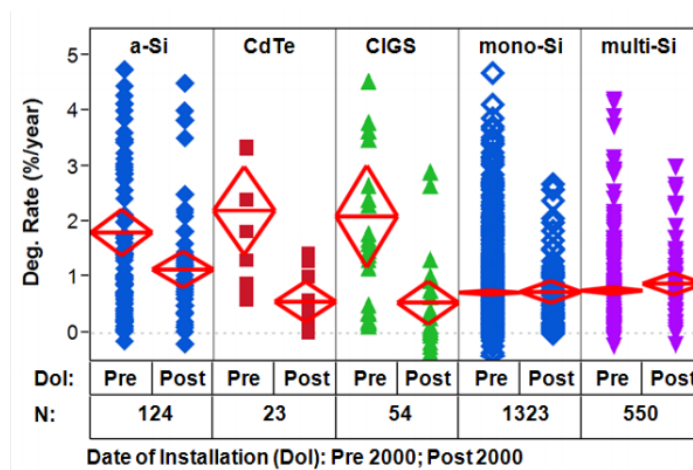


Figure 116 – Historical PV module degradation rates split by technology. The diamonds represents the mean and 95% confidence interval. [107].

An interestingly remark is that the data is not separated geographically or on the basis of climate of PV system surroundings. Is number of years the best way of describing the degradation rate towards? Would it be more precise to estimate the accumulated irradiation on the PV module surface? And/or also taken the temperature into account? And is the degradation rate correlated to the irradiance intensity? This is unanswered questions that might speak in favour of lower annual degradation rates for PV modules mounted further north.

As the level of degradation might speak in favour for PV systems at northern latitudes, the physical stress might indicate otherwise. As illustrated earlier in chapter 2.3.5. Several modules used in the Acusticum PV system got a rather severely bent lower frame due to force from the snow, not perpendicular on the module. Whether or not this is within warranty, the modules should be mounted another way in order to withstand the pressure or if the external forces are just outside what one should expect for solar modules in accordance to the standards is also an unknown question.

However, Innotech Solar, the supplier of PV modules for the Acusticum, filed for insolvency at 26th of March 2015. Swemodule, the PV module producer, two weeks earlier [109].

3.3.1.2 Inverter

The power optimizers used have a warranty of 25 years. The inverters 12 years, with the option of paying extra to reach a warranty of 25 years. As this is not done a change of inverters are calculated after 15 years in service.

Øystein Kleven have commented the electrician participating in mounting the inverter had a look inside the inverters and said that he was impressed by the good quality components chosen for the inverter.

In the last ten years the amount of materials used in inverters have been reduced from 12 kg/kW to 2 kg/kW [3]. BoS learning rate is about 20%, with the inverters considered to be

in the area of 5-20% [98]. Industry analysts IHS are predicting an inverter price reduction of 8% annually through to 2019 [110]. This is the rate used for later calculations.

3.3.2 Other annual costs

According to Pite Energy, the owner of the Acusticum PV system, the only annual operation and maintenance cost is the cost of renting the Acusticum roof of SEK 5 000. Also, the PV system is not insured as a separate asset, but as a part of the whole company [111]. According to Morales (2015) the insurance rates ranges from 0.6 to 1.2% of the total system cost [98]. 1% will be used for further calculations and an annual operation and maintenance cost of SEK 25 000 will be used. The extra SEK 20 000 as it is more than likely that other operation and maintenance cost will accrue, especially towards the PV system end of life.

In end of chapter 2.2.2 an annual increase of irradiation of 0.3 % is suggested based on historical data. This effect is not taken into further calculations as no future estimates are made.

3.4 The cost of capital

As capital for most people is not free, this must be taken into account when calculating the cost of a PV system. This is done through the discount rate. The interest rate usually reflects the inflation, risk and alternative cost of a project and depends on the perspective the interest rate is viewed in.

As the interest rate in the chosen LCOE method primarily affects the physical electricity and not the invested money, it is as earlier discussed not directly intuitive to understand the reason. One way to look at it is if the energy have not been discounted, the corresponding increase in the invested money had to be done in order to reflect the cost of capital. For further details, please refer to chapter 3.1.

For discount rates it is some distinguish between whether or not it is nominal, the inflation is not taken into account, or real, the inflation is taken into account. Norway has an inflation target of 2.5 % [112]. It is considered easier to communicate real values as consumer often

thinks in real world prices [98]. However, when supplying the interest rate LCOE sensitivity, as this thesis does, this distinguish is of less importance as the result of all realistic interest rates are also given.

The Norwegian Water Resource and Energy Directorate uses in their 2015 report “Costs in the energy sector” a discount rate of 4%. Pite Energy has not done any profitability analyses and naturally the discount rate is not given [111]. For further calculations a discount rate of 4 % will be used. It could be considered low if this is a real interest rate, or high if this is nominal. Please refer to the LCOE discount rate sensitivity for the value of choice.

The wanted return on capital is different whether the capital is your own equity or debt, with the return on debt often lower. To account for this a Weighted Average Cost of Capital (WACC) is often used. “*A standard result in corporate finance is that if the project in question keeps the firms leverage ratio (debt over total assets) constant, then the appropriate discount rate is the Weighted Average Cost of Capital.*”[11] I.e. if the project financing is fifty/fifty split between equity and debt with a wanted return of capital of 5 and 10 %, the WACC would be 7.5 %. Although not used as an explicit concept in this thesis, it is used in several other private and corporate PV system LCOE calculations and is a concept that should be known.

The last years the cost of capital has gone down dramatically. Some countries central banks even have negative interest rates. Patric Jonsson at Pite Energy also commented on the fact that money these days are cheap [111]. As renewable energy in most cases have the majority of the cost in the beginning of the project and is therefore subject to a relatively large investment, the low interest rates speaks in favour of renewable energy projects as PV systems.

The fact that almost all of the expenses for most renewable energy, like PV systems, comes in the start of the project can make it difficult to obtain the necessary capital. In fact, the initial investment in PV is an important roadblock in pursuit of a higher rate of PV installations. Not only for private households, but maybe especially for public buildings that

have very different budgets for constructing and operating the building. To lower the high threshold that the initial investment represent, other financing options like third party ownership (TPO), leasing, have been developed. This is I.e. a popular option in California.

To summarize, the discount rate is essentially your total rate of return on invested capital given the resulting LCOE. So, with a discount rate of 10%, you get 10% return on your investment for the guaranteed electric cost equal the LCOE.

Interest during construction is disregarded.

3.5 The LCOE for the Acusticum PV system

For the calculations the decommission cost and residual value combined are assumed zero.

The summary of LCOE input factors and the calculated LCOE can be seen in Figure 117. As seen the LCOE is found to be 1.22 SEK/kWh. Converter to other currencies this equals 0.148 USD/kWh, 0.132 EUR/kWh, 0.0953 GBP/kWh or 1.10 NOK/kWh. The LCOE calculation model can be found as an add-on to the electronic publication of this thesis.

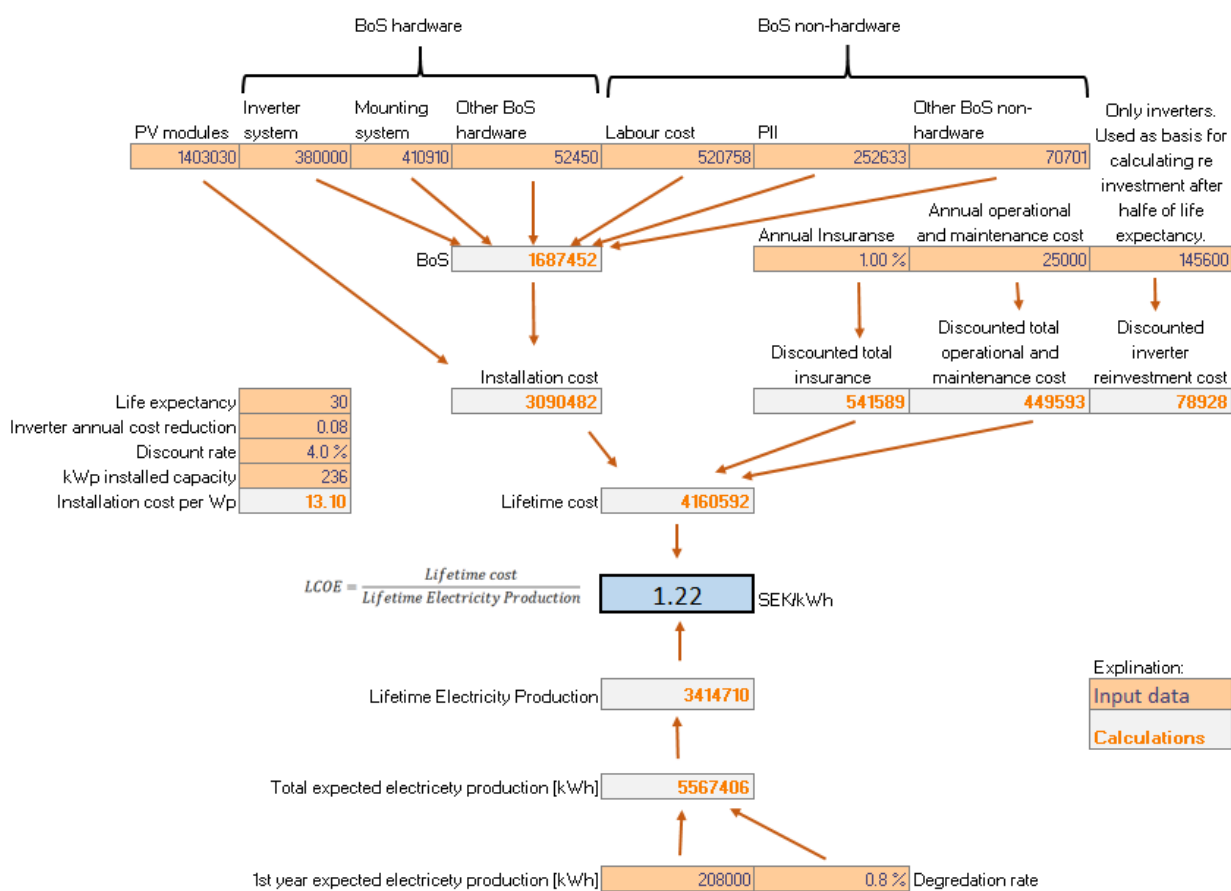


Figure 117 - The LCOE for the Acusticum PV system.

Comparing to other LCOE studies referred to in chapter 0 we see that the LCOE is in most cases at the lower end. In fact the Acusticum PV system was below the world average LCOE in 2014 according to the report “Renewable Power Generation Costs in 2014” by the International Renewable Energy Agency as illustrated in Figure 12 [12].

If one compare the Acusticum PV system LCOE to a LCOE study in Germany by the Fraunhofer Institute for Solar Energy from 2013, we see that the Acusticum PV system performs a little above average for large PV systems as illustrated in Figure 13 [1]. This despite that the Fraunhofer Institute used a GHI of 1000 kWh/m² compared to Piteå 900 kWh/m².

The study by Good et.al (2011), found a LCOE of 0.27 EUR/kWh for a PV system in Piteå as illustrated in Figure 14 [18]. This is over twice the LCOE found at the Acusticum PV system. Also a remarkable cost reduction over just a few years.

An interesting finding is that the LCOE found for the Acusticum PV system is exactly the same as Stridh et al. (2013) presented at PVSEC 28. They also had a scenario without any subsidies and a specific production of 900 kWh/kW_p, but an investment cost of 20 SEK/W_p reflecting a “typical residential installation” [17]. The same specific production and LCOE indicates an unrealistically low discount rate.

According to the report “Costs in the energy sector” from 2015 by the Norwegian Water Resource and Energy Directorate, the lowest LCOE estimate for Norway was just above 1 NOK/kWh as illustrated in Figure 16 [21]. This is about the same as the Acusticum PV system, despite that the Acusticum PV system have considerable lower irradiation levels than used to get to the low estimate above. Indicating that the Norwegian LCOE estimate could be lower, especially since these lowest estimates are for utility size PV systems.

Even though the assumptions made between the above studies varies some, and because of this the LCOE results is not directly comparable, there is no doubt that the LCOE of the Acusticum PV system is in world class. However, it should also be noted that the best

projects in 2014 was estimated to 0.08 USD/kWh [12]. This is of course completely other irradiation levels.

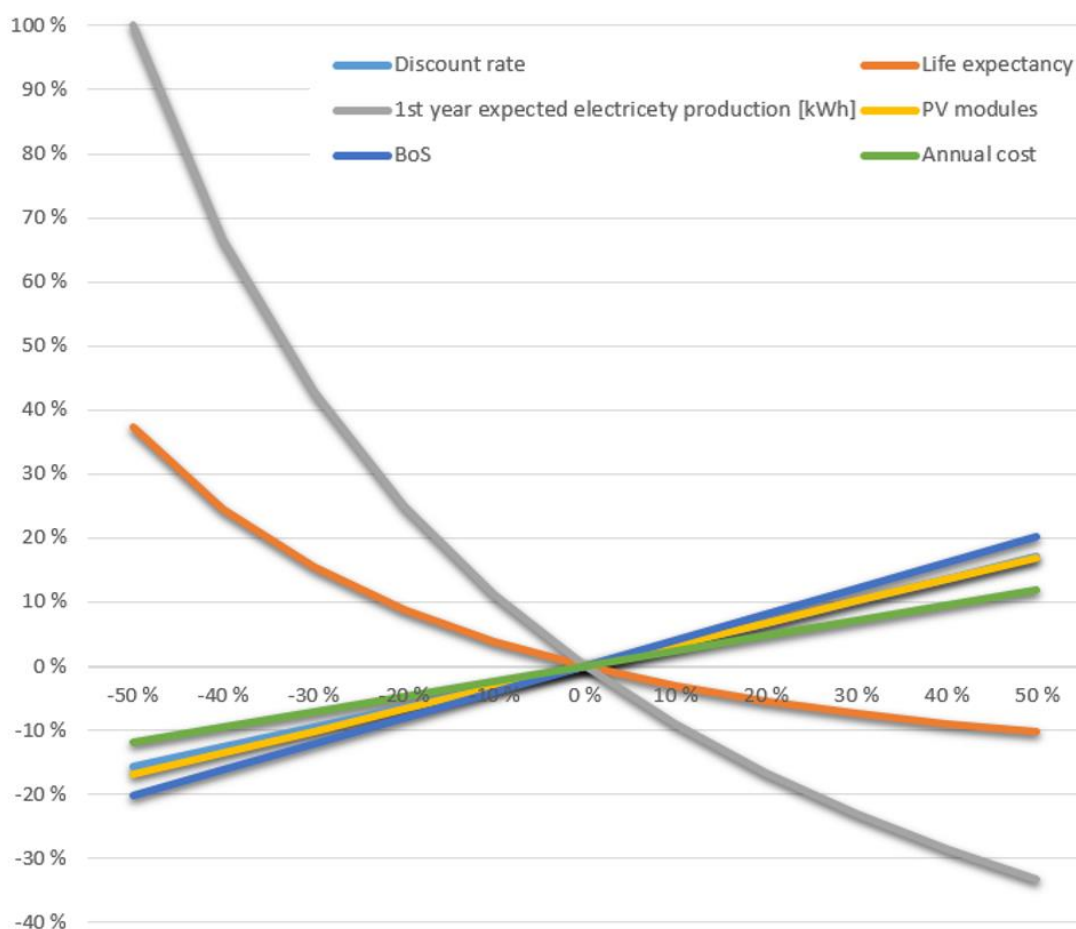


Figure 118 - The Acusticum LCOE sensitivity related to relative change in input parameters.

As for the LCOE sensitivity to the relative change in input parameters can be seen in the spider graph in Figure 118. As expected a change in the 1st year expected electricity production⁸, the basis for total expected electricity production, will have the highest impact on the LCOE. In fact, about 10 % increase of annual electricity production will reduce the LCOE with about the same. This is quite much, not just relative to the other input factors, but PV energy technology is in fact on of the technologies that is most sensitive to change

⁸ The 1st year expected electricity production can also be interpreted as the capacity factor. This concept is used in some other publications and is a more generic term in order to compare different energy technology LCOE sensitivities.

in the energy production as seen in Figure 119. Placing the system at a site with higher irradiation levels, or using modules with a higher degree of efficiency have a relatively high impact on the LCOE.

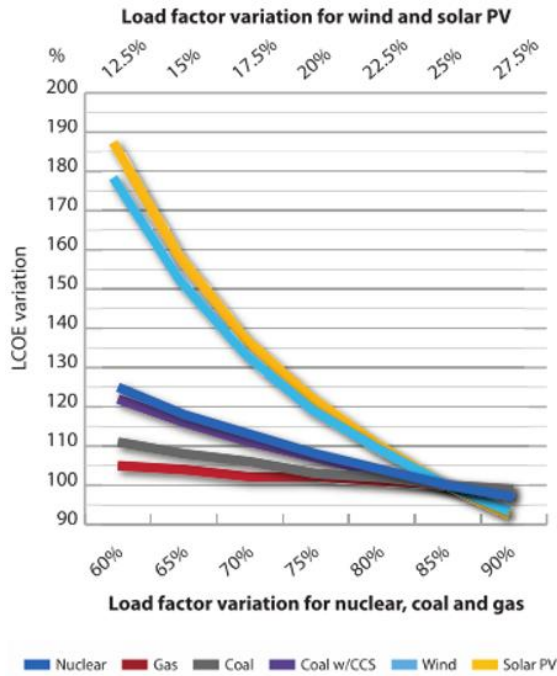


Figure 119 - LCOE as a function of a variation in the load factor (5 % discount rate) [92].

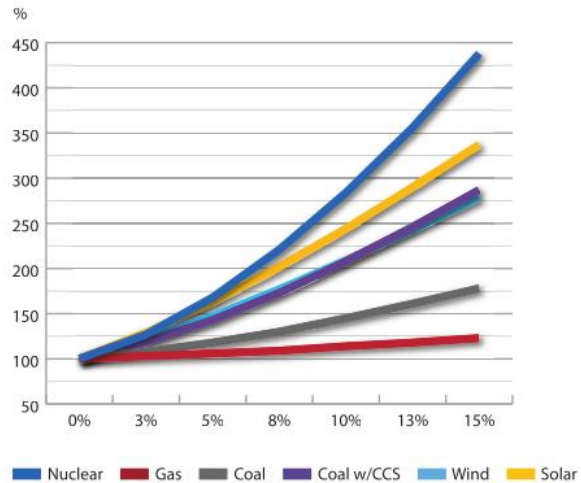


Figure 120 - LCOE sensitivity for different discount rate for different technologies [92].

Also note that the reduction of the discount rate from 4 to 2 %, a reduction of 50%, would decrease the LCOE with about 15 %. This would result in a new LCOE of 1.04 SEK/kWh. PV energy technology is one of the energy technologies that is most sensitive to a change in the discount rate as illustrated in Figure 120.

Another interesting observation is that a 50 % increase in life expectancy from 30 to 45 years will only reduce the LCOE by 10 %. However, the life expectancy sensitivity is also affected by the discount rate. A lower discount rate would raise the sensitivity of the life expectancy.

The sensitivity calculations, in addition to an automated sensitivity graph as shown in Figure 118, can be found as an add-on to the electronic publication of this thesis.

3.6 LCOE future development

The LCOE of PV systems have always been decreasing and there is nothing pointing against this development. The only question is how fast.

As seen in Figure 121, the International Renewable Energy Agency (IRENA) gathered in 2012 several possible future scenarios from 2010 to 2030. Interestingly enough, despite the low irradiation potential at Piteå, the Acusticum PV system is just above the lowest scenario. According to this scenario the LCOE rate of reduction will steadily decline until reaching a steady-state of 0.050 USD/kWh in 2030 [113]. However, this is average scenarios. IRENA already in 2015 gave examples of PV projects producing electricity at an estimated LCOE of 0.08 USD/kWh and projects in construction with an estimated LCOE of 0.06 USD/kWh [12].

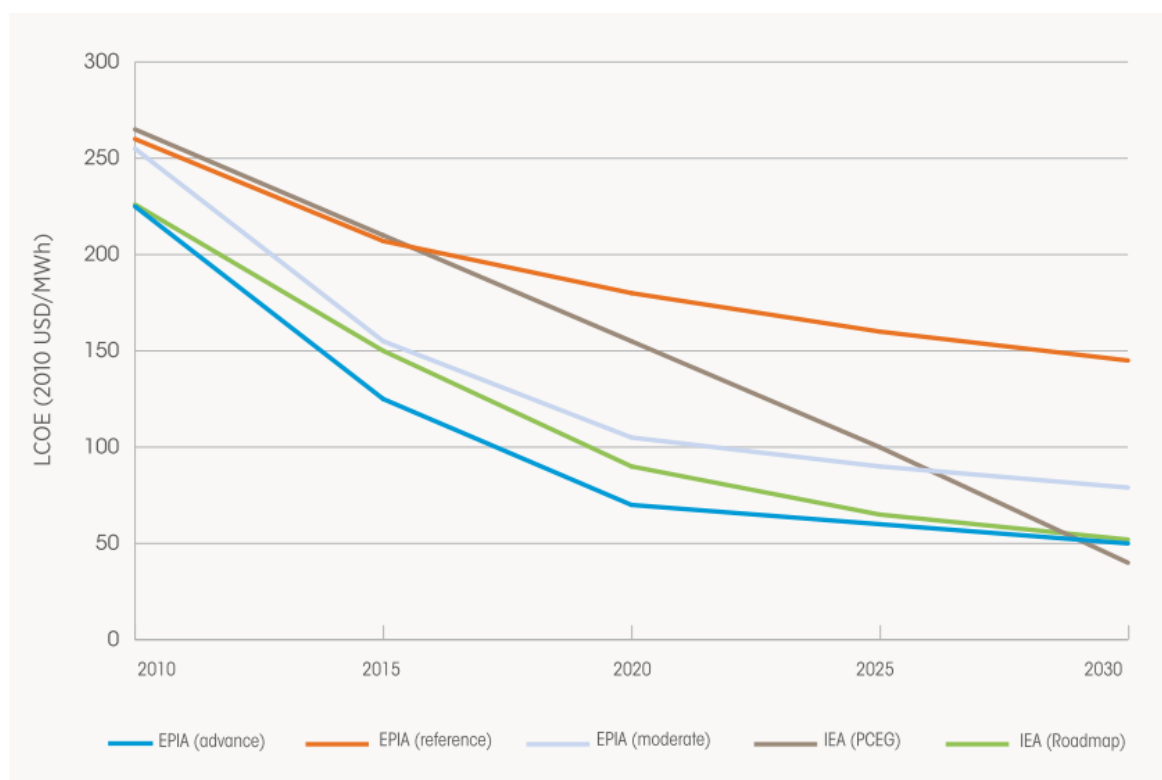


Figure 121 – Different LCOE scenarios for PV systems from 2010 to 2030 [113].

The Fraunhofer Institute for Solar Energy also predicts a decline as the scenarios presented by IRENA as seen in Figure 122. However, the rate of reduction is much lower, not

reaching the low 2030 levels predicted by the lowest scenario presented by IRENA. A reason being that IRENA presents global scenarios and Fraunhofer Institute for Germany, having relatively low irradiation levels compared to most people in the world. Also, the LCOE in Germany is now one of lowest in the world. This after several years of attractive governmental support attracting several participates to the marked, increasing competition and pressing cost as the support is reduced. A method increasingly used at different degrees in several other countries, continuing pushing the LCOE down.

As the LCOE of the Acusticum PV system fitted quite well with the earlier estimates by the Fraunhofer Institute as seen in Figure 13, the LCOE projection presented in Figure 122 might be one of the better estimates for LCOE at northern latitudes. Although it is quite interesting than one can compare a PV system as the Acusticum at these latitudes to a marked of this high degree of development. Maybe the relatively close geographical proximity has a rather high influence on also the market at more northern latitudes as Scandinavia?

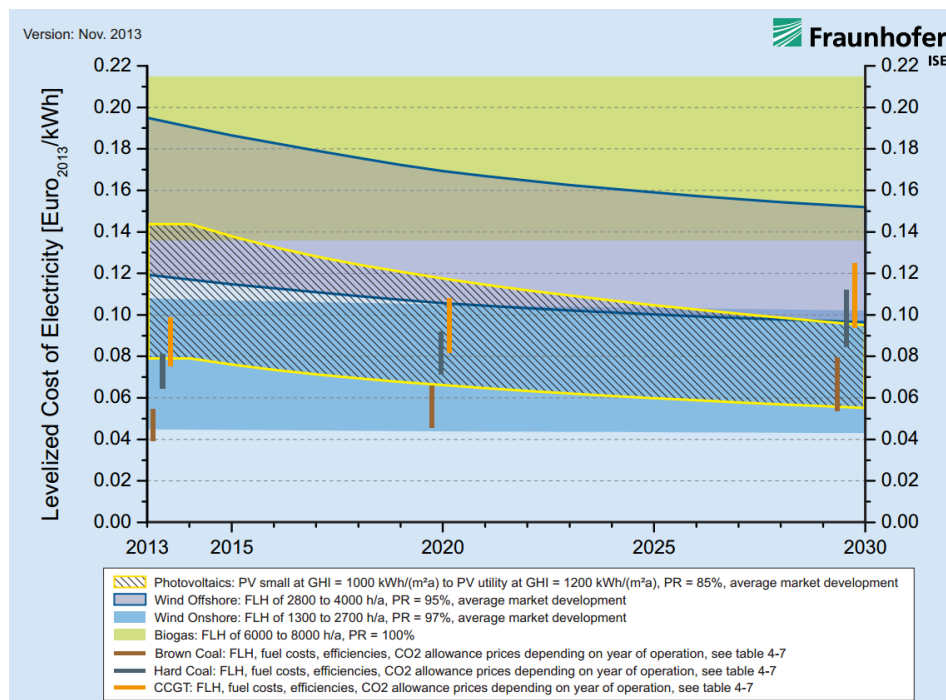


Figure 122 - LCOE forecasts for different energy technologies [1, 15].

So why should the LCOE continue to drop? Breyer (2013) argues that the key drivers in continued cost reduction is the historical learning rate seen in PV modules, industry growth rate with 45% in the last 15 years, increased PV system performance, the continuing rise of electricity prices (4.3 % annually 2000-2007 in EU, 3.6 % in US 2000-06) and last; 1.5 billion people is not connected to the grid [19]. All reasonable and sound arguments.

What the future will bring, and how it will develop is off course a big unknown. History has shown that changes have a tendency to happen rather fast. Jumps instead of incremental changes. The fact that the LCOE of PV systems these days all over the globe are now competing, without subsidies, to other electricity sources is interesting to say the least. Taken the continued LCOE reduction into account, making electricity from PV the most economical choice in more and more countries, might indicate we are close to a paradigm shift.

“The dynamics of solar PV costs and prices as a challenge for technology forecasting” by Candelise et al. (2013) is recommended for a more detailed discussion regarding the forces affecting also PV system LCOE prognosis [104].

4 PV system investment profitability in Norway

As the LCOE only looks at the direct cost related to the energy production, there are several other costs aspects to take into account. In addition, to put the costs into context some revenue aspects is also discussed. This is used to in order to shed some light on the PV system profitability in Norway. Although the Acusticum PV system will in some cases be used as an example.

Firs the indirect revenues and cost are discussed. Next the policy instruments currently available in Norway for the increased used for renewable energy is calculated for a scenario where the Acusticum PV system was placed in Norway. Then the electricity price, and some aspects concerning this will be discussed as this is an important factor whether or not a PV system is profitable or not. Last, the question on profitability is tried to be answered.

4.1 Indirect revenues and cost

Indirect cost and revenues today might become direct tomorrow. Two areas will bi focused on; advantages and disadvantages for transmission system operators, and the costs and opportunities that lay in area of social responsibility. Last other indirect revenues and costs will be mentioned.

4.1.1 Advantages and disadvantages for transmission system operators

The International Energy Agency argues in their 2014 report “The power of transformation” that a high share of variable renewable energy (VRE) like PV have some challenges that must be addressed. One of them being able to ensure sufficient generation capacity when VRE in unavailable and another the ability to control the production at short notice according to consumption needs. Increased share of VRE in the grid calls for increased flexibility. There are four different flexible resources: grid infrastructure, dispatchable generation, storage and demand-side integration. Grid infrastructure has a double benefit; reaching resources and distributing VRE over a larger area [93]. Some of the different storage technologies and the corresponding power system application can be seen in Figure 123.

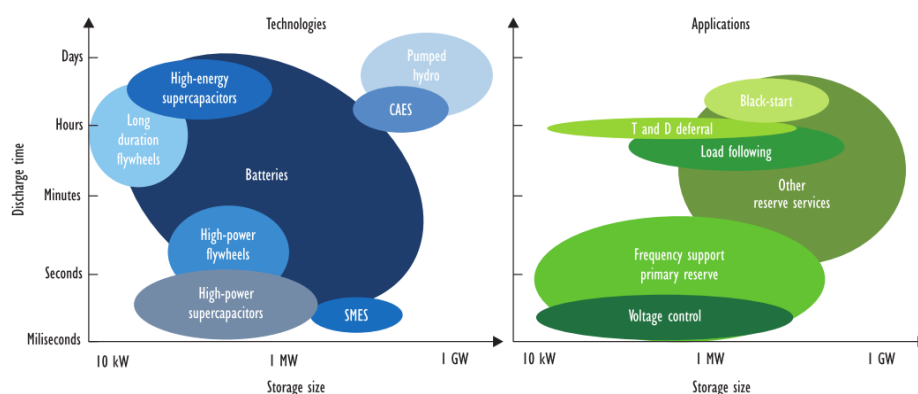


Figure 123 - Different storage technologies for corresponding power system applications [93].

Even though PV presently are mostly variable source of energy it presents also some interesting possibilities, most credited the inverter. One aspect regarding inverters is their possible ability to be used to compensate the reactive power demand and by doing so serving as a grid stabilization measure [114, 115]. Not nearly all inverters can do so, but most producers have inverters with this capability. Also, work is being done in order to standardize the communication and control requirements for future “smart” inverters where some of the abilities is watt-voltage management, watt-frequency management and storage management [116].

As the PV industry have grown, complementary systems have also been developing trying so solve some of the challenges. One of the biggest off course the ability to control when to use the energy generated as IEA have pointed out as one of the solutions of increased shares of VRE. Tesla, one of the few car manufactures only producing battery powered cars, have just released a battery pack intended for storing energy from VRE sources. The battery pack is about set world record in value of product sold in a short time – of any available product. This shows that there is a huge market, and that it is possible to produce storage solutions at a cost consumers are willing to pay.

However, as large successful technologies companies like Google and Apple have shown, people would like advanced solutions, but simple. If the ability the inverter represents and the storage capacity added should be used at its full potential this must be easy to use. Again, both Google and Apple are using a lot of resources in smart-home technologies. Combined

by the fact that controlling a lot of small inverters and small batteries add up to a whole swarm that combined could represent very significant amount, controlling this ability can be quite profitable. Lowering the energy bill at one end, and delivering power systems services at the other. A possible example of demand-side integration.

4.1.2 Social responsibility costs and opportunities

As the LCOE from PV system from a purely economic view are on the road of being a very realistic choice, this should not be the only variable when considering the source of energy. In this chapter some background on the environmental impact of PV systems are given, before relating this to more tangible opportunities.

4.1.2.1 Environmental effects of PV production and operation

As PV is new to most people it is often met with some level of uncertainty and scepticism in regards to the environmental friendliness. To reduce this uncertainty it is important to point out that most of the module often is an aluminium frame, glass front, some plastic in the middle and Silicon. As silicon not is that usual in its purest form it is still an abundant asset on earth making up for about 20% of the earth's crust, making it the second most common material on earth after oxygen [25].

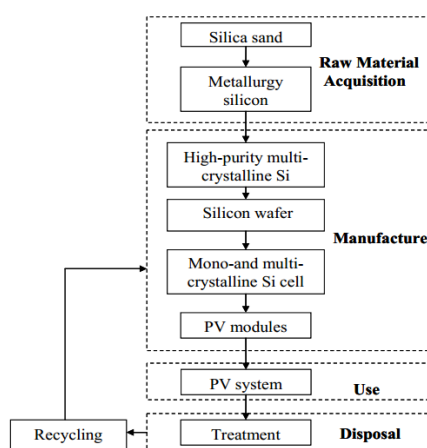


Figure 124 - Life cycle stages of crystalline PV system [117].

To assess the environmental impact of PV systems the life cycle assessment (LCA) methodology is used. This have a holistic approach considering in most cases the whole lifespan of the product, and the impact on much more than the present overwhelming focus on greenhouse gas (GHG) emissions and its impact on global warming. Nevertheless, the focus here is mainly on GHG.

In a comparative LCA analysis between European and China manufactures of PV modules, they found that the GHG emissions is about double for silicon based PV modules produced in China in comparison to modules produced in Europe [118]. They also found that the modules manufactured in China consume 28-48% more primary energy than the manufactures in Europe [118]. Graphs illustrating this can be found in Figure 125.

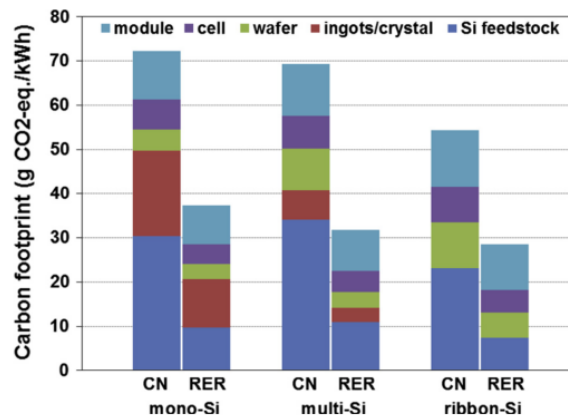


Figure 125 - Results of carbon footprints of Si-PV modules

(CN: China, RER: Europe) [118].

The energy payback time (EPBT) is often used as a measure to show the sustainability of PV systems. Some studies suggest an EPBT of down to two years for multi-Ci modules, and as little as half a year for CdTe modules [119]. Another study on hybrid solar systems suggest that the EPBT is less than half of that of crystalline technologies, and the GHG emissions is even less [120].

All LCA calculations on PV systems show that the EPBT is always smaller than the life expectancy of the systems [121]. In this view, PV systems seem environmental friendly.

Nevertheless, the procedures, boundaries and assumptions the LCA studies have used differs a lot. Important factors as end of life handling and studies mostly in high irradiation areas are often not taken into account [121]. This all stresses the importance, as for all scientific work, to read it with a critical eye. However, studies conclude with a reasonable large margin that electricity from PV also with respect to GHG emissions is environmental friendly [122].

To get a sense of the scale between different energy sources with regards to CO₂-eq., NO_x and SO₂ emissions, this is shown in Table 8. For solar energy the we see that it is in the lower scale of GHG emissions, but the span in relative huge indicating uncertainties, deviations in different production processes, different LCA approaches, geographical differences, different PV technologies and so on. Some of this difference is illustrated in the comparison of European and China manufactures earlier.

Table 8 - CO₂-eq., NO_x and SO₂ emissions from different sources of energy [123].

Energy source	CO ₂ -eq	NO _x	SO ₂
<i>Electricity output [kg/MWh_{out}]</i>			
Hard coal	660–1050	0.3–3.9	0.03–6.7
Lignite	800–1300	0.2–1.7	0.6–7
Natural gas	380–1000	0.2–3.8	0.01–0.32
Oil	530–900	0.5–1.5	0.85–8
Nuclear power	3–35	0.01–0.04	0.003–0.038
Biomass	8.5–130	0.08–1.7	0.03–0.94
Hydropower	2–20	0.004–0.06	0.001–0.03
Solar energy	13–190	0.15–0.40	0.12–0.29
Wind	3–41	0.02–0.11	0.02–0.09
<i>Fuel input [kg/GJ_{in}]</i>			
Hard coal	46–125	0.028–0.352	0.003–0.596
Lignite	91–141	0.025–0.161	0.047–0.753
Natural gas	57–85	0.037–0.277	0.0002–0.044
Oil	75–94	0.081–0.298	0.112–0.698
Biomass	0.1–10	0.007–0.128	0.004–0.094

As Table 8 illustrates the difference between the CO₂-eq emission in the high scale for solar energy and low case for natural gas, the difference is just half in favour of the solar energy. From this perspective, is it fair that one have to buy CO₂ quotas when producing energy from natural gas, and not from solar? These indirect emissions are off course difficult to estimate on a case to case basis, but an increased public awareness of this fact, and maybe a later direct taxation is not unlikely to expect.

The development in the PV industry and the continuously new incentives and policy to reduce GHG emissions means that LCA of PV systems is a continuously work. Both as a decision tool to make new policies, but also to see the effect of them. As late as 2014 the EU Waste Electrical and Electronic Equipment (WEEE) Directive made it compulsory for PV manufacturers to take back and recycle at least 85% of their PV modules free of charge [3].

In an environmental perspective, the production of PV systems in Norway makes a lot of sense as the input energy used in production is mostly renewable and the production would be regulated through rather strong environmental directives.

4.1.2.2 Social responsibility opportunities

As focus on the environment are in general high, showing social responsibility will in most cases draw in attention. According to Patric Jonsson, head of Research and Development at Pite Energi, this was a very important motivation for trying out PV systems. A lot have been written their PV systems. School classes are visiting in average once a week. It also draw a picture of Pite Energi as a progressive place to work, making them a more attractive employer. The value of this publicity is huge compare to the cost of installing their PV systems.

The effect of very high publicity is likely to believe that will be reduced, however when this happens the direct cost of the PV systems will have been reduced to a level of preferred choice of electricity. Also, the focus on social responsibility in general are showing no sign of getting lower. Perhaps those not focusing enough on social responsible solutions are getting an increasingly bad publicity instead.

Another interesting aspect regarding social responsibility opportunities, borderline direct revenues, is the increased demand for office buildings with a higher energy rating. Not just those that owns the buildings they are operating in, but also for renting. Making the demand for high energy buildings lower, vice versa. Especially reaching the highest grade of A,

meaning that the building have to produce some energy itself. Solar power being one of the obvious choices.

4.1.3 Other indirect revenues or costs

Another way of looking at PV systems, and especially PV modules, is not as only an addition to a building, but as a substitute. The warranty, just for guaranteed module performance, is in most cases 25 years. One could expect the module itself to last even longer. The PV module could isolated be considered a robust façade materials, the energy it produces just an extra bonus.

A combination of VRE and the highly controllable hydro power is a very good combination. Storing the surplus energy from the VRE source as water in the hydro magazine by pumping the water up into the reservoir. However, experience from Italy shows a distinct invers correlation between the utilization of pumped hydro and installed PV capacity as illustrated in Figure 126. Traditionally the prices during the day is higher than during the night, and pumped hydro utilizes this. Introduction of PV lowers this price difference and might be the reason for this lower utilization. The IEA also states that with a higher shares of VRE, one can expect a lower utilization of available energy sources [93].

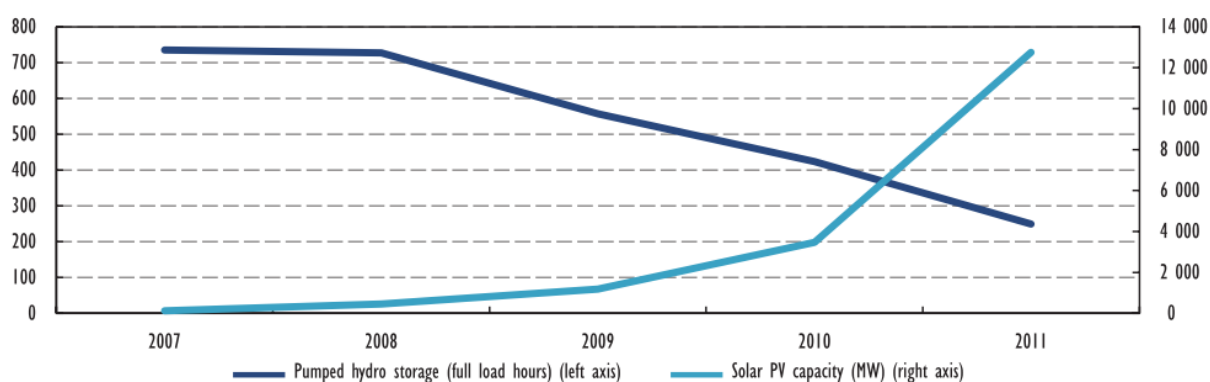


Figure 126: Utilization of Italian pumped hydro storage and installed PV capacity [93].

4.2 Policy instruments and their influence on PV profitability

In addition to the challenges represented by solar as a variable energy source, the necessary assistance by policy support mechanisms are considered by the IEA to be the two biggest challenges towards a higher share of VRE [3].

In this chapter two policy instruments are look into. The investment support and feed in tariffs.

4.2.1 Investment support

Oslo municipality announced in November 2014 that they would support the installation of PV systems with 40 % of the total installation costs. The campaign started at 10th of December 2014 and stop when they reach a granted amount of support of NOK 2 mill [124]. As this is a rather small amount this probably has been granted. An evaluation of the project has not been released and whether this initiative will continues is not known.

However, Enova SF introduced in 2015 an investment support scheme with the ability to get back 35 % of the documented total installation costs. Though at maximum NOK 10 000 plus NOK 1 250 per installed kW limited upwards to 15 kW [125]. For a 15 kW PV system this equals to a support of NOK 28 750.

If linearly scaling down the installation cost of the Acusticum PV system to 15 kW, this would cost NOK 176 786. The investment support is 16 % of this sum. In addition during the lifetime an additional 1/3 of the investment cost would be total annual costs , according to the Acusticum PV calculations, reaching a total cost of about NOK 235 000. The support is now down to about 12 %. Considering a linearly scaling is most likely a very optimistic estimation, the total cost would be even higher, and the relative support even lower.

So, even if the initial support of 35 % sounds promising, the actual support of the total cost is more in the line of 10 %, also reflecting the LCOE reduction.

According to Patric Jonsson, the Acusticum PV system got an investment support of SEK 1 037 000 [111]. As earlier described, SEK 280 000 of this has been used to cover expenses

related to the research and development part of the Acusticum PV system. If reducing the investment cost in the LCOE model with SEK 757, the lifetime cost of energy for the Acusticum PV system is reduced to 0.96 SEK/kWh.

4.2.2 Feed in tariffs (FiT) and Green certificates

As opposed to investment support as a one-time payment, instead with FiT schemes you get a payment for the energy you produce. How, and how much you are compensated differs from country to country and is also in most places adjusted, manually or automatic (i.e. through a marked mechanism), from time to time.

Germany is one of the countries that have been using FiT schemes very actively as an incentive to increase the amount of renewable energy, making them the biggest PV market for several years. As the market has matured, the FiT have been reduced. However, as FiT are being reduced in a now relatively big PV market, this is forcing the PV installers to reduce prices [105]. This is most likely one of the important reasons behind the large reduction in LCOE in Germany the last years as illustrated in Figure 127. As expected, a study investigating the influence of FiTs on the investments in renewables in five countries concludes that this has had a significant positive effect [126].

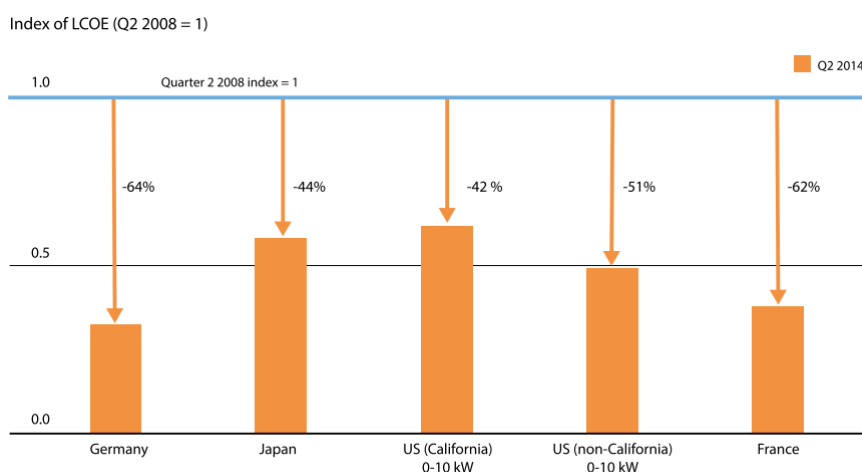


Figure 127 – LCOE reduction for residential PV from Q2 2008 to Q2 2014 [12].

In Norway and Sweden the electric power distributors, and some big consumers, are obliged to buy a certain amount of these green certificates. The share they have to buy increases until 2020 and from then decreases to zero in 2035. The certificates are issued to producers that invest in new renewable energy capacity. Both a demand and supply is now made and a market is created where these certificates can be bought and sold [127].

The aim is to build 26.4 TWh by the end of 2020. The arrangement with certificates is technology neutral.

In Norway the fee for being able to receive these certificates are NOK 15 000,- for systems less than 100 kW, and NOK 30 000,- for systems further up to 5 MW⁹ [127]. As of the 7th of May 2015 the price for one certificate is 165.13 NOK/MWh. The average price in 2013 was 183.80 NOK/MWh, in 2014 it was 177.73 NOK/MWh and for the first quarter of 2015 165.82 NOK/MWh [128]. As also seen in Figure 128, the price trend from 2013 and onwards are steadily decreasing despite the annual increase in obliged share of certificates the power distributors have to buy.

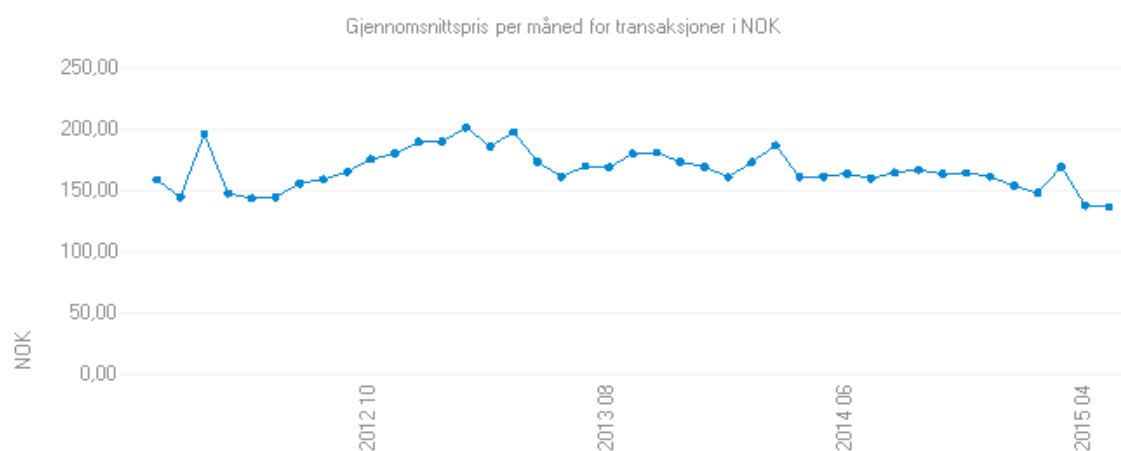


Figure 128 - Green certificates price development 01.2012 - 05.2015 [128].

⁹ For other rates: <http://www.nve.no/no/Kraftmarked/Elsertifikater/Kraftprodusenter/Gebyr/>

Green certificates have been used in Sweden since 1st of May 2003. Norway and Sweden combined from 1st of January 2012.

How the price will evolve is very difficult to predict. However we know it will steadily move towards zero at 2035, meaning the Acusticum PV system will only be able to sell certificates in 20 of the 30 years of the analysed period. As the uncertainty is high, only a rough estimate will be done. A discounted certificate price of 0.07 SEK/kWh is assumed for the whole analysed period, reducing the cost of energy from the Acusticum PV system down to 0.89 SEK/kWh when also including the investment support. The connection fee for being able to receive certificates are neglected.

The direct positive economic effect of investment support or as a FiT is not difficult to see. It is however important to point out that it is the long term effect that is interesting. As any emerging industry the starting cost is high because of investments that have to be done, uncertainty is higher and have to be valued, the customer knowledge about the product is lower and so on. A positive economic policy instrument is to facilitate a faster and easier transition.

4.3 Electricity price development

If the PV system investment is profitable or not is off course closely related to the marked electricity price development. First a closer look on the annual average, next on grid rent and taxes as these also are an important part of the actual price paid, and last on other time periods as the cost structure of electricity might be changing.

4.3.1 Annual average

Just before the reason finance crisis, 10-year future contracts for electrical power in the Nordic was traded for over 70 EUR/MWh. As seen in Figure 129, Markedskraft predicted in 2012 a price of about 45 EUR/MWh in 2020. In 2015 the electricity price in 2020 is trade at about 30 EUR/MWh as illustrated in Figure 130. All graphs are pointing up, but the trend is down.

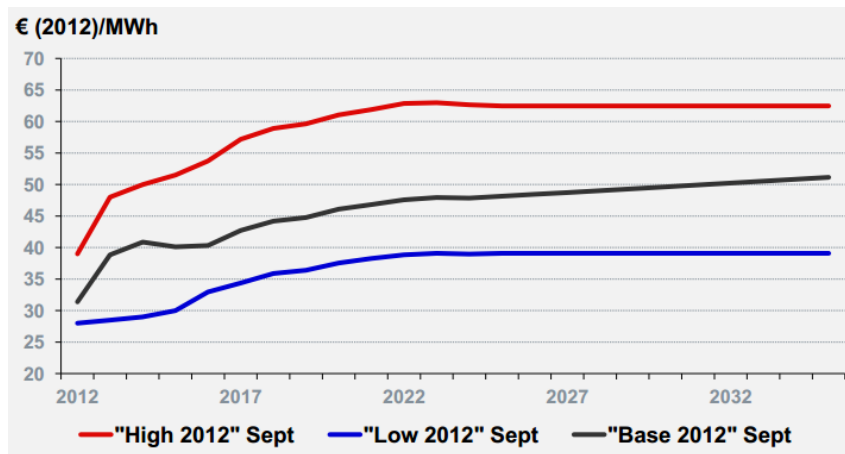


Figure 129 - Forecasted Nordic spot price of base load power in real 2012 Euros from Markedskraft [129].

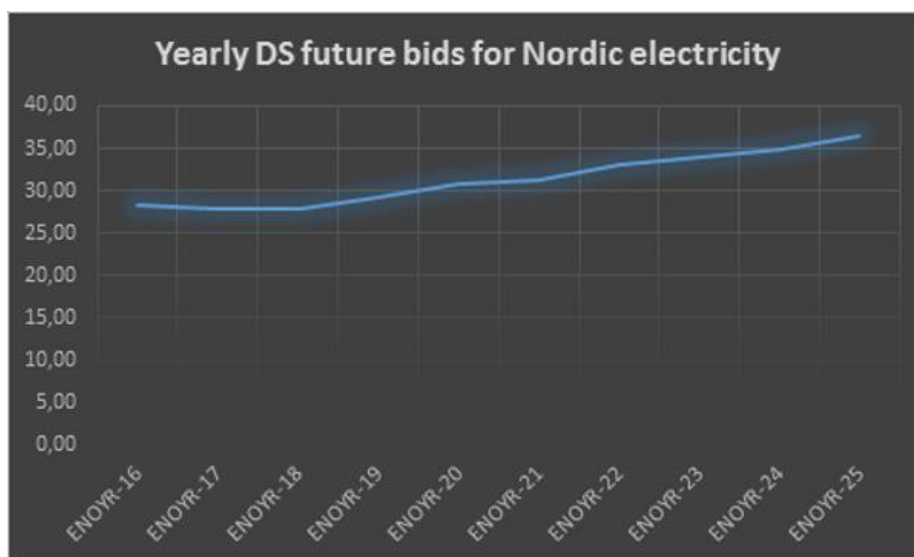


Figure 130 - Future bids for Nordic electricity in EUR/MWh. Data from Nordpool [130].

As the price of electricity is market controlled it is regulated through supply and demand. Norway and Sweden have a goal of 26.4 TWh of annual new renewable energy within 2020. Most of which is VRE. Will other sources, like nuclear in Sweden, be reduced? Will the demand increase? If not, prices might decline fast. As VRE has a very low short run marginal cost, it will push the supply curve and thereby the price equilibrium down to a new level as illustrated in Figure 131.

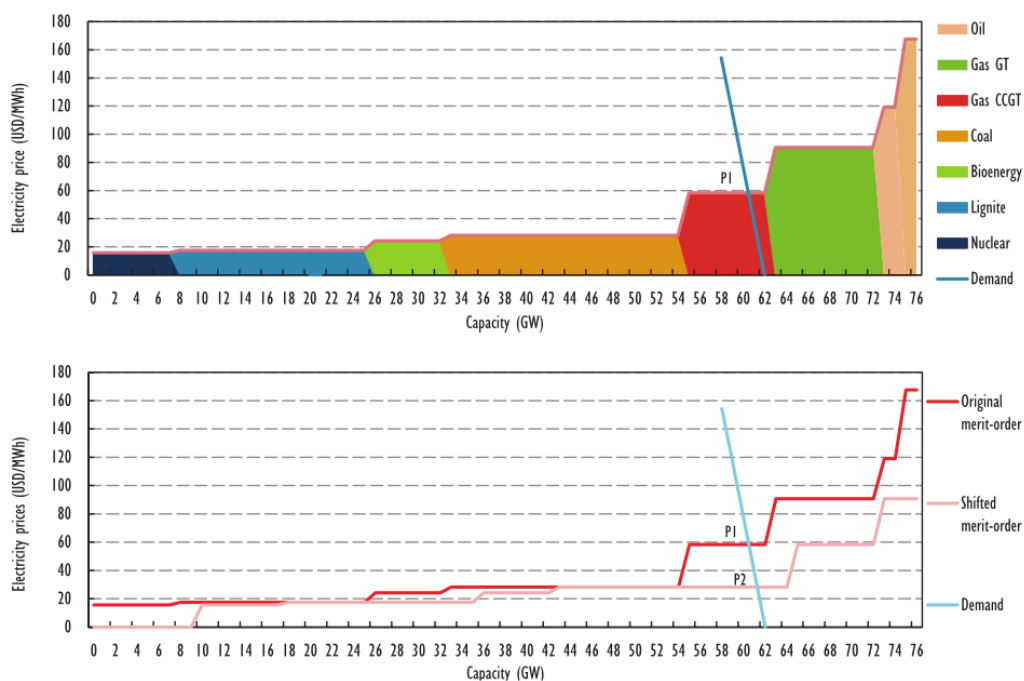


Figure 131 - Shift in merit-order and system price with the introduction of renewables with a SRMC close to zero. CCGT = combined-cycle gas turbine; GT = gas turbine; P1 = price without additional generation; P2 with additional generation [103].

However, the physical and monetary electricity market in the Nordics are expanding. Interconnections to Europe are under construction, and more are planned. A milestone was reached the spring of 2014 when the system price one day was the same in northern Norway as in Spain. As Europe is moving against a backbone high voltage DC grid, this might become the rule, and not the exception. Although, even if the prices in Europe historically have been higher than in the Nordics, the introduction of PV in Europe might flip this around.

But what the electricity consumer actually pays is more than just the electricity as the next chapter will demonstrate.

4.3.2 Grid rent cost, tax, VAT and development in these

How much the grid rent is and how it is divided between annual fixed cost and cost related to energy used depends on where in Norway you are. I.e. for private households including VAT the fixed cost ranged from NOK 750 in Oslo, to NOK 3868 in Hedemark. Also the cost related to energy used is not the same all over the country, ranging from NOK 0.113 per kWh in Vestfold to NOK 0.366 per kWh in Sogn og Fjordane. Adding these two components together to NOK per kWh for a household using 20 000 kWh, the range is from 0.256 to 0.499, with a national average in January 2015 on NOK 0.315 per kWh [131]. Adding tax this becomes NOK 0.478 per kWh as seen in Figure 132. Also the business and industry have relatively large variations. National average including tax in January 2015 of NOK 0.408 per kWh.

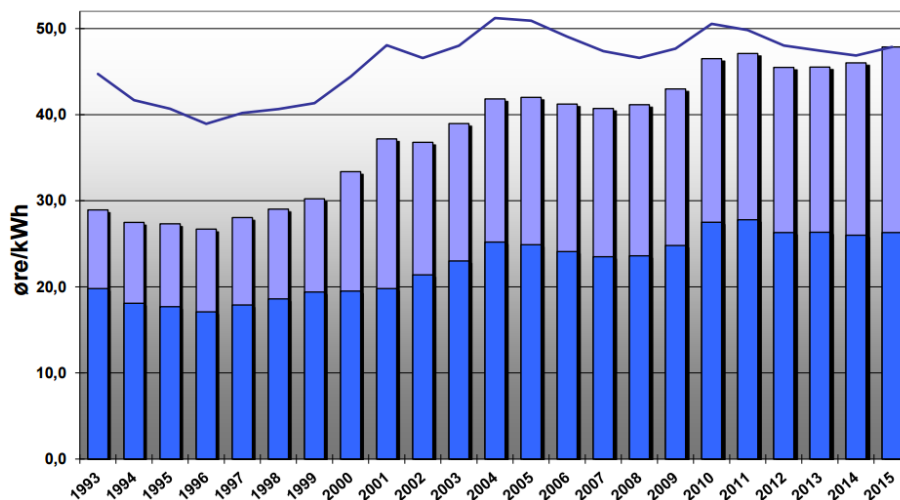


Figure 132 - Grid rent statistics for private households in Norway. Blue is grid rent for a household using 20 000 kWh, purple is tax and VAT, and line is prices in 2015 currency [131].

Although the real price as seen in Figure 132 have been about the same for the last 15 years, huge investments are on its way in the national central grid. The central grid development plan describes an annual investment of between NOK 5 to 7 billions the next 10 years [132]. This is considerable amounts compared to earlier periods as seen in Figure 133. As the grid rent is calculated on the basis of grid investment and maintenance, this might indicate a higher grid rent the next years. I should be noted that the graph is only the central

grid, and the regional and district grid is not included. No indications on national average changes in these have been found.

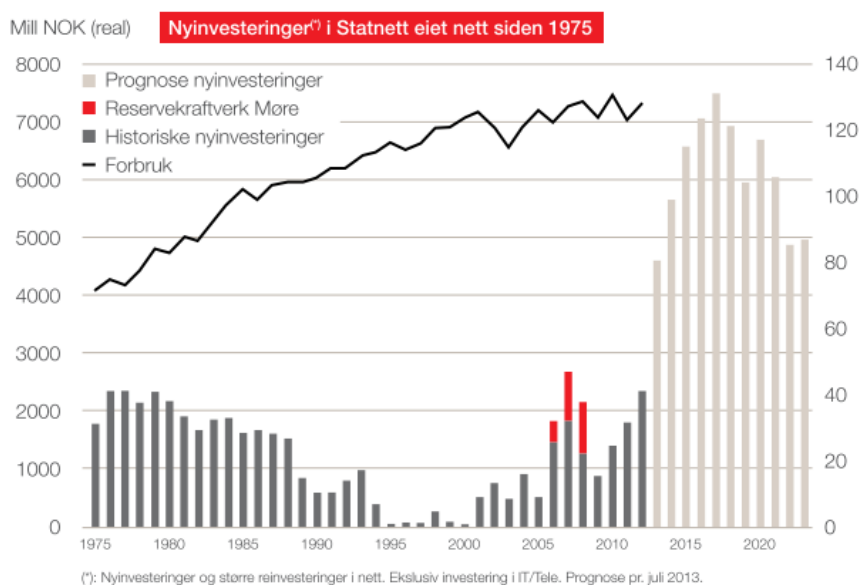


Figure 133 - Investment in the central grid. Historically and prognosis [132].

If distributed generation, as PV systems, are getting more common, it is difficult to believe that several grid operators will still collect a big portion of the grid rent through a cost related to energy use. As IEA states: “Moreover, for reasons of efficiency, tariff simplicity and fair cost allocation, electricity tariffs tend to recover a significant part of fixed infrastructure costs – which may or may not be reduced by distributed PV – via per-kilowatt-hour charges.” [5]. So if not the need for grid investments go down because of increased PV, the consumers will in fact subsidize the connection to the grid for the PV owners. A subject also discussed in the IEA [133]. The IEA goes as far as saying that; “Reaching socket parity dramatically increases the relevance of cost-reflective electricity tariff design.” [5].

The grid infrastructure is dimensioned by the peak demand. If the PV was to reduce the grid system cost, it have to reduce the peak demand. This can only be the case in systems where the peak demand is during daytime. The California independent system operator have simulated a higher PV penetration, and as the Figure 134 illustrates they have not found the increased use of PV to reduce peak load.

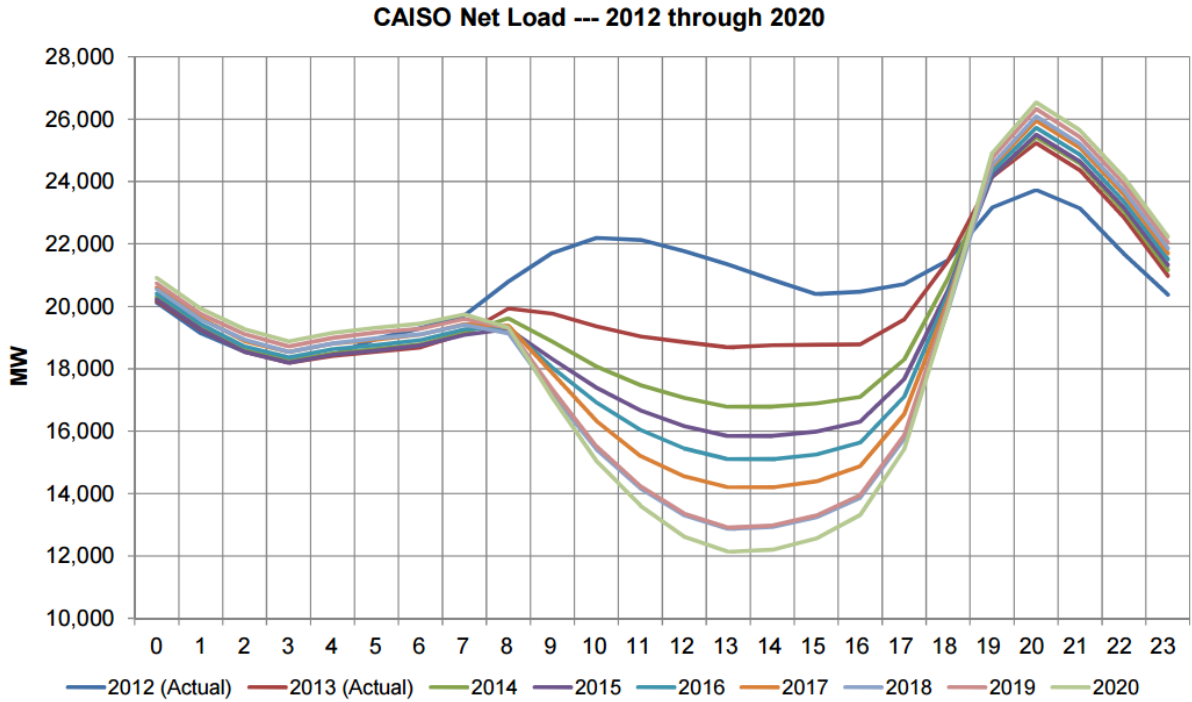


Figure 134 - Actual and projected energy demand during a single day in March from the California Independent System Operator Corporation (CAISO) [134, 135].

However, it might seem that the conclusion from CAISO is not generic. As seen in Figure 135 the peak load in Germany has in fact been reduced, although it might indicate that the peak load reduction potential has been taken out. The same can be seen for Italy in Figure 136.

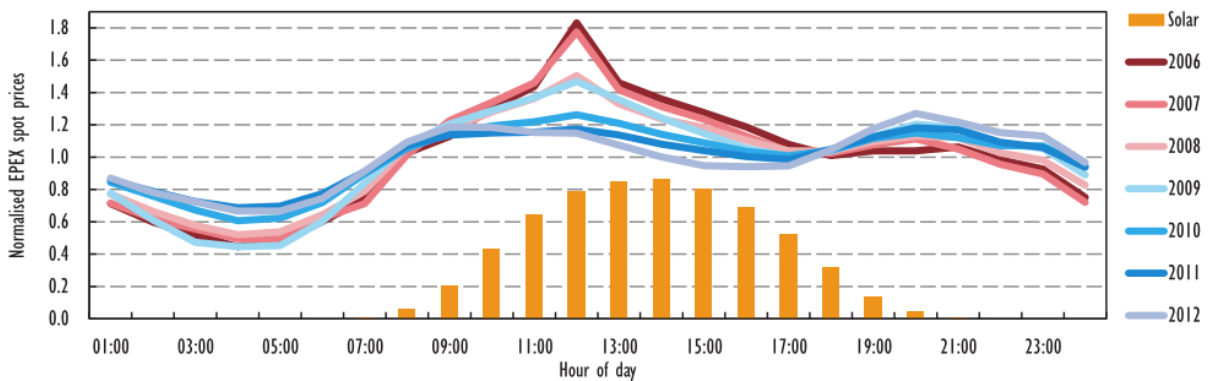


Figure 135 – Shift in the spot market price structure. Germany 2006-2012 [93].

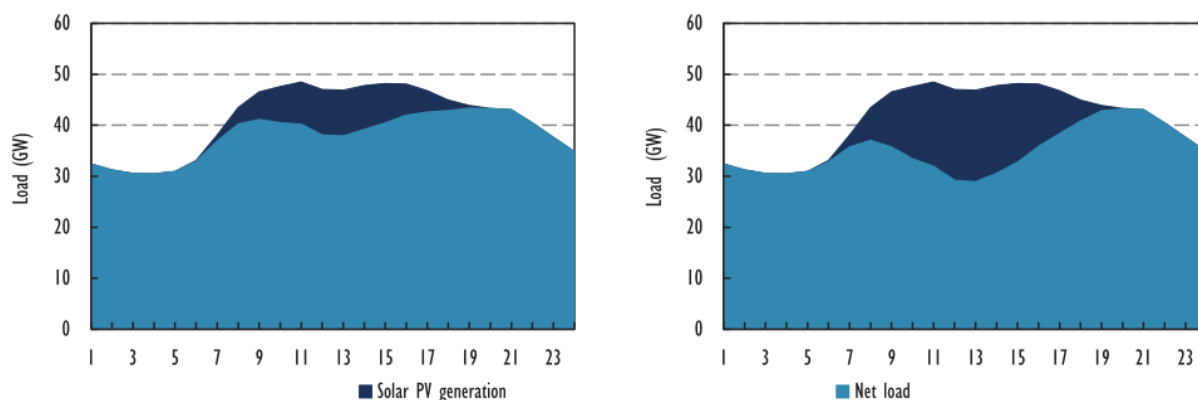


Figure 136 – Net load and the impact of solar PV generation in Italy. Left: A sunny day in July 2012. Right: Simulated doubling of PV capacity [93].

To summarize, it looks like the grid rent might increase some, assumed 0.5 NOK/kWh for further calculations. As more distributed generation like PV is introduced to the grid is less likely that current cost structure for grid rent is continuing, collecting a higher share from the annual fixed cost. The tax and VAT is assumed following the inflation level.

4.3.3 Demand- and price fluctuations during the day

Electricity is not a homogenous good as the value of it changes over time. The daily fluctuations have until just a few years ago largely been the result of changes in daily demand as the sources of supply in a large share of the world is generating the same amount of power all day due to the technology used. Although where the supply is easier to control the fluctuations is much lower, as seen in Figure 137 comparing the Nordic towards Germany.

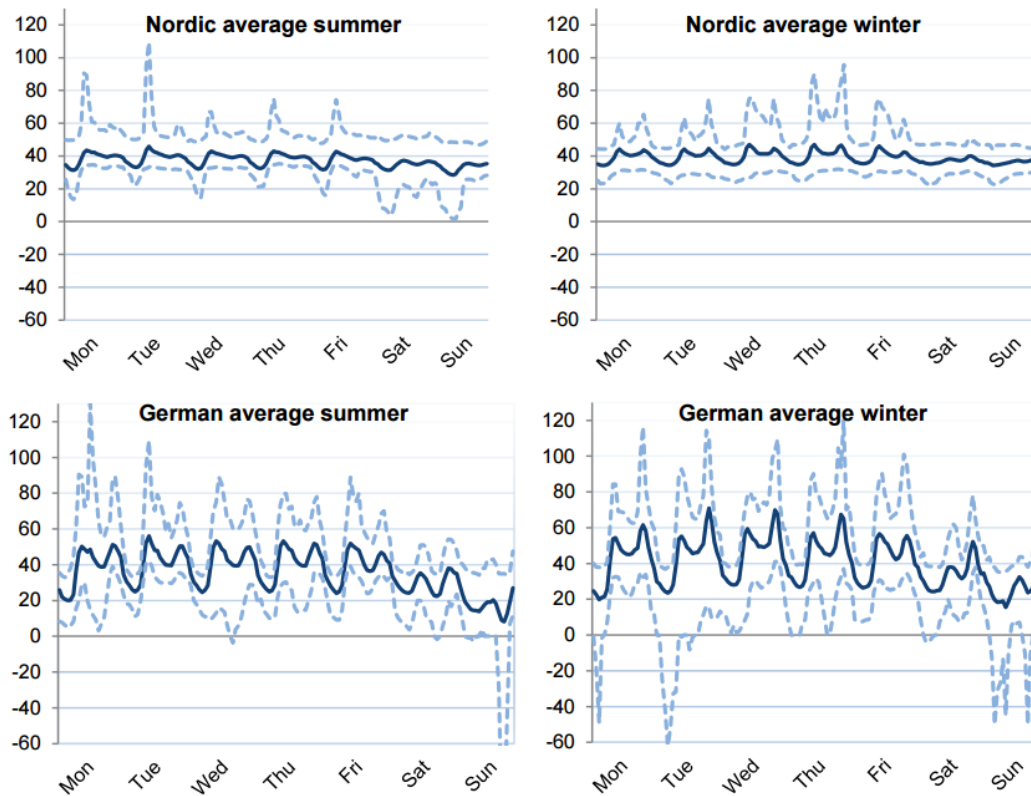


Figure 137 - Nordic and German average price of electricity in 2013 [136].

The prices during daytime is still in most places higher than night, but if the share of PV system in the grid continues to rise this might change. As electricity from PV has a short run marginal cost of close to zero, when the PV system is built it will deliver electricity almost regardless of price. In fact, there have been days in Germany with even negative prices.

If it will go as far as making day cheap and night expensive may be unlikely. However, the fluctuations is likely to be faster, instead of day vs night, it is morning and evening vs mid-day and night, a doubling in frequency. But as the prices might be more volatile, it opens other opportunities. As fluctuations may be doubling, this reduces the time the energy have to be stored, and also reduces the need for storing capacity by half.

4.4 PV system investment profitable in Norway?

As both the cost- and revenue side of this question as seen in this thesis have a lot of variables, with also large variations within Norway, a definite answer depends on each case examined and the assumptions made. Although it may look like the average is getting close to a tipping point, meaning several PV projects are already profitable today.

The different aspects discussed in the above sections in chapter four and comparison to the statements in the introduction will be taken in the following section, and the last section some of the interesting elements concerning electricity from PV and self-use vs self-sufficiency. Interesting factors when assessing future PV investment profitability.

4.4.1 Reaching socket parity

The normal way of starting the assessment of whether or not an energy technology is competitive, and thereby profitable, is to compare it to the alternatives. As illustrated in Figure 138 the LCOE on PV systems in Germany already in 2013 was competing with other technologies – at irradiation levels comparable to southern Norway.

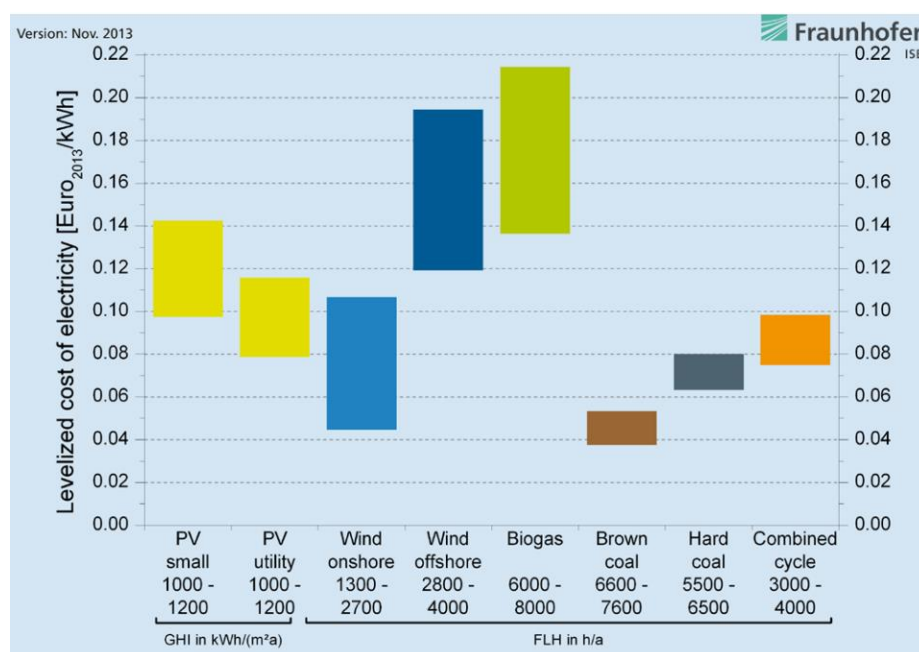


Figure 138 – LCOE for different energy technologies in Germany 2013 [1].

However, the price for electricity in the grid is for a given site at a given time the same, regardless of which source. This is the price that for most energy technologies is interesting. Reaching this level is also referred to grid parity. Grid parity has already happened several places and will occur throughout the next decade in the majority of the world for solar electricity [19]. Although, one should be aware that the grid parity concept is interpreted and used differently.

The interesting characteristic property of PV technology, in comparison to most other energy technologies, is that is extremely scalable without affecting the energy output. Meaning that even small systems can generate electricity with the same efficiency as larger systems at almost the same price. As seen in the previous chapters the price paid for the electricity by the consumer is more than just the cost of electricity. By mounting a PV system on a consumer property, one can compare the cost of electricity from the PV system to total price of electricity. Reaching this level is referred to at the socket parity. As the price paid is different between private households and the industry mainly due to VAT, it is normal to make this differentiating.

Whether a PV system investment is profitable or not depends on whether the socket cost of electricity is higher or lower than the LCOE adjusted for policy instruments. In other words; having reached socket parity or not.

Germany, Denmark, Italy, Spain and parts of Australia have in 2013 already reached socket parity, defined here as the point where a household can make 5% or more return on investment in a PV system just by using the energy generated to replace household energy consumption, while countries like Japan, France, Brazil or Turkey are expected to reach it by 2015 [94]. An illustration of countries that have reach, or is close to reach, socket parity can be seen in Figure 139.

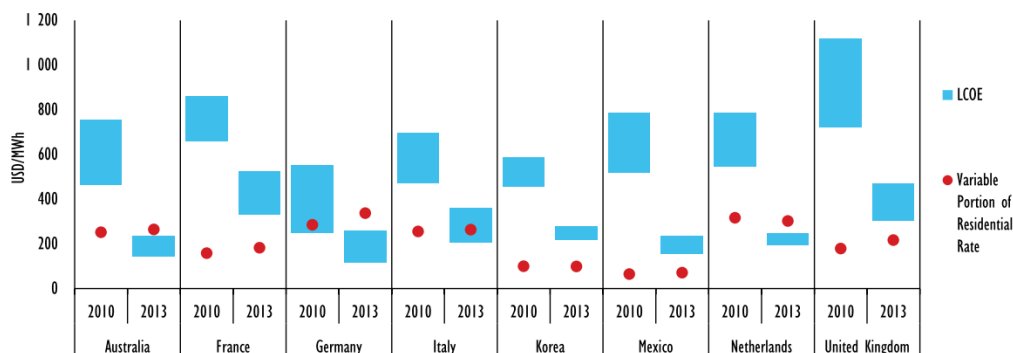


Figure 139 – The LCOE compared to the variable portion of electricity tariffs in selected countries [5, 133].

So what is the status on socket parity for private households in Norway? The LCOE found for the Acusticum PV system was 0.132 EUR/kWh. However private households have to pay tax for the PV system, and the size of the Acusticum PV system means some lower installation cost. On the other hand, most of the population in Norway are living in the southern part of Norway as illustrated in Figure 140. As this is further south than Piteå, it is likely to assume that the irradiation levels are higher. The LCOE found for the Acusticum PV system is used.

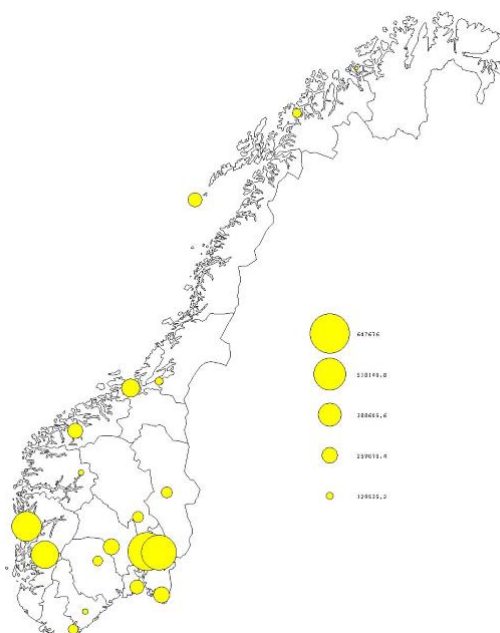


Figure 140 - The population distribution in Norway as of 1st of January 2015 [137].

As found in the chapter regarding policy instruments, it was found that the investment support had a LCOE reduction impact of about 10 %. Reducing the cost of PV electricity to about 0.12 EUR/kWh.

As for the socket cost of electricity, the price of electricity was found to be about 0.03 EUR/kWh incl. VAT this is 0.0375 EUR/kWh. The grid rent, tax and VAT was found to be about 0.06 EUR/kWh. In total this is just below 0.1 EUR/kWh.

With this rough estimate, private households in Norway have not reached grid parity for PV systems. However it is close. Taking into account that this is a rather rough average estimate, and no indirect revenues have been taken into consideration, the cost of PV electricity is most likely low enough for a lot of private households in Norway.

If one compare these results to the socket parity calculations illustrated in Figure 15, we notice that the estimated average cost of electricity in 2016 is just below 0.2 EUR/kWh. This is twice the amount found in this thesis. However, the best LCOE estimates are just below 0.17 EUR/kWh in 2016. Although not taking any policy instruments into account this is higher than the LCOE used in the calculations above. This might indicate that assumptions made for the LCOE estimated used for private households in Norway are somewhat optimistic. Also, as discussed during the chapter on grid rent, it is likely that one might see an increase in the fixed grid rent cost at the expense of the part of the grid rent related to the energy used. This will in turn make the socket cost lower and move the socket parity forward in time.

At the company level, the socket price of electricity is lower than for households. However, the PV LCOE is also most likely somewhat lower. In addition, the indirect revenues are also more closely related to actual revenues as discussed earlier. So even as the industry is further from socket parity than the private households, the total value of a PV system might still be worth it also today.

Although grid parity has not been reached for most actors in Norway, it will be reached in a few years. No present energy technology are experiencing growth rates as seen by the PV industry.

The IEA states in their 2014 “Technology Roadmap: Solar Photovoltaic Energy” that they envision a 4600 GW of installed PV capacity by 2050 [3]. A considerable increase from today's 150 GW. It should also be mentioned that this estimate is about 50 % higher than their estimate from just four years earlier [3].

4.4.2 Self-use and self-sufficient

One important assumption made by most socket parity analysis, also the estimates above, is that all energy produced are used by the consumer. As also mentioned in chapter 4.3.3, this is problematic.

As the direct power output from a PV system cannot be controlled by time, and the fact that energy have to be consumed the moment it is produced, the generation of PV electricity and consumption of electricity will not always converge.

As illustrated in Figure 141 PV systems will most likely not be able to cover the power needed during nights, and depending on the system size it will most likely produce more power than the consumer needs during some days.

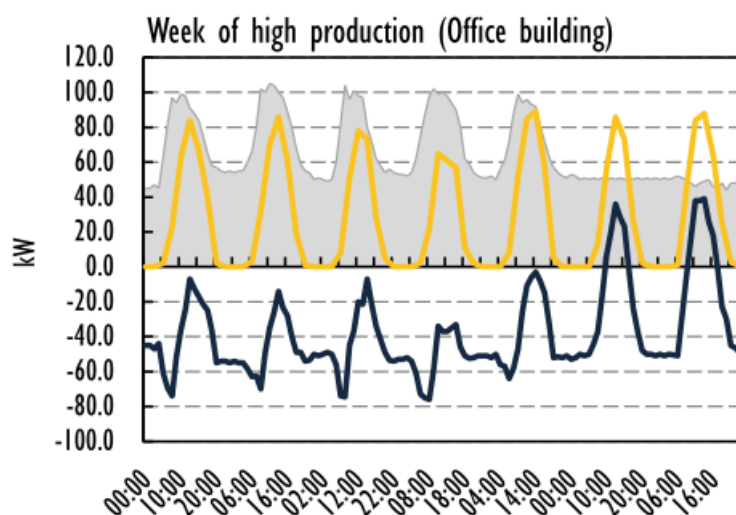


Figure 141 - The influence on electricity demand and supply by a PV system on a office building in southern France [5].

If dimensioning the PV system to use all of what is generated, 100 % self-use, there will be huge periods of power deficit. The result being that a lot of power must be imported from

the grid, low self-sufficiency. Increasing the size of the PV system will on the other hand increase self-sufficiency, but decrease self-use. As the value of the power sold is much lower than the power used from the PV system, a PV system designed for 100 % self-sufficiency could be a poor economical choice. It is a trade-off between self-use and self-sufficiency as illustrated in Figure 142. A 100 % self-use results in very low self-sufficiency, and vice versa.

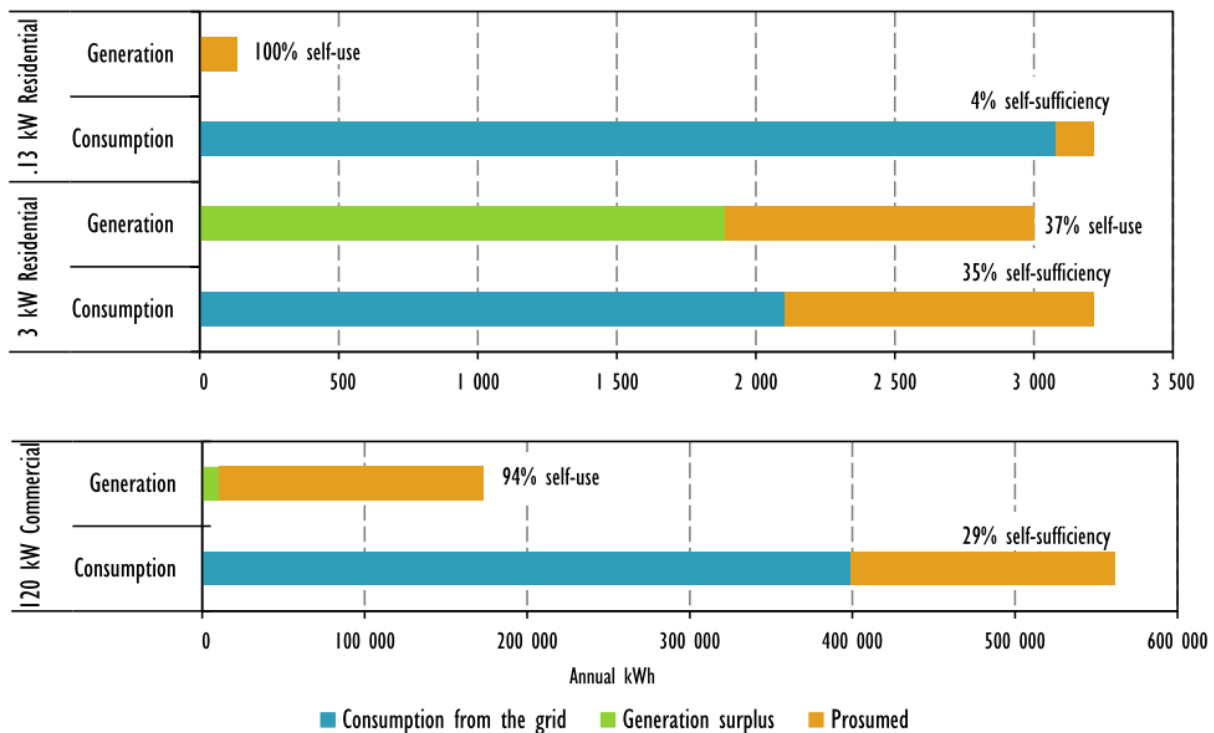


Figure 142 - Self-use and self-sufficiency shares by PV system size and consumer segment [5].

Achieving high levels of self-sufficiency, and still maintaining high levels of self-use depends on how well the consumption pattern correlates to the PV electricity generation pattern. As illustrated in Figure 143, the power consumption pattern for office buildings are especially suited for PV electricity.

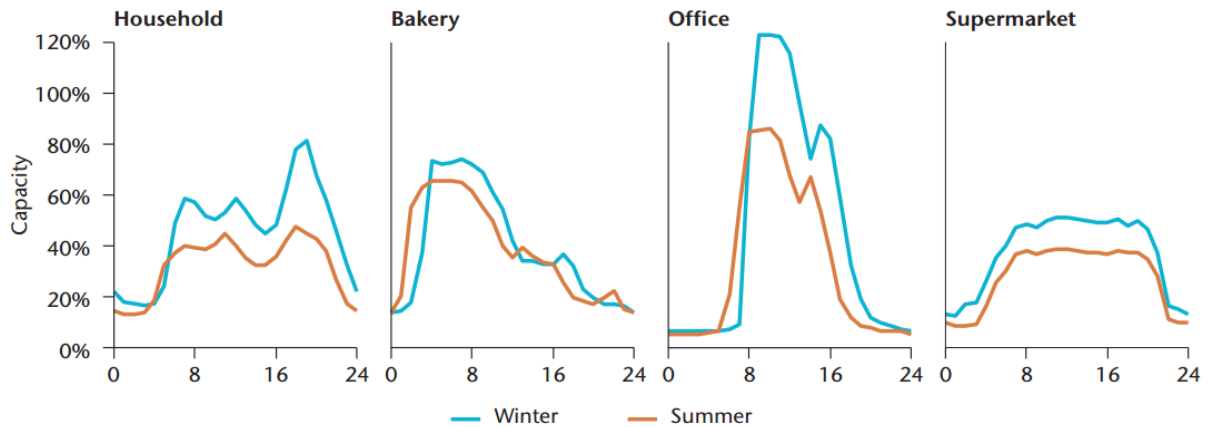


Figure 143 - Electricity consumption profiles for building types in Germany [3].

The best profitability is of course reached when the degree of self-use is at its highest. However, as the degree of self-use declines so does the PV system profitability as illustrated in Figure 144. The dimensioning of the PV system should not be arbitrary, but seen in self-use vs. self-sufficiency context.

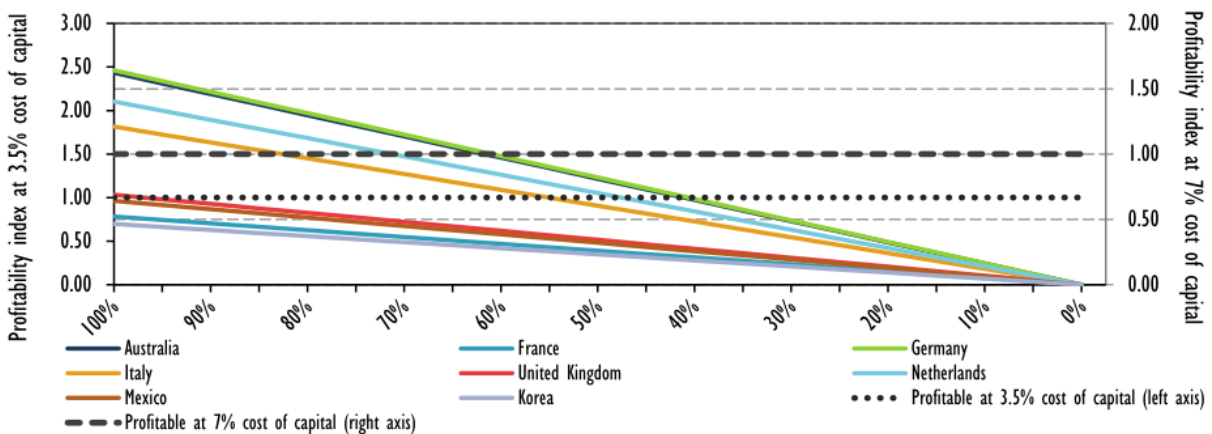


Figure 144 – PV system profitability for different rates of self-use [5]. Profitability index = $1 + \text{net present value} / \text{investment}$. A value over 1 means the project is profitable.

The question on self-use vs. self-sufficiency makes the notion on socket parity somewhat harder to use. More variables to take into account. The PV system investment profitability not only depends on whether or not the price of electricity have reach grid parity, but also

what the consumer gets paid for the excess electricity delivered to the grid and the cost of storage at the consumer [5].

As storage capacity is one of the few components that can increase the self-sufficiency, and still maintain a high degree of self-use, PV system owners are off course very interested in storage solutions. The huge interest in the home battery solution Power Wall by Tesla, was no surprise.

5 Conclusion

5.1 Summary

So, what is the performance and potential for PV energy in northern latitudes?

In order to calculate the performance of a PV system it is important to know the solar potential. For the northern latitudes, these data are of relatively low quality due to few good ground measurement stations and high uncertainty of satellite data. This is also confirmed for Piteå by rather high differences in levels and composition of the irradiation. The most likely best generic irradiation database for northern latitudes was found to be the NASA/SSE database.

It may also look like the current mechanical PV module standard is not suited for some of the climate at northern latitudes as several of the modules at the Acusticum got a bent frame during this winter. The reason for this was high pressure on the frame. This might indicate that frame-less modules are a better choice at northern latitudes.

Northern latitudes have large shares of low light conditions, meaning the inverters are performing at a lower power than normal compared to the rest of the world. This might result in lower efficiencies. However, results from the inverters at the Acusticum PV system indicate that also high power input have much lower than reported efficiency. Whether or not this is related to northern latitudes is not known.

The simulated performance of the 236 kW_p PV system at the Acusticum reported an annual yield of 208 kW_p. A specific production of 897 kWh/kW_p and a performance ratio of 0.850. The biggest loss was 7.1 % due to snow, but this was put in manually in the simulation. How big impact this actually have is not known, but this winter it was much higher for the PV system. This might indicate that the optimal tilt and azimuth for PV modules should take the snow also into consideration, allowing for passive removal.

The Acusticum PV system LCOE was calculated to be 0.132 EUR/kWh. The cost level was found to be close to world best practice. However, as the cost in the industry are

declining at all levels, it is highly likely to believe that the next PV system will have an even lower LCOE.

A LCOE reduction of about 10 % was found in the investment support for a 15 kWp private household using the Acusticum PV system as base case. The resulting cost of PV energy was 0.12 EUR/kWh.

Current and near future electricity price for households was estimated to 0.1 EUR/kWh in Norway. This means that the direct cost difference is 0.02 EUR/kWh against investing in a PV system. However, several assumptions have been made during these calculations where changes of some of these would decrease the difference. In addition, indirect revenues points to values much higher than the cost difference found.

There are some issues as mentioned above to be aware of, but the end conclusion is that the performance and potential for PV systems in northern latitudes is overall very good.

5.2 Further research

Mechanical pressure due to snow on PV modules. Modules are rated for horizontal pressure, especially modules at northern latitudes are not mounted horizontal. Adding snow results in high pressure on the frame. Is there a critical tilt angle for PV modules related to snow? Must the angle be either low enough in order to not pressure the frame, or high enough for the snow to easier fall off. Is the solution frame-less modules for northern latitudes?

Low snow accumulation position of modules vs optimal irradiation angle. Lowering the loss due to temporary shading vs increased collection in the snow free months. Could also be considered in a time perspective, as probably energy at the cold season is worth more. An optimal tilt angle in northern latitudes must take the snow accumulation into account, but how much, and what are the effect on performance?

The lifetime of PV modules at northern latitudes. Is the rate of degradation different at northern latitudes with its climate conditions? (Colder, more wind, less intensive irradiance). Should the degradation rate be related to another variable than years?

How can the new properties of inverters be controlled in order to be an instrument for the system operator?

The low quality of irradiation data in northern latitudes, and especially Norway. Continued validation of the solar data collected by Kjeller Vindteknikk. The use of polar orbiting satellites for estimation of irradiation. Could the new 2012 polar satellite contribute?

What is the environmental effect of a PV system mounted in Norway?

Energy from PV systems are already affecting Norway indirectly from especially Germany, and it is likely that it is just a matter of time before the direct effect is considerable. The effects of PV systems are slowly lining up. How to exploit the positive effects and dodge the bad ones are the challenge.

Electricity cost structure. Electricity is not a homogenous good related to time. This is poorly reflected in the price of electricity. Electricity from PV have a short run marginal cost of close to zero, and some research suggest that increased number for PV systems does not reduce the power peaks. There will be challenges. What are those, and how to handle them?

What is the optimal self-sufficiency and self-use for which values of input? Optimization formula connecting socket parity, grid parity, LCOE, storage cost and location. Telling the optimal PV system at which timeframe. Could also be used to predict critical storage cost.

5.3 Recommended reading

For basic and a practical focused introduction to PV technology, a big recommendation goes to the book “Planning and installing Photovoltaic Systems” by the Deutsche Gesellschaft für Sonnenenergie.

Also the latest publication of “Technology Roadmap: Solar Photovoltaic Energy” (2014) by the International Energy Agency (IEA) gives some interesting aspects about the future of photovoltaic.

For assessment of different policy instruments the publication “The Power of Transformation”. (2014) Chapter 8 by the IEA is recommended.

References

1. Fraunhofer Institute for Solar Energy Systems, *Levelized Cost of Electricity Renewable Energy Technologies*. 2013.
2. Tao, M., *Terawatt Solar Photovoltaics: Roadblocks and Opportunities*. 2014: Springer. 9-20.
3. International Energy Agency, *Technology Roadmap: Solar Photovoltaic Energy*, in *Energy Technology Perspectives*. 2014.
4. International Energy Agency - Photovoltaic Power Systems Programme, *Snapshot of Global PV Markets*. 2015.
5. International Energy Agency, *Medium-Term Renewable Energy Market Report 2014*. 2014: IEA.
6. Ellabban, O., H. Abu-Rub, and F. Blaabjerg, *Renewable energy resources: Current status, future prospects and their enabling technology*. *Renewable and Sustainable Energy Reviews*, 2014. **39**: p. 748-764.
7. International Energy Agency, *World Energy Outlook 2013*. 2013: IEA.
8. European Photovoltaic Industry Association, *Global Market Outlook For Photovoltaics 2014-2018*. 2014.
9. DN.no, I.G.R. *Byttet oljefyr med soltak*. 2015 06.06.15]; Available from: <http://www.dn.no/nyheter/energi/2015/03/17/2150/Solenergi/byttet-oljefyr-med-soltak>.
10. International Energy Agency, *Energy technology perspectives 2014: harnessing electricity's potential*. 2014, Paris: OECD/IEA. 376 s. : ill.
11. Reichelstein, S. and M. Yorston, *The prospects for cost competitive solar PV power*. *Energy Policy*, 2013. **55**(0): p. 117-127.
12. International Renewable Energy Agency, *Renewable Power Generation Costs in 2014*. 2015, IRENA.
13. Spatuzza, A. *Brazil contracts 890MW solar PV*. 2014 06.06.15]; totaling 889.7MW of solar PV from 31 projects at an average price of R\$215.12/MWh (\$86.8MWh)]. Available from: <http://www.rechargenews.com/solar/1382254/Brazil-contracts-890MW-solar-PV>.
14. Roselund, C. *890 MW of solar PV clears in Brazil's reserve auction*. 2014 06.06.15]; average clearing bid price of \$0.087 per kilowatt hour]. Available from: http://www.pv-magazine.com/news/details/beitrag/890-mw-of-solar-pv-clears-in-brazils-reserve-auction_100017022/#axzz3I5SAf76I.
15. Christoph Kost, J.N.M., Jessica Thomsen, Niklas Hartmann, Charlotte Senkpiel, Simon P. Philipps, Sebastian Nold, Simon Lude, Noha Saad, Jan Schmid, Thomas Schlegl, *Levelized Cost of Electricity: PV and CPV in Comparison to Other Technologies*, in *29th European Photovoltaic Solar Energy Conference and Exhibition*. 2014: Amsterdam.
16. Carlstedt, N.-E.K., Bjørn; Kjellson, Elisabeth; Neij, Lena; Samuelsson, Olof, *Konkurrenskraft för nätansluten sol i Sverige -sett ur kraftföretagens och nätägarnas perspektiv*. 2006, Elforsk.
17. Stridh, B., et al., *Production Cost of PV Electricity in Sweden*. 2013, WIP.

18. Good, C., et al., *Towards cost-efficient grid-connected PV power plants in Northern Scandinavia*, in *26th European Photovoltaic Solar Energy Conference*. 2011: Hamburg, Germany.
19. Breyer, C. and A. Gerlach, *Global overview on grid-parity*. *Progress in Photovoltaics: Research and Applications*, 2013. **21**(1): p. 121-136.
20. Multiconsult, *Kostnadsstudie, Solkraft i Norge 2013*. 2013, Enova SF.
21. Norwegian Water Resource and Energy Directorate, *Kostnader i energisektoren - Kraft, varme og effektivisering*. 2015.
22. Lont, A. *Our Electrical future*. in *2014 autumn conference*. 2014. Oslo: Statnett.
23. Mertens, K. and G. Roth, *Photovoltaics : fundamentals, technology and practice*. 2014, Wiley: Chichester, England. p. 1 online resource (297 pages).
24. Deutsche Gesellschaft für Sonnenenergie, *Planning and installing photovoltaic systems a guide for installers, architects, and engineers*. 2013, Routledge: Oxfordshire, England New York. p. 1 online resource (xii, 521 s.).
25. Masters, G.M., *Renewable and efficient electric power systems*. 2013, John Wiley & Sons: Hoboken, NJ. p. 1 b.
26. Kleissl, J., *Solar energy forecasting and resource assessment*. 2013, Oxford: Elsevier Academic Press. XXII, 416 s. : ill.
27. Reno, M.J., C.W. Hansen, and J.S. Stein, *Global horizontal irradiance clear sky models: implementation and analysis*. SAND2012-2389, Sandia National Laboratories, Albuquerque, NM, 2012.
28. Eissa, Y., M. Chiesa, and H. Ghedira, *Assessment and recalibration of the Heliosat-2 method in global horizontal irradiance modeling over the desert environment of the UAE*. *Solar Energy*, 2012. **86**(6): p. 1816-1825.
29. Gueymard, C.A. *Progress in direct irradiance modeling and validation*. in *Proc. ASES Annual Conf. Phoenix, AZ, USA*. 2010.
30. Vignola, F., et al., *Building a bankable solar radiation dataset*. *Solar Energy*, 2012. **86**(8): p. 2218-2229.
31. Szokolay, S.V. *Solar geometry*. 1996. PLEA.
32. Gueymard, C.A., *Clear-sky irradiance predictions for solar resource mapping and large-scale applications: Improved validation methodology and detailed performance analysis of 18 broadband radiative models*. *Solar Energy*, 2012. **86**(8): p. 2145-2169.
33. Paulescu, M., et al., *Weather Modeling and Forecasting of PV Systems Operation*. 2013, Springer London : Imprint: Springer: London. p. XVIII, 355 s. 166 illus.
34. World Radiation Data Centre. *World Radiation Data Centre*. 2015 06.06.15]; Available from: <http://wrdc.mgo.rssi.ru/>.
35. World Radiation Monitoring Center - Baseline Surface Radiation Network. *World Radiation Monitoring Center - Baseline Surface Radiation Network*. 2015 06.06.15]; Available from: <http://bsrn.awi.de/>.

36. Swedish Meteorological and Hydrological Institute. *Strålingsnat*. 2013 06.06.15]; Available from: http://www.smhi.se/polopoly_fs/1.3260!/Stralningsstationer_1_6000000_2013_08.pdf.
37. Kjeller Vindteknikk, *Resource mapping of solar energy - An overview of available data in Norway*. 2013, Kjeller Vindteknikk.
38. Byrkjedal, Ø., *Questions regarding the report on resource mapping for solar energy in Norway by Kjeller Vindteknikk*, E.O. Lockertsen, Editor. 2015.
39. Persson, T., *Solar radiation climate in Sweden*. Physics and Chemistry of the Earth, Part B: Hydrology, Oceans and Atmosphere, 1999. **24**(3): p. 275-279.
40. Zelenka, A., et al., *Effective Accuracy of Satellite-Derived Hourly Irradiances*. Theoretical and Applied Climatology, 1999. **62**(3-4): p. 199-207.
41. Committee on Earth Observation Satellites. *World weather satellites*. 2015 06.06.15]; Available from: http://www.eohandbook.com/eohb05/images/fig_03_%28weather%29.jpg.
42. EUMETSAT. *Sample Meteosat Colour Images & Animations*. 2012 06.06.15]; Available from: http://www.geo-web.org.uk/MSGimagery_files/MSG2-fulldisk-hires.jpg.
43. Ineichen, P., *Global irradiation: average and typical year, and year to year annual variability*. 2011.
44. Hagen, L., *Measured, modelled and satellite derived solar radiation in Scandinavia*. 2011.
45. CEOS. *CEOS EO HANDBOOK – MISSION SUMMARY - Metop-B*. 2015 06.06.15]; Available from: <http://database.eohandbook.com/database/missionsummary.aspx?missionID=230>.
46. Liu, Y. and R. Liu, *Evaluation of the Spatial and Temporal Uncertainties Distribution of Daily-Integrated Shortwave Downward Radiation Estimated from Polar-Orbiting Satellite Observation*. Journal of Atmospheric and Oceanic Technology, 2012. **29**(10): p. 1481-1491.
47. Godøy, Ø. *Estimation of surface solar irradiance using polar orbiting satellites*. in *Midnight Sun Seminar 2012 - Using Solar Energy in the North*. 2012.
48. Ramedani, Z., M. Omid, and A. Keyhani, *Modeling Solar Energy Potential in a Tehran Province Using Artificial Neural Networks*. International Journal of Green Energy, 2013. **10**(4): p. 427-441.
49. Sözen, A., et al., *Use of artificial neural networks for mapping of solar potential in Turkey*. Applied Energy, 2004. **77**(3): p. 273-286.
50. Reddy, K.e. and M. Ranjan, *Solar resource estimation using artificial neural networks and comparison with other correlation models*. Energy Conversion and Management, 2003. **44**(15): p. 2519-2530.
51. Storvold, R. *Ground and airborne measurements and modelling of solar irradiance and albedo in arctic regions*. in *Midnight Sun Seminar 2012 - Using Solar Energy in the North*. 2012.
52. Ineichen, P., *Long term satellite hourly, daily and monthly global, beam and diffuse irradiance validation. Interannual variability analysis*. 2013.
53. Ineichen, P., *Long Term Satellite Global, Beam and Diffuse Irradiance Validation*. Energy Procedia, 2014. **48**(0): p. 1586-1596.

54. Landelius, T. *Gridded solar radiation data in the North*. in *Midnight Sun Seminar 2012 - Using Solar Energy in the North*. 2012. STRÅNG/SMHI.
55. PVSYST. *NASA-SSE data*. 2015 06.06.15]; Available from: http://files.pvsyst.com/help/meteo_source_nasa.htm.
56. Andersen, M., *Analysis of actual and forecasted power production for a solar energy system in Norway*, in *Norwegian University of Life Sciences*. 2014, Norwegian University of Life Sciences: Ås.
57. Huld, T., R. Müller, and A. Gambardella, *A new solar radiation database for estimating PV performance in Europe and Africa*. *Solar Energy*, 2012. **86**(6): p. 1803-1815.
58. HelioClim. *European Solar Radiation Atlas*. 2001 06.06.15]; Available from: <http://www.soda-is.com/esra/map.html>.
59. Müller, R.P., Uwe; Träger-Chatterjee, Christine; Cremer, Roswitha; Trentmann, Jörg; Hollmann, Rainer, *Surface Solar Radiation Data Set - Heliosat (SARAH) - Edition 1, in 1983 to 2013*. 2015, EUMETSAT Satellite Application Facility on Climate Monitoring (CM SAF).
60. Šúri, M., et al., *Potential of solar electricity generation in the European Union member states and candidate countries*. *Solar Energy*, 2007. **81**(10): p. 1295-1305.
61. Meteonorm, *Global Meteorological Database - Handbook Part 1: Software*. 2014.
62. Lundström, L., *Weather data for building simulation - New actual weather files for North Europe combining observed weather and modeled solar radiation*, in *School of Sustainable Development of Society and Technology*. 2012, Mälardalen University: Västerås, Sweden.
63. Swedish Meteorological and Hydrological Institute. *STRÅNG - a solar radiation model*. 2015 06.06.15]; Available from: <http://www.smhi.se/en/research/research-departments/atmospheric-remote-sensing/strang-a-solar-radiation-model-1.4893>.
64. SolarGIS. *Accuracy of SolarGIS data*. 2015 06.06.15]; Available from: <http://solargis.info/doc/accuracy>.
65. Swedish Meteorological and Hydrological Institute. *Solstrålning i Sverige sedan 1983*. 2015 06.06.15]; Available from: <http://www.smhi.se/klimatdata/meteorologi/stralning/solstralning-i-sverige-sedan-1983-1.8243>.
66. Swedish Meteorological and Hydrological Institute, S.E.P.A., ; Swedish Radiation Safety Authority,, *Extracting STRÅNG data, in 1999 to 2014*. 2015, Swedish Meteorological and Hydrological Institute,: SMHI.se.
67. European Commission - Joint Research Centre - Institute for Energy and Transport, *Photovoltaic Geographical Information System - Interactive Maps, in 1981-1990*. 2015, European Commission.
68. NASA Langley Research Center Atmospheric Science Data Center Surface meteorological and Solar Energy (SSE), *NASA Surface meteorology and Solar Energy - Location, in 1983 to 2005*. 2015, NASA.
69. The European Space Agency, *Satel-Light - The European Database of Daylight and Solar Radiation, in 1996 to 2000*. 2015, The European Space Agency.
70. Meteonorm 6.1, *Irradiation data, in 1981 to 2000*. 2015, Meteonorm through PVSYST v6.32.

71. Meeonorm 7.1, *Irradiation data, in 1991 to 2010*. 2015, Meeonorm through PVSYST v6.35.
72. Lave, M. and J. Kleissl, *Optimum fixed orientations and benefits of tracking for capturing solar radiation in the continental United States*. *Renewable Energy*, 2011. **36**(3): p. 1145-1152.
73. Bugler, J., *The determination of hourly insolation on an inclined plane using a diffuse irradiance model based on hourly measured global horizontal insolation*. *Solar Energy*, 1977. **19**(5): p. 477-491.
74. National Renewable Energy Laboratory, *Best Research-Cell Efficiencies*. 2014.
75. Masters, G.M., *Renewable and Efficient Electric Power Systems*. 2004, Hoboken, NJ, USA: John Wiley & Sons, Incorporated.
76. Wallace, P.D. *Electric Sunshine*. 2005 06.06.15]; Available from: http://ffden-2.phys.uaf.edu/631fall2008_web.dir/wallace_webpage/8_Sun.html.
77. Kleven, Ø., *Solparken Acusticum - Teknisk beskrivelse av solcelleinstallasjonen på Solparken Acusticum*. 2014.
78. Tyagi, V., et al., *Progress in solar PV technology: research and achievement*. *Renewable and sustainable energy reviews*, 2013. **20**: p. 443-461.
79. Eikelboom, J. and M. Jansen, *Characterisation of PV modules of new generations*. Results of tests and simulations, 2000.
80. Thevenard, D., et al. *Performance monitoring of a northern 3.2 kWp grid-connected photovoltaic system*. in *Photovoltaic Specialists Conference, 2000. Conference Record of the Twenty-Eighth IEEE*. 2000.
81. Kendall B.D. Esmeijer, A.L., Wilfried G.J.H.M. van Sark, *PV Performance During Low Irradiance and Rainy weather Conditions*, in *29th European Photovoltaic Solar Energy Conference and Exhibition*. 2014: Amsterdam.
82. Deline, C., et al., *A performance and economic analysis of distributed power electronics in photovoltaic systems*. *Contract*, 2011. **303**: p. 275-3000.
83. Scholten, D.M., N. Ertugrul, and W.L. Soong. *Micro-inverters in small scale PV systems: A review and future directions*. in *Power Engineering Conference (AUPEC), 2013 Australasian Universities*. 2013.
84. SolarEdge. *SolarEdge Three Phase Inverters*. 2015 06.06.15]; Available from: <http://www.solaredge.com/files/pdfs/products/inverters/se-three-phase-inverter-datasheet.pdf>.
85. SweModule. *Installation instruction for Solar Photovoltaic Modules*. 2013 06.06.15]; Available from: http://www.swemodule.com/assets/files/pdf/Swemodule_Installation%20instruction_2013-07-10%20rev%2007.pdf.
86. REC. *Installation manual - REC peak energy series*. 2015 06.06.15]; Available from: <http://www.recgroup.com/Documents/Downloadcenter/Solar%20product%20downloads/Solar%20Installation%20and%20Maintenance/REC%20Peak%20Energy%20Installation%20Manual%20IEC%20ENG.pdf?epslanguage=en>.
87. Verlinden, P.J., et al., *Optimized PV Modules for Tropical, Mountain and Desert Climates*, in *29th European Photovoltaic Solar Energy Conference and Exhibition*. 2014, WIP.

88. Energirådgivningen. *Stockholm solinventering - Stocholms solkarta*. 2015 06.06.15]; Available from: <http://www.energiradgivningen.se/stockholm-solinventering>.
89. Widèn, J. *Beräkningsverktyg*. 2011 06.06.15]; Available from: <http://www.solelprogrammet.se/projekteringsverktyg/berakningsverktyg/>.
90. Widen, J., *Beräkningsmodell för ekonomisk optimering av soleanläggningar*. 2011, Elforsk.
91. McConnell, P.H.D., *Renewable Energy Technology Cost Review*, in *Technical Paper Series*. 2011, The University of Melbourne - Melbourne Energy Institute: Melbourne.
92. OECD/NEA, *Projected Costs of Generating Electricity 2010*. 2010: OECD Publishing.
93. International Energy Agency, *The Power of Transformation*. 2014: IEA.
94. Bazilian, M., et al., *Re-considering the economics of photovoltaic power*. *Renewable Energy*, 2013. **53**(0): p. 329-338.
95. Alexander Hauser, A.R., Sylvère Leu, *Cell and Module Desing in Dependence of Quality, Climate and LCOE*, in *29th European Photovoltaic Solar Energy Conference and Exhibition*. 2014: Amsterdam.
96. Branker, K., M.J.M. Pathak, and J.M. Pearce, *A review of solar photovoltaic levelized cost of electricity*. *Renewable and Sustainable Energy Reviews*, 2011. **15**(9): p. 4470-4482.
97. He, F., Z. Zhao, and L. Yuan, *Impact of inverter configuration on energy cost of grid-connected photovoltaic systems*. *Renewable Energy*, 2012. **41**(0): p. 328-335.
98. Morales, J.I.B.M.J.B.R.M., *PV Grid Parity Monitor - Residential Sector - 3rd issue*. 2015, CREARA.
99. Norrga, S.S., Bengt; Meier, Stephan; Nee, Hans-Peter, *Renewable Energy Sources for Electricity Generation*. 2012, KTH Royal Institute of Technology.
100. Ransome, S. and J. Sutterlueti, *The Sensitivity of LCOE to PV Technology Including Degradation, Seasonal Annealing, Spectral and Other Effects*. 2012, WIP.
101. National Renewable Energy Laboratory. *Levelized Cost of Energy Calculator*. 2015 06.06.15]; Available from: http://www.nrel.gov/analysis/tech_lcoe.html.
102. Ueckerdt, F., et al., *System LCOE: What are the costs of variable renewables?* *Energy*, 2013. **63**(0): p. 61-75.
103. International Energy Agency, *The Power of Transformation*. 2014, IEA.
104. Candelise, C., M. Winkler, and R.J. Gross, *The dynamics of solar PV costs and prices as a challenge for technology forecasting*. *Renewable and Sustainable Energy Reviews*, 2013. **26**: p. 96-107.
105. Seel, J., G.L. Barbose, and R.H. Wiser, *An analysis of residential PV system price differences between the United States and Germany*. *Energy Policy*, 2014. **69**(0): p. 216-226.
106. International Energy Agency, *Review of Failures of Photovoltaic Modules*, in *Photovoltaic Power Systems Programme*. 2014, International Energy Agency,.
107. Jordan, D.C. and S.R. Kurtz, *Photovoltaic Degradation Risk*, in *2012 World Renewable Energy Forum*, National Renewable Energy Laboratory, Editor. 2012: Denver, Colorado.
108. Jordan, D.C. and S.R. Kurtz, *Photovoltaic Degradation Rates—an Analytical Review*. *Progress in Photovoltaics: Research and Applications*, 2013. **21**(1): p. 12-29.

109. Innotech Solar. *Innotech Solar AS to file for insolvency*. 2015 06.06.15]; Available from: <http://www.innotechsolar.com/en/news/single/artikel/innotech-solar-as-beantragt-insolvenz.html>.
110. Gifford, J. *IHS: Inverter price declines to lead BoS cost reductions*. 2015 06.06.15]; Available from: <http://www.pv-magazine.com/news/details/beitrag/ihs--inverter-price-declines-to-lead-bos-cost-reductions-100018462/#ixzz3TuSg2023>.
111. Jonsson, P., *Questions regarding the PV system at Acusticum*, E.O. Lockertsen, Editor. 2015: Piteå.
112. Bank, N. *Inflasjon*. 2015 06.06.15]; Available from: <http://www.norges-bank.no/Statistikk/Inflasjon/>.
113. International Renewable Energy Agency, *Solar Photovoltaics*, in *Renewable Energy Technologies: Cost Analysis Series*, I. Secretariat, Editor. 2012.
114. Kabiri, R., D.G. Holmes, and B.P. McGrath. *The influence of pv inverter reactive power injection on grid voltage regulation*. in *Power Electronics for Distributed Generation Systems (PEDG), 2014 IEEE 5th International Symposium on*. 2014.
115. Youngsang, B., V. Trung-Kien, and K. Rae-Young, *Implemental Control Strategy for Grid Stabilization of Grid-Connected PV System Based on German Grid Code in Symmetrical Low-to-Medium Voltage Network*. *Energy Conversion, IEEE Transactions on*, 2013. **28**(3): p. 619-631.
116. Yaosuo, X., et al. *Towards next generation photovoltaic inverters*. in *Energy Conversion Congress and Exposition (ECCE), 2011 IEEE*. 2011.
117. Zhang, J., F. Lv, and L. Zhang, *Discussion on environment impact assessment in the lifecycle of PV systems*. *Energy Procedia*, 2012. **16**: p. 234-239.
118. Yue, D., F. You, and S.B. Darling, *Domestic and overseas manufacturing scenarios of silicon-based photovoltaics: Life cycle energy and environmental comparative analysis*. *Solar Energy*, 2014. **105**: p. 669-678.
119. Baharwani, V., et al. *Life cycle inventory and assessment of different solar photovoltaic systems*. in *Power and Energy Systems Conference: Towards Sustainable Energy, 2014*. 2014.
120. Azzopardi, B. and J. Mutale, *Life cycle analysis for future photovoltaic systems using hybrid solar cells*. *Renewable and Sustainable Energy Reviews*, 2010. **14**(3): p. 1130-1134.
121. Gerbinet, S., S. Belboom, and A. Léonard, *Life Cycle Analysis (LCA) of photovoltaic panels: A review*. *Renewable and Sustainable Energy Reviews*, 2014. **38**: p. 747-753.
122. Sherwani, A. and J. Usmani, *Life cycle assessment of solar PV based electricity generation systems: A review*. *Renewable and Sustainable Energy Reviews*, 2010. **14**(1): p. 540-544.
123. Turconi, R., A. Boldrin, and T. Astrup, *Life cycle assessment (LCA) of electricity generation technologies: overview, comparability and limitations*. *Renewable and Sustainable Energy Reviews*, 2013. **28**: p. 555-565.
124. Oslo Municipality. *The clima- and energy found solar campaign*. 2014 06.06.15]; Available from: <http://www.enoketaten.oslo.kommune.no/article287767-5667.html>.
125. Enova SF. *Tilskudd for el-produksjon*. 2015 06.06.15]; Available from: <http://www.enova.no/finansiering/privat/enovatilskuddet-/el-produksjon/914/0/>.

126. Bolkesjø, T.F., P.T. Eltvig, and E. Nygaard, *An Econometric Analysis of Support Scheme Effects on Renewable Energy Investments in Europe*. Energy Procedia, 2014. **58**(0): p. 2-8.
127. Norwegian Water Resources and Energy Directorate. *Electricity certificates*. 2015 06.06.15]; Available from: <http://www.nve.no/en/Electricity-market/Electricity-certificates/>.
128. STATNETT SF. *Norwegian Energy Certificate System*. 2015 06.06.15]; Available from: <http://necs.statnett.no/default.aspx>.
129. Botnen, O.J., *Long Term Expectations for price development in the Nordic Power Market 2013-2035*. 2012, Markedskraft: PF Norsk Energiforening, Oslo, 27. nov. 2012.
130. Nordpool. *Yearly DS future bids for Nordic electricity*. 2015 06.06.15]; Available from: <http://www.nordpoolspot.com/>.
131. Norwegian Water Resource and Energy Directorate. *Grid rent statistics*. 2015 06.06.15]; Available from: <http://www.nve.no/no/Kraftmarked/Nettleie1/Nettleiestatistikk/>.
132. Statnett SF, *Nettutviklingsplan 2013*. 2013.
133. International Energy Agency, *Energy - Issue 7*. 2014.
134. Bouillon, B. *Prepared Statement of Brad Bouillon on behalf of the California Independent System Operator Corporation*. in *Reliability Technical Conference 2014*.
135. Bernstein Research, *Bernstein Energy & Power Blast: Equal and Opposite... If Solar Wins, Who Loses?*, in *Commodities and Power*. 2014.
136. Nordic Energy Regulators, *Development in the Nordic Electricity Market*. 2014.
137. Statistics Norway. *Norwegian population statistics*. 2015 06.06.15]; Available from: <https://www.ssb.no/befolkning>.

Appendix 1 – Extraction of STRÅNG data

<http://strang.smhi.se/extraction/index.php?data=tmsrs&lev=3>

Date of extraction: 09.04.2015

Datatype: Time series

Time resolution: Yearly

Parameter: Global and direct irradiation [Wh/m²]

From: 1999

To: 2014

Latitude: 65.30 Longitude: 21.48

Year	month	day	hour	Global irradiation [Wh/m ²]	Direct irradiation [Wh/m ²]
1999	12	31	23	920256.3	1135000.8
2000	12	31	23	894294.1	1129606.8
2001	12	31	23	885540.2	1028521.5
2002	12	31	23	960342.1	1222044.2
2003	12	31	23	931726.6	1149160.0
2004	12	31	23	870708.7	1048381.4
2005	12	31	23	864875.6	1009359.0
2006	12	31	23	925194.6	1216909.6
2007	12	31	23	853109.9	1066556.6
2008	12	31	23	850922.8	955772.1
2009	12	31	23	868089.9	1076951.4
2010	12	31	23	754300.6	948716.7
2011	12	31	23	851280.7	956742.6
2012	12	31	23	830149.2	861427.9
2013	12	31	23	907960.9	1070725.2
2014	12	31	23	906748.6	1023362.8

Appendix 2 – Extraction of PVGIS-classic data

<http://re.jrc.ec.europa.eu/pvgis/apps4/pvest.php>

Date of extraction: 09.04.2015

Latitude: 65.30 Longitude: 21.48

Monthly Solar Irradiation

PVGIS Estimates of long-term monthly averages

Location: 65°17'59" North, 21°28'48" East, Elevation: 0 m a.s.l.,

Solar radiation database used: PVGIS-classic

Optimal inclination angle is: 47 degrees
Annual irradiation deficit due to shadowing (horizontal): 0.0 %

Month	H_h	DNI	I_{opt}	D/G	T_{24h}	N_{DD}
Jan	110	915	86	0.57	-7.7	841
Feb	620	1900	78	0.54	-9.1	754
Mar	1720	2930	64	0.53	-4.5	635
Apr	3630	5090	49	0.45	1.0	463
May	4880	5410	33	0.47	8.0	275
Jun	5530	5580	26	0.49	13.4	105
Jul	4990	4850	29	0.52	16.8	49
Aug	3370	3140	38	0.58	14.7	145
Sep	1900	2260	55	0.60	9.9	337
Oct	781	1420	70	0.63	3.4	540
Nov	169	603	82	0.71	-1.9	692
Dec	35.4	382	87	0.74	-6.2	838
Year	2320	2880	47	0.51	3.2	5674

H_h : Irradiation on horizontal plane (Wh/m²/day)

DNI : Direct normal irradiation (Wh/m²/day)

I_{opt} : Optimal inclination (deg.)

D/G : Ratio of diffuse to global irradiation (-)

T_{24h} : 24 hour average of temperature (°C)

N_{DD} : Number of heating degree-days (-)

PVGIS © European Communities, 2001-2012

Appendix 3 – Extraction of NASA/SSE data

<https://cosweb.larc.nasa.gov/cgi-bin/sse/grid.cgi?email=skip@larc.nasa.gov>

Date of extraction: 09.04.2015

Latitude: 65.30 Longitude: 21.48

9.4.2015

NASA Surface meteorology and Solar Energy - Available Tables

[SSE
Homepage](#)

[Find A Different Location](#)

[Accuracy](#)

[Methodology](#)

[Parameters
\(Units & Definition\)](#)



NASA Surface meteorology and Solar Energy - Available Tables



Latitude **65.3** / Longitude **21.48** was chosen.

Geometry Information

Elevation: **157** meters
taken from the
NASA GEOS-4
model elevation

Northern boundary
66

Western boundary **21** Center
Latitude **65.5**
Longitude **21.5** Eastern boundary
22

Southern boundary
65

Parameters for Sizing and Pointing of Solar Panels and for Solar Thermal Applications:

Monthly Averaged Insolation Incident On A Horizontal Surface (kWh/m²/day)

Lat 65.3 Lon 21.48	Jan	Feb	Mar	Apr	May	Jun	Jul	Aug	Sep	Oct	Nov	Dec	Annual Average
22-year Average	0.09	0.66	1.99	3.84	5.09	5.50	5.01	3.82	2.25	0.91	0.22	0.02	2.46

Minimum And Maximum Difference From Monthly Averaged Insolation (%)

Lat 65.3 Lon 21.48	Jan	Feb	Mar	Apr	May	Jun	Jul	Aug	Sep	Oct	Nov	Dec
Minimum	-11	-12	-13	-15	-16	-19	-12	-23	-22	-25	-14	n/a
Maximum	11	18	15	8	16	29	23	25	19	23	23	n/a

Parameter Definition

Monthly Averaged Diffuse Radiation Incident On A Horizontal Surface (kWh/m²/day)

Lat 65.3 Lon 21.48	Jan	Feb	Mar	Apr	May	Jun	Jul	Aug	Sep	Oct	Nov	Dec	Annual Average
22-year Average	0.07	0.44	1.16	1.90	2.47	2.69	2.62	2.18	1.28	0.60	0.16	n/a	n/a
Minimum	0.07	0.50	1.24	1.92	2.45	2.69	2.62	2.22	1.38	0.70	0.18	n/a	n/a
Maximum	n/a	0.40	1.09	1.90	2.43	2.47	2.58	2.06	1.16	n/a	0.14	n/a	n/a
22-year Average K	0.30	0.43	0.50	0.53	0.51	0.48	0.47	0.47	0.44	0.39	0.37	0.28	0.43
Minimum K	0.26	0.37	0.43	0.45	0.42	0.38	0.41	0.36	0.34	0.29	0.32	0.14	0.35
Maximum K	0.33	0.50	0.57	0.58	0.59	0.62	0.57	0.58	0.53	0.49	0.46	0.28	0.51

NOTE: *Diffuse radiation, direct normal radiation and tilted surface radiation are not calculated when the clearness index (K) is below 0.3 or above 0.8.*

Parameter Definition

Monthly Averaged Direct Normal Radiation (kWh/m²/day)

Lat 65.3 Lon 21.48	Jan	Feb	Mar	Apr	May	Jun	Jul	Aug	Sep	Oct	Nov	Dec	Annual Average
22-year Average	n/a	1.44	3.06	5.07	6.01	6.53	5.46	3.97	3.05	1.61	0.78	n/a	n/a

Minimum And Maximum Difference From Monthly Averaged Direct Normal Radiation (%)

Lat 65.3 Lon 21.48	Jan	Feb	Mar	Apr	May	Jun	Jul	Aug	Sep	Oct	Nov	Dec
Minimum	n/a	-65	-41	-31	-30	-38	-25	-55	-61	n/a	n/a	n/a
Maximum	n/a	74	43	16	31	63	49	66	55	n/a	111	n/a

NOTE: *Diffuse radiation, direct normal radiation and tilted surface radiation are not calculated when the clearness index (K) is below 0.3 or above 0.8.*

Parameter Definition

Meteorology (Temperature):

Monthly Averaged Air Temperature At 10 m Above The Surface Of The Earth (°C)

Lat 65.3 Lon 21.48	Jan	Feb	Mar	Apr	May	Jun	Jul	Aug	Sep	Oct	Nov	Dec	Annual Average
22-year Average	-9.66	-9.16	-5.59	-0.27	6.66	12.6	15.1	13.0	7.94	2.33	-3.67	-7.67	1.87
Minimum	-13.1	-12.9	-9.73	-4.55	2.54	8.73	11.4	9.46	5.14	0.12	-6.35	-11.0	-1.62
Maximum	-6.14	-5.66	-1.56	3.65	10.2	16.2	18.4	16.2	10.9	4.51	-1.34	-4.55	5.14

Parameter Definition

Meteorology (Wind):

Monthly Averaged Wind Speed At 50 m Above The Surface Of The Earth (m/s)

Lat 65.3 Lon 21.48	Jan	Feb	Mar	Apr	May	Jun	Jul	Aug	Sep	Oct	Nov	Dec	Annual Average
10-year Average	5.71	5.62	4.83	4.61	4.49	4.18	4.51	4.47	4.68	5.54	5.57	5.77	4.99

Minimum And Maximum Difference From Monthly Averaged Wind Speed At 50 m (%)

Lat 65.3 Lon 21.48	Jan	Feb	Mar	Apr	May	Jun	Jul	Aug	Sep	Oct	Nov	Dec	Annual Average
Minimum	-13	-21	-12	-12	-13	-9	-14	-11	-10	-19	-11	-15	-13
Maximum	15	20	20	13	16	10	9	18	10	18	15	11	15

It is recommended that users of these wind data review the SSE [Methodology](#). The user may wish to correct for biases as well as local effects within the selected grid region.

All height measurements are from the soil, water, or ice/snow surface instead of "effective" surface, which is usually taken to be near the tops of vegetated canopies.

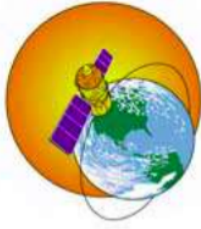
[Parameter Definition](#) [Units Conversion Chart](#)

Supporting Information:

Monthly Averaged Top-of-atmosphere Insolation (kWh/m²/day)

Lat 65.3 Lon 21.48	Jan	Feb	Mar	Apr	May	Jun	Jul	Aug	Sep	Oct	Nov	Dec	Annual Average
22-year Average	0.30	1.53	3.97	7.12	9.96	11.4	10.6	8.11	5.03	2.28	0.57	0.07	5.10

[Parameter Definition](#)



[Back to SSE
Data Set
Home Page](#)

Responsible > Data: Paul W. Stackhouse, Jr., Ph.D.
 Officials > Archive: John M. Kusterer
 Site Administration/Help: NASA Langley [ASDC](#) User
 Services ([Contact Us](#))
[\[Privacy Policy and Important Notices\]](#)
 Document generated on Thu Apr 9 04:24:09 EDT 2015

Appendix 4 – Extraction of Meteonorm 7.1 data

Collected through PVSYST v6.35

Date of extraction: 09.04.2015

Latitude: 65.30 Longitude: 21.48

Site: **Piteå (Sweden)**

Data source:

	Global Irrad. kWh/m ² .mth	Diffuse kWh/m ² .mth	Temper. °C	Wind Vel. m/s
January	3.6	2.3	-6.1	4.60
February	18.3	9.9	-7.6	4.39
March	59.7	24.4	-4.4	3.98
April	110.1	44.6	0.9	3.89
May	154.3	69.2	6.7	3.90
June	168.7	80.7	12.3	4.00
July	160.7	78.8	16.0	4.00
August	117.7	57.3	15.1	3.89
September	65.5	35.3	9.7	4.39
October	25.5	16.8	3.9	4.70
November	5.7	3.9	-1.0	4.79
December	0.0	0.0	-4.1	4.70
Year	889.9	423.1	3.5	4.3

Required Data:

- Horizontal global irradiation
- Average Ext. Temperature

Extra data:

- Horizontal diffuse irradiation
- Wind velocity

Irradiation units:

- kWh/m².day
- kWh/m².mth
- MJ/m².day
- MJ/m².mth
- W/m²
- Clearness Index Kt

Buttons: ? Paste Paste Paste Paste

Meteo File SE_Pite_MN71_SYN.MET, Monthly accumulations

Close Print Export

Meteo for Piteå, Reference year

Interval beginning	GlobHor kWh/m ² .mth	DiffHor kWh/m ² .mth	BeamNor kWh/m ² .mth
January	3.6	2.27	15.7
February	18.3	9.91	47.4
March	59.7	24.37	113.6
April	110.1	44.59	156.0
May	154.3	69.15	176.0
June	168.7	80.69	177.1
July	160.7	78.83	168.7
August	117.7	57.32	135.3
September	65.5	35.31	88.9
October	25.5	16.80	42.8
November	5.7	3.88	18.6
December	0.0	0.00	0.0
Year	889.9	423.11	1140.1

Appendix 5 – Extraction of Meteonorm 6.1 data

Collected through PVSYST v6.32

Date of extraction: 09.04.2015

Latitude: 65.30 Longitude: 21.48

Site: **Piteå (Sweden)**

Data source:

	Global Irrad. kWh/m ² .mth	Diffuse kWh/m ² .mth	Temper. °C	Wind Vel. m/s
January	3.4	2.6	-6.8	4.31
February	18.2	10.4	-7.6	4.51
March	56.9	28.1	-4.8	4.12
April	111.6	48.5	0.5	3.71
May	151.8	69.6	6.1	3.88
June	169.9	81.7	12.1	3.95
July	155.1	72.8	16.0	3.90
August	108.3	57.8	14.6	3.90
September	58.4	30.6	9.7	4.35
October	22.7	14.2	4.0	4.54
November	5.4	4.1	-1.2	4.67
December	0.5	0.1	-5.1	4.44
Year	862.1	420.6	3.1	4.2

Required Data

Horizontal global irradiation

Average Ext. Temperature

Extra data

Horizontal diffuse irradiation

Wind velocity

Irradiation units

kWh/m².day

kWh/m².mth

MJ/m².day

MJ/m².mth

W/m²

Clearness Index Kt

Meteo File SE_Pite_MN61_SYN.MET, Monthly accumulations

Close Print Export

Meteo for Piteå, Reference year

Interval beginning	GlobHor kWh/m ² .mth	DiffHor kWh/m ² .mth	BeamNor kWh/m ² .mth
January	3.4	2.62	8.9
February	18.2	10.44	44.8
March	56.9	28.05	93.9
April	111.6	48.50	160.1
May	151.8	69.60	169.9
June	169.9	81.71	178.8
July	155.1	72.79	166.9
August	108.3	57.80	114.4
September	58.4	30.63	82.8
October	22.7	14.22	36.4
November	5.4	4.10	11.8
December	0.0	0.00	0.0
Year	861.6	420.46	1068.5

Appendix 6 – Extraction of Satel-Light data

Date of extraction: 09.04.2015

Latitude: 65.00 Longitude: 21.48

9.4.2015

Satel-Light: your site information.

S@tel-Light Your Site Outdoor Information

Created: 04/09/2015 14:28 - Copyright Satel-Light

The information presented in this document is based on Meteosat Satellite images obtained every half hour - See our [advanced guide](#) for more information.

Report problems to the [Satel-Light WebMaster](#).

S@tel-Light

Lat: 55°0'0"N Lon: 21°29'0"E Alt: 20 m Clock Time: GMT+1 (Summer: GMT+2)
 From: Sunrise To: Sunset Using: Clock Time Years: 1996 to 2000
 Jan Feb Mar Apr May Jun Jul Aug Sep Oct Nov Dec All Months

Warning !, this section of the server is still in development !
 During that time, it produces a file containing half hour values of all the parameters you requested.

[Download your parameter information file \(1319 k\)](#)

This file has been compressed using the ZIP format. To uncompress it, use [WinZip](#) (Windows), [PKZIP](#) (Windows, Unix) or [ZipIt](#) (MacOS).

S@tel-Light Lat: 55°0'0"N Lon: 21°29'0"E Alt: 20 m
 From: Sunrise To: Sunset Using: Clock Time Years: 1996 to 2000
 Information: Percentage of Known, Derived, Missing and Night data (%)

	Jan.	Feb.	Mar.	Apr.	May	Jun.	Jul.	Aug.	Sep.	Oct.	Nov.	Dec.	Total
Known	10	68	80	73	67	62	65	72	77	74	31	0	64
Derived	90	32	20	27	33	38	35	28	23	26	68	100	36
Missing	0	0	0	0	0	0	0	0	0	1	1	0	0
Night	0	0	0	0	0	0	0	0	0	0	0	0	0

S@tel-Light Lat: 55°0'0"N Lon: 21°29'0"E Alt: 20 m
 From: Sunrise To: Sunset Using: Clock Time Years: 1996 to 2000
 Parameter: Global Horizontal Irradiance
 Information: Monthly Mean of daily sums (Wh/m2)

	Jan.	Feb.	Mar.	Apr.	May	Jun.	Jul.	Aug.	Sep.	Oct.	Nov.	Dec.	Total
Mean	98	482	1697	3277	5069	5504	5155	4012	2346	825	165	36	2401

S@tel-Light Lat: 55°0'0"N Lon: 21°29'0"E Alt: 20 m
 From: Sunrise To: Sunset Using: Clock Time Years: 1996 to 2000
 Parameter: Diffuse Horizontal Irradiance
 Information: Monthly Mean of daily sums (Wh/m2)

	Jan.	Feb.	Mar.	Apr.	May	Jun.	Jul.	Aug.	Sep.	Oct.	Nov.	Dec.	Total
Mean	84	362	1037	1888	2431	2618	2470	1877	1167	517	130	35	1223

S@tel-Light Lat: 55°0'0"N Lon: 21°29'0"E Alt: 20 m
 From: Sunrise To: Sunset Using: Clock Time Years: 1996 to 2000
 Parameter: Direct Horizontal Irradiance
 Information: Monthly Mean of daily sums (Wh/m2)

	Jan.	Feb.	Mar.	Apr.	May	Jun.	Jul.	Aug.	Sep.	Oct.	Nov.	Dec.	Total

Mean	14	120	660	1389	2638	2886	2686	2135	1179	308	35	1	1178
------	----	-----	-----	------	------	------	------	------	------	-----	----	---	------

S@tel-Light Lat : 55°0'0"N Lon : 21°29'0"E Alt : 20 m
From : Sunrise **To :** Sunset **Using :** Clock Time **Years :** 1996 to 2000
Parameter : Global Horizontal Illuminance
Information : Monthly Mean of daily sums (klxh)

	Jan.	Feb.	Mar.	Apr.	May	Jun.	Jul.	Aug.	Sep.	Oct.	Nov.	Dec.	Total
Mean	10.4	51.6	183.8	360.0	562.2	619.6	583.1	451.7	259.5	89.6	17.7	3.8	267.4

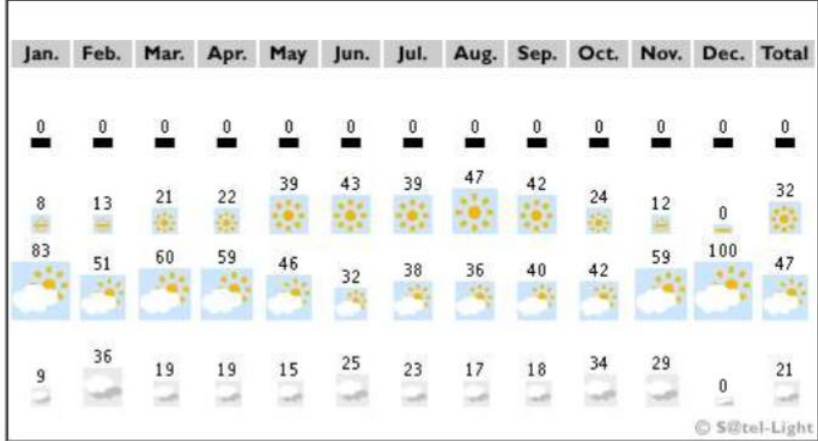
S@tel-Light Lat : 55°0'0"N Lon : 21°29'0"E Alt : 20 m
From : Sunrise **To :** Sunset **Using :** Clock Time **Years :** 1996 to 2000
Parameter : Diffuse Horizontal Illuminance
Information : Monthly Mean of daily sums (klxh)

	Jan.	Feb.	Mar.	Apr.	May	Jun.	Jul.	Aug.	Sep.	Oct.	Nov.	Dec.	Total
Mean	9.8	42.9	123.1	223.5	293.0	319.4	301.3	230.3	143.5	63.0	15.5	3.8	148.1

S@tel-Light Lat : 55°0'0"N Lon : 21°29'0"E Alt : 20 m
From : Sunrise **To :** Sunset **Using :** Clock Time **Years :** 1996 to 2000
Parameter : Direct Horizontal Illuminance
Information : Monthly Mean of daily sums (klxh)

	Jan.	Feb.	Mar.	Apr.	May	Jun.	Jul.	Aug.	Sep.	Oct.	Nov.	Dec.	Total
Mean	0.7	8.8	60.6	136.5	269.2	300.2	281.7	221.4	116.0	26.6	2.1	0.0	119.4

S@tel-Light Lat : 55°0'0"N Lon : 21°29'0"E Alt : 20 m
From : Sunrise **To :** Sunset **Using :** Clock Time **Years :** 1996 to 2000
Information : Frequency of Night, Sunny, Intermediate and Cloudy skies (%)



Appendix 7 – Inverter simplification calculations for PVSYST

Inverter rated power [kW]		17							
Module average STC power [kWp]		0.26484							
	String 1		String 2		Total			Fraction of inverter used by each string	
Inverter	# modules	String name	# modules	String name	# modules	Module/inverter power ratio		String 1	String 2
7E18255C-17	31	G1	34	G2	65	1.013		0.477	0.523
7E18253B-F6	32	G3	33	G4	65	1.013		0.492	0.508
7E182562-1D	33	F4	35	F5	68	1.059		0.485	0.515
7E18257B-36	38	F6	32	F2	70	1.091		0.543	0.457
7E182540-FB	32	F3	35	F1	67	1.044		0.478	0.522
7E18257A-35	39	A5	32	B1	71	1.106		0.549	0.451
7E182573-2E	33	A3	34	B2	67	1.044		0.493	0.507
7E182550-OB	40	B3	30	A2	70	1.091		0.571	0.429
7E18254F-0A	42	B4	30	A1	72	1.122		0.583	0.417
7E18256E-29	36	A4	33	HI1	69	1.075		0.522	0.478
7E182569-24	40	HI3	29	HI4	69	1.075		0.580	0.420
7E182571-2C	38	HI2	30	D2	68	1.059		0.559	0.441
7E182561-1C	40	E1	30	D1	70	1.091		0.571	0.429
TOTAL					891	1.068			
HI4 have all 29 modules from roof I. HI1 have 18 modules from roof I.									
Number for strings for each lenght					Number for strings for each lenght simplified for PVSYST				
			Total fraction of inverter used					Total fraction of inverter used	
# modules	# strings	sum modules	Sum	PVSYST string name	# modules	# strings	sum modules		Module/inverter power ratio
29	1	29	0.420						
30	4	120	1.715	5x30	30	5	150	2.135	1.09
31	1	31	0.477						
32	4	128	1.878	5x32	32	5	160	2.355	1.06
33	4	132	1.964	4x33	33	4	132	1.964	1.05
34	2	68	1.031	2x34	34	2	68	1.031	1.03
35	2	70	1.037	3x35	35	3	105	1.559	1.05
36	1	36	0.522						
38	2	76	1.102	3x38	38	3	114	1.651	1.08
39	1	39	0.549						
40	3	120	1.723	3x40	40	3	120	1.723	1.09
42	1	42	0.583	1x42	42	1	42	0.583	1.12
		891	13.000				891	13.000	
		# modules	# inverters				# modules	# inverters	

Appendix 8 – Simulation report. Expected scenario.

PVSYST V6.32	Eirik Oksavik Lockertsen			13/06/15	Page 1/6
Grid-Connected System: Simulation parameters					
Project :	Piteå (NASA-SSE) 236kWp Solbes Eirik				
Geographical Site	Piteå (NASA-SSE)	Country	Sweden		
Situation	Latitude	65.3°N	Longitude	21.5°E	
Time defined as	Legal Time	Time zone UT+1	Altitude	20 m	
	Albedo	0.20			
Meteo data:	Piteå (NASA-SSE)	Synthetic - NASA-SSE satellite data, 1983-2005			
Simulation variant :	String setup Innotech Solar EcoPlus 260 Wp (with different orientations)				
	Simulation date	13/06/15 14h41			
Simulation parameters					
3 orientations	Tilts/Azimuths	27°/39°, 27°/-51°, 30°/39°			
Models used	Transposition	Perez	Diffuse	Erbs, Meteororm	
Horizon	Free Horizon				
Near Shadings	Linear shadings				
PV Arrays Characteristics (8 kinds of array defined)					
PV module	Si-poly	Model	EcoPlus260		
	Manufacturer	Innotech Solar			
Sub-array "5x30"	Orientation	#1	Tilt/Azimuth	27°/39°	
Nb. of PowerBoxes	In series	30	In parallel	5 strings	
Total number of PV modules	Nb. modules	150	Unit Nom. Power	260 Wp	
Array global power	Nominal (STC)	39.0 kWp	At operating cond.	35.3 kWp (50°C)	
Output of Power Boxes	U oper	750 V	I at Poper	47 A	
Sub-array "5x32"	Orientation	#1	Tilt/Azimuth	27°/39°	
Nb. of PowerBoxes	In series	32	In parallel	5 strings	
Total number of PV modules	Nb. modules	160	Unit Nom. Power	260 Wp	
Array global power	Nominal (STC)	41.6 kWp	At operating cond.	37.7 kWp (50°C)	
Output of Power Boxes	U oper	750 V	I at Poper	50 A	
Sub-array "4x33"	Orientation	#3	Tilt/Azimuth	30°/39°	
Nb. of PowerBoxes	In series	33	In parallel	4 strings	
Total number of PV modules	Nb. modules	132	Unit Nom. Power	260 Wp	
Array global power	Nominal (STC)	34.3 kWp	At operating cond.	31.1 kWp (50°C)	
Output of Power Boxes	U oper	750 V	I at Poper	41 A	
Sub-array "2x34"	Orientation	#1	Tilt/Azimuth	27°/39°	
Nb. of PowerBoxes	In series	34	In parallel	2 strings	
Total number of PV modules	Nb. modules	68	Unit Nom. Power	260 Wp	
Array global power	Nominal (STC)	17.68 kWp	At operating cond.	16.01 kWp (50°C)	
Output of Power Boxes	U oper	750 V	I at Poper	21 A	
Sub-array "3x35"	Orientation	#1	Tilt/Azimuth	27°/39°	
Nb. of PowerBoxes	In series	35	In parallel	3 strings	
Total number of PV modules	Nb. modules	105	Unit Nom. Power	260 Wp	
Array global power	Nominal (STC)	27.30 kWp	At operating cond.	24.73 kWp (50°C)	
Output of Power Boxes	U oper	750 V	I at Poper	33 A	

Grid-Connected System: Simulation parameters (continued)

Sub-array "3x38"	Orientation	#1	Tilt/Azimuth	27°/39°
Nb. of PowerBoxes	In series	38	In parallel	3 strings
Total number of PV modules	Nb. modules	114	Unit Nom. Power	260 Wp
Array global power	Nominal (STC)	29.64 kWp	At operating cond.	26.84 kWp (50°C)
Output of Power Boxes	U oper	750 V	I at Poper	36 A
Sub-array "3x40"	Orientation	#1	Tilt/Azimuth	27°/39°
Nb. of PowerBoxes	In series	40	In parallel	3 strings
Total number of PV modules	Nb. modules	120	Unit Nom. Power	260 Wp
Array global power	Nominal (STC)	31.2 kWp	At operating cond.	28.26 kWp (50°C)
Output of Power Boxes	U oper	750 V	I at Poper	38 A
Sub-array "1x42"	Orientation	#2	Tilt/Azimuth	27°/-51°
Nb. of PowerBoxes	In series	42	In parallel	1 strings
Total number of PV modules	Nb. modules	42	Unit Nom. Power	260 Wp
Array global power	Nominal (STC)	10.92 kWp	At operating cond.	9.89 kWp (50°C)
Output of Power Boxes	U oper	750 V	I at Poper	13 A
Total Arrays global power	Nominal (STC)	232 kWp	Total	891 modules
	Module area	1470 m²	Cell area	1301 m ²
Inverter	Model	SE17k		
	Manufacturer	SolarEdge		
	Operating Voltage	750 V	Unit Nom. Power	17.0 kW AC
Sub-array "5x30"	Nb. of inverters	2.1 units	Total Power	36 kW AC
Sub-array "5x32"	Nb. of inverters	2.4 units	Total Power	41 kW AC
Sub-array "4x33"	Nb. of inverters	2 units	Total Power	34 kW AC
Sub-array "2x34"	Nb. of inverters	1 units	Total Power	17.0 kW AC
Sub-array "3x35"	Nb. of inverters	1.6 units	Total Power	27 kW AC
Sub-array "3x38"	Nb. of inverters	1.7 units	Total Power	29 kW AC
Sub-array "3x40"	Nb. of inverters	1.7 units	Total Power	29 kW AC
Sub-array "1x42"	Nb. of inverters	0.6 units	Total Power	10.2 kW AC
Total	Nb. of inverters	13	Total Power	223 kW AC

PV Array loss factors

Array Soiling Losses

Jan.	Feb.	Mar.	Apr.	May	June	July	Aug.	Sep.	Oct.	Nov.	Dec.
80.0%	80.0%	50.0%	0.0%	0.0%	0.0%	0.0%	0.0%	0.0%	0.0%	0.0%	50.0%

Thermal Loss factor	Uc (const)	29.0 W/m ² K	Uv (wind)	0.0 W/m ² K / m/s
Wiring Ohmic Loss	Array#1	115 mOhm	Loss Fraction	0.8 % at STC
	Array#2	108 mOhm	Loss Fraction	0.8 % at STC
	Array#3	131 mOhm	Loss Fraction	0.8 % at STC
	Array#4	254 mOhm	Loss Fraction	0.8 % at STC
	Array#5	165 mOhm	Loss Fraction	0.8 % at STC
	Array#6	152 mOhm	Loss Fraction	0.8 % at STC
	Array#7	144 mOhm	Loss Fraction	0.8 % at STC
	Array#8	412 mOhm	Loss Fraction	0.8 % at STC
	Global		Loss Fraction	0.8 % at STC
LID - Light Induced Degradation			Loss Fraction	0.7 %
Module Quality Loss			Loss Fraction	-1.7 %
Module Mismatch Losses			Loss Fraction	0.0 % (fixed voltage)
Incidence effect, ASHRAE parametrization	IAM = 1 - bo (1/cos i - 1)	bo Param.		0.02

Grid-Connected System: Simulation parameters (continued)

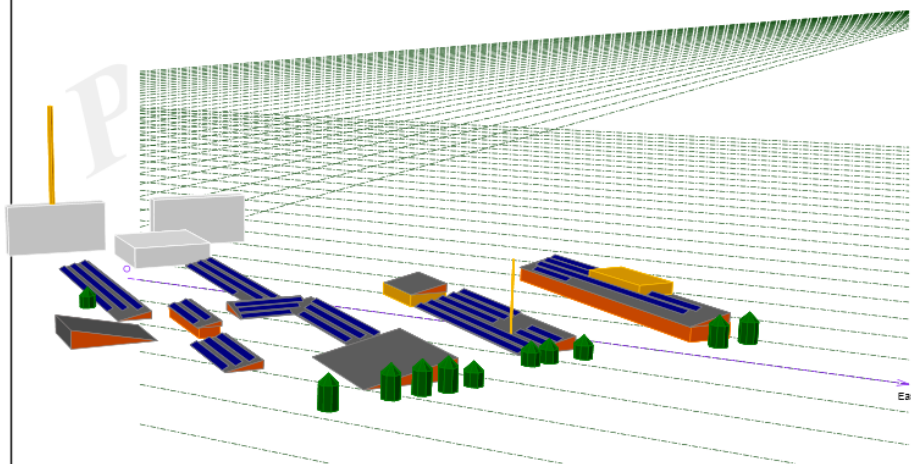
User's needs : Unlimited load (grid)

Grid-Connected System: Near shading definition

Project : Piteå (NASA-SSE) 236kwp Solbes Eirik
Simulation variant : String setup Innotech Solar EcoPlus 260 Wp (with different orientations)

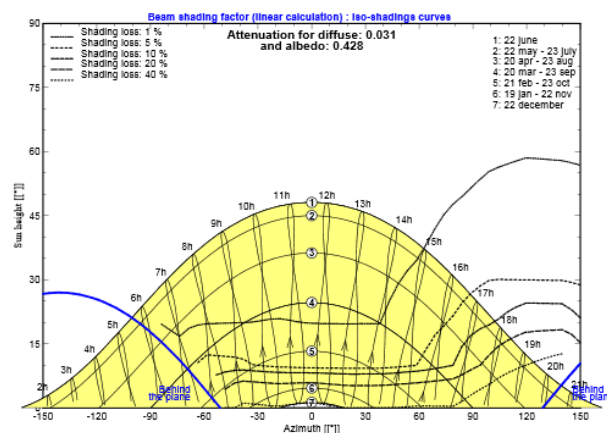
Main system parameters	System type	Grid-Connected	
Near Shadings	Linear shadings		
PV Field Orientation	3 orientations	Tilt/Azimuth = 27°/39°, 27°/-51°, 30°/39°	
PV modules	Model	EcoPlus260	Pnom 260 Wp
PV Array	Nb. of modules	891	Pnom total 232 kWp
Inverter	Model	SE17k	Pnom 17.00 kW ac
Inverter pack	Nb. of units	13.1	Pnom total 223 kW ac
User's needs	Unlimited load (grid)		

Perspective of the PV-field and surrounding shading scene



Iso-shadings diagram

Piteå (NASA-SSE) 236kwp Solbes Eirik



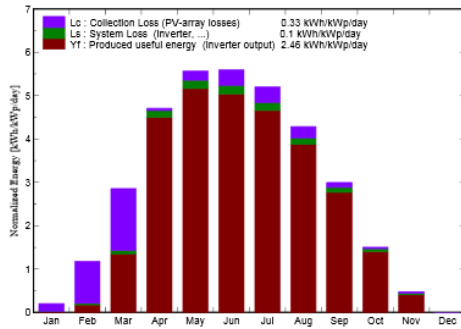
Grid-Connected System: Main results

Project : Piteå (NASA-SSE) 236kwp Solbes Eirik
Simulation variant : String setup Innotech Solar EcoPlus 260 Wp (with different orientations)

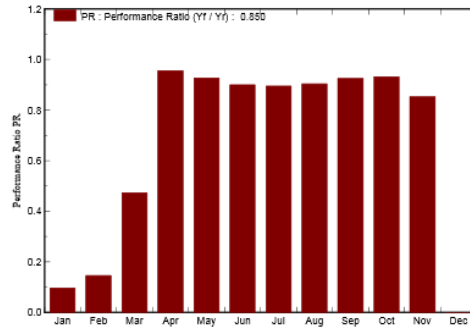
Main system parameters System type **Grid-Connected**
Near Shadings Linear shadings
 PV Field Orientation 3 orientations Tilt/Azimuth = 27°/39°, 27°/-51°, 30°/39°
 PV modules Model EcoPlus260 Pnom 260 Wp
 PV Array Nb. of modules 891 Pnom total **232 kWp**
 Inverter Model SE17k Pnom 17.00 kW ac
 Inverter pack Nb. of units 13.1 Pnom total **223 kW ac**
 User's needs Unlimited load (grid)

Main simulation results
 System Production **Produced Energy 207.7 MWh/year** Specific prod. 897 kWh/kWp/year
 Performance Ratio PR 85.0 %

Normalized productions (per installed kWp): Nominal power 232 kWp



Performance Ratio PR



String setup Innotech Solar EcoPlus 260 Wp (with different orientations)
 Balances and main results

	GlobHor	T Amb	GlobInc	GlobEff	EArray	E_Grid	EffArrR	EffSysR
	kWh/m²	°C	kWh/m²	kWh/m²	MWh	MWh	%	%
January	2.8	-9.70	6.3	1.1	0.20	0.14	2.14	1.52
February	18.5	-9.20	32.9	6.2	1.36	1.12	2.81	2.30
March	61.7	-5.60	88.5	42.5	10.26	9.69	7.89	7.45
April	115.2	-0.30	141.2	135.9	32.37	31.27	15.60	15.06
May	157.8	6.70	172.7	165.6	38.48	37.10	15.15	14.61
June	165.0	12.70	167.9	161.0	36.41	34.99	14.75	14.17
July	155.6	15.10	161.3	154.8	34.77	33.45	14.66	14.10
August	118.4	13.00	132.9	127.4	28.91	27.82	14.80	14.24
September	67.8	7.90	89.8	86.3	20.04	19.26	15.18	14.59
October	28.2	2.30	46.6	44.4	10.56	10.07	15.41	14.69
November	6.6	-3.70	14.3	12.9	3.07	2.83	14.56	13.45
December	0.0	-7.70	0.0	0.0	0.00	0.00	0.00	0.00
Year	897.6	1.86	1054.4	938.2	216.44	207.74	13.96	13.40

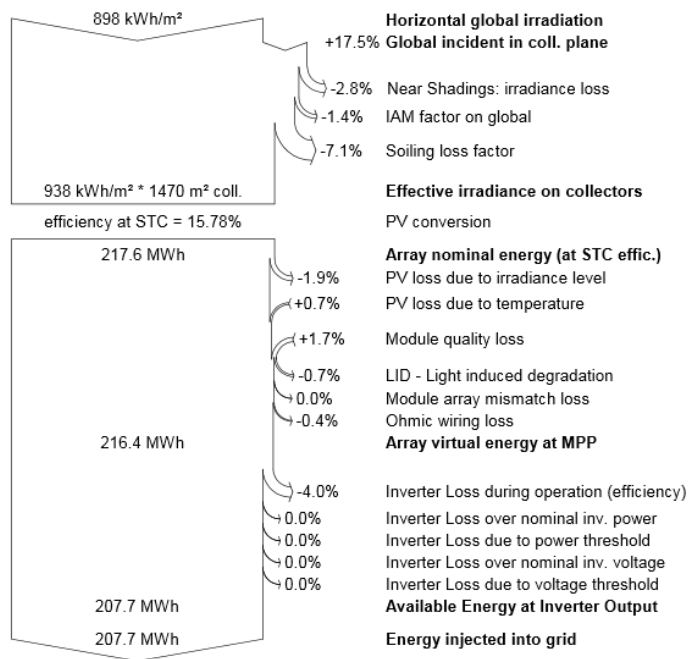
Legends: GlobHor Horizontal global irradiation EArray Effective energy at the output of the array
 T Amb Ambient Temperature E_Grid Energy injected into grid
 GlobInc Global incident in coll. plane EffArrR Effc. Eout array / rough area
 GlobEff Effective Global, corr. for IAM and shadings EffSysR Effc. Eout system / rough area

Grid-Connected System: Loss diagram

Project : Piteå (NASA-SSE) 236kwp Solbes Eirik
Simulation variant : String setup Innotech Solar EcoPlus 260 Wp (with different orientations)

Main system parameters	System type	Grid-Connected	
Near Shadings	Linear shadings		
PV Field Orientation	3 orientations	Tilt/Azimuth = 27°/39°, 27°/-51°, 30°/39°	
PV modules	Model	EcoPlus260	Pnom 260 Wp
PV Array	Nb. of modules	891	Pnom total 232 kWp
Inverter	Model	SE17k	Pnom 17.00 kW ac
Inverter pack	Nb. of units	13.1	Pnom total 223 kW ac
User's needs	Unlimited load (grid)		

Loss diagram over the whole year



Appendix 9 – Acusticum AC energy report May 2015



Periodic AC Energy Report for Site Solparken Acusticum

Report Period: From 2015-05-01 to 2015-05-31.

Location: Pitea, Sweden
Peak Power: 236 kWp
Installation Date: 2014-11-27
Intäktsberäkning: Enkel Tariff

Inverter	Serial Number	AC Energy (kWh)	Total intäkt (kr)
Inverter 1	7E18255C-17	1909,83	0,00
Inverter 2	7E182DA7-6A	1966,48	0,00
Inverter 2 (Disconnected)	7E18253B-F6	0,00	0,00
Inverter 3	7E182562-1D	1898,63	0,00
Inverter 4	7E18257B-36	2094,58	0,00
Inverter 5	7E182540-FB	1984,32	0,00
Inverter 6	7E18257A-35	1899,63	0,00
Inverter 7	7E182573-2E	1917,48	0,00
Inverter 8	7E182550-0B	1998,66	0,00
Inverter 9	7E18254F-0A	2073,37	0,00
Inverter 10	7E18256E-29	2024,88	0,00
Inverter 11	7E182569-24	2004,18	0,00
Inverter 12	7E182571-2C	1920,51	0,00
Inverter 13	7E182561-1C	2113,59	0,00
Total for site		25806,13	0,00

Appendix 10 – Simulation report. May, Acusticum data.

PVSYST V6.32	Eirik Oksavik Lockertsen		13/06/15	Page 1/6
Grid-Connected System: Simulation parameters				
Project :	Acusticum 236kwp Solbes Eirik			
Geographical Site	Piteå (NASA-SSE)	Country	Sweden	
Situation	Latitude	65.3°N	Longitude	21.5°E
Time defined as	Legal Time	Time zone UT+1	Altitude	20 m
	Albedo	0.20		
Meteo data:	Piteå (Meteonorm 7.1)	Imported - ASCII file		
Simulation variant :	String setup Innotech Solar EcoPlus 260 Wp (with different o			
	Simulation date	13/06/15 18h47		
Simulation parameters				
3 orientations	Tilts/Azimuths	27°/39°, 27°/-51°, 30°/39°		
Models used	Transposition	Hay	Diffuse	Erbs, Meteonorm
Horizon	Free Horizon			
Near Shadings	Linear shadings			
PV Arrays Characteristics (8 kinds of array defined)				
PV module	Si-poly	Model	EcoPlus260	
	Manufacturer	Innotech Solar		
Sub-array "5x30"	Orientation	#1	Tilt/Azimuth	27°/39°
Nb. of PowerBoxes	In series	30	In parallel	5 strings
Total number of PV modules	Nb. modules	150	Unit Nom. Power	260 Wp
Array global power	Nominal (STC)	39.0 kWp	At operating cond.	35.3 kWp (50°C)
Output of Power Boxes	U oper	750 V	I at Poper	47 A
Sub-array "5x32"	Orientation	#1	Tilt/Azimuth	27°/39°
Nb. of PowerBoxes	In series	32	In parallel	5 strings
Total number of PV modules	Nb. modules	160	Unit Nom. Power	260 Wp
Array global power	Nominal (STC)	41.6 kWp	At operating cond.	37.7 kWp (50°C)
Output of Power Boxes	U oper	750 V	I at Poper	50 A
Sub-array "4x33"	Orientation	#3	Tilt/Azimuth	30°/39°
Nb. of PowerBoxes	In series	33	In parallel	4 strings
Total number of PV modules	Nb. modules	132	Unit Nom. Power	260 Wp
Array global power	Nominal (STC)	34.3 kWp	At operating cond.	31.1 kWp (50°C)
Output of Power Boxes	U oper	750 V	I at Poper	41 A
Sub-array "2x34"	Orientation	#1	Tilt/Azimuth	27°/39°
Nb. of PowerBoxes	In series	34	In parallel	2 strings
Total number of PV modules	Nb. modules	68	Unit Nom. Power	260 Wp
Array global power	Nominal (STC)	17.68 kWp	At operating cond.	16.01 kWp (50°C)
Output of Power Boxes	U oper	750 V	I at Poper	21 A
Sub-array "3x35"	Orientation	#1	Tilt/Azimuth	27°/39°
Nb. of PowerBoxes	In series	35	In parallel	3 strings
Total number of PV modules	Nb. modules	105	Unit Nom. Power	260 Wp
Array global power	Nominal (STC)	27.30 kWp	At operating cond.	24.73 kWp (50°C)
Output of Power Boxes	U oper	750 V	I at Poper	33 A

Grid-Connected System: Simulation parameters (continued)

Sub-array "3x38"	Orientation	#1	Tilt/Azimuth	27°/39°
Nb. of PowerBoxes	In series	38	In parallel	3 strings
Total number of PV modules	Nb. modules	114	Unit Nom. Power	260 Wp
Array global power	Nominal (STC)	29.64 kWp	At operating cond.	26.84 kWp (50°C)
Output of Power Boxes	U oper	750 V	I at Poper	36 A
Sub-array "3x40"	Orientation	#1	Tilt/Azimuth	27°/39°
Nb. of PowerBoxes	In series	40	In parallel	3 strings
Total number of PV modules	Nb. modules	120	Unit Nom. Power	260 Wp
Array global power	Nominal (STC)	31.2 kWp	At operating cond.	28.26 kWp (50°C)
Output of Power Boxes	U oper	750 V	I at Poper	38 A
Sub-array "1x42"	Orientation	#2	Tilt/Azimuth	27°/-51°
Nb. of PowerBoxes	In series	42	In parallel	1 strings
Total number of PV modules	Nb. modules	42	Unit Nom. Power	260 Wp
Array global power	Nominal (STC)	10.92 kWp	At operating cond.	9.89 kWp (50°C)
Output of Power Boxes	U oper	750 V	I at Poper	13 A
Total Arrays global power	Nominal (STC)	232 kWp	Total	891 modules
	Module area	1470 m²	Cell area	1301 m ²
Inverter	Model	SE17k		
	Manufacturer	SolarEdge		
	Operating Voltage	750 V	Unit Nom. Power	17.0 kW AC
Sub-array "5x30"	Nb. of inverters	2.1 units	Total Power	36 kW AC
Sub-array "5x32"	Nb. of inverters	2.4 units	Total Power	41 kW AC
Sub-array "4x33"	Nb. of inverters	2 units	Total Power	34 kW AC
Sub-array "2x34"	Nb. of inverters	1 units	Total Power	17.0 kW AC
Sub-array "3x35"	Nb. of inverters	1.6 units	Total Power	27 kW AC
Sub-array "3x38"	Nb. of inverters	1.7 units	Total Power	29 kW AC
Sub-array "3x40"	Nb. of inverters	1.7 units	Total Power	29 kW AC
Sub-array "1x42"	Nb. of inverters	0.6 units	Total Power	10.2 kW AC
Total	Nb. of inverters	13	Total Power	223 kW AC

PV Array loss factors

Array Soiling Losses

Jan.	Feb.	Mar.	Apr.	May	June	July	Aug.	Sep.	Oct.	Nov.	Dec.
80.0%	80.0%	50.0%	0.0%	0.0%	0.0%	0.0%	0.0%	0.0%	0.0%	0.0%	50.0%

Thermal Loss factor	Uc (const)	29.0 W/m ² K	Uv (wind)	0.0 W/m ² K / m/s
Wiring Ohmic Loss	Array#1	115 mOhm	Loss Fraction	0.8 % at STC
	Array#2	108 mOhm	Loss Fraction	0.8 % at STC
	Array#3	131 mOhm	Loss Fraction	0.8 % at STC
	Array#4	254 mOhm	Loss Fraction	0.8 % at STC
	Array#5	165 mOhm	Loss Fraction	0.8 % at STC
	Array#6	152 mOhm	Loss Fraction	0.8 % at STC
	Array#7	144 mOhm	Loss Fraction	0.8 % at STC
	Array#8	412 mOhm	Loss Fraction	0.8 % at STC
	Global		Loss Fraction	0.8 % at STC
LID - Light Induced Degradation			Loss Fraction	0.7 %
Module Quality Loss			Loss Fraction	-1.7 %
Module Mismatch Losses			Loss Fraction	0.0 % (fixed voltage)
Incidence effect, ASHRAE parametrization	IAM =	1 - bo (1/cos i - 1)	bo Param.	0.02

Grid-Connected System: Simulation parameters (continued)

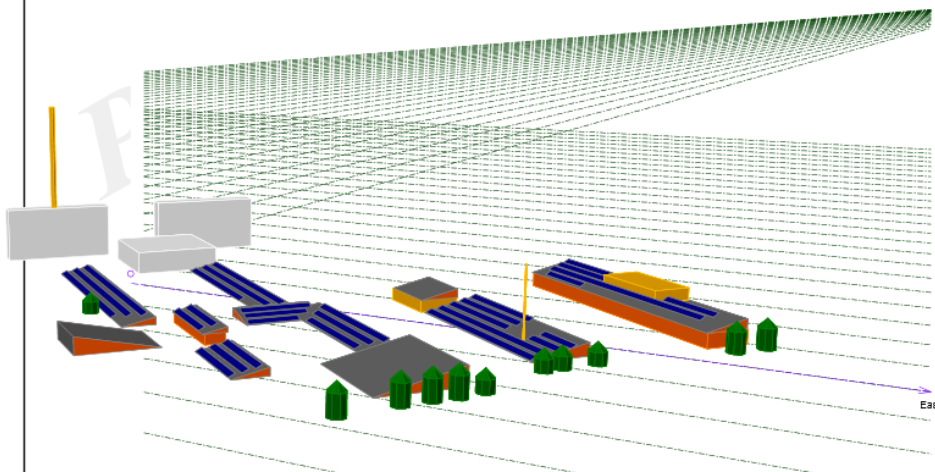
User's needs : Unlimited load (grid)

Grid-Connected System: Near shading definition

Project : Acusticum 236kwp Solbes Eirik
Simulation variant : String setup Innotech Solar EcoPlus 260 Wp (with different o

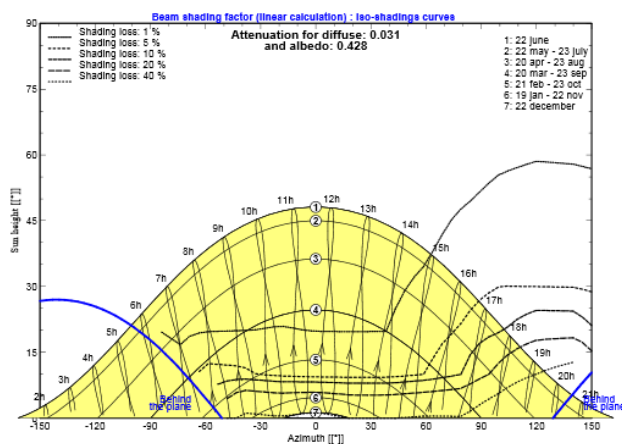
Main system parameters	System type	Grid-Connected	
Near Shadings	Linear shadings		
PV Field Orientation	3 orientations	Tilt/Azimuth = 27°/39°, 27°/-51°, 30°/39°	
PV modules	Model	EcoPlus260	Pnom 260 Wp
PV Array	Nb. of modules	891	Pnom total 232 kWp
Inverter	Model	SE17k	Pnom 17.00 kW ac
Inverter pack	Nb. of units	13.1	Pnom total 223 kW ac
User's needs	Unlimited load (grid)		

Perspective of the PV-field and surrounding shading scene



Iso-shadings diagram

Acusticum 236kwp Solbes Eirik



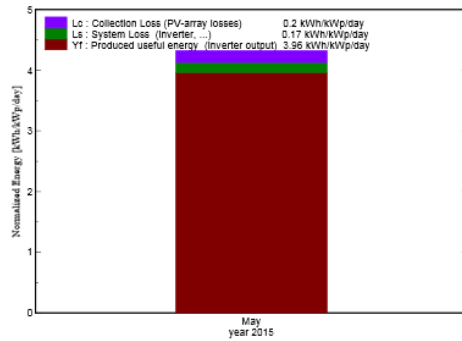
Grid-Connected System: Main results

Project : Acusticum 236kwp Solbes Eirik
Simulation variant : String setup Innotech Solar EcoPlus 260 Wp (with different o

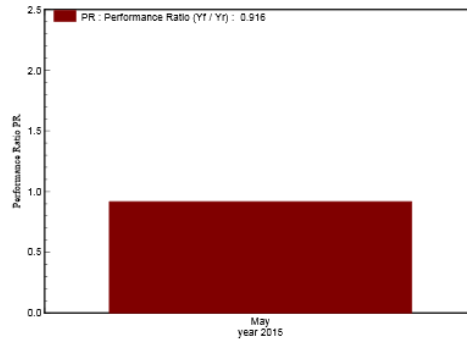
Main system parameters	System type	Grid-Connected		
Near Shadings	Linear shadings			
PV Field Orientation	3 orientations	Tilt/Azimuth = 27°/39°, 27°/-51°, 30°/39°		
PV modules	Model	EcoPlus260	Pnom	260 Wp
PV Array	Nb. of modules	891	Pnom total	232 kWp
Inverter	Model	SE17k	Pnom	17.00 kW ac
Inverter pack	Nb. of units	13.1	Pnom total	223 kW ac
User's needs	Unlimited load (grid)			

Main simulation results	System Production	Produced Energy	28.46 MWh	Specific prod.	123 kWh/kWp
		Performance Ratio PR	91.6 %		

Normalized productions (per installed kWp): Nominal power 232 kWp



Performance Ratio PR



String setup Innotech Solar EcoPlus 260 Wp (with different o
Balances and main results

	GlobHor kWh/m²	T_Amb °C	GlobInc kWh/m²	GlobEFF kWh/m²	EArray MWh	E_Grid MWh	EffArrR %	EffSysR %
May 15	126.1	8.75	134.1	128.9	29.66	28.46	15.05	14.44
Period	126.1	8.75	134.1	128.9	29.66	28.46	15.05	14.44

Legends: GlobHor Horizontal global irradiation EArray Effective energy at the output of the array
 T_Amb Ambient Temperature E_Grid Energy injected into grid
 GlobInc Global incident in coll. plane EffArrR Effc. Eout array / rough area
 GlobEFF Effective Global, corr. for IAM and shadings EffSysR Effc. Eout system / rough area

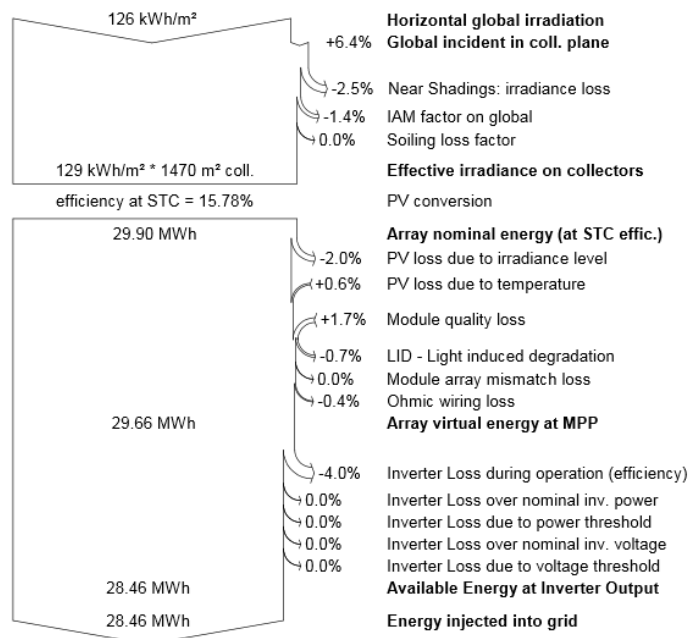
Grid-Connected System: Loss diagram

Project : Acusticum 236kwp Solbes Eirik

Simulation variant : String setup Innotech Solar EcoPlus 260 Wp (with different o

Main system parameters	System type	Grid-Connected	
Near Shadings	Linear shadings		
PV Field Orientation	3 orientations	Tilt/Azimuth = 27°/39°, 27°/-51°, 30°/39°	
PV modules	Model	EcoPlus260	Pnom 260 Wp
PV Array	Nb. of modules	891	Pnom total 232 kWp
Inverter	Model	SE17k	Pnom 17.00 kW ac
Inverter pack	Nb. of units	13.1	Pnom total 223 kW ac
User's needs	Unlimited load (grid)		

Loss diagram over the whole year



Appendix 11 – Simulation report. May, STRÅNG data.

Wind- and temperature data is from the Acusticum sensors.

PVSYST V6.32	Eirik Oksavik Lockertsen		13/06/15	Page 1/6
Grid-Connected System: Simulation parameters				
Project : Acusticum 236kwp Solbes Eirik				
Geographical Site		Piteå (NASA-SSE)	Country	Sweden
Situation		Latitude 65.3°N	Longitude	21.5°E
Time defined as		Legal Time	Time zone	UT+1
		Albedo	Altitude	20 m
Meteo data:		Piteå, Akusticum	Imported - ASCII file	
Simulation variant : Acusticum. Real data May 2015. STRÅNG database.				
Simulation date 13/06/15 18h18				
Simulation parameters				
3 orientations		Tilts/Azimuths 27°/39°, 27°/-51°, 30°/39°		
Models used		Transposition	Hay	Diffuse Erbs, Meteonorm
Horizon		Free Horizon		
Near Shadings		Linear shadings		
PV Arrays Characteristics (8 kinds of array defined)				
PV module		Si-poly	Model	EcoPlus260
		Manufacturer	Innotech Solar	
Sub-array "5x30"		Orientation	#1	Tilt/Azimuth 27°/39°
Nb. of PowerBoxes		In series	30	In parallel 5 strings
Total number of PV modules		Nb. modules	150	Unit Nom. Power 260 Wp
Array global power		Nominal (STC)	39.0 kWp	At operating cond. 35.3 kWp (50°C)
Output of Power Boxes		U oper	750 V	I at Poper 47 A
Sub-array "5x32"		Orientation	#1	Tilt/Azimuth 27°/39°
Nb. of PowerBoxes		In series	32	In parallel 5 strings
Total number of PV modules		Nb. modules	160	Unit Nom. Power 260 Wp
Array global power		Nominal (STC)	41.6 kWp	At operating cond. 37.7 kWp (50°C)
Output of Power Boxes		U oper	750 V	I at Poper 50 A
Sub-array "4x33"		Orientation	#3	Tilt/Azimuth 30°/39°
Nb. of PowerBoxes		In series	33	In parallel 4 strings
Total number of PV modules		Nb. modules	132	Unit Nom. Power 260 Wp
Array global power		Nominal (STC)	34.3 kWp	At operating cond. 31.1 kWp (50°C)
Output of Power Boxes		U oper	750 V	I at Poper 41 A
Sub-array "2x34"		Orientation	#1	Tilt/Azimuth 27°/39°
Nb. of PowerBoxes		In series	34	In parallel 2 strings
Total number of PV modules		Nb. modules	68	Unit Nom. Power 260 Wp
Array global power		Nominal (STC)	17.68 kWp	At operating cond. 16.01 kWp (50°C)
Output of Power Boxes		U oper	750 V	I at Poper 21 A
Sub-array "3x35"		Orientation	#1	Tilt/Azimuth 27°/39°
Nb. of PowerBoxes		In series	35	In parallel 3 strings
Total number of PV modules		Nb. modules	105	Unit Nom. Power 260 Wp
Array global power		Nominal (STC)	27.30 kWp	At operating cond. 24.73 kWp (50°C)
Output of Power Boxes		U oper	750 V	I at Poper 33 A

Grid-Connected System: Simulation parameters (continued)

Sub-array "3x38"	Orientation	#1	Tilt/Azimuth	27°/39°
Nb. of PowerBoxes	In series	38	In parallel	3 strings
Total number of PV modules	Nb. modules	114	Unit Nom. Power	260 Wp
Array global power	Nominal (STC)	29.64 kWp	At operating cond.	26.84 kWp (50°C)
Output of Power Boxes	U oper	750 V	I at Poper	36 A
Sub-array "3x40"	Orientation	#1	Tilt/Azimuth	27°/39°
Nb. of PowerBoxes	In series	40	In parallel	3 strings
Total number of PV modules	Nb. modules	120	Unit Nom. Power	260 Wp
Array global power	Nominal (STC)	31.2 kWp	At operating cond.	28.26 kWp (50°C)
Output of Power Boxes	U oper	750 V	I at Poper	38 A
Sub-array "1x42"	Orientation	#2	Tilt/Azimuth	27°/-51°
Nb. of PowerBoxes	In series	42	In parallel	1 strings
Total number of PV modules	Nb. modules	42	Unit Nom. Power	260 Wp
Array global power	Nominal (STC)	10.92 kWp	At operating cond.	9.89 kWp (50°C)
Output of Power Boxes	U oper	750 V	I at Poper	13 A
Total Arrays global power	Nominal (STC)	232 kWp	Total	891 modules
	Module area	1470 m²	Cell area	1301 m ²
Inverter	Model	SE17k		
	Manufacturer	SolarEdge		
	Operating Voltage	750 V	Unit Nom. Power	17.0 kW AC
Sub-array "5x30"	Nb. of inverters	2.1 units	Total Power	36 kW AC
Sub-array "5x32"	Nb. of inverters	2.4 units	Total Power	41 kW AC
Sub-array "4x33"	Nb. of inverters	2 units	Total Power	34 kW AC
Sub-array "2x34"	Nb. of inverters	1 units	Total Power	17.0 kW AC
Sub-array "3x35"	Nb. of inverters	1.6 units	Total Power	27 kW AC
Sub-array "3x38"	Nb. of inverters	1.7 units	Total Power	29 kW AC
Sub-array "3x40"	Nb. of inverters	1.7 units	Total Power	29 kW AC
Sub-array "1x42"	Nb. of inverters	0.6 units	Total Power	10.2 kW AC
Total	Nb. of inverters	13	Total Power	223 kW AC

PV Array loss factors

Array Soiling Losses

Jan.	Feb.	Mar.	Apr.	May	June	July	Aug.	Sep.	Oct.	Nov.	Dec.
80.0%	80.0%	50.0%	0.0%	0.0%	0.0%	0.0%	0.0%	0.0%	0.0%	0.0%	50.0%

Thermal Loss factor	Uc (const)	29.0 W/m ² K	Uv (wind)	0.0 W/m ² K / m/s
Wiring Ohmic Loss	Array#1	115 mOhm	Loss Fraction	0.8 % at STC
	Array#2	108 mOhm	Loss Fraction	0.8 % at STC
	Array#3	131 mOhm	Loss Fraction	0.8 % at STC
	Array#4	254 mOhm	Loss Fraction	0.8 % at STC
	Array#5	165 mOhm	Loss Fraction	0.8 % at STC
	Array#6	152 mOhm	Loss Fraction	0.8 % at STC
	Array#7	144 mOhm	Loss Fraction	0.8 % at STC
	Array#8	412 mOhm	Loss Fraction	0.8 % at STC
	Global		Loss Fraction	0.8 % at STC
LID - Light Induced Degradation			Loss Fraction	0.7 %
Module Quality Loss			Loss Fraction	-1.7 %
Module Mismatch Losses			Loss Fraction	0.0 % (fixed voltage)
Incidence effect, ASHRAE parametrization	IAM =	1 - bo (1/cos i - 1)	bo Param.	0.02

Grid-Connected System: Simulation parameters (continued)

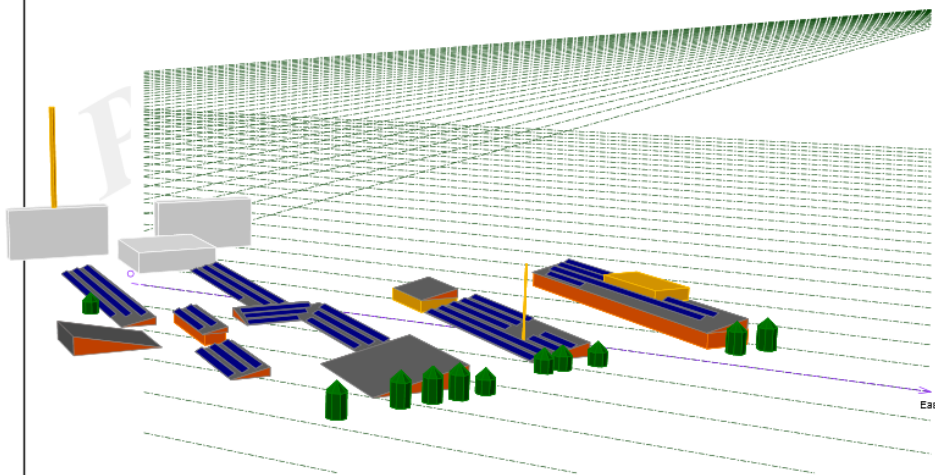
User's needs : Unlimited load (grid)

Grid-Connected System: Near shading definition

Project : Acusticum 236kwp Solbes Eirik
Simulation variant : Acusticum. Real data May 2015. STRÅNG database.

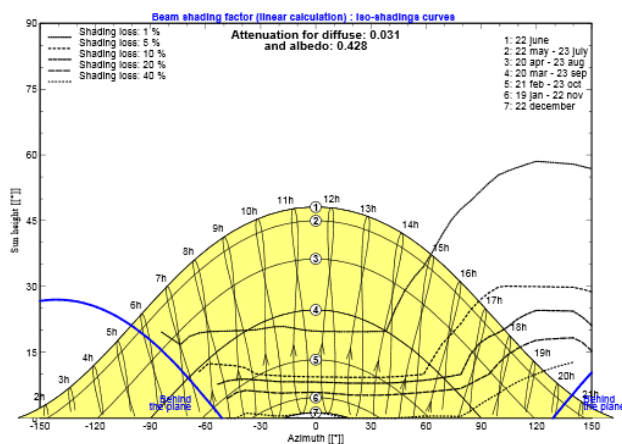
Main system parameters	System type	Grid-Connected		
Near Shadings	Linear shadings	3 orientations		
PV Field Orientation	Model	Tilt/Azimuth = 27°/39°, 27°/-51°, 30°/39°		
PV modules	Nb. of modules	EcoPlus260	Pnom	260 Wp
PV Array	Model	891	Pnom total	232 kWp
Inverter	Nb. of units	SE17k	Pnom	17.00 kW ac
Inverter pack	Unlimited load (grid)	13.1	Pnom total	223 kW ac
User's needs				

Perspective of the PV-field and surrounding shading scene



Iso-shadings diagram

Acusticum 236kwp Solbes Eirik



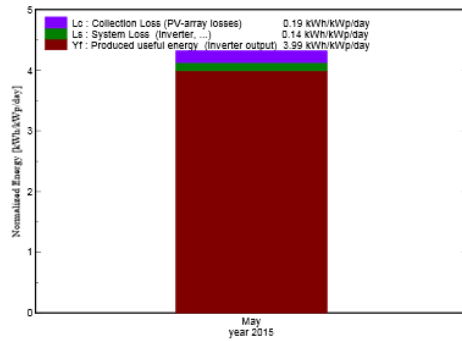
Grid-Connected System: Main results

Project : Acusticum 236kwp Solbes Eirik
Simulation variant : Acusticum. Real data May 2015. STRÅNG database.

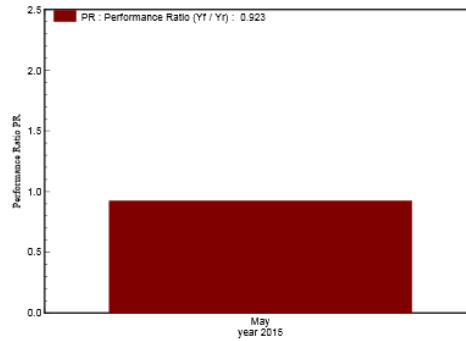
Main system parameters	System type	Grid-Connected		
Near Shadings	Linear shadings			
PV Field Orientation	3 orientations	Tilt/Azimuth = 27°/39°, 27°/-51°, 30°/39°		
PV modules	Model	EcoPlus260	Pnom	260 Wp
PV Array	Nb. of modules	891	Pnom total	232 kWp
Inverter	Model	SE17k	Pnom	17.00 kW ac
Inverter pack	Nb. of units	13.1	Pnom total	223 kW ac
User's needs	Unlimited load (grid)			

Main simulation results	System Production	Produced Energy	28.65 MWh	Specific prod.	124 kWh/kWp
		Performance Ratio PR	92.3 %		

Normalized productions (per installed kWp): Nominal power 232 kWp



Performance Ratio PR



Acusticum. Real data May 2015. STRÅNG database.
Balances and main results

	GlobHor kWh/m²	T_Amb °C	GlobInc kWh/m²	GlobEFF kWh/m²	EArray MWh	E_Grid MWh	EffArrR %	EffSysR %
May 15	116.2	8.75	133.9	128.3	29.64	28.65	15.05	14.55
Period	116.2	8.75	133.9	128.3	29.64	28.65	15.05	14.55

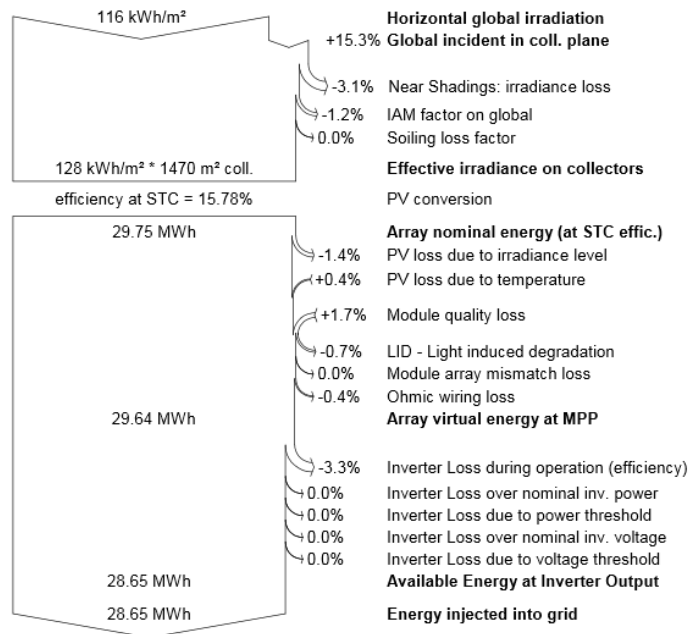
Legends: GlobHor Horizontal global irradiation EArray Effective energy at the output of the array
 T_Amb Ambient Temperature E_Grid Energy injected into grid
 GlobInc Global incident in coll. plane EffArrR Effc. Eout array / rough area
 GlobEFF Effective Global, corr. for IAM and shadings EffSysR Effc. Eout system / rough area

Grid-Connected System: Loss diagram

Project : Acusticum 236kwp Solbes Eirik
Simulation variant : Acusticum. Real data May 2015. STRÅNG database.

Main system parameters	System type	Grid-Connected	
Near Shadings	Linear shadings		
PV Field Orientation	3 orientations	Tilt/Azimuth = 27°/39°, 27°/-51°, 30°/39°	
PV modules	Model	EcoPlus260	Pnom 260 Wp
PV Array	Nb. of modules	891	Pnom total 232 kWp
Inverter	Model	SE17k	Pnom 17.00 kW ac
Inverter pack	Nb. of units	13.1	Pnom total 223 kW ac
User's needs	Unlimited load (grid)		

Loss diagram over the whole year



Appendix 12 - Simulation report. May, E-roof.

Real values May 2015. Acusticum data.

PVSYST V6.32	Eirik Oksavik Lockertsen		13/06/15	Page 1/3																															
Grid-Connected System: Simulation parameters																																			
Project :	Acusticum 236kwp Solbes Eirik																																		
Geographical Site	Piteå (NASA-SSE)	Country	Sweden																																
Situation	Latitude	65.3°N	Longitude	21.5°E																															
Time defined as	Legal Time	Time zone UT+1	Altitude	20 m																															
	Albedo	0.20																																	
Meteo data:	Piteå (Meteonorm 7.1)	Imported - ASCII file																																	
Simulation variant : E roof																																			
	Simulation date	13/06/15 19h33																																	
Simulation parameters																																			
Collector Plane Orientation	Tilt	27°	Azimuth	39°																															
Models used	Transposition	Hay	Diffuse	Erbs, Meteonorm																															
Horizon	Free Horizon																																		
Near Shadings	No Shadings																																		
PV Array Characteristics																																			
PV module	Si-poly	Model	EcoPlus260																																
	Manufacturer	Innotech Solar																																	
SolarEdge PowerBox		Model	P350	Unit nom. power 350 W																															
PV modules on one Powerbox		in series	1	in parallel 1																															
Number of PowerBoxes		In series	40	In parallel 1 strings																															
Total number of PV modules	Nb. modules	40	Unit Nom. Power	260 Wp																															
Array global power	Nominal (STC)	10.40 kWp	At operating cond.	9.42 kWp (50°C)																															
Output of Power Boxes	U oper	750 V	I at Poper	13 A																															
Total area	Module area	66.0 m²	Cell area	58.4 m²																															
Inverter		Model	SE17k																																
	Manufacturer	SolarEdge																																	
Characteristics	Operating Voltage	750 V	Unit Nom. Power	17.0 kWac																															
Inverter pack	Nb. of inverters	1 units	Total Power	10.2 kWac																															
PV Array loss factors																																			
Array Soiling Losses	<table border="1"> <thead> <tr> <th>Jan.</th> <th>Feb.</th> <th>Mar.</th> <th>Apr.</th> <th>May</th> <th>June</th> <th>July</th> <th>Aug.</th> <th>Sep.</th> <th>Oct.</th> <th>Nov.</th> <th>Dec.</th> </tr> </thead> <tbody> <tr> <td>80.0%</td> <td>80.0%</td> <td>50.0%</td> <td>0.0%</td> <td>0.0%</td> <td>0.0%</td> <td>0.0%</td> <td>0.0%</td> <td>0.0%</td> <td>0.0%</td> <td>0.0%</td> <td>50.0%</td> </tr> </tbody> </table>											Jan.	Feb.	Mar.	Apr.	May	June	July	Aug.	Sep.	Oct.	Nov.	Dec.	80.0%	80.0%	50.0%	0.0%	0.0%	0.0%	0.0%	0.0%	0.0%	0.0%	0.0%	50.0%
Jan.	Feb.	Mar.	Apr.	May	June	July	Aug.	Sep.	Oct.	Nov.	Dec.																								
80.0%	80.0%	50.0%	0.0%	0.0%	0.0%	0.0%	0.0%	0.0%	0.0%	0.0%	50.0%																								
Thermal Loss factor	Uc (const)	29.0 W/m²K	Uv (wind)	0.0 W/m²K / m/s																															
Wiring Ohmic Loss	Global array res.	144 mOhm	Loss Fraction	0.3 % at STC																															
LID - Light Induced Degradation			Loss Fraction	0.7 %																															
Module Quality Loss			Loss Fraction	-1.7 %																															
Module Mismatch Losses			Loss Fraction	0.0 % (fixed voltage)																															
Incidence effect, ASHRAE parametrization	IAM =	1 - bo (1/cos i - 1)	bo Param.	0.02																															
User's needs :	Unlimited load (grid)																																		

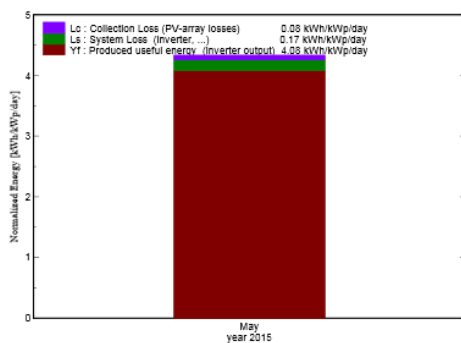
Grid-Connected System: Main results

Project : Acusticum 236kwp Solbes Eirik
Simulation variant : E roof

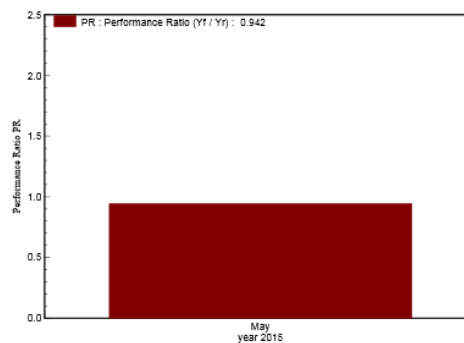
Main system parameters	System type	Grid-Connected		
PV Field Orientation	tilt	27°	azimuth	39°
PV modules	Model	EcoPlus260	Pnom	260 Wp
PV Array	Nb. of modules	40	Pnom total	10.40 kWp
Inverter	Model	SE17k	Pnom	17.00 kW ac
User's needs	Unlimited load (grid)			

Main simulation results	System Production	Produced Energy	1317 kWh	Specific prod.	127 kWh/kWp
		Performance Ratio PR	94.2 %		

Normalized productions (per installed kWp): Nominal power 10.40 kWp



Performance Ratio PR



E roof Balances and main results

	GlobHor	T Amb	GlobInc	GlobEff	EArray	E_Grid	EffArrR	EffSysR
	kWh/m ²	°C	kWh/m ²	kWh/m ²	kWh	kWh	%	%
May 15	126.1	8.75	134.4	132.4	1372	1317	15.47	14.85
Period	126.1	8.75	134.4	132.4	1372	1317	15.47	14.85

Legends:	GlobHor	Horizontal global irradiation	EArray	Effective energy at the output of the array
	T Amb	Ambient Temperature	E_Grid	Energy injected into grid
	GlobInc	Global incident in coll. plane	EffArrR	Effic. Eout array / rough area
	GlobEff	Effective Global, corr. for IAM and shadings	EffSysR	Effic. Eout system / rough area

Grid-Connected System: Loss diagram

Project : Acusticum 236kwp Solbes Eirik

Simulation variant : E roof

Main system parameters

	System type	Grid-Connected		
PV Field Orientation	tilt	27°	azimuth	39°
PV modules	Model	EcoPlus260	Pnom	260 Wp
PV Array	Nb. of modules	40	Pnom total	10.40 kWp
Inverter	Model	SE17k	Pnom	17.00 kW ac
User's needs	Unlimited load (grid)			

Loss diagram over the whole year

